forests

Disturbance Effects on Soil Carbon and Greenhouse Gas Emissions in Forest Ecosystems

Edited by
Scott X. Chang and Yanjiang Cai

Printed Edition of the Special Issue Published in *Forests*

www.mdpi.com/journal/forests

Disturbance Effects on Soil Carbon and Greenhouse Gas Emissions in Forest Ecosystems

Disturbance Effects on Soil Carbon and Greenhouse Gas Emissions in Forest Ecosystems

Special Issue Editors

Scott X. Chang
Yanjiang Cai

MDPI • Basel • Beijing • Wuhan • Barcelona • Belgrade • Manchester • Tokyo • Cluj • Tianjin

Special Issue Editors
Scott X. Chang
University of Alberta
Canada

Yanjiang Cai
Zhejiang A&F University
China

Editorial Office
MDPI
St. Alban-Anlage 66
4052 Basel, Switzerland

This is a reprint of articles from the Special Issue published online in the open access journal *Forests* (ISSN 1999-4907) (available at: https://www.mdpi.com/journal/forests/special_issues/Disturbance_Effects_on_Soil_Carbon_and_Greenhouse_Gas_Emissions).

For citation purposes, cite each article independently as indicated on the article page online and as indicated below:

LastName, A.A.; LastName, B.B.; LastName, C.C. Article Title. *Journal Name* **Year**, *Article Number*, Page Range.

ISBN 978-3-03928-666-9 (Pbk)
ISBN 978-3-03928-667-6 (PDF)

Cover image courtesy of Scott X. Chang

Contents

About the Special Issue Editors

Scott X. Chang (Professor of Forest Soils and Nutrient Dynamics) received his B.Sc. from Zhejiang Agricultural University, his M.Sc. from the Chinese Academy of Sciences, and his Ph.D. from the University of British Columbia. He has held academic positions in New Zealand and the United States prior to taking up his current position at the University of Alberta. His main research interests are in forest soils, soil nutrient cycling, and plant nutrition. He served as Chair of the Soil Fertility and Plant Nutrition Commission of the International Union of Soil Science; President of the Association of Chinese Soil & Plant Scientists in North America; Chair for the Forest, Range, and Wildland Soils Division of the Soil Science Society of America; and Chair of the Alberta Soil Science Workshop. He has served as an Associate/Guest Editor or Editorial Board member for Biology and Fertility of Soils, Pedosphere, Soil Science Society of America Journal, Canadian Journal of Soil Science, Journal of Environmental Quality, Environmental Science and Pollution Research, Forests, and Forest Ecology and Management. He is a fellow of the Soil Science Society of America, the American Society of Agronomy, and the Canadian Society of Soil Science.

Yanjiang Cai (Professor of Soil Science) received his B.Sc. from the Hebei University, his M.Sc. from the Dalian Jiaotong University, and his Ph.D. from the Chinese Academy of Sciences. He was a visiting Professor at the University of Alberta in Canada and a JSPS postdoctoral researcher at the National Agriculture and Food Research Organization in Japan. He held an academic position in Chinese Academy of Sciences prior to taking up his current position at the Zhejiang A&F University. His main research interests are soil carbon and nitrogen transformations and fluxes in forest and grassland ecosystems, as well as management options towards greenhouse gas mitigation and climate change adaptation. He has served as an Editorial Board member for Biology and Fertility of Soils and a Guest Editor for Forests. He received the JSPS Fellowship for Overseas Researchers and the Excellent Young Scientist Award from the Association of Chinese Soil and Plant Scientists in North America.

forests

MDPI

Editorial

Disturbance Effects on Soil Carbon and Greenhouse Gas Emissions in Forest Ecosystems

Yanjiang Cai [1] and Scott X. Chang [1,2,*]

[1] State Key Laboratory of Subtropical Silviculture, Zhejiang A&F University, Hangzhou 311300, China; yjcai@zafu.edu.cn

[2] Department of Renewable Resources, University of Alberta, 442 Earth Sciences Building, Edmonton, AB T6G 2E3, Canada

* Correspondence: scott.chang@ualberta.ca; Tel.: +1-780-492-6375

Received: 28 February 2020; Accepted: 5 March 2020; Published: 7 March 2020

Abstract: Forests cover around 30% of the global land area and forest ecosystems can store over 70% of total soil organic carbon (SOC) of all terrestrial ecosystems, but SOC stocks and greenhouse gas (GHG) emissions may be affected by both natural and anthropogenic disturbances. Even though the changes in forest soil C pool can have a significant effect on climate change, there are some contradictory results regarding the role of forest disturbance on SOC sequestration, GHG emissions, and the mitigation of global changes. Therefore, there is a need to better understand the impact of different disturbance regimes on forest soil C storage and GHG emissions. A Special Issue was therefore organized for discussing the responses of soil C storage and GHG emissions to various types of disturbances in forest ecosystems and a total of 15 studies were accepted for this special issue to assess these responses. This Special Issue includes the effects of storms and beetle outbreaks, Karstification, rock desertification, warming, nitrogen addition, land-use change, field tillage, and biochar application on soil C dynamics and/or GHG emissions.

Keywords: CH_4 emissions; CO_2 emissions; climate change mitigation; global change; land-use change; N_2O emissions; soil carbon sequestration

Disturbances from natural (e.g., insect outbreaks, geologic processes and wildfires) and anthropogenic (e.g., logging, applying soil amendments and land use change) are important drivers of changes of ecological processes in forest ecosystems, and the impact of disturbances on ecosystem processes may vary with the type and level of disturbances [1–3]. These disturbances are expected to markedly affect the amount, form and stability of soil organic carbon (SOC) and the emission of three major trace greenhouse gases (GHGs) (CO_2, CH_4 and N_2O) from forest ecosystems [4,5]. More than 70% of total SOC of all terrestrial ecosystems can be found in forest ecosystems [6] and thus, a minor change in the size of the forest SOC pool can exert a large impact on climate change on a global scale. The assessment of the variability in forest SOC storage and GHG emissions is thus a critical consideration for evaluating regional and global climate change [7]. It is vitally important to improve the understanding of the impact of different disturbance regimes on forest SOC storage and GHG emissions for guiding future research, forest management practices, and policy development. We therefore organized a Special Issue to bring together researchers working on different aspects of forest ecology to share their findings on disturbance effects on SOC storage and GHG emissions in forest ecosystems. We are pleased that we received a strong response from the scientific community to this call for the Special Issue and a total of 15 papers have ultimately been accepted for inclusion in this Special Issue.

Three papers in this Special Issue address the effect of natural disturbances on SOC content and GHG emissions. Storms and beetle outbreaks are two major forms of disturbance in European forests,

but Kosunen et al. did not find any consistent effect of either storm or European spruce bark beetle (*Ips typographus* L.) outbreak on soil total and heterotrophic respiration, and soil total respiration rates were found to be related to the basal area of living trees, and also to soil temperature and soil moisture content [8]. Karstification, the dissolution of calcite and the formation of the karst landform in an area where the bedrock is dominated by limestone, can also affect soil C dynamics; in this respect, Huang et al. found that the C sink in karstified calcareous soils was 11.97 times that of non-karstified red soils, while the role of calcareous soils as a C source was only 1.12 times that in red soils [9]. The overall mean $\delta^{13}C$-CO_2 value in calcareous soils was 0.87‰ higher than that in red soils, and these results indicate that karst soils play a key role in the reduction of atmospheric CO_2 [9]. Rock desertification is a process of land degradation that may reduce soil productivity and some natural environmental factors can induce this process [10], but the effect of desertification on forest soil stoichiometry remains poorly understood. Yang et al. reported that soil C:N (nitrogen) ratio was not significantly affected by the degree of desertification, but soil C:P (C: phosphorus) and N:P ratios increased with increasing degree of desertification [11]. Yang et al. also pointed out that P might be the limiting factor for plant growth during restoration and calcium could play an important role in soil C, N and P stoichiometry in the ecosystem they studied [11].

Eleven papers in this Special Issue address the effect of anthropogenic disturbances on soil C and GHG emissions. Soil C and N cycling can be significantly affected by climate warming and N deposition that are caused by human activities [12,13]. An eight-year experiment with warming and N addition treatments in a subalpine spruce (*Picea asperata* Mast.) plantation forest showed that soil CO_2 emissions were solely influenced by warming while both N addition and its interaction with warming significantly elevated soil N_2O emissions, there were different response patterns and different factors governed soil CO_2 and N_2O emissions in the forest ecosystem [14]. Interestingly, Zhou et al. found that in a subtropical forest dominated by *Castanopsis carlesii* Hayata and *Schima superba* Gardn. et Champ, a high-level N addition treatment significantly reduced but a low-level N addition treatment markedly enhanced soil respiration, with the high-level N addition treatment reduced soil pH and increased C and P co-limitation of microorganisms, which resulted in decreases in total phospholipid fatty acid (PLFA) content and alterations in microbial community structures [15]. Zhou et al. also concluded that the altered microbial community structure and suppressed microbial biomass under increasing N deposition could ultimately lead to the accumulation of recalcitrant C and reduction in soil C emissions in the studied subtropical forest [15].

Changes in land use patterns can also alter soil C and N cycling and the structure of soil microbial communities [5,6]. The research in Qiu et al. indicated that *Proteobacteria*, *Verrucomicrobia* and *Acidobacteria* were the dominant bacteria and their relative abundances were different in the woodland, shrubland and grassland soils in a karst graben basin in subtropical China, and soil bacterial communities were markedly influenced by SOC, total N, and available potassium contents [16]. Studying SOC mineralization under different land uses is essential for improving our understanding of SOC responses to land-use change. The study of Yang et al. in the karst region showed that the establishment of plum (*Prunus salicina* Lindl.) plantations markedly reduced the SOC content as compared with abandoned lands, but the SOC content did not vary with plum plantation age; however, the cumulative and potential SOC mineralization rates were different among plum plantation ages, and both increased with increasing soil calcium concentration; thus, more attention should be paid in the future to the critical role of calcium in SOC mineralization in the studied subtropical area [17]. In contrast, the study conducted by Zhao et al. in a larch (*Larix principis-rupprechtii* Mayr) forest showed that the contents of SOC, total N and total K were all increased with increasing stand age, and clear-cutting reduced SOC, total N, and total K contents [18]. The effect of the conversion of natural evergreen broadleaved forests to an assisted natural regeneration and Chinese fir (*Cunninghamia lanceolata* (Lamb.) Hook) and mason pine (*Pinus massoniana* Lamb.) plantations was conducted by Yang et al. in subtropical China [19]. The conversion led to 42%, 60%, and 64% reductions in SOC contents for assisted natural regeneration, Chinese fir, and mason pine plantations, respectively, with

microbial residue C accumulation varying with SOC content and rate of litter input [19]. In addition, Zhu et al. investigated the responses of SOC and soil organic N to soil erosion and forest conversion in the development of sloping economic forests in mountain areas in Jiangsu province in China; they reported that the conversion of coniferous broadleaved mixed forests into economic forests aggravated soil erosion, and the intensive management of the economic forest also reduced soil C storage and increased the loss of soil nutrients; the loss of soil C and N caused by soil erosion can therefore be detrimental to the development of local agriculture and forestry [20].

Although tillage in forest ecosystems does not take place as often as in agricultural ecosystems, tree planting and tillage are practices commonly used for vegetation restoration [21]. In a forest soil profile inversion and mixing study, Wang et al. showed that CO_2 concentration in forest soil profiles was governed by both soil properties related to CO_2 production such as SOC and soil microbial biomass content and those related to gas diffusion, such as soil bulk density and gas molecular weight; however, soil surface CO_2 emissions were not affected by soil profile inversion but were increased by soil profile mixing; soil surface CO_2 emissions were mainly controlled by soil surface temperature [21].

Mangrove wetlands are a potential source for atmospheric CH_4, but there remain considerable uncertainties regarding the importance of mangrove wetlands for contributing climate warming [22]. Through a field study at three tidal zones of two mangrove ecosystems in southeastern China, Zheng et al. found highly variable CH_4 emission patterns among the three zones and attributed this phenomenon to the heterogeneity in the mangrove soil environment [23]. After analyzing the data from these three zones and those from 24 mangrove wetlands worldwide, the authors summarized that undisturbed mangrove sites had very low rates of CH_4 emissions, which were much lower than the global warming potentials generated by soil CO_2 emissions from the same sites. Although CH_4 emissions from mangrove soils were not significantly affected by plant species, study site, tidal position, sampling time, and soil characteristics, the nutrient inputs driven by anthropogenic activities could markedly elevate mangrove soil CH_4 emissions, and the estimates of regional or biglobal inventory of CH_4 emission should affirmatively consider the part from mangrove wetlands intensively affected by human activities [23].

Even though biochar has a great potential to mitigate climate change, much less research on biochar effects has been carried out in forest ecosystems in comparison to agricultural ecosystems [24]. Two papers in this Special Issue address the effect of biochar on altering forest soil C storage and mitigating GHG emissions. The study of Criscuoli et al. in northern Italy showed that conifer woodchip-derived biochar application did not significantly influence the temperature sensitivity of soil CO_2 and N_2O emissions, but significantly reduced the sensitivity of soil CH_4 uptake [25]. In the second biochar study included in this Special Issue, Deng et al. conducted an in situ experiment to examine the effects of shell-derived biochar and dicyandiamide (DCD) on soil N_2O emissions from a tea oil camellia (*Camellia oleifera* Abel) plantation with intensive N application in Jiangxi province, China [26]. The authors found that N application enhanced cumulative soil N_2O emissions by 307%, adding biochar and DCD to the N-fertilized field reduced cumulative soil N_2O emissions by 36 and 44%, respectively, suggesting that the mitigation potential of biochar on soil N_2O emissions may reach that of DCD under the conditions studied [26].

It should be noted that estimating forest C stock and improving the accuracy of GHG inventory for each country are very important for evaluating the impact of land management and land use change on regional and global climate change [5–7]. The work done by Lee et al. in South Korea showed that forests could continue to store C and absorb CO_2 even under the declining total forest area and their study provides methodologies to facilitate the estimation of C stock changes and CO_2 removal by different forest types or plant species [27].

We are pleased to make this Special Issue available to readers. As guest editors, we would like to thank the authors for their valuable contribution to this Special Issue and express our deep appreciation to the many reviewers for their insightful comments that improved the quality of an earlier version

of each of the published papers. We would also like to express our sincere gratitude to the Editorial Office for their valuable assistance throughout the publication process.

Author Contributions: Y.C. wrote the first draft. S.X.C. went through several rounds of review/editing and added content. All authors have read and agreed to the published version of the manuscript.

Funding: This work was supported by the National Natural Science Foundation of China (41877085, 41877088), the Research and Development Fund of Zhejiang A&F University (2018FR005, 2018FR006), the Open Research Fund Program of the State Key Laboratory of Subtropical Silviculture, Zhejiang A&F University (ZY20180301, ZY20180205).

Conflicts of Interest: The authors declare no conflict of interest.

References

1. Danneyrolles, V.; Dupuis, S.; Fortin, G.; Leroyer, M.; de Römer, A.; Terrail, R.; Vellend, M.; Boucher, Y.; Laflamme, J.; Bergeron, Y.; et al. Stronger influence of anthropogenic disturbance than climate change on century-scale compositional changes in northern forests. *Nat. Commun.* **2019**, *10*, 1265. [CrossRef]
2. Moreno-Mateos, D.; Barbier, E.B.; Jones, P.C.; Jones, H.P.; Aronson, J.; López-López, J.A.; McCrackin, M.L.; Meli, P.; Montoya, D.; Rey Benayas, J.M. Anthropogenic ecosystem disturbance and the recovery debt. *Nat. Commun.* **2017**, *8*, 14163. [CrossRef]
3. Thom, D.; Seidl, R. Natural disturbance impacts on ecosystem services and biodiversity in temperate and boreal forests. *Biol. Rev.* **2016**, *91*, 760–781. [CrossRef]
4. Bradford, J.B.; Birdsey, R.A.; Joyce, L.A.; Ryan, M.G. Tree age, disturbance history, and carbon stocks and fluxes in subalpine Rocky Mountain forests. *Glob. Change Biol.* **2008**, *14*, 2882–2897. [CrossRef]
5. Oertel, C.; Matschullat, J.; Zurba, K.; Zimmermann, F.; Erasmi, S. Greenhouse gas emissions from soils—A review. *Geochemistry* **2016**, *76*, 327–352. [CrossRef]
6. Jandl, R.; Lindner, M.; Vesterdal, L.; Bauwens, B.; Baritz, R.; Hagedorn, F.; Johnson, D.W.; Minkkinen, K.; Byrne, K.A. How strongly can forest management influence soil carbon sequestration? *Geoderma* **2007**, *137*, 253–268. [CrossRef]
7. IPCC. Climate Change 2014: Synthesis Report. In *Contribution of Working Groups I, II and III to the Fifth Assessment Report of the Intergovernmental Panel on Climate Change*; Core Writing Team, Pachauri, R.K., Meyer, L.A., Eds.; IPCC: Geneva, Switzerland, 2014; p. 151.
8. Kosunen, M.; Lyytikäinen-Saarenmaa, P.; Ojanen, P.; Blomqvist, M.; Starr, M. Response of soil surface respiration to storm and *Ips typographus* (L.) disturbance in boreal Norway spruce stands. *Forests* **2019**, *10*, 307. [CrossRef]
9. Huang, F.; Cao, J.; Zhu, T.; Fan, M.; Ren, M. CO_2 transfer characteristics of calcareous humid subtropical forest soils and associated contributions to carbon source and sink in Guilin, southwest China. *Forests* **2020**, *11*, 219. [CrossRef]
10. Yang, Q.Q.; Wang, K.L.; Zhang, C.; Yue, Y.M.; Tian, R.C.; Fan, F.D. Spatio-temporal evolution of rocky desertification and its driving forces in karst areas of Northwestern Guangxi, China. *Environ. Earth Sci.* **2011**, *64*, 383–393. [CrossRef]
11. Yang, H.; Zhang, P.; Zhu, T.; Li, Q.; Cao, J. The characteristics of soil C, N, and P stoichiometric ratios as affected by geological background in a karst graben area, southwest China. *Forests* **2019**, *10*, 601. [CrossRef]
12. Battye, W.; Aneja, V.P.; Schlesinger, W.H. Is nitrogen the next carbon? *Earth's Future* **2017**, *5*, 894–904. [CrossRef]
13. Reay, D.S.; Dentener, F.; Smith, P.; Grace, J.; Feely, R.A. Global nitrogen deposition and carbon sinks. *Nat. Geosci.* **2008**, *1*, 430–437. [CrossRef]
14. Li, D.; Liu, Q.; Yin, H.; Luo, Y.; Hui, D. Differential responses and controls of soil CO_2 and N_2O fluxes to experimental warming and nitrogen fertilization in a subalpine coniferous spruce (*Picea asperata* Mast.) plantation forest. *Forests* **2019**, *10*, 808. [CrossRef]
15. Zhou, J.; Liu, X.; Xie, J.; Lyu, M.; Zheng, Y.; You, Z.; Fan, Y.; Lin, C.; Chen, G.; Chen, Y.; et al. Nitrogen addition affects soil respiration primarily through changes in microbial community structure and biomass in a subtropical natural forest. *Forests* **2019**, *10*, 435. [CrossRef]
16. Qiu, J.; Cao, J.; Lan, G.; Liang, Y.; Wang, H.; Li, Q. The influence of land use patterns on soil bacterial community structure in the karst graben basin of Yunnan province, China. *Forests* **2019**, *11*, 51. [CrossRef]

17. Yang, H.; Mo, B.; Zhou, M.; Zhu, T.; Cao, J. Effects of plum plantation ages on soil organic carbon mineralization in the karst rocky desertification ecosystem of southwest China. *Forests* **2019**, *10*, 1107. [CrossRef]
18. Zhao, K.; Fahey, T.J.; Liang, D.; Jia, Z.; Ma, L. Effects of long-term successive rotations, clear-cutting and stand age of prince rupprecht's larch (*Larix principis-rupprechtii* Mayr) on soil quality. *Forests* **2019**, *10*, 932. [CrossRef]
19. Yang, L.; Chen, S.; Li, Y.; Wang, Q.; Zhong, X.; Yang, Z.; Lin, C.; Yang, Y. Conversion of natural evergreen broadleaved forests decreases soil organic carbon but increases the relative contribution of microbial residue in subtropical China. *Forests* **2019**, *10*, 468. [CrossRef]
20. Zhu, X.; Lin, J.; Dai, Q.; Xu, Y.; Li, H. Evaluation of forest conversion effects on soil erosion, soil organic carbon and total nitrogen based on ^{137}Cs tracer technique. *Forests* **2019**, *10*, 433. [CrossRef]
21. Wang, X.; Fu, S.; Li, J.; Zou, X.; Zhang, W.; Xia, H.; Lin, Y.; Tian, Q.; Zhou, L. Forest soil profile inversion and mixing change the vertical stratification of soil CO_2 concentration without altering soil surface CO_2 Flux. *Forests* **2019**, *10*, 192. [CrossRef]
22. Chen, G.; Chen, B.; Yu, D.; Tam, N.F.Y.; Ye, Y.; Chen, S. Soil greenhouse gas emissions reduce the contribution of mangrove plants to the atmospheric cooling effect. *Environ. Res. Lett.* **2016**, *11*, 124019. [CrossRef]
23. Zheng, X.; Guo, J.; Song, W.; Feng, J.; Lin, G. Methane emission from mangrove wetland soils is marginal but can be stimulated significantly by anthropogenic activities. *Forests* **2018**, *9*, 738. [CrossRef]
24. Li, Y.; Hu, S.; Chen, J.; Mueller, K.; Li, Y.; Fu, W.; Lin, Z.; Wang, H. Effects of biochar application in forest ecosystems on soil properties and greenhouse gas emissions: A review. *J. Soils Sediments* **2018**, *18*, 546–563. [CrossRef]
25. Criscuoli, I.; Ventura, M.; Sperotto, A.; Panzacchi, P.; Tonon, G. Effect of woodchips biochar on sensitivity to temperature of soil greenhouse gases emissions. *Forests* **2019**, *10*, 594. [CrossRef]
26. Deng, B.; Fang, H.; Jiang, N.; Feng, W.; Luo, L.; Wang, J.; Wang, H.; Hu, D.; Guo, X.; Zhang, L. Biochar is comparable to dicyandiamide in the mitigation of nitrous oxide emissions from *Camellia oleifera* Abel. fields. *Forests* **2019**, *10*, 1076. [CrossRef]
27. Lee, S.J.; Yim, J.S.; Son, Y.M.; Son, Y.; Kim, R. Estimation of forest carbon stocks for national greenhouse gas inventory reporting in South Korea. *Forests* **2018**, *9*, 625. [CrossRef]

forests

MDPI

Article

Response of Soil Surface Respiration to Storm and *Ips typographus* (L.) Disturbance in Boreal Norway Spruce Stands

Maiju Kosunen *, Päivi Lyytikäinen-Saarenmaa, Paavo Ojanen, Minna Blomqvist and Mike Starr

Department of Forest Sciences, University of Helsinki, P.O. Box 27, FI-00014, 00100 Helsinki, Finland; paivi.lyytikainen-saarenmaa@helsinki.fi (P.L.-S.); paavo.ojanen@helsinki.fi (P.O.); minna.blomqvist@helsinki.fi (M.B.); mike.starr@helsinki.fi (M.S.)

* Correspondence: maiju.kosunen@helsinki.fi

Received: 28 February 2019; Accepted: 24 March 2019; Published: 3 April 2019

Abstract: Disturbances such as storm events and bark beetle outbreaks can have a major influence on forest soil carbon (C) cycling. Both autotrophic and heterotrophic soil respiration may be affected by the increase in tree mortality. We studied the effect of a storm in 2010 followed by an outbreak of the European spruce bark beetle (*Ips typographus* L.) on the soil surface respiration (respiration by soil and ground vegetation) at two Norway spruce (*Picea abies* L.) dominated sites in southeastern Finland. Soil surface respiration, soil temperature, and soil moisture were measured in three types of plots—living trees (undisturbed), storm-felled trees, and standing dead trees killed by *I. typographus*—during the summer–autumn period for three years (2015–2017). Measurements at storm-felled tree plots were separated into dead tree detritus-covered (under storm-felled trees) and open-vegetated (on open areas) microsites. The soil surface total respiration for 2017 was separated into its autotrophic and heterotrophic components using trenching. The soil surface total respiration rates at the disturbed plots were 64%–82% of those at the living tree plots at one site and were due to a decrease in autotrophic respiration, but there was no clear difference in soil surface total respiration between the plots at the other site, due to shifts in either autotrophic or heterotrophic respiration. The soil surface respiration rates were related to plot basal area (living and all trees), as well as to soil temperature and soil moisture. As storm and bark beetle disturbances are predicted to become more common in the future, their effects on forest ecosystem C cycling and CO_2 fluxes will therefore become increasingly important.

Keywords: forest soils; autotrophic respiration; heterotrophic respiration; CO_2 effluxes; decomposition; forest disturbance; tree mortality; storm damage; insect outbreak

1. Introduction

Abiotic disturbances, such as storms, and biotic disturbances, such as bark beetle outbreaks, are important drivers of forest ecosystem functioning [1,2]. Such disturbances increase tree mortality, resulting in—at least temporarily—diminished forest C fixation (CO_2 influx) and autotrophic respiration (CO_2 efflux from plant and rhizosphere metabolism) and, in some cases, increased heterotrophic respiration (CO_2 efflux from organic matter decomposition) due to increased decomposition [2–6]. Over extended periods of time, the effect of natural disturbances on the carbon (C) balance can thus result in a forest turning from being a C sink into a C source and so add to global warming [4,7]. However, the effects on C balance may be less drastic and transient if the productivity of the remaining trees and secondary structure is increased or if decreased forest stand productivity is accompanied with a reduction in ecosystem respiration [8,9]. Besides disturbance severity, changes in forest ecosystem C fluxes are dependent on several other factors, e.g., pre-disturbance forest composition

and structure, growth of the remaining trees and ground vegetation, and tree regeneration [5,8,10–12]. Hence, the responses and recovery of a forest after disturbance may differ among forest management strategies as well as between non-managed and commercially managed forests [3,8,13–15].

Soil respiration is one of the largest terrestrial C fluxes globally [16]. It has been estimated that 55% of the C fixed annually by forests in gross primary production is returned back to the atmosphere as a result of soil respiration [17]. Disturbance may alter soil respiration in several ways. Tree death reduces soil autotrophic respiration due to the cessation of C allocation to roots and soil [18,19]. Disturbance-induced tree mortality also results in changes in litter quality and quantity [20,21], light and water availability and soil temperature and moisture [2,6,12,22,23], soil microbial community dynamics [24–26], and the composition of the ground vegetation [13,27], all of which can be expected to lead to changes in the decomposition process and, hence, soil heterotrophic respiration.

Besides spatial variation in the alterations, the direction and magnitude of these alterations may change with time after the disturbance [5]. As a result, both increases [23,28] and decreases [9,29] as well as no change [6,22,23,30,31] in soil total respiration over periods varying from months to several years after disturbance have been reported. However, few studies have studied the effects of natural disturbance separately on the autotrophic and heterotrophic components of soil respiration. Mayer et al. [6,23] found that storm disturbance increased heterotrophic respiration for some years after the storm and attributed this to increases in soil temperature and associated accelerated decomposition of soil organic matter, whereas in another study [29], storm and bark beetle disturbance was shown to have decreased autotrophic soil respiration but to have had no clear effect on heterotrophic respiration.

Storms and European spruce bark beetle (*Ips typographus* L.) outbreaks are two major forms of disturbance in European forests [32,33], and both are predicted to result in greater tree damage in the future [34,35]. Whilst storms immediately alter the structure and functioning of the forest by breaking and uprooting (killing) trees and mixing soil [1], the changes brought about by bark beetle outbreaks are gradual [2]. Wind disturbance especially creates various microsites [1,36] where tree stand and soil properties differ. For example, undisturbed soil with decomposing residue piles [37] or gaps [38,39] created after disturbance can have different soil properties and dynamics compared to the less affected areas or pre-disturbance conditions. Storm events can predispose forests to insect outbreaks, as wind-fallen trees provide optimal breeding material for bark beetles [40,41]. Where there is more than one disturbance event, changes in the C balance and soil respiration can be expected to be more complicated.

In this study, the effects of a storm event followed by an outbreak of *I. typographus* on soil surface total (SR_{tot}, soil CO_2 efflux from soil and ground vegetation), autotrophic (SR_a), and heterotrophic (SR_h) respiration were investigated at two forest sites in southeastern Finland. The aims of the study were to determine the effect of storm damage and *I. typographus* outbreak on (1) SR_{tot} and its autotrophic and heterotrophic components and (2) the degree to which disturbance-related differences in respiration were due to differences in tree stand characteristics and tree mortality or in environmental conditions. We hypothesized that (1) SR_a from storm-damaged and from *I. typographus*-infested plots would be lower and SR_h higher compared to control (undisturbed) plots; (2) storm-damaged SR_a and SR_h would differ between open microsites having ground vegetation and microsites under storm-felled trees covered with dead tree detritus; and (3) respiration would be related to stand basal area (dead tree basal area resulting from the storm and *I. typographus* disturbances), disturbance-related differences in soil microclimate (temperature and moisture), or both.

2. Materials and Methods

2.1. Research Area

The study was carried out in two Norway spruce (*Picea abies* L.) dominated forest sites, Paajasensalo (56 ha) and Viitalampi (73 ha), located in the municipality of Ruokolahti (61°17′30″ N, 28°49′10″ E) in southeastern Finland. The distance between the two sites is about 6 km. A large-scale storm occurred

in the region in July 2010 and was followed by an outbreak of *I. typographus* from 2011 onwards. The forests at the Paajasensalo site were in commercial use until 2010 and those in the Viitalampi site until 2011, but afterwards they were conserved as METSO (Forest Biodiversity Program for Southern Finland) sites and no forest management actions have been carried out since. Thus, contrary to normal forestry practice, all the trees killed by the storm and bark beetle were left in the forest after the disturbance events, making the sites ideal for the purposes of this research.

The soils at the study sites were Podzols, mostly cambic, and developed in till deposits. The soil texture (fine-earth fraction) was either sandy loam or loamy sand, and the thickness of the surface humus layer varied between 2.3 and 8.0 cm. According to the Cajanderian site type classification [42], which describes site stand productivity, the sites were mainly medium-rich Myrtillus (MT) and rich Oxalis-Myrtillus (OMT) types. The ground vegetation under closed canopy was dominated by blueberry (*Vaccinium myrtillus* L.), with lingonberry (*Vaccinium vitis-idaea* L.) and several herbaceous species (e.g., small cow-wheat (*Melampyrum sylvaticum* L.), twinflower (*Linnea borealis* L.), wood sorrel (*Oxalis acetosella* L.), and oak fern (*Gymnocarpium dryopteris* L. Newman)) being present. The forest floor moss layer was dominated by red-stemmed feather-moss (*Pleurozium schreberi* (Brid.) Mitt.), stairstep moss (*Hylocomium splendens* (Hedw.) BSG), and fork-moss (*Dicranum* sp.). The storm and, to a lesser degree, the bark beetle outbreaks modified the ground vegetation composition towards more light-demanding pioneer species such as fireweed (*Chamerion angustifolium* L.), wavy hair-grass (*Deschampsia flexuosa* L. Trin), and raspberry (*Rubus ideaus* L.). Although dominated by spruce, isolated Scots pine (*Pinus sylvesteris* L.), silver birch (*Betula pendula* Roth), downy birch (*Betula pubescens* L.), European aspen (*Populus tremula* L.), grey alder (*Alnus incana* L.), common alder (*Alnus glutinosa* L. Gaertn), rowen (*Sorbus aucuparia* L.), and willow (*Salix* spp.) trees also grew within the stands. The long-term (1981–2010) mean annual air temperature for the study sites was 4.2 °C and the mean annual precipitation was 653 mm [43]. The mean air temperature and precipitation for the study months (May–Oct) were 12.3 °C and 38 mm in 2015, 13.0 °C and 52 mm in 2016, and 11.3 °C and 61 mm in 2017 [44].

2.2. Study Layout

After exploring both study sites, three types of disturbance areas were identified: those having living trees with no clear signs of storm or bark beetle damage (LT), areas with fallen trees resulting from the storm (SF), and areas of living and dead standing trees showing bark beetle attack (ID). A circular plot (radius 11.28 m, area 400 m^2) was then established in each of three areas in both study sites in June 2015 (Figure 1), resulting in a total of 12 plots (6 in Paajasensalo and 6 in Viitalampi). In order to have a more encompassing data set, another set (block) of plots were established in both study sites in June 2016 (Figure 1). Photographs of each plot type (LT, SF, and ID) are presented in Figure S1. As the three plots (disturbance treatments) were spatially interspersed within the two blocks and the blocks were replicated at two study sites, bias and problems of pseudoreplication were reduced [45].

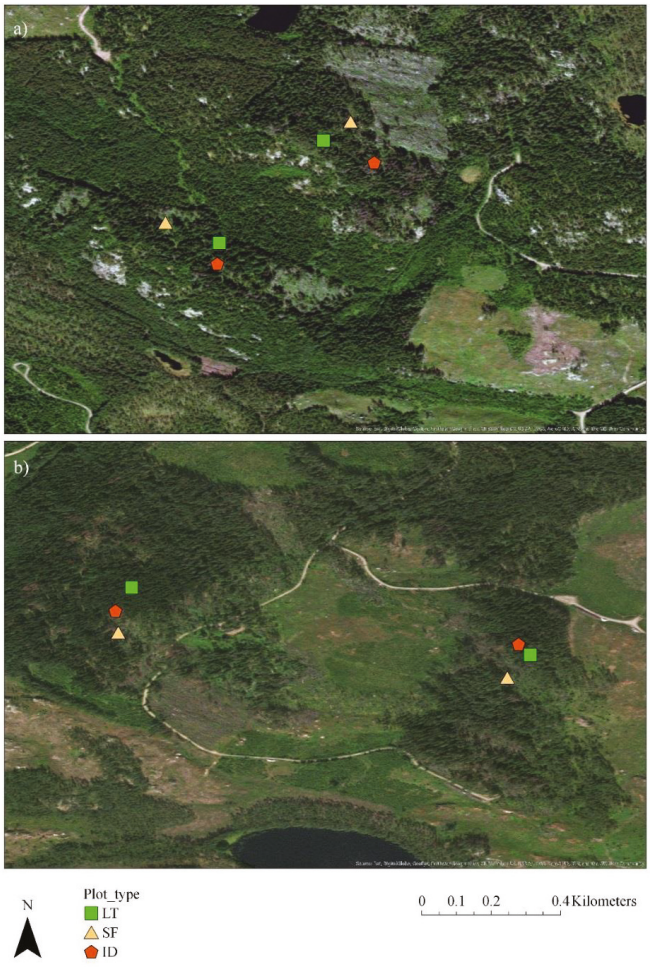

Figure 1. Locations of study plots in Paajasensalo (**a**) where plots established in 2015 are on the left and plots established in 2016 are on the right, and Viitalampi (**b**) where plots established in 2015 are on the right and plots established in 2016 are on the left. LT = living tree plot (green squares), SF = storm-felled tree plot (light brown triangles), and ID = tree killed by *I. typographus* plot (red pentagons). Created using ArcGIS (ESRI, Redlands, CA, USA).

2.3. Tree Measurements

All trees growing on the plots were numbered and the diameter at breast height (dbh) of each living and dead tree, both standing and fallen, with a dbh of >6 cm was measured. All spruce trees were inspected for symptoms of *I. typographus* colonization (discoloration, defoliation, entrance and exit holes, resin flow spots, and bark loss) [46] to confirm the initial cause of each spruce tree's death as *I. typographus* and to monitor the population level of the living trees during the study. Although some spruce trees on the LT plots showed incipient symptoms caused by *I. typographus*, they remained living and vigorous during the study period. We are not able to identify the specific time of death of the *I. typographus*-killed trees in our plots, but it took place during 2013–2014 [47]. In addition to the storm in July 2010, the warm summers of 2010, 2011, and 2013 [48] likely contributed to the development of the *I. typographus* outbreak. The two disturbance types also interacted on some of the

plots. For example, 50% of the standing dead trees on the Viitalampi ID plot established in 2015 broke and fell due to another storm in October 2015. On the other plots, however, only single standing dead trees and none of the living trees fell during the study period. In addition, many of the wind-thrown trees on the SF plots had maternal galleries of *I. typographus*. However, the initial cause of tree death on SF plots was the storm in 2010 and the beetle outbreak on the ID plots that occurred from 2011 onwards. Some dead trees were also found at the LT plots, but they had already died before the 2010 storm and start of the beetle outbreak.

2.4. Soil Surface Respiration, Temperature, and Moisture Measurements

Soil surface respiration, soil temperature, and soil moisture were measured at a number of locations in each plot. For the LT and ID plots, the location of the sampling point was based on a random selection of the numbered trees. A stone-free sampling area ≥2 m from the randomly selected tree stem (or other measurement point) was selected. In the case of the SF plots, all fallen tree(s)–detritus-covered microsites (SF_d) and ground vegetated–open (i.e., no fallen trees above) microsites (SF_o) were identified and numbered, and then a set of each microsite type was chosen using a random number sequence generator. These two types of microsite reflected a clear dichotomy in conditions created by the storm. If a respiration measurement point was considered unsuitable (stony or <1.5 m to another measurement point or tree), it was rejected and the next measurement point in the random sequence was chosen. Accordingly, 30 soil respiration measurement points were established in each study site in summer 2015: eight in the LT plots, seven each in the SF_d and SF_o microsites, and eight in ID plots at each forest (Figure S2). A PVC collar (diameter = 20.1 cm, height ~ 15 cm) for respiration measurements was installed at each selected measurement point by pressing the collar into the ground to a depth of ca. 1 cm and sealed from the outside with sand (Figure 2, Figure S2). At this stage, vegetation was not removed from inside the collars so that SR_{tot} measurements included respiration by soil and ground vegetation. In 2016, collars were installed in the new plots using the same procedure as in 2015: three collars in the LT plots, three in each of the two microsites in the SF plots, and three in ID plots at both study sites.

Figure 2. Soil surface respiration chamber darkened with aluminum foil and containing the CARBOCAP® GMP343 CO_2 probe and a data logger on the ground in front. The measurement point is one of the trenched measurement points. Photo: Maiju Kosunen.

In order to quantify the proportions of SR_a and SR_h, 15 of the measurement points in the plots established in 2015 (4 in LT, 3 or 4 in SF_d and 3 or 4 in SF_o, and 4 in ID selected at random in both study sites) were trenched in July–August 2016. A knife and a spade were used to cut the roots in an area of ca 0.25 m^2 surrounding the selected collars to a depth of ca. 30 cm, the maximum depth of most *P. abies* roots in Finnish conditions [49]. A 30 cm wide strip of strong fabric was then inserted into the cut to inhibit further root ingrowth. After trenching, the ground vegetation was carefully removed from inside the collars. Mosses were, however, left growing in the collars to avoid direct radiation from topsoil, but were not considered to have significantly affected the respiration measurements. Any regrowth of vegetation was removed inside the trenched collars before each measurement.

Trenching may bias soil autotrophic and heterotrophic respiration estimates, for example, because of changes in the soil microclimate brought about by root decease [50]. In our study, trenching, however, had no clear effect on soil moisture and increased the soil temperature only slightly at some plots. Nevertheless, for example, re-sprouting of the clipped vegetation at trenched points in between measurements as well as inclusion of ground vegetation respiration to measurements at intact collars may have also caused inaccuracy to estimations. Thus, the SR_a and SR_h values should only be considered as estimates of the proportions.

The respiration measurements were carried out approximately weekly during 18 Jun–6 Oct 2015 and 24 May–27 Sept 2016 and approximately biweekly during 16 May–19 Oct 2017 (intervals varying from 4 to 18 days) using a closed and darkened chamber (D = 19.0 cm, height = 24.7 cm) made of Perspex fitted with a CARBOCAP®GMP343 CO_2 probe (Vaisala Ltd., Vantaa, Finland) and an air mixing fan (Figure 2). After carefully placing the chamber on top of the collar, the increase in the CO_2 concentration inside the chamber was recorded every 5 seconds over a 5 minute period. The lower edge of the chamber was fitted with a rubber O-ring washer so as to prevent any airflow between the collar and chamber. The air in the chamber was mixed during each measurement by means of a small fan fitted inside the chamber. Between each measurement, the chamber was ventilated by exposing the chamber to the air. Immediately following the respiration measurements, soil temperature and moisture were measured at three spots around each collar (ca. 0.2 m distance from the collar). Soil temperature (°C) was measured at a depth of 10.5 cm using a S3 11B thermometer (Fluke corp., Everett, WA, USA) probe and the soil moisture (% vol) was measured at a depth of 6.0 cm with a ML3 ThetaKit soil moisture meter (Delta-T devices Ltd., Cambridge, UK).

2.5. Calculation of Soil Surface Total, Heterotrophic, and Autotrophic Respiration

Respiration (mg CO_2 m^{-2} s^{-1}) was calculated as the slope of the linear regression between CO_2 concentration in the chamber and time. Respiration measurements from the intact (non-trenched) collars (n = 30 in both Paajasensalo and Viitalampi until Aug 2016, after which n = 27) in both study sites over the whole study period in 2015–2017 were taken to be SR_{tot}. Respiration measured from the trenched collars (n = 15 in both Paajasensalo and 15 in Viitalampi) was considered to be SR_h, and the difference between SR_{tot} and SR_h was therefore assumed to be SR_a.

However, as we observed a difference in the mean SR_{tot} values between the intact collars and the collars to be trenched already before the trenching for some plots, we used linear regression to estimate the SR_{tot} values for the trenched collars in order to correct for this baseline difference. Thus, for each plot established in 2015, a linear regression model was computed using pre-trench data (up to June 2016) to predict the SR_{tot} of the collars to be trenched from that of the collars that would remain intact. These regression models were then used to derive post-trenching SR_{tot} values for the trenched collars as if they had not been trenched. All regression models had high R^2 values (0.73–0.96). The difference between the predicted mean SR_{tot} values and the measured mean values from the trenched collars (SR_h) was then taken to be SR_a. Values of SR_a were thus weekly treatment means, including one value that was negative. The SR_h values were individual collar measurements; however, weekly treatment means of SR_h for each plot were used to compare with SR_a values.

The disturbance caused by root cutting and fast decay could be expected to keep the levels of respiration high for some time after trenching. In our treatments, respiration of the trenched collars in comparison to the intact collars decreased mostly 1–3 weeks (but ca. 2 months at the latest) after the root cutting; therefore, only the respiration measurements starting from 2017 were used to estimate the proportions of SR_a and SR_h.

2.6. Statistical Analyses

For comparing SR_{tot} and SR_h (measured and temperature-adjusted), temperature, and moisture between treatments, analyses of variance (ANOVA) with a linear mixed-effects model structure followed by Scheffe's post hoc tests were used. Treatment (LT, SF_o, SF_d, and ID) was set as a fixed variable, and measurement date (running number of days cumulated over the study period) and collar number were set as random crossed variables. If the produced linear mixed model did not fulfil the assumptions of normality and homogeneity of residuals, appropriate transformations were applied. Because there was only one value for SR_a at each treatment for each measurement day in 2017, it was not appropriate to test for differences in SR_a between treatments.

To control for the effect of treatment differences in soil temperature on respiration, each measured SR_{tot} and SR_h value was adjusted to a soil temperature value of 10 °C. This was done by fitting a nonlinear regression [51] between soil temperature and respiration for each collar separately. The adjusted flux at a soil temperature at 10 °C was then calculated by adding the estimated value of respiration at 10 °C of each collar to the residual of each measurement.

Spearman's rank correlation coefficients were computed to describe the relationship between the plot (n = 16) mean SR_{tot} (measured and temperature-adjusted), soil temperature and soil moisture, and plot basal area (living, dead, and total), i.e., across treatments. Basal area values of the entire SF plots were used for both SF_d and SF_o microsites. Spearman's rank correlation coefficients were also computed to describe the relationship between plot (n = 8) mean SR_a and SR_h and plot basal area, i.e., across treatments.

All the analyses were done using the R statistical computing environment [52] with utilization of *lme4* [53] for the mixed modeling, *car* [54] for ANOVA, and *emmeans* [55] for the post hoc tests.

3. Results

3.1. Tree Mortality

The characteristics of the stands on each plot are shown in Table 1. Spruce was the dominant species, although several plots also had a considerable proportion of pine (*Pinus sylvestris* L.) and broadleaved trees (mostly silver birch, *Betula Pendula* Roth) present. An exception was the Viitalampi LT plot established in 2016, where only 45% of the trees were spruce; however, 59% of the living trees on that plot were spruce. The Viitalampi ID plot established in 2016 had the highest stem density, and the Viitalampi SF plot established in 2015 had the lowest, with all being dead. Of the disturbed plots (SF and ID), the greatest proportion of dead trees was in the Viitalampi SF plot established in 2015 (100%) and the lowest was in the Viitalampi ID plot established in 2015 (69%). The proportion of dead trees on the LT plots varied between 8% and 27%.

Table 1. Study plot disturbance and stand characteristics (mean ± standard deviation). Abbreviations: Year = year of plot establishment, dbh = tree diameter at breast height, Stems/ha = number of trees per hectare, Basal area = basal area of trees, Species (%) = percentage of basal area of certain tree species from all measured trees on plot, Sp = spruce, Pi = pine, De = deciduous, PS = Paajasensalo, VL = Viitalampi, LT = living trees, ID = trees killed by *I. typographus*, SF = storm-felled trees, MT = medium-rich Myrtillus type, OMT = Oxalis-Myrtillus type.

						Basal Area (m^2/ha)			Species (%)		
Site	**Year**	**Plot Type**	**Site Type**	**dbh (cm)**	**Stems/ha**	**Living**	**Dead**	**Total**	**Sp**	**Pi**	**De**
PS	2015	LT	MT	21 ± 8	1350	42.2 ± 0.6	9.3 ± 1.4	51.5 ± 0.8	65	22	13
PS	2015	SF	MT	22 ± 7	925	13.6 ± 0.7	24.6 ± 0.6	38.2 ± 0.7	81	14	5
PS	2015	ID	OMT	25 ± 8	625	5.5 ± 1.2	27.4 ± 0.7	33.0 ± 0.8	96	0	4
PS	2016	LT	MT	20 ± 10	925	34.3 ± 0.8	0.9 ± 0.2	35.2 ± 0.8	89	0	11
PS	2016	SF	MT	17 ± 7	1725	10.6 ± 0.3	36.8 ± 0.7	47.4 ± 0.6	88	0	12
PS	2016	ID	MT	15 ± 7	1525	2.3 ± 0.3	29.3 ± 0.5	31.7 ± 0.5	100	0	0
VL	2015	LT	MT	21 ± 7	975	35.9 ± 0.4	0.4 ± 0.0	36.3 ± 0.5	97	0	3
VL	2015	SF	MT	25 ± 3	600	0 ± 0.0	28.6 ± 0.3	28.6 ± 0.3	100	0	0
VL	2015	ID	MT	24 ± 4	650	9.8 ± 0.4	20.1 ± 0.3	30.0 ± 0.3	100	0	0
VL	2016	LT	MT	20 ± 10	1275	39.8 ± 0.8	9.5 ± 1.0	49.2 ± 0.9	45	4	51
VL	2016	SF	MT	19 ± 9	800	0.7 ± 0.1	26 ± 0.8	26.7 ± 0.8	63	0	38
VL	2016	ID	OMT	19 ± 9	1800	22.8 ± 0.7	39.7 ± 0.7	62.5 ± 0.7	96	0	4

3.2. Soil Surface Total Respiration, Soil Temperature, and Soil Moisture

At Paajasensalo, the mean SR_{tot} of the three disturbed treatments was lower than that of the LT treatment, although only significantly so in the case of the SF_o treatment (Table 2). At Viitalampi, the disturbed treatment mean SR_{tot} was also lower than that of the LT treatment, but none of the differences were significant. After adjusting SR_{tot} for soil temperature, the differences in mean values between treatments were reduced, but LT and SF_o still significantly differed from each other at Paajasensalo (Table 2). Adjusting the respiration values for soil temperature did not change the pattern in SR_{tot} among the treatments at Viitalampi.

Table 2. Treatment mean total soil surface respiration (SR_{tot}) and soil-temperature-adjusted soil surface total respiration values ($SR_{tot\_ST\ adj.}$), soil temperature (ST) and soil moisture (SM; non-trenched collars 2015–2017 data only), and heterotrophic soil respiration (SR_h) and soil-temperature-adjusted heterotrophic soil respiration (SR_{tot_STadj}; 2017 data from trenched collars only) for the Paajasensalo and Viitalampi study sites. Values are linear mixed-effects model adjusted means. Treatment means followed by the same subscript letter are not significantly different (p = 0.05; Scheffe's post hoc tests). LT = living trees, SF_d = storm damaged, tree detritus, SF_o = storm damaged, open-vegetated, ID = trees killed by *I. typographus*.

	LT		**SF_d**		**SF_o**		**ID**	
Paajasensalo								
SR_{tot} (mg CO_2 m^{-2} s^{-1})	0.28	a	0.23	ab	0.18	b	0.22	ab
$SR_{tot\_STadj.}$ (mg CO_2 m^{-2} s^{-1})	0.24	a	0.22	ab	0.17	b	0.20	ab
ST (°C)	10.7	a	10.2	b	10.2	b	10.5	ab
SM (% vol/vol)	13.3	a	18.3	b	22.8	bc	26.0	c
SR_h (mg CO_2 m^{-2} s^{-1})	0.14	a	0.13	ab	0.10	b	0.12	ab
$SRh_{\_STadj.}$ (mg CO_2 m^{-2} s^{-1})	0.15	a	0.15	a	0.12	a	0.13	a
Viitalampi								
SR_{tot} (mg CO_2 m^{-2} s^{-1})	0.22	a	0.18	a	0.21	a	0.20	a
$SR_{tot\_STadj.}$ (mg CO_2 m^{-2} s^{-1})	0.20	a	0.17	a	0.19	a	0.17	a
ST (°C)	10.5	a	10.3	a	10.6	a	11.0	b
SM (% vol/vol)	20.1	a	26.1	a	26.3	a	26.3	a
SR_h (mg CO_2 m^{-2} s^{-1})	0.11	a	0.14	a	0.12	a	0.11	a
$SRh_{\_STadj.}$ (mg CO_2 m^{-2} s^{-1})	0.12	a	0.15	a	0.12	a	0.11	a

Mean soil temperatures were slightly lower, but significantly so only at SF_d and SF_o for the disturbed treatments compared to the LT treatment at Paajasensalo (Table 2). At Viitalampi, mean soil temperatures were significantly highest in the case of the ID treatment. The mean soil moisture content at Paajasensalo was significantly higher for the three disturbed treatments compared to the LT treatment. At Viitalampi, the disturbed treatment mean soil moisture was also higher than the LT treatment mean value, but not significantly so (Table 2). The mean SR_{tot}, temperature, and moisture of plots established in 2015 and 2016 as well as those of the to-be-trenched and intact collars are presented in Table S1.

The seasonal patterns in SR_{tot}, soil temperature, and soil moisture contents for the three study years are shown in Figure 3. At Paajansensalo, the LT treatment had higher SR_{tot} values compared to the disturbed treatments during the mid-summer to autumn months, whereas the differences between treatments were not that visible in the early summer periods (Figure 3a). At Viitalampi, no clear differences in the seasonal pattern of SR_{tot} among the treatments were observed (Figure 3b). However, at both Paajasensalo and Viitalampi, SR_{tot} followed the seasonal pattern in soil temperature (Figure 3c,d). The seasonal pattern in soil moisture in each year was similar at both Paajasensalo and Viitalampi. At Paajasensalo, soil moisture was consistently the highest in the ID treatment and lowest in the LT treatment throughout each year (Figure 3e). While the treatment differences in soil moisture at Viitalampi during 2015 were similar to those at Paajasensalo, the differences evened out during 2016 and 2017 (Figure 3f).

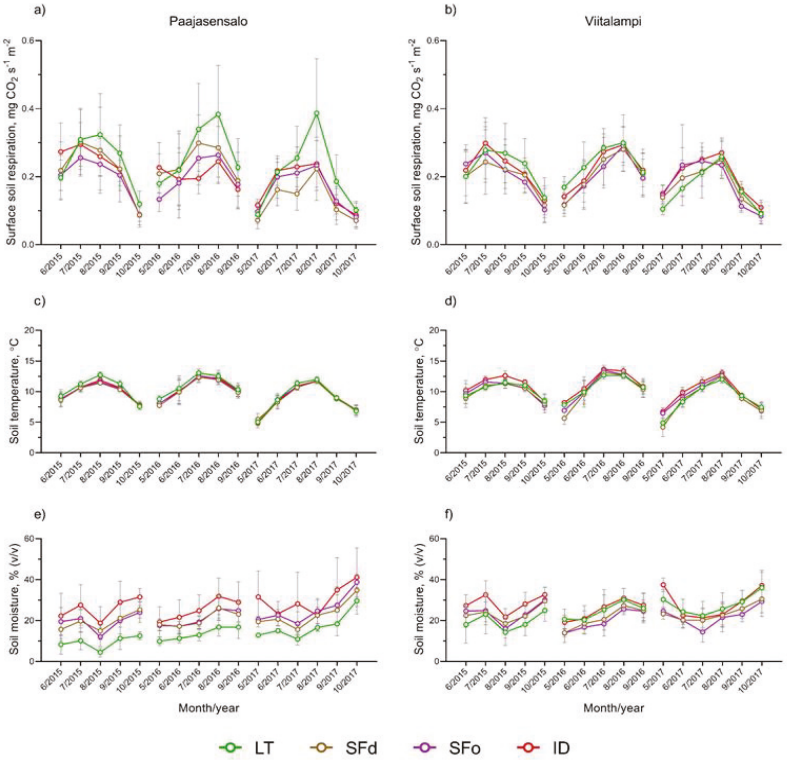

Figure 3. Monthly means and standard deviations for soil surface total respiration (**a,b**), soil temperature (**c,d**), and soil moisture (**e,f**) of each treatment in Paajasensalo (left) and Viitalampi (right). Values are based on measurements from the intact collars on plots established in 2015, i.e., the data set is consistent throughout 2015–2017. LT = living trees, SF_d = storm dead tree detritus, SF_o = storm open-vegetated, and ID = trees killed by *I. typographus*.

3.3. Heterotrophic and Autotrophic Soil Respiration

At Paajasensalo, the mean SR_a values from the disturbed plots were 23% (SF_d), 39% (SF_o), and 57% (ID) of the mean value from LT. At Viitalampi, the mean SR_a value from the SF_d treatment was 45% of the mean value in LT, whereas the mean values from the SF_o microsite and ID plot were 195% and 124%, respectively, of the mean value of LT. The mean SR_h at Paajansensalo was lowest in SF_o (70% of the mean in LT) (Figure 4) and differed significantly from LT. The respective soil-temperature-adjusted mean respiration values, however, did not differ significantly from each other (Table 2). At Viitalampi, the highest mean SR_h was found in SF_d (124% of mean in LT), but the mean did not differ significantly from those of other treatments (Table 2).

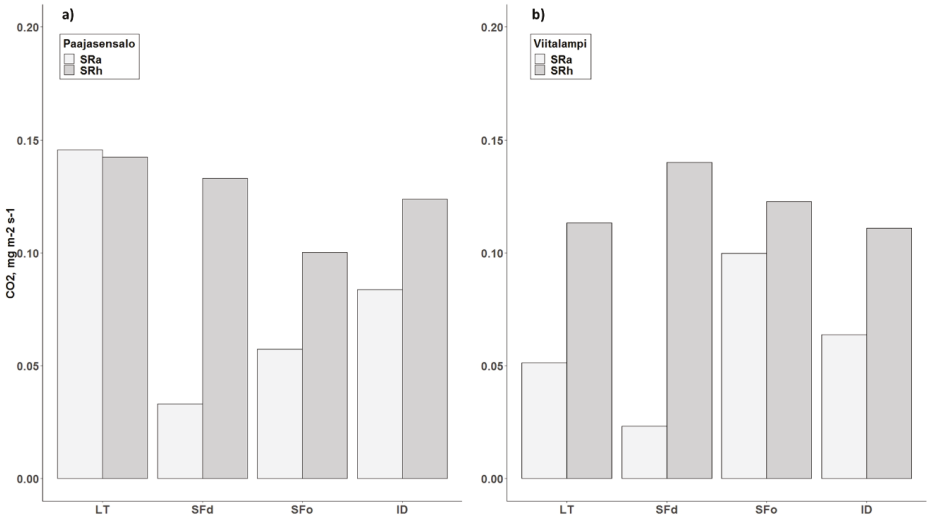

Figure 4. Means of autotrophic (SR_a) and heterotrophic (SR_h) soil surface respiration, based on the measurements in May–Sept 2017, of each treatment (one weekly mean value per treatment) in plots established in 2015 for (**a**) Paajasensalo and (**b**) Viitalampi. LT = living trees, SF_d = storm dead tree detritus, SF_o = storm open-vegetated, ID = trees killed by *I. typographus*.

The proportion of SR_a relative to SR_{tot} at Paajasensalo was 51% for LT, 20% for SF_d, 36% for SF_o, and 40% for ID treatment. The corresponding proportions at Viitalampi were 31% for LT, 14% for SF_d, 45% for SF_o, and 36% for ID. This resulted in a shift in SR_{tot} towards SR_h at disturbed plots with exception of the SF_o microsite and ID plot in Viitalampi, where the proportions of SR_a were higher than at the LT plot.

3.4. Relationships between Variables

Combining data from both sites, the plot mean (treatment mean in SF) SR_{tot} was significantly and positively correlated with the basal area of living trees (Table 3). SR_a or SR_h, however, were not significantly correlated with the basal area of living trees or that of all trees. Neither did soil temperature correlate with the tree stand variables, but soil moisture showed a significant negative correlation with both basal areas of living and all trees (Table 3). Using soil-temperature-adjusted SR_{tot} values for correlations did lower the correlations. Across both sites, treatment and plot mean soil temperature also showed a significant positive correlation with soil total respiration (Table 3), as it did inside each treatment (Table S2). Mean soil moisture, on the contrary, showed significant negative correlations with SR_{tot} and SR_h across both sites and treatments (Table 3) but showed weaker correlations inside each treatment (Table S2).

Table 3. Spearman's correlation coefficients between various plot mean soil surface respiration and soil temperature, soil moisture, and stand basal area. BA_L = living, BA_D = dead, and BA_{tot} = all trees, ST = soil temperature, SM = soil moisture, SR_{tot} = soil surface total respiration, $SR_{tot\_STadj.}$ = temperature-adjusted soil surface total respiration (Aug–Oct 2016 and May–Oct 2017 data, n = 16). SR_a = autotrophic respiration, SR_h = measured, and $SR_{h\_STadj.}$ = soil-temperature-adjusted heterotrophic respiration (May–Oct 2017 data, n = 8).

	BA_L	BA_D	BA_{tot}	ST	SM
SR_{tot}	0.55 *	−0.41	0.40	0.54 *	−0.67 **
$SR_{tot\_STadj.}$	0.43	−0.36	0.31	-	−0.69 **
SR_a	0.14	−0.12	0.17	-	-
SR_h	0.02	0.17	0.12	−0.29	−0.83 *
$SR_{h\_STadj.}$	0.16	0.13	0.33	-	−0.88 **
ST	0.17	−0.18	−0.01	-	−0.13
SM	−0.56 *	0.25	−0.59 **	−0.13	-

* = $p < 0.05$ and ** = $p < 0.01$.

4. Discussion

4.1. Soil Surface Total, Autotrophic, and Heterotrophic Respiration

We hypothesized that the loss of living trees (roots) resulting from storm damage (5–7 years ago) and *I. typographus* infestation (tree mortality circa 2–4 years ago) would result in reduced SR_a, while the death of trees and roots would increase the amount of surface organic debris and soil organic matter available for microbial decomposition and hence increase SR_h. Our results went some way to supporting this hypothesis. Thus, SR_a at both the *I. typographus*-infested and storm-damaged plots was lower than at the living tree plot in Paajasensalo, and the same was true for the storm-damaged SF_d microsite, but not for the storm-damaged SF_o microsite and *I. typographus*-infested plot, at Viitalampi. Furthermore, the lower SR_a/SR_{tot} ratios of the disturbed plots compared to the living tree plots supported the hypothesis that disturbance results in a shift in total respiration away from SR_a towards SR_h at Paajasensalo, but not at Viitalampi. Although significant differences in SR_h were only found between the SF_o and LT treatments in Paajasensalo, the values at disturbed treatments were mainly lower in Paajasensalo and higher in Viitalampi in comparison to LT. As a result of these patterns in SR_a and SR_h, significant differences (lower) in SR_{tot} compared to living tree plots were only associated with the storm-damaged open microsites at Paajasensalo.

The higher-than-expected level of SR_a at the Viitalampi SF_o microsite and ID plot might have been due to a response of ground vegetation cover and/or the remaining living trees to changes brought about by the tree mortality. As the ground vegetation at the Viitalampi SF_o microsite was observed to be more developed than at the other plots, the higher-than-expected SR_a value was however probably due to the inclusion of the associated autotrophic respiration. The ID plot was also damaged by a storm which broke and felled 50% of the beetle-killed standing dead trees, resulting in increased light to the forest floor and subsequent development of the ground vegetation, which is typical especially after wind disturbance [27]. The effect of developing ground vegetation after disturbance (bark beetle, storm and clearance) has been implicated in increased autotrophic soil respiration observed in a study carried out in Norway spruce stands in Austria [50]. In addition, the productivity of the remaining living trees at the ID plot may have been stimulated by an increase in light, water, and nutrient availability after the death of surrounding trees by *I. typographus*, as was shown in a study on mountain pine beetle (*Dendroctonus ponderosae* Hopkins) attack on lodgepole pine stands in British Columbia [8], and resulted in increased SR_a. Also, seedlings which were growing at all plot types may have contributed to some extent to the SR_a at the disturbed treatment plots. However, rather than stimulating growth, mechanical damage to the remaining living trees caused by the storm-felled trees may have hampered their growth [56], resulting in the lower SR_a in SF_d plot compared to the ID plot at Paajasensalo. That

there was still relatively high SR_a in the SF_d microsite in Viitalampi in spite of there being no living mature trees, may be because some of the respiration measurement points also had living ground vegetation, which would have contributed to the SR_a component.

That the difference in SR_h rates between treatments was weaker than expected may be related to the length of time since tree mortality. Following tree mortality, the C/N and lignin/N ratios of the needle litter decrease [20,22], while litterfall [21] and the mortality of fine roots and ectomycorrhizal fungi [19,57] increase, all of which could potentially stimulate decomposition and SR_h. With time after disturbance, the more easily decomposable compounds would be utilized, leaving more recalcitrant debris and lowering the rate of decomposition [24]. The SR_h rates at our disturbed plots may thus have been considerably higher in the first weeks, or even years, following the death of the trees, i.e., before our measurements started. Nevertheless, small branches and twigs on the SF_d microsites were probably a sufficiently good substrate for decomposition, keeping SR_h rates relatively high even seven years after the storm. However, such an effect could be expected to be less visible in the case of managed forests where trees are cleared away after disturbance. Increasing ground vegetation growth accompanied with lowering heterotrophic respiration can considerably mitigate C emissions already three to six years after storm and beetle disturbance and clearing of damaged trees [50]. In our study, the higher SR_a at the SF_o microsite in comparison to LT at Viitalampi and lower (although not significantly) SR_h at SF_o microsite in comparison to SF_d at both sites could indicate such a pattern. However, we have no data to support this possibl effect.

On a larger spatial scale with greater variability in tree mortality, forest structure and composition, and disturbance-created microhabitats, different or more notable effects in soil surface respiration after the two disturbance types could possibly be found. Although our disturbed study plots on average had a similar dead tree basal area, storm- and *I. typographus*-induced tree mortality patterns across the study forests were rather heterogeneous, varying from individual to stand-level tree decease. Noteworthy also is that at our sites, trees were not cleared away after the events, which would be expected to lead to differing response and recovery patterns of C balance compared to managed forests, due to differences in, e.g., litter quantity, incoming radiation, and ground vegetation changes [13,27].

4.2. Relationships between Basal Area, Soil Microclimate, and Respiration

Although we hypothesized that respiration would be related to the amount of dead tree biomass resulting from the disturbances, SR_{tot} was more strongly correlated to the basal area of living trees than to that of the dead trees. The weaker correlations with dead tree basal area are probably because much of the dead fine root biomass, needles, and small branch detritus that decompose much faster than the bigger tree parts [58,59] had already decomposed by the time of our respiration measurements. Also, since detritus for decomposition is also supplied by the living trees, SR_h cannot be attributed to dead trees only; therefore, correlations with basal area likely were relatively weak.

As we had hypothesized, soil temperature and moisture conditions differed among the treatments. The higher soil moisture contents in the disturbed plots compared to the living tree plots in Paajasensalo are likely related to a reduction in transpiration resulting from tree mortality. The effect of tree mortality on transpiration and soil moisture contents was also clearly indicated by a significant negative correlation between soil moisture content and living tree basal area. However, in Viitalampi, the diminishing soil moisture differences between treatments during the study period may be related to the dense herbaceous ground vegetation further developing during the study and potentially enhanced tree growth taking up moisture from the soil. Soil temperature did not differ so clearly between treatments as moisture, but the higher soil temperatures recorded in Viitalampi ID treatment compared to other treatments may be explained by an increase in light (radiation) conditions brought about by the storm felling of dead trees, as discussed earlier.

To assess the extent to which soil surface respiration were determined more by soil temperature than by plant metabolism and the supply of detritus (living and dead basal area), we examined temperature-adjusted respiration values. However, adjusting respiration for temperature had little

effect on the treatment mean respiration rates, indicating that treatment differences in soil surface respiration were determined more by differences in plant metabolism and the supply of detritus than by differences in soil temperature per se.

Collar-wise correlations between soil moisture and SR_{tot} were generally poor, which is why we were not able to examine the effect of soil moisture on respiration differences between treatments. There were, however, clear differences in mean soil moisture contents between treatments, and plot-wise mean SR_{tot} and SR_h rates were strongly and significantly correlated to plot mean soil moisture contents, indicating that disturbance-driven effects on soil surface respiration are related to changes in soil moisture conditions. However, as basal area and soil moisture were also strongly correlated, it is not possible to determine whether differences in respiration were due to differences in basal area or soil moisture.

5. Conclusions

We found no consistent effect of either storm or *I. typographus* disturbances (tree mortality) on SR_{tot} and SR_h. However, SR_a was lower and SR_{tot} rates showed a shift towards a greater proportion of SR_h in the disturbed forest areas, except at the SF_o microsite and ID plot at Viitalampi, where SR_a was higher than expected. These higher-than-expected SR_a values may have been related to the development of ground vegetation and growth stimulation of remaining living trees. Soil surface respiration was found to be related to basal area (living trees) and soil moisture and temperature conditions, factors which would further relate to plant metabolism, the supply and availability of organic matter for decomposition, forest floor light (radiation) conditions, and stand transpiration.

Despite the mainly similar effects of the two disturbances on soil C dynamics found in this study, the influence of the disturbances on tree mortality patterns, stand structure and composition, and created microsites differs over larger areas. Since storm and bark beetle disturbances are predicted to become more common in the future, their effects on forest C dynamics may become even more complex and considerable. Therefore, for future research, studies concentrating on several disturbances and their effects on forest C fluxes and C balance at greater spatial and temporal scales would be important in order to clarify and estimate the potential effects of disturbances on forest C dynamics.

Supplementary Materials: The following are available online at http://www.mdpi.com/1999-4907/10/4/307/s1, Figure S1: Example photos of plot types, Figure S2: Example photos of soil surface respiration measurement points, Table S1: Mean soil surface respiration, temperature and moisture of each treatment at each plot separately, Table S2: Correlation coefficients between soil surface total and heterotrophic respiration, temperature and moisture.

Author Contributions: Conceptualization, M.K., P.L.-S., M.B. and M.S.; Data curation, M.K. and M.B.; Formal analysis, M.K.; Funding acquisition, M.K., P.L.-S. and M.S.; Investigation, M.K., P.O. and M.S.; Methodology, M.K., P.L.-S., P.O. and M.S.; Project administration, M.K. and M.S.; Resources, M.K.; Software, M.K.; Supervision, P.L.-S., P.O. and M.S.; Visualization, M.K. and M.S.; Writing—original draft, M.K.; Writing—review and editing, P.L.-S., P.O., M.B. and M.S.

Funding: This research was funded by AGFOREE Doctoral Programme, Finnish Cultural Foundation—South-Karelia Regional Fund, Nessling Foundation, Niemi Foundation and Societas pro Fauna et Flora Fennica.

Acknowledgments: We wish to thank Pentti Henttonen, Eetu Hirvonen, Risto Tanninen and Jaana Turunen for irreplaceable help with field work. Tuula Kantola, Kajar Köster and Jukka Pumpanen we acknowledge for their valuable advice in relation to the study design and field measurements. Stora Enso and Tornator Ltd, especially Jarmo Hakalisto and Maarit Sallinen, we thank for enabling this study to be carried out in the Viitalampi and Paajasensalo forests.

Conflicts of Interest: The authors declare no conflict of interest.

References

1. Mitchell, S.J. Wind as a natural disturbance agent in forests: A synthesis. *Forestry* **2013**, *86*, 147–157. [CrossRef]
2. Edburg, S.L.; Hicke, J.A.; Brooks, P.D.; Pendall, E.G.; Brent, E.; Norton, U.; Gochis, D.; Gutmann, E.D.; Meddens, A.J.H.; Edburg, S.L.; et al. Cascading impacts of bark beetle-c mortality on coupled biogeophysic biogeochemical processes. *Front. Ecol. Environ.* **2012**, *10*, 416–424. [CrossRef]

3. Knohl, A. Carbon exchange of a Russian boreal forest after windthrow Carbon dioxide exchange of a Russian boreal forest after disturbance by wind throw. *Glob. Chang. Biol.* **2002**, *8*, 231–246. [CrossRef]
4. Kurz, W.A.; Dymond, C.C.; Stinson, G.; Rampley, G.J.; Neilson, E.T.; Carroll, A.L.; Ebata, T.; Safranyik, L. Mountain pine beetle and forest carbon feedback to climate change. *Nature* **2008**, *452*, 987–990. [CrossRef]
5. Hicke, J.A.; Allen, C.D.; Desai, A.R.; Dietze, M.C.; Hall, R.J.; Hogg, E.H.T.; Kashian, D.M.; Moore, D.; Raffa, K.F.; Sturrock, R.N.; et al. Effects of biotic disturbances on forest carbon cycling in\r\nthe United States and Canada. *Glob. Chang. Biol.* **2012**, *18*, 7–34. [CrossRef]
6. Mayer, M.; Sandén, H.; Rewald, B.; Godbold, D.L.; Katzensteiner, K. Increase in heterotrophic soil respiration by temperature drives decline in soil organic carbon stocks after forest windthrow in a mountainous ecosystem. *Funct. Ecol.* **2017**, *31*, 1163–1172. [CrossRef]
7. Lindroth, A.; Lagergren, F.; Grelle, A.; Klemedtsson, L.; Langvall, O.; Weslien, P.; Tuulik, J. Storms can cause Europe-wide reduction in forest carbon sink. *Glob. Chang. Biol.* **2009**, *15*, 346–355. [CrossRef]
8. Brown, M.; Black, T.A.; Nesic, Z.; Foord, V.N.; Spittlehouse, D.L.; Fredeen, A.L.; Grant, N.J.; Burton, P.J.; Trofymow, J.A. Impact of mountain pine beetle on the net ecosystem production of lodgepole pine stands in British Columbia. *Agric. For. Meteorol.* **2010**, *150*, 254–264. [CrossRef]
9. Moore, D.J.P.; Trahan, N.A.; Wilkes, P.; Quaife, T.; Stephens, B.B.; Elder, K.; Desai, A.R.; Negron, J.; Monson, R.K. Persistent reduced ecosystem respiration after insect disturbance in high elevation forests. *Ecol. Lett.* **2013**, *16*, 731–737. [CrossRef]
10. Hicke, J.A.; Meddens, A.J.H.; Allen, C.D.; Kolden, C.A. Carbon stocks of trees killed by bark beetles and wildfire in the western United States. *Environ. Res. Lett.* **2013**, *8*, 035032. [CrossRef]
11. Hansen, E.M.; Amacher, M.C.; Van Miegroet, H.; Long, J.N.; Ryan, M.G. Carbon dynamics in central US Rockies lodgepole pine type after mountain pine beetle outbreaks. *For. Sci.* **2015**, *61*, 665–679. [CrossRef]
12. Reed, D.E.; Ewers, B.E.; Pendall, E. Impact of mountain pine beetle induced mortality on forest carbon and water fluxes. *Environ. Res. Lett.* **2014**, *9*, 105004. [CrossRef]
13. Jonášová, M.; Prach, K. The influence of bark beetles outbreak vs. salvage logging on ground layer vegetation in Central European mountain spruce forests. *Biol. Conserv.* **2008**, *141*, 1525–1535. [CrossRef]
14. Seidl, R.; Rammer, W.; Jäger, D.; Lexer, M.J. Impact of bark beetle (*Ips typographus* L.) disturbance on timber production and carbon sequestration in different management strategies under climate change. *For. Ecol. Manag.* **2008**, *256*, 209–220. [CrossRef]
15. Jonášová, M.; Vávrová, E.; Cudlín, P. Western Carpathian mountain spruce forest after a windthrow: Natural regeneration in cleared and uncleared areas. *For. Ecol. Manag.* **2010**, *259*, 1127–1134. [CrossRef]
16. Schlesinger, W.; Andrews, J. Soil Respiration and Global Carbon Cycle. *Biogeochemistry* **2000**, *48*, 7–20. [CrossRef]
17. Janssens, I.A.; Lankreijer, H.; Matteucci, G.; Kowalski, A.S.; Buchmann, N.; Epron, D.; Pilegaard, K.; Kutsch, W.; Longdoz, B.; Grünwald, T.; et al. Productivity overshadows temperature in determining soil and ecosystem respiration across European forests. *Glob. Chang. Biol.* **2002**, *7*, 269–278. [CrossRef]
18. Bhupinderpal-Singh; Nordgren, A.; Löfvenius Ottosson, M.; Högberg, M.N.; Mellander, P.E.; Högberg, P. Tree root and soil heterotrophic respiration as revealed by girdling of boreal Scots pine forest: Extending observations beyond the first year. *Plant Cell Environ.* **2003**, *26*, 1287–1296. [CrossRef]
19. Högberg, P.; Bhupinderpal-Singh; Löfvenius, M.O.; Nordgren, A. Partitioning of soil respiration into its autotrophic and heterotrophic components by means of tree-girdling in old boreal spruce forest. *For. Ecol. Manag.* **2009**, *257*, 1764–1767.
20. Sariyildiz, T.; Akkuzu, E.; Küçük, M.; Duman, A.; Aksu, Y. Effects of *Ips typographus* (L.) damage on litter quality and decomposition rates of oriental spruce [*Picea orientalis* (L.) Link.] in Hatila Valley National Park, Turkey. *Eur. J. For. Res.* **2008**, *127*, 429–440. [CrossRef]
21. Kopáček, J.; Cudlín, P.; Fluksová, H.; Kaňa, J.; Picek, T.; Šantrůčková, H.; Svoboda, M.; Vaněk, D. Dynamics and composition of litterfall in an unmanaged *Norway spruce* (*Picea abies*) forest after bark-beetle outbreak. *Boreal Environ. Res.* **2015**, *20*, 305–323.
22. Morehouse, K.; Johns, T.; Kaye, J.; Kaye, M. Carbon and nitrogen cycling immediately following bark beetle outbreaks in southwestern ponderosa pine forests. *For. Ecol. Manag.* **2008**, *255*, 2698–2708. [CrossRef]
23. Mayer, M.; Matthews, B.; Schindlbacher, A.; Katzensteiner, K. Soil CO_2 efflux from mountainous windthrow areas: Dynamics over 12 years post-disturbance. *Biogeosciences* **2014**, *11*, 6081–6093. [CrossRef]

24. Šťursová, M.; Šnajdr, J.; Cajthaml, T.; Bárta, J.; Šantrůčková, H.; Baldrian, P. When the forest dies: The response of forest soil fungi to a bark beetle-induced tree dieback. *ISME J.* **2014**, *8*, 1920–1931. [CrossRef]
25. Mikkelson, K.M.; Brouillard, B.M.; Bokman, C.M.; Sharpa, J.O. Ecosystem resilience and limitations revealed by soil bacterial community dynamics in a bark beetle-impacted forest. *MBio* **2017**, *8*, 1–13. [CrossRef]
26. Pec, G.J.; Karst, J.; Taylor, D.L.; Cigan, P.W.; Erbilgin, N.; Cooke, J.E.K.; Simard, S.W.; Cahill, J.F. Change in soil fungal community structure driven by a decline in ectomycorrhizal fungi following a mountain pine beetle (*Dendroctonus ponderosae*) outbreak. *New Phytol.* **2017**, *213*, 864–873. [CrossRef] [PubMed]
27. Fischer, A.; Lindner, M.; Abs, C.; Lasch, P. Vegetation dynamics in central european forest ecosystems (near-natural as well as managed) after storm events. *Folia Geobot.* **2002**, *37*, 17–32. [CrossRef]
28. Zhang, B.; Zhou, X.; Zhou, L.; Ju, R. A global synthesis of below-ground carbon responses to biotic disturbance: A meta-analysis. *Glob. Ecol. Biogeogr.* **2015**, *24*, 126–138. [CrossRef]
29. Kobler, J.; Jandl, R.; Dirnböck, T.; Mirtl, M.; Schindlbacher, A. Effects of stand patchiness due to windthrow and bark beetle abatement measures on soil CO_2 efflux and net ecosystem productivity of a managed temperate mountain forest. *Eur. J. For. Res.* **2015**, *134*, 683–692. [CrossRef]
30. Köster, K.; Püttsepp, Ü.; Pumpanen, J. Comparison of soil CO_2 flux between uncleared and cleared windthrow areas in Estonia and Latvia. *For. Ecol. Manag.* **2011**, *262*, 65–70. [CrossRef]
31. Borkhuu, B.; Peckham, S.D.; Ewers, B.E.; Norton, U.; Pendall, E. Does soil respiration decline following bark beetle induced forest mortality? Evidence from a lodgepole pine forest. *Agric. For. Meteorol.* **2015**, *214–215*, 201–207. [CrossRef]
32. Schelhaas, M.-J.; Nabuurs, G.-J.; Schuck, A. Natural disturbances in the European forests in the 19th and 20th centuries. *Glob. Chang. Biol.* **2003**, *9*, 1620–1633. [CrossRef]
33. Jeger, M.; Bragard, C.; Caffier, D.; Candresse, T.; Chatzivassiliou, E.; Dehnen-Schmutz, K.; Gilioli, G.; Jaques Miret, J.A.; MacLeod, A.; Navajas Navarro, M.; et al. Pest categorisation of *Ips amitinus*. *EFSA J.* **2017**, *15*, 5038.
34. Seidl, R.; Thom, D.; Kautz, M.; Martin-Benito, D.; Peltoniemi, M.; Vacchiano, G.; Wild, J.; Ascoli, D.; Petr, M.; Honkaniemi, J.; et al. Forest disturbances under climate change. *Nat. Clim. Chang.* **2017**, *7*, 395–402. [CrossRef] [PubMed]
35. Seidl, R.; Schelhaas, M.J.; Lexer, M.J. Unraveling the drivers of intensifying forest disturbance regimes in Europe. *Glob. Chang. Biol.* **2011**, *17*, 2842–2852. [CrossRef]
36. Ulanova, N.G. The effects of windthrow on forest at different spatial scales: A review. *For. Ecol. Manag.* **2000**, *135*, 155–167. [CrossRef]
37. Pumpanen, J.; Westman, C.J.; Ilvesniemi, H. Soil CO_2 efflux from a podzolic forest soil before and after forest clear-cutting and site preparation. *Boreal Environ. Res.* **2004**, *9*, 199–212.
38. Müller, K.H.; Wagner, S. Fine root dynamics in gaps of Norway spruce stands in the German Ore Mountains. *Forestry* **2003**, *76*, 149–158. [CrossRef]
39. Gray, A.N.; Spies, T.A.; Easter, M.J. Microclimatic and soil moisture responses to gap formation in coastal Douglas-fir forests. *Can. J. For. Res.* **2002**, *32*, 332–343. [CrossRef]
40. Wermelinger, B. Ecology and management of the spruce bark beetle Ips typographus—A review of recent research. *For. Ecol. Manag.* **2004**, *202*, 67–82. [CrossRef]
41. Eriksson, M.; Pouttu, A.; Roininen, H. The influence of windthrow area and timber characteristics on colonization of wind-felled spruces by *Ips typographus* (L.). *For. Ecol. Manag.* **2005**, *216*, 105–116. [CrossRef]
42. Mikola, P. Application of vegetation science to forestry in Finland. In *Handbook of Vegetation Science, Part 12*; Jahn, G., Ed.; Dr W. Junk Publishers: The Hague, The Netherlands; Boston, MA, USA; London, UK, 1982; pp. 199–224.
43. Pirinen, P.; Simola, H.; Aalto, J.; Kaukoranta, J.-P.; Karlsson, P.; Ruuhela, R. *CLIMATOLOGICAL statistics of Finland 1981–2010*; Reports 2012-1; Finnish Meteorological Institute: Helsinki, Finland, 2012.
44. Finnish Meteorological Institute. Open Source Weather Observations. Available online: https://en.ilmatieteenlaitos.fi/download-observations#!/ (accessed on 19 October 2018).
45. Hurlbert, S.H. Pseudoreplication and the Design of Ecological Field Experiments. *Ecol. Monogr.* **1984**, *54*, 187–211. [CrossRef]
46. Blomqvist, M.; Kosunen, M.; Starr, M.; Kantola, T.; Holopainen, M.; Lyytikäinen-Saarenmaa, P. Modelling the predisposition of Norway spruce to *Ips typographus* L. infestation by means of environmental factors in southern Finland. *Eur. J. For. Res.* **2018**, *137*, 675–691. [CrossRef]

47. Lyytikäinen-Saarenmaa, P.; (Department of Forest Sciences, University of Helsinki). Personal communication, 2014.
48. Finnish Meteorological Institute. Annual Weather Statistics. Available online: https://ilmatieteenlaitos.fi/vuositilastot (accessed on 3 January 2019).
49. Helmisaari, H.-S.; Derome, J.; Nojd, P.; Kukkola, M. Fine root biomass in relation to site and stand characteristics in Norway spruce and Scots pine stands. *Tree Physiol.* **2007**, *27*, 1493–1504. [CrossRef]
50. Zehetgruber, B.; Kobler, J.; Dirnböck, T.; Jandl, R.; Seidl, R.; Schindlbacher, A. Intensive ground vegetation growth mitigates the carbon loss after forest disturbance. *Plant Soil* **2017**, *420*, 239–252. [CrossRef] [PubMed]
51. Lloyd, J.; Taylor, J. On the Temperature Dependence of Soil Respiration. *Funct. Ecol.* **1994**, *8*, 315–323. [CrossRef]
52. R Core Team. *R: A Language and Environment for Statistical Computing*; R Foundation for Statistical Computing: Vienna, Austria, 2018.
53. Bates, D.; Maechler, M.; Bolker, B.; Walker, S. Fitting Linear Mixed-Effects Models Using lme4. *J. Stat. Softw.* **2015**, *67*, 1–48. [CrossRef]
54. Fox, J.; Weisberg, S. *An {R} Companion to Applied Regression*, 2nd ed.; Sage: Thousand Oaks, CA, USA, 2011.
55. Lenth, R. *Emmeans: Estimated Marginal Means, aka Least-Squares Means*; R Core Team: Vienna, Austria, 2018.
56. Seidl, R.; Blennow, K. Pervasive Growth Reduction in Norway Spruce Forests following Wind Disturbance. *PLoS ONE* **2012**, *3*, e33301. [CrossRef]
57. Högberg, M.N.; Högberg, P.; Högberg, M.N. Extramatrical ectomycorrhizal mycelium contributes one-third of microbial biomass and produces, together with associated roots, half the dissolved organic carbon in a forest soil. *New Phytol.* **2002**, 791–795. [CrossRef]
58. Lõhmus, K.; Ivask, M. Decomposition and nitrogen dynamics of fine roots of Norway spruce (*Picea abies* (L.) Karst.) at different sites. *Plant Soil* **1995**, *168*, 89–94. [CrossRef]
59. Hyvonen, R.; Olsson, B.A.; Lundkvist, H.; Staaf, H. Decomposition and nutrient release from *Picea abies* (L.) Karst. and *Pinus sylvestris* L. logging residues. *For. Ecol. Manag.* **2000**, *126*, 97–112. [CrossRef]

forests

MDPI

Article

CO_2 Transfer Characteristics of Calcareous Humid Subtropical Forest Soils and Associated Contributions to Carbon Source and Sink in Guilin, Southwest China

Fen Huang [1,2], Jianhua Cao [1,2,*], Tongbin Zhu [1,2], Mingzhu Fan [1,2] and Mengmeng Ren [1,3]

1 Key Laboratory of Karst Dynamics, Institute of Karst Geology (CAGS), Ministry of Natural Resourses (MNR) and Guangxi, Guilin 541004, China; hfen@karst.ac.cn (F.H.); zhutongbin@gmail.com (T.Z.); fanmingzhu3071@163.com (M.F.); luckdevin@163.com (M.R.)

2 International Research Center on Karst, Under the Auspices of United Nations Educational, Scientific and Cultural Organization (UNESCO), Guilin 541004, China

3 School of Water Resources and Environment, China University of Geosciences (Beijing), Beijing 100083, China

* Correspondence: jhcaogl@163.com; Tel.: +86-773-779-6626

Received: 4 January 2020; Accepted: 11 February 2020; Published: 14 February 2020

Abstract: In karst landscapes, soil CO_2 is a key factor in weathering processes and carbon cycling, where its distribution and migration characteristics directly affect fluxes in carbon source–sink dynamics. We measured the CO_2 emission and dissolution rates of carbonate tablets in calcareous soil developed from limestone and red soil developed from clastic rock, in karst and non-karst subtropical forests, in Guilin, southwest China between 2015 and 2018, to analyze their CO_2 transfer characteristics and source–sink effects. The results showed similar average soil respiration rates between calcareous soil and red soil, with an average CO_2 emission flux of 1305 and 1167 t C km^{-2} a^{-1}, respectively. Carbonate tablet dissolution rates were bidirectional with increasing depth and were greater in red soil than calcareous soil, averaging 13.88 ± 5.42 and 7.20 ± 2.11 mg cm^{-2} a^{-1}, respectively. CO_2 concentration was bidirectional with increasing soil depth, reaching a maximum at the base of the soil–atmosphere interface (50–60 cm), and the bidirectional gradient was more distinctive in red soil. Change in the carbon isotope value of soil CO_2 was also bidirectional in calcareous soils, for which the overall average was 0.87‰ heavier in calcareous than red soil. The carbon sink in calcareous soil in karst regions was estimated to be 11.97 times that of red soil in non-karst regions, whereas its role as a carbon source is just 1.12 times that of red soil, thus indicating the key role of karst soil in the reduction of atmospheric CO_2.

Keywords: subtropical forest; calcareous soils; red soils; soil CO_2; carbon source–sink

1. Introduction

As the largest carbon pool of the terrestrial ecosystem, the amount of total carbon stored in soil (2300 Pg) is about two times and three times higher than the amount stored in the atmosphere (750 Pg) and in living biomass (650 Pg), respectively [1]. Global soil CO_2 emission rates are now up to approximately 98 ± 12 Pg a^{-1}, which is an order of magnitude greater than total annual CO_2 emissions from human activities (6.8 Pg a^{-1}); thus, small fluctuations in soil CO_2 emissions can greatly affect concentrations of atmospheric CO_2 [2,3].

Notably, soil CO_2 is soluble in water and readily forms carbonic acid, which can react with some types of bedrock (e.g., carbonate rock) to consume soil CO_2 and act as an important carbon sink of atmospheric CO_2 [4]. China has a karst area of 3.44 million km^2 [5], and the net recovery of atmospheric

CO_2 from the weathering of carbonate rocks (karstifiction) can reach 36 million t C a^{-1} [6], accounting for 48% of China's forest carbon sink (75 million t C a^{-1}) [7] between 1981 and 2000. The karst area of eight provinces in southwest China totals 1.12 million km^2, of which the bare karst area, depicted as carbonate rock exposed to the atmosphere directly, is 460,000 km^2 [5].

According to previous studies, the karstification that occurred in the soil–rock interface has affected the carbon isotope value ($\delta^{13}C$) of CO_2 from soil respiration and its distribution in the soil profile [8–12]. The CO_2 concentration in the limestone soil profile has a bidirectional gradient, with CO_2 concentration peaks typical in the middle layer [8–11]. In contrast, the CO_2 concentration in the red soil profile has a unidirectional gradient; that is to say, the deeper the red soil layer, the higher the CO_2 concentration [9]. However, unidirectional gradients with depth have also been recorded from 60 cm depths in limestone and dolomite soil profiles [12]. In the non-karst soil profile, the bidirectional gradient of CO_2 distribution was also reported [13,14]. The CO_2 concentration and amount of CO_2 emitted from soil respiration in limestone soil are both lower in karst areas than those of red soil in non-karst areas [9]. The $\delta^{13}C$ value of CO_2 from soil respiration in the karst area is 4‰ heavier than that of the non-karst area [9]. This difference may be related to consummation and absorption of soil CO_2 in the carbonate rock dissolution at the soil–rock interface of karst regions [9]. In the soil–atmosphere interface layer, the $\delta^{13}C$ value of soil CO_2 ($\delta^{13}C$-CO_2) decreased with an increase in soil depth; whereas, below the soil–atmosphere interface layer, the $\delta^{13}C$-CO_2 is basically unchanged in a karst soil [15].

Analysis of the $\delta^{13}C$ may be used to explore the source of CO_2 in soil. If the karstification effect is sufficiently large enough to influence soil CO_2 concentration distribution, it should first arouse the CO_2 isotope's response to the soil profiles, because the CO_2 dissociated from bicarbonate formed by karstification is one of the sources of the soil CO_2 in karst areas [12]. Therefore, to understand how it may affect $\delta^{13}C$-CO_2 and the release of CO_2, and evaluate the CO_2 source and sink effect of karst soils, we determined the CO_2 concentration and isotope value in three calcareous soil profiles, developed from limestone found in a subtropical forest, for three years, for which red soils developed from clastic rock of the same zone were chosen for comparison. The source of CO_2 emission in calcareous soil was collected by the chamber method, and the sink produced by karstification was calculated by the standard carbonate tablet method.

2. Materials and Methods

2.1. Study Site

The study area was located near Maocun village, about 30 km southeastof Guilin (110°30′00″–110°33′45″ E, 25°10′11″–25°12′30″ N), in a typical karst peak cluster depression and valley landscape, with a catchment of about 10 km^2 (Figure 1). The climate in the area is mid-subtropical humid monsoon, hot and humid summer, characterized by spatio–temporal variations in rainfall; the annual average temperature is 19.64–20.39 °C, and the annual average rainfall is 1160–1378 mm (Figure S1). The geology of karst areas consists of Upper Devonian Rongxian Formation (D_3r) pure limestone. Vegetation in the studied sites was comprised of an evergreen broad-leaved forest dominated by *Cyclobalanopsis glauca*, *Loropetalum chinense*, *Alchornea trewioides*, and *Nephrolepis auriculata*, whose soil type was brown calcareous soil of the primosol order in the genetic soil classification of China (GSCC) [16], with a depth of 0.2–1 m. The geology of non-karst areas comprises iron clastic rock (D_2^1). Vegetation in this studied site was comprised of an evergreen broad-leaved forest, dominated by *Castanopsis fargesii*, *Schima superba*, *Itea chinensis*, and a small amount of *Miscanthus* spp.; the soil type was red soil of the ferralosol order in GSCC [16], with a depth of >1 m [9].

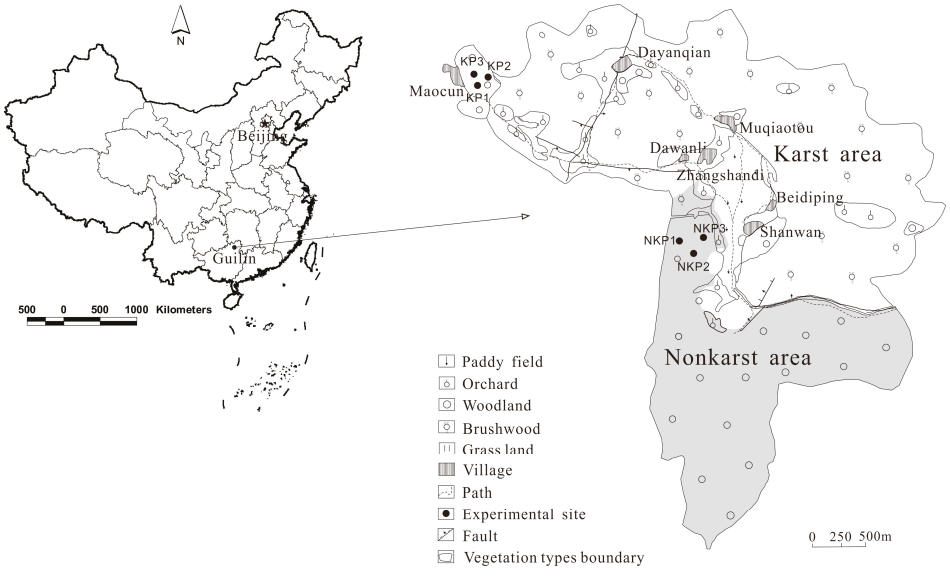

Figure 1. Land use of study area and location of study sites.

2.2. Soil Physicochemical Properties

For each layer (10, 20, 30, 40, 50, 60, 80, and 100 cm) in the 1-m deep soil profiles, we recorded water volume concentration, conductivity, and temperature using a WET sensor and HH2 moisture meter (Delta, Wakefield, UK); the corresponding range and resolutions are 0–100%, 0.1%, 0–300 mS m^{-1}, 1.0 mS m^{-1} and–5–+50 °C, 0.1 °C. Soil pH was measured by a US IQ150 (0.00–14.00, 0.01) soil in situ acidity meter on 24 March 2015. The water volume concentration, conductivity, and temperature of the surface calcareous soil and red soil were measured monthly for one year (Table 1; Figure 2). Soil organic matter was determined by the potassium dichromate volumetric method.

Table 1. Properties at different depths in calcareous and red soils.

	Depth (cm)	pH	Organic Matter (%)	Water Content (%)	Conductivity (mS m^{-1})	Soil Temperature (°C)
Calcareous soil (KP1)	10	7.32	4.57 ± 0.05	26.7	92	16.3
	20	7.29	2.57 ± 0.03	22.6	106	16.4
	30	7.35	1.92 ± 0.04	23.4	112	16.1
	40	7.27	1.78 ± 0.03	22.3	115	16.1
	50	7.25	1.89 ± 0.08	22.2	118	16.0
	60	7.13	2.02 ± 0.05	20.8	123	16.0
	80	7.21	1.34 ± 0.01	26.2	117	15.8
	100	7.24	0.86 ± 0.00	32.2	116	15.7
Red soil (NKP1)	10	5.48	4.02 ± 0.03	21.9	12	17.1
	20	5.96	3.67 ± 0.05	23.3	16	16.6
	30	5.33	3.15 ± 0.05	20.3	12	16.6
	40	5.40	2.72 ± 0.03	22.0	13	16.8
	50	5.48	2.01 ± 0.08	19.5	11	17.0
	60	5.36	1.65 ± 0.00	18.1	10	17.4
	80	5.69	1.14 ± 0.01	16.2	7	17.6
	100	6.39	1.04 ± 0.06	10.7	7	17.5

Data are the mean ± standard deviation (SD). N = 3.

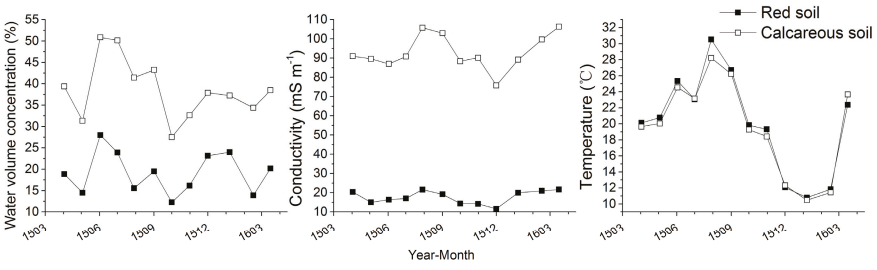

Figure 2. Temperature, water volume concentration and conductivity in the calcareous and red soils.

2.3. Soil CO_2 Concentrations and Emissions

We installed a CO_2 collection pipe in the calcareous (KP1) and red (NKP1) soil profiles in March 2015; two additional profiles in each soil type were included in January 2016 (KP2, KP3, and NKP2, NKP3), and monitoring points were separated by 5–50 m. Monthly monitoring continued from April 2015 to March 2018.

CO_2 concentrations in the eight soil layers were measured and recorded monthly (April 2015–March 2018) using a self-made soil collection pipe, comprising a 100 mL test tube in which gas was collected using a vacuum pump (GAS-TECQ Kitagawa, Japan). If CO_2 concentration >2.6%, we collected 50 mL of gas, and CO_2 concentration was doubled to give a concentration per 100 mL of gas.

Soil respiration CO_2 was collected from relatively flat ground, from which litter and weeds were removed to control for photosynthesis and the respiration of plants; the bare ground was immediately covered with a metal cylinder (25 cm diameter, 32 cm high), and the lower, open end of the cylinder was embedded 2 cm below the soil surface. A rubber tube was embedded in the soil within the cylinder and exposed to the atmosphere; a water stop clip was used to seal the end of the tube exposed to the atmosphere. Monthly atmospheric samples (April 2015–March 2018) were taken from the profiles at about 2 m above ground level to calculate background CO_2 levels; 1 h later, 200 mL of gas in the cylinder was continuously collected using a 100 mL medical syringe and injected into a vacuumed aluminum foil gas sampling bag. CO_2 concentration (ppm) was determined using an Agilent SP1 7890-0468 meteorological chromatograph (Agilent, Santa Clara, CA, USA) at the Ministry of Natural Resources/Guangxi Key Laboratory of Karst Dynamics, Guilin, Guangxi. Air pressure and temperature were simultaneously recorded. Sampling was done between 09:00 and 11:00, when soil respiration rates tend to reflect daily averages [17], to minimize diurnal variations in emissions. Soil CO_2 concentration and respiration in KP1 and NKP1 were sampled 33 times, and 23 times from the remaining profiles.

The $\delta^{13}C$-CO_2 was measured from the eight layers in the soil profiles in June and December 2015, and July 2017, where we used a vacuum to extract soil CO_2 into sealed aluminum bags. The $\delta^{13}C$-CO_2 analysis was completed at the isotope laboratory of the Chinese Academy of Agricultural Sciences, Beijing, China using a MAT253 mass spectrometer. Samples were collected from KP1 and NKP1 three times, and once from the remaining profiles.

2.4. Dissolution Rate of Carbonate Rock

The rate was acquired through the standard carbonate tablet method [18]. Carbonate tablets were determined from high purity, 4 cm diameter × 0.3 cm thick calcareous tablets that were washed and subsequently dried at 70 °C to constant weight after cooling, through a repeated dry-weigh process. In March 2015, in KP1 and NKP1, three tablets were placed 150 cm above the ground, at the soil surface, and inserted at the 20, 50, and 100 cm soil layers. In June, September, and December 2015, and March 2016, the tablets were recovered, analyzed, and re-buried following the washing and drying process described above.

2.5. Data Analysis

The units of CO_2 measurement (ppm) were converted to mg m^{-3} using:

$$CO_2 = \frac{M}{22.4} \times ppm \times \frac{273}{273 + T} \times \frac{Ba}{101325} \quad (1)$$

where M is the molecular weight of the gas; ppm is the measured volume concentration; T is the atmospheric temperature (°C); and, Ba is atmospheric pressure (Pa).

Soil respiration rate (V_R; mg C m^{-2} h^{-1}) was calculated as:

$$V_R = \frac{(C_1 - C_0) \times V}{S \times h} \times \frac{12}{44} \quad (2)$$

where C_1 is CO_2 concentration in the cylinder (mg m^{-3}); C_0 is the corresponding background CO_2 concentration (mg m^{-3}); V is the sampling box volume (m^3); S is the area of sampled soil (m^2); and, h is the monitoring time (h).

Annual soil CO_2 emission flux (F; t C km^{-2} a^{-1}) was calculated as:

$$F = \frac{\sum_{i=1}^{n} V_n \times (T_n - T_{n-1}) \times 24 \times 10^{-3}}{\frac{(T_n - T_1)}{365}} \quad (3)$$

where V_n is the nth measured soil respiration rate (mg C m^{-2} h^{-1}); $T_n - T_{n-1}$ and $T_n - T_1$ are the nth and (n−1)th, the nth and 1st sampling intervals (d), respectively.

The annual dissolution rate of the carbonate tablet (ER; mg cm^{-2} a^{-1}) was calculated as:

$$ER = (W_1 - W_2) \times 1000 \times \frac{T}{365 \times S} \quad (4)$$

where W_1 is the initial weight of the tablet (g); W_2 is the weight after embedding (g); T is the embedding duration (d); and S is the tablet surface area (about 28.9 cm^2).

CO_2 recovery in calcareous soil (CR_C; t C km^{-2} a^{-1}) was calculated according to the stoichiometric coefficient ratio of the carbonate dissolution reaction:

$$CaCO_3 + CO_2 + H_2O \leftrightarrow Ca^{2+} + HCO_3^- \quad (5)$$

$$CR_C = ER \times 97\% \times \frac{12}{100} \times 10 \quad (6)$$

where ER is the annual dissolution rate of the carbonate tablet (mg cm^{-2} a^{-1}); 97% is the purity of the standard carbonate tablet.

The dissolution rate of carbonate rocks in calcareous soil is 23.8 times that of clastic rocks in red soil at the study site [19]. According to the clastic rock dissolution reaction:

$$2CO_2 + 3H_2O + CaSiO_3 = Ca^{2+} + 2HCO_3^- + H_4SiO_4 \quad (7)$$

the CO_2 recovery in red soil (CR_R; t C km^{-2} a^{-1}) was calculated this way:

$$CR_R = \frac{CR_C}{23.8} \times 2 \quad (8)$$

We used one-way analysis of variance (ANOVA) to analyze the differences in soil respiration rate, CO_2 concentration, and $\delta^{13}C$-CO_2 among the soil layers between the two soil types at $p = 0.05$. A Pearson correlation analysis was used to test for association between CO_2 concentration and $\delta^{13}C$-CO_2 in different layers. Analyses were performed in Statistical Package Social Science (SPSS ver. 20.0; IBM Crop., Armonk, NY, USA).

3. Results

3.1. Soil Respiration Rate and Flux

There was a single peak in the soil respiration rate in one year of the karst and non-karst soil profiles, and soil respiration rates varied among the three calcareous soil profiles (range: 9.02–437.33 mg C m^{-2} h^{-1}, average: 134.84 mg C m^{-2} h^{-1}), where they were greater in KP2 than KP1; there were no differences among the red soil profiles (range: 23.21–361.42 mg C m^{-2} h^{-1}, average: 137.93 mg C m^{-2} h^{-1}) (Figure 3). No difference in the mean soil respiration rate was found between the two soil types, but the variation was greater in calcareous soil. The average CO_2 emission flux in calcareous soil and red soil was 1305 and 1167 t C km^{-2} a^{-2} (Table S1), being 12% higher in calcareous soil.

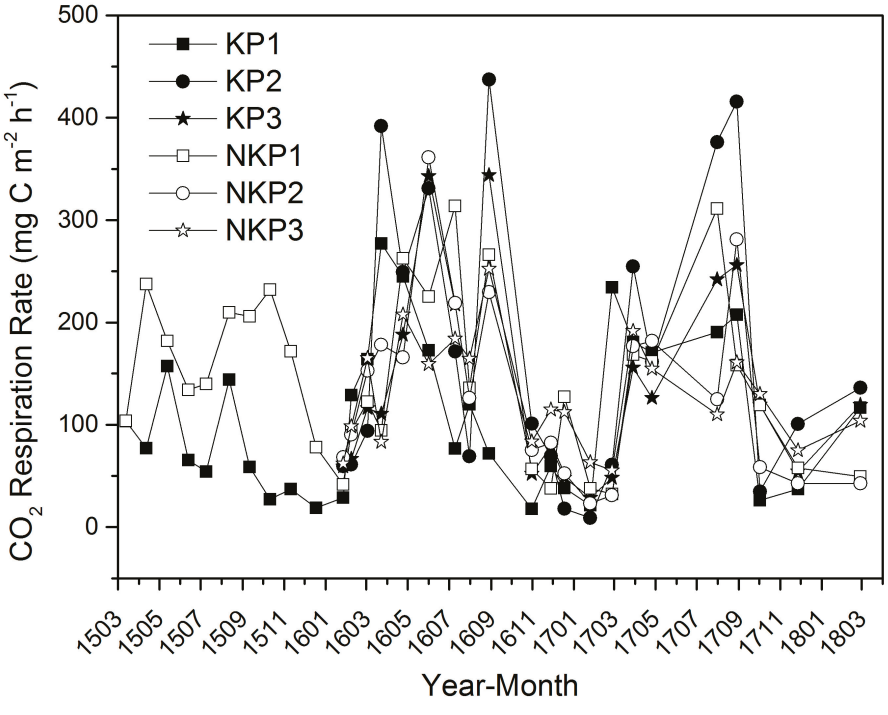

Figure 3. Respiration rates in the calcareous and red soils.

3.2. Variation in CO_2 Concentration among Soil Layers

Consistent with changes in soil respiration rate, the seasonal variation in soil CO_2 concentration in the layers tended to be unimodal, and concentrations were universally greater in summer and autumn than in winter and spring; an anomaly was the low value recorded in July 2015 and August 2016 (Figure 4). Overall, CO_2 concentrations were greatest and most variable in KP2, and lowest in KP1. There were no differences in CO_2 concentrations among the three red profiles.

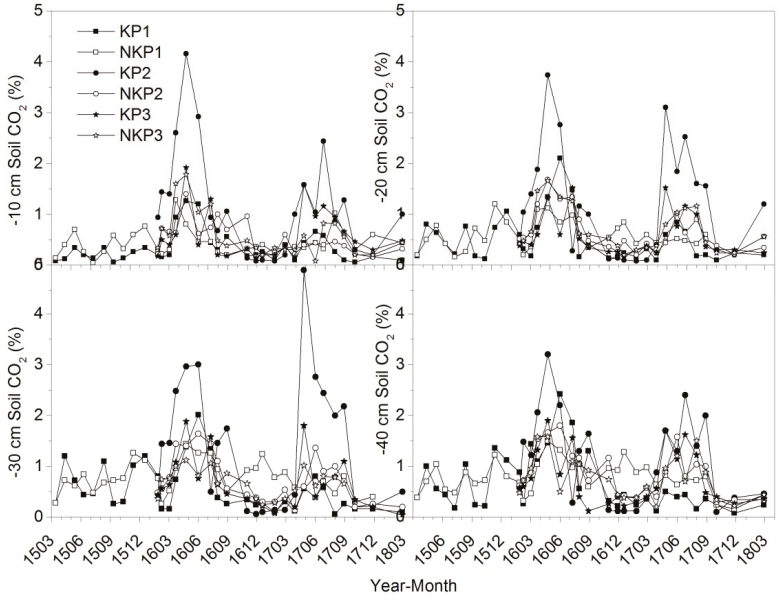

(**a**)

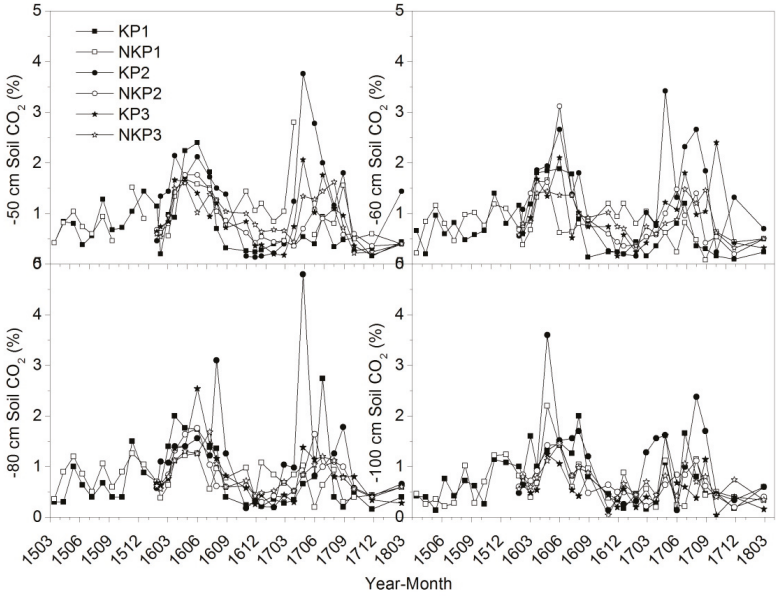

(**b**)

Figure 4. Soil CO_2 concentrations at 10–40 cm (**a**) and 50–100 cm (**b**) depths in calcareous and red soils.

Soil CO_2 concentration in the calcareous soil and red soil profiles varied with depth, where it tended to be higher at 50–60 cm and lower in the upper and deeper layers; this pattern was clearer in the red soils (Figure 5). The mean CO_2 concentrations in the three calcareous soils were 11% greater than in the red soils (Table S2).

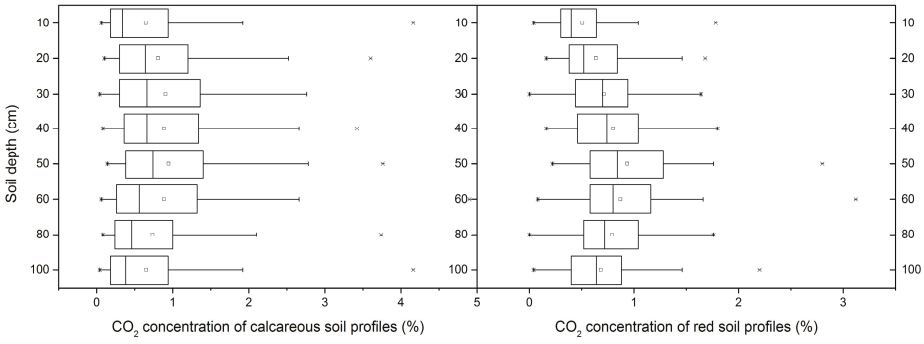

Figure 5. Summary statistics of overall mean soil CO_2 concentrations in calcareous and red soils. Open square: average; vertical line: median; box: upper and lower quartiles; horizontal lines: 1st and 99th percentiles; ×: minimum and maximum values. N = 168.

3.3. Changes in δ^{13}C-CO_2 among Soil Layers

In the calcareous soils, there was a bidirectional gradient of δ^{13}C-CO_2 with a depth in KP1 and KP3, and values at 60 cm were lighter than those of either the upper or deeper layers; the δ^{13}C-CO_2 values were lightest in KP2 and heaviest in KP1, with respective averages of −26.28‰ and −24.24‰ (Figure 6). In the red soils, δ^{13}C-CO_2 decreased with a depth of up to 50 cm, but it remained stable from 50 cm to 100 cm. The mean value of three plots for all layers was 0.87‰ heavier in calcareous soil than red soil (Table S3).

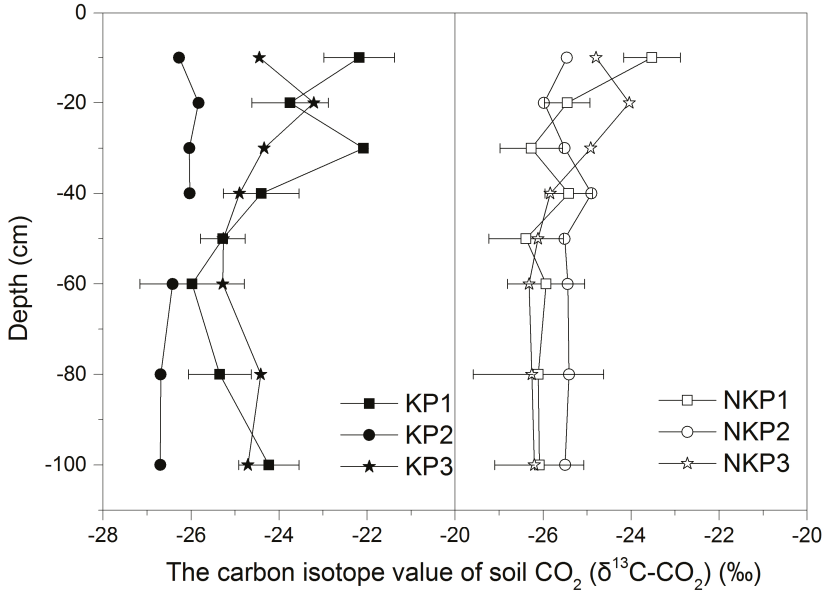

Figure 6. δ^{13}C-CO_2 values in different depth layers of the calcareous and red soils.

3.4. Dissolution Rates of the Carbonate Tablets in Different Layers

The dissolution rates of carbonate tablets were greater in the two soil types than in the air above the profiles, and their rates were greatest in the summer (Figure 7). The rates were bidirectional with

increasing depth and were greater in red soil than calcareous soil, except in calcareous soil during summer. There was no difference in the mean rates in the air above the calcareous and red soils, with averages of 2.50 ± 0.91 and 2.03 ± 1.07 mg cm^{-2} a^{-1}, respectively. The corresponding rates in the soil were 7.20 ± 2.11 and 13.88 ± 5.42 mg cm^{-2} a^{-1}, being 48% lower in calcareous soil (Table S4).

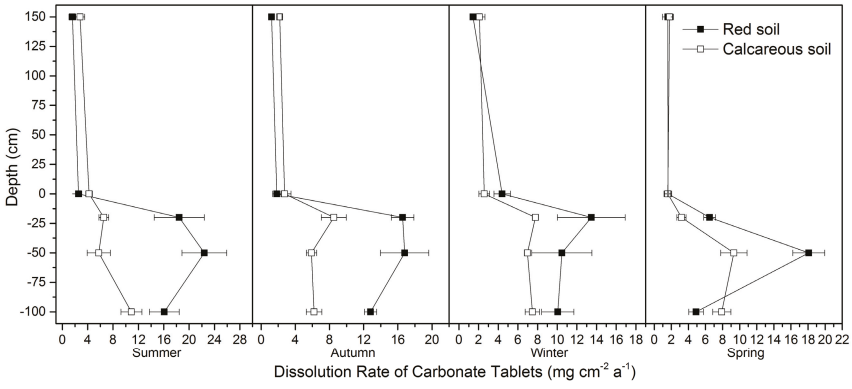

Figure 7. Dissolution rates in calcareous and red soils.

4. Discussion

4.1. Bidirectional Gradient of Soil CO_2 Concentrations and CO_2 Emissions in Red and Calcareous Soil Profile

Wang [13] and Dai [14] found that soil concentrations of CO_2 increased with a greater depth (up to 50 cm) but then diminished below 60 cm, due to the low associated organic carbon content. In our study, soil CO_2 concentrations in the two soil types had a bidirectional gradient trend, though this was more pronounced in the red soil, where the maximum values were recorded in the 50–60 cm layer. Soil organic matter (SOM) on the surface of calcareous soil was clearly higher than that of red soil (Table 1), but it exhibited the opposite trend deeper in the profile. Additionally, there is only a single trend of a gradually decreasing SOM content in red soil, while calcareous soil has a tendency to increase slightly at 50–60 cm. Therefore, the distribution of SOM should be a major reason why the concentration of CO_2 in deep layers of red soil decreases faster than in calcareous soil.

Our experiment showed that the diffusion input of atmospheric CO_2 was greater until the 50–60 cm layer, indicating that the thickness of the soil–atmosphere interface layer was 50–60 cm, while soil CO_2 in deeper layers was probably controlled by oxidative decomposition of organic matter. It is likely that the physical structure of soil particles and porosity, clay content, and soil flooding may also affect the thickness of the soil–atmosphere interface layer [20–22].

The annual soil respiration flux varies greatly in southwest China, ranging from 4.5 t C ha^{-1} a^{-1} (450 t C km^{-2} a^{-1}) in Yaji, Guilin, Guangxi, to 150 mg C m^{-2} h^{-1} (1314 t C km^{-2} a^{-1}) in Qingmuguan, Chongqing [9,23–25]. The results of our study are close to the largest value in those studies. The results were four to six times greater than those of typical meadow and dryland systems in a temperate continental monsoon climate zone (2.8–4.8 t C ha^{-1} a^{-1} = 280–480 t C km^{-2} a^{-1}) [22], perhaps due to lower temperatures in the temperate zone. Soil temperature, which is a key driver of soil respiration, is exponentially related to soil CO_2 [26].

Soil moisture also drives the soil respiration rate, and directly and indirectly regulates soil CO_2 emissions. It is believed that soil respiration increases with increasing soil moisture, until it reaches a threshold, after which it declines [20]. For example, when soil moisture is >60% in shallow soil, CO_2 flux rapidly decreases, due to the restriction of gas transport by the moisture [21], and a soil water content of 25–45% is optimal for microbe activity [27]. Soil moisture in the profile of calcareous soil was horizontally and vertically higher than that of the profile of red soil (Table 1, Figure 2), which may

have been responsible for the higher CO_2 concentration and respiration characterizing the calcareous soil profile.

4.2. Soil CO_2 Concentration and δ^{13}C-CO_2 Affected by Karstification

Consistent with our results, the CO_2 produced in soil had a lighter mean δ^{13}C value of −21 ± 1.5‰ than CO_2 with heavier isotopes in the surface atmosphere did (−9.82‰) [15], indicating a greater exchange of soil and air CO_2 at the soil–atmosphere interface. Therefore, δ^{13}C-CO_2 from the soil–atmosphere interface layer and upward gradually becomes heavier.

We found heavier δ^{13}C-CO_2 in the calcareous karst soils below 50–60 cm, due to two possible reasons. Firstly, karstification consumes soil CO_2, and lighter C is moved downward; the nearer the bedrock, the greater the likelihood of consumption of lighter C, resulting in heavier δ^{13}C-CO_2 in the soil. Secondly, the δ^{13}C of the rock is 0‰, and the theoretical CO_2 isotope value for bicarbonate formed by karstification at the soil–rock interface dissociation into soil CO_2 is −14‰ [28]; therefore, lighter δ^{13}C-CO_2 derived from root respiration, soil organic matter oxidative decomposition, and soil microbe activity could be mixed with this part of CO_2, resulting in a decreased overall CO_2 isotope value.

The δ^{13}C-CO_2 in the red soil below 50–60 cm tended to be stable; this finding is consistent with other studies in non-karst areas [29]. This stability with increasing soil depth may be attributed to the composition of stable carbon isotopes of CO_2 produced from the soil or the limited impacts of the climate on the physical properties of deep soils. The lightest value of soil CO_2 occurred at 50–60 cm, both in calcareous and red soils, which further corroborated that the 50–60 cm layer was the bottom of the soil–atmosphere interface layer.

Below the soil–atmosphere interface layer, karstification at the soil–rock interface consumes CO_2 and drives the downward migration of CO_2 [9]. This process may also have caused slow declines in CO_2 concentration at the bottom profile of the calcareous soil, resulting in a less pronounced bidirectional gradient than in the red soil profile. The δ^{13}C-CO_2 in calcareous soil became heavier: both the CO_2 concentration and its isotopes of calcareous soil show a bidirectional gradient due to the contribution from karstification, so a significant positive correlation arose between the CO_2 concentration and its isotopes (Figure 8). However, this was not the case in the red soil profile.

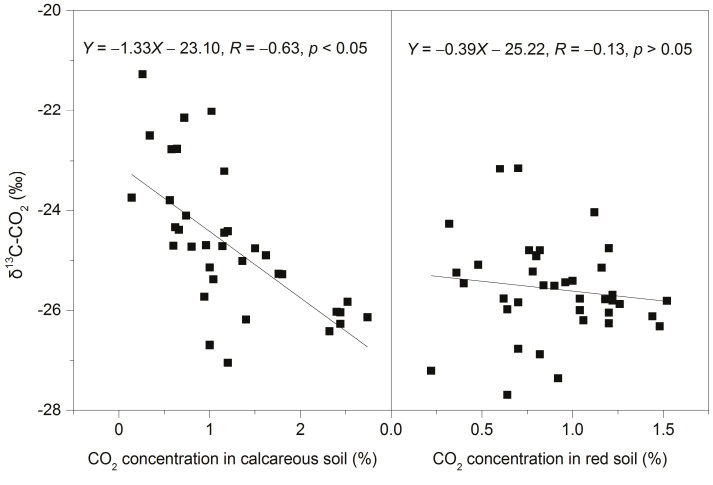

Figure 8. Association between δ^{13}C-CO_2 and the CO_2 concentration in calcareous and red soils.

4.3. Source–Sink Effect of Karst Soil Carbon Pools

In this study, the dissolution rate of the carbonate tablet in the red soil was found to be 1.93 times that of the calcareous soil (Table 2); however, soil CO_2 concentration and soil respiration rates were not as high (1.16 and 1.42 times, respectively, for NKP1 versus KP1), possibly due to a lower soil pH in the red soil affecting the rate of soil organic matter decomposition and erosion by soil microorganisms [30].

Table 2. The ratio of CO_2 recovery to CO_2 emission in calcareous soil and red soil.

	Calcareous Soil	Red Soil
Carbonate dissolution rate in air (mg cm^{-2} a^{-1})	2.50	2.03
Carbonate dissolution rate in soil (mg cm^{-2} a^{-1})	7.20	13.88
CO_2 recovery (t C km^{-2} a^{-1})	8.38	0.70
Soil CO_2 emission flux (t C km^{-2} a^{-1})	1305	1167
CO_2 recovery/CO_2 emission (%)	0.64	0.06

Influenced by soil temperature, water, soil CO_2, soil organic matter and pH, in addition to soil pores and other conditions [31], the dissolution rate of carbonate tablets in the soil in forests in karst areas in southwest China vary widely, ranging from 1.99 mg cm^{-2} a^{-1} in Yaji, Guilin, Guangxi [24], to 357.93 mg m^{-2} d^{-1} (13.06 mg cm^{-2} a^{-1}) in Dalongdong, Hunan [32]. The corresponding value obtained in our study is in the middle of these (Table 2), which can be considered as a better representative. The dissolution rate of carbonate tablets in the air is mainly controlled by the concentration of atmospheric CO_2 and rainfall intensity [18], and the difference between the data in this study (Table 2) and that from Jinfo Mountain, Chongqing, (21.4 t km^{-2} a^{-1} = 2.14 mg cm^{-2} a^{-1}) [18] is not large.

According to Table 2, CO_2 recovery accounts for 0.64% of the soil carbon source for calcareous soil. It is clear, then, that although karstification is an active weathering process, decomposition of soil organic matter and associated CO_2 respiratory emissions dominate the transport and cycling of carbon in the soil system. Thus, karstification and its impact on the carbon cycle represent an Earth-surface carbon transfer process.

Although the carbon source of calcareous soil was 1.12 times that of red soil, its carbon sink effect is 11.97 times that of red soil, suggesting that karst soil contributes greatly to the reduction of atmospheric CO_2. Nonetheless, the dissolution rate of carbonate tablets in the air could be indicative of the carbonate rock dissolution rate in bare karst areas, which is only 0.35 times that of calcareous soil. However, due to the wide distribution of bare karst in southwest China, its carbon sink potentiality cannot be ignored. The high carbonate dissolution rate in red soil also indicated the huge carbon sink potential of zonal red soil-intercalated carbonate rocks.

5. Conclusions

The CO_2 concentrations in calcareous and red soil layers exhibited bidirectional responses to soil depth. The influence of the soil–atmosphere interface on CO_2 exchange extended to a depth of 50–60 cm, where CO_2 concentration increased with depth; below this, CO_2 concentration decreases with depth and is mainly controlled by organic matter decomposition.

Soil $\delta^{13}C$-CO_2 in the two soils was controlled by CO_2 exchange at the soil–atmosphere interface and downward—where isotopes become lighter with depths of 50–60 cm; beyond this, $\delta^{13}C$-CO_2 gradually became heavier in calcareous soil layers, being mainly controlled by karstification. The CO_2 in the red clastic soils was derived from organic matter with stable isotopes, and so $\delta^{13}C$-CO_2 values were stable at depths >50–60 cm. The overall average of $\delta^{13}C$-CO_2 was 0.87‰ heavier in calcareous soils than red soils.

There were also bidirectional differences evident in the dissolution rates of carbonate rock in the two contrasting soils. The rates in the calcareous soil and red soil were 7.20 ± 2.11 and 13.88 ± 5.42 mg cm^{-2} a^{-1}, and, thus, almost half as low (48% lower) in calcareous soil.

Although karstification is an active weathering process, the decomposition of soil organic matter and associated CO_2 respiratory emissions dominate the transport and cycling of carbon in the system. The soil carbon sink only accounts for 0.64% of carbon sources in the karst areas. However, the CO_2 recovery in karst soil is estimated to be 11.97 times that of the clastic rock area and 1.12 times the latter as a carbon source, indicating the key role of karst soil in reducing atmospheric CO_2.

Supplementary Materials: The following are available online at http://www.mdpi.com/1999-4907/11/2/219/s1, Figure S1: Temperature and rainfall in Maocun village, Table S1: Respiration rates in calcareous and red soils, Table S2: CO_2 Concentrations in different layers in calcareous and red soils, Table S3: $\delta^{13}C$-CO_2 values at different depths of calcareous and red soils, Table S4: Seasonal carbonate dissolution rates in calcareous and red soils.

Author Contributions: Conceptualization, J.C.; writing—original draft preparation, F.H.; investigation, M.R. and M.F., writing—review and editing, J.C. and T.Z. All authors have read and agreed to the published version of the manuscript.

Funding: This study was supported by the National and Guangxi Natural Science Foundation of China (Grant Nos. 41772385, 2016GXNSFAA380034, 41530316), the National Key Research Projects (Grant No. 2016YFC05025), and the China Geological Survey (Grant No. DD20160305).

Acknowledgments: Special thanks go to the anonymous referees for their valuable comments and suggestions.

Conflicts of Interest: The authors declare no conflict of interest.

References

1. Jobbagy, E.G.; Jackson, R. The Vertical Distribution of Soil Organic Carbon and Its Relation to Climate and Vegetation. *Ecol. Appl.* **2000**, *10*, 423–436. [CrossRef]
2. Sheng, H.; Yang, Y.S.; Yang, Z.J.; Chen, G.S.; Xie, J.S.; Guo, J.F.; Zou, S.Q. The dynamic response of soil respiration to land-use changes in subtropical China. *Glob. Chang. Biol.* **2010**, *16*, 1107–1121. [CrossRef]
3. Ben, B.L.; Allison, T. Temperature-associated increases in the global soil respiration record. *Nature* **2010**, *464*, 579–582.
4. Cao, J.; Yang, H.; Kang, Z. Preliminary regional estimation of carbon sink flux by carbonate rock corrosion: A case study of the Pearl River Basin. *Chin. Sci. Bull.* **2011**, *56*, 3766–3773. [CrossRef]
5. Li, D.; Luo, Y. Measurement of carbonate rocks distribution area in China. *Carsologica Sin.* **1983**, *2*, 147–150. (In Chinese)
6. Liu, Z.; Wolfgang, D. Comparison of carbon sequestration capacity between carbonate weathering and forests: The necessity to change traditional ideas and methods of study of carbon sinks. *Carsologica Sin.* **2012**, *31*, 345–348. (In Chinese)
7. Fang, J.; Guo, Z.; Piao, S.; Chen, A. Estimation of terrestrial vegetation carbon sink in China from 1981 to 2000. *Sci. China Ser. D* **2007**, *37*, 804–812. (In Chinese)
8. Huang, Q.; Qin, X.; Liu, P.; Zhang, L.; SU, C. Proportion of pedogenic carbonates and the impact on carbon sink calculation in karst area with semiarid environment. *Carsologica Sin.* **2016**, *35*, 164–172. (In Chinese)
9. Cao, J.; Zhou, L.; Yang, H.; Lu, Q.; Kang, Z. Comparison of carbon transfer between forest soils in karst and clasolite areas and the karst carbon sink effect in Maocun village of Guilin. *Quat. Sci.* **2011**, *31*, 431–437. (In Chinese)
10. He, S.; Zhang, M.; Xu, S. Observation on soil CO_2 concentration, hydrochemistry, and thier relationship with karst processes. *Carsologica Sin.* **1997**, *16*, 319–324.
11. Xu, S.; He, S. The CO_2 regime of soil profile and its drive to dissolution of carbonbate rock. *Carsologica Sin.* **1996**, *15*, 50–57. (In Chinese)
12. Li, T.; Wang, S.; Zheng, L. Comparative study on sources of CO_2 from overlying carbonate rocks and non-carbonate rocks, in the middle parts of Guizhou province. *Sci. China Ser. D* **2001**, *31*, 777–782. (In Chinese)
13. Wang, C.; Huang, Q.; Yang, Z.; Huang, R.; Chen, G. Analysis of vertical profiles of soil CO_2 efflux in Chinese fir plantation. *Acta Ecol. Sin.* **2011**, *31*, 5711–5719. (In Chinese)
14. Dai, W.; Wang, Y.; Huang, Y.; Liu, J.; Zhao, L. Seasonal dynamic of CO_2 concentration in lou soil and impact by environmental factors. *Acta Pedol. Sin.* **2004**, *41*, 827–831. (In Chinese)
15. Zheng, L. The stable carbon isotope composition of soil CO_2 in the karst areas, the middle parts of Guizhou province. *Sci. Chin. Ser. D* **1999**, *29*, 514–519. (In Chinese)

16. Huang, C. *Soil Science*; China Agriculture Press: Beijing, China, 2000; pp. 224–227. (In Chinese)
17. Bubier, J.; Crill, P.; Mosedale, A.; Frolking, S.; Linder, E. Peatland responses to varying interannual moisture conditions as measured by automatic CO_2 chambers. *Glob. Biogeochem. Cycles* **2003**, *17*. [CrossRef]
18. Zhang, C. Carbonate rock dissolution rates in different landuses and their carbon sink effect. *Chin. Sci. Bull.* **2011**, *56*, 2174–2180. [CrossRef]
19. Huang, F.; Zhang, C.L.; Xie, Y.C.; Li, L.; Cao, J.H. Inorganic carbon flux and its source in the karst catchment of Maocun, Guilin, China. *Environ. Earth Sci.* **2015**, *74*, 1079–1089. [CrossRef]
20. Gong, X.; Li, Y.; Wang, X.; Niu, Y.; Lian, J.; Luo, Y. Characteristics of soil CO_2 emission in relation to hydrothermal factors during the growing season in horqin sandy land. *Ecol. Environ.* **2018**, *27*, 634–642. (In Chinese)
21. Gabriel, C.E.; Kellman, L. Investigating the role of moisture as an environmental constraint in the decomposition of shallow and deep mineral soil organic matter of a temperate coniferous soil. *Soil Biol. Biochem.* **2014**, *68*, 373–384. [CrossRef]
22. Jiang, C.; Hao, Q.; Song, C.; Hu, B. Effects of marsh reclamation on soil respiration in the Sanjiang Plain. *Acta Ecol. Sin.* **2010**, *30*, 4539–4548. (In Chinese)
23. Wu, X.; Pan, M.; Zhu, X.; Zhang, M.; Bai, X.; Zhang, B. Precipitation effect on soil respiration in epikarst during summer. *J. South. Agric.* **2015**, *46*, 575–580. (In Chinese)
24. Pan, G.; He, S.; Cao, J.; Tao, Y.; Sun, Y. Variation of $\delta^{13}C$ value in karst soil system in the surface zone of Yaji Village, Guilin. *Chin. Sci. Bull.* **2001**, *46*, 1919–1922. (In Chinese)
25. Li, L.; Xian, H.; Kuang, M.; Xie, S.; Zhang, Y.; Jiang, Y.; Liu, Y. The regularity of CO_2 release from soils of the epikarst ecosystem in the Jinfu mountain, Chongqing. *Acta Geosci. Sin.* **2006**, *27*, 329–334. (In Chinese)
26. Wang, X.; Wang, X.; Han, G.; Wang, J.; Song, W.; You, Z. Dynamics of soil CO_2 concentration and CO_2 efflux in non-growing season of the Yellow River Delta wetland. *Chin. J. Ecol.* **2018**, *37*, 2698–2706.
27. Schindlbacher, A.; Zechmeister-Boltenstern, S.; Kitzler, B.; Jandl, R. Experimental forest soil warming: Response of autotrophic and heterotrophic soil respiration to a short-term 10 °C temperature rise. *Plant Soil* **2008**, *303*, 323–330. [CrossRef]
28. Jiang, Y.J. The contribution of human activities to dissolved inorganic carbon fluxes in a karst underground river system: Evidence from major elements and delta $\delta^{13}C_{DIC}$ Nandong, Southwest China. *J. Contam. Hydrol.* **2013**, *152*, 1–11. [CrossRef]
29. Ding, P.; Shen, C.; Wang, N.; Yi, W.; Ding, X.; Fu, D.; Liu, K.; Zhao, P. Carbon isotopic composition turnover and origins of soil of soil CO_2 in a monsoon evergreen hroad leaf forest in Dinghushan Biosphere Reservior, South China. *Chin. Sci. Bull.* **2010**, *55*, 779–787. (In Chinese) [CrossRef]
30. Zhao, R.; Lv, X.; Jiang, J.; Duan, Y. Factors affecting soil CO_2 and karst carbon cycle. *Acta Ecol. Sin.* **2015**, *35*, 4257–4264. (In Chinese)
31. Liu, W.; Zhang, Q.; Jia, Y. The influence of meteorological factors and soil physicochemical properties on karst processes in six land-use patterns in summer and winter in a typical karst valley. *Acta Ecol. Sin.* **2014**, *34*, 1418–1428. (In Chinese)
32. Wang, W.; Lan, F.; Jiang, Z.; Qin, X.; Lao, W. Corrosion rate of carbonate tablet under diverse land use and lithology in the Dalongdong basin, Hunan. *Carsologica Sin.* **2013**, *32*, 29–33. (In Chinese)

forests

MDPI

Article

The Characteristics of Soil C, N, and P Stoichiometric Ratios as Affected by Geological Background in a Karst Graben Area, Southwest China

Hui Yang [1,2], Peng Zhang [1,2,3], Tongbin Zhu [1,2,*], Qiang Li [1,2] and Jianhua Cao [1,2]

1 Institute of Karst Geology, CAGS, Karst Dynamics Laboratory, MNR and Guangxi, Guilin 541004, China
2 International Research Centre on Karst, Under the Auspices of UNESCO, Guilin 541004, China
3 School of Water Resources and Environment, China University of Geosciences (Beijing), Beijing 100083, China
* Correspondence: zhutongbin@gmail.com; Tel.: +86-773-5837840

Received: 31 May 2019; Accepted: 17 July 2019; Published: 19 July 2019

Abstract: Understanding ecological stoichiometric characteristics of soil nutrient elements is crucial to guide ecological restoration and agricultural cultivation in karst rocky desertification region, but the information about the effect of the geological background on ecological stoichiometric ratios remains unknown. Soils from different landforms, including a basin, slope, and plateau, were sampled to investigate the spatial variance of the ecological stoichiometric characteristics of soil carbon (C), nitrogen (N), and phosphorus (P) under different rocky desertification grades (LRD: light rocky desertification; MRD: moderate rocky desertification; and SRD: severe rocky desertification) in a karst graben basin of Southwest China. Soil C:N ratio was not significantly influenced by rocky desertification grade, which was at a relatively stable level in the same landform, but soil C:P and N:P ratios increased with increasing rocky desertification grade. This change was consistent with increased soil organic carbon (SOC) and total nitrogen (TN) concentrations in the same geomorphic location along with the intensification of rocky desertification, but soil P concentration remained at a relatively stable level, indicating that P may be the limiting macronutrient for plant growth during vegetation restoration in a karst graben area. The soil C:N ratio of slope land was larger than that of the basin and plateau, while the soil C:P ratio and N:P ratio of the slope and plateau were significantly larger than that of the basin. The correlations between pH and C, N, and P stoichiometry decreased significantly when Ca was used as a control variable. In sharp contrast, the correlations between Ca and C, N, and P stoichiometry were highly significant no matter whether pH was used as a control variable, suggesting the important role of Ca in soil C, N, and P stoichiometry in karst graben basins.

Keywords: stoichiometric ratios; landform; rocky desertification; karst graben basin

1. Introduction

Karst, which accounts for 12% of the world's total land area, is a calcium (Ca)-rich environment and a unique ecological system [1]. China has approximately 3.44 million km^2 of karst areas, including buried, covered, and exposed carbonate rock areas, accounting for 15.6% of all karst areas in the world [2]. The karst ecosystem is extremely fragile, and it is ranked as the four fragile eco-environmental zones in China along with loess, desert, and cold desert [3]. Due to the fragile ecological environment, complex human-land system, and unreasonable social and economic activities, the rocky desertification widely occurs in the southwest karst region of China (Figure S1) [4]. Noticeably, the karst graben basin is a unique geomorphological form, more fragile than other karst regions in the Southwest China, due to the obvious differences in the topography and climate between basins and mountainous areas in graben basins. Furthermore, geographical environment factors (e.g., hydrology, climate,

and soil) are complex and vegetation site conditions are poor, all of which induce serious rocky desertification [5,6]. Thus, rocky desertification control has become an important part of China's social and economic construction. In addition, vegetation after rocky desertification control is characterized by simple structure, poor stability, and weak resistance. However, the theoretical research of karst rocky desertification restoration lags far behind the practice of rocky desertification control, which seriously limits the restoration and reconstruction of rocky desertification.

It has been widely accepted that the eco-stoichiometry in terrestrial ecosystems plays an important role in biogeochemical cycle research, because it can be used to evaluate the equilibrium and coupling relationships of the main components of an ecosystem [7,8]. Among various elements, soil carbon (C), nitrogen (N), and phosphorus (P) are considered to be the most important components, because the soil C:N:P stoichiometric ratio can reflect soil fertility, plant nutritional status, and the coupling changes between these elements can also affect the growth and distribution of vegetation [9]. In the past several decades, the ratios and relationships among soil C, N, and P have been extensively studied to indicate whether plant growth is limited by these nutrients [10]. The stoichiometric ratio of soil C, N, and P is strongly influenced by soil type, vegetation community characteristics, climatic condition, and vegetation development stage [11,12]. Noticeably, soil is highly heterogeneous in time and space, especially for karst landform. With the development of rock desertification grades, except for plant loss (i.e., the reverse succession of plant communities), the changes in soil quality (e.g., physical, chemical, and biological properties) and quantity have also been significantly taken place [13,14]. In general, the positive succession of plant communities facilitates soil nutrient accumulation, while the reverse succession of plant communities exacerbates soil degradation [15], which can be further enhanced with an increasing rocky desertification grade [16–18]. However, the response of soil physical and chemical properties during the evolution of rocky desertification can show the different patterns as follows: With the increasing rocky desertification grade, the aggregation effect of bare rocks becomes more and more obvious, and the input of soil total N (TN) and soil organic carbon (SOC) is increased through atmospheric sedimentation nutrients and the karst process, while soil erosion becomes weak due to the less soil that can be lost, and subsequently soil nutrient loss is weak, which may improve soil nutrients and physical properties in a rocky desertification environment [16]. Thus, it is possible that soil quality varies with the grade of rocky desertification. Noticeably, soils that widely exist in different landforms in the karst graben basin also have different physical and chemical properties. Therefore, soil stoichiometry may be simultaneously affected by rocky desertification and topography. However, the existing reports mainly focus on the spatial distribution characteristics of soil nutrients and changing patterns during rocky desertification evolution [19]. There is no systematic study on the relationships, ratios between soil C, N, and P elements, and the affecting factors under different rocky desertification in different landforms in the karst graben basin. In addition, calcareous soil developed on carbonate rock is characterized by high pH, magnesium (Mg), and Ca materials in a karst region [2,20], which may lead to the obvious differences in the eco-stoichiometry of soil C, N, and P compared to other soil types. We hypothesized that the karst geological background, especially soil pH, Mg, and Ca concentrations, may play an important role in controlling soil C, N, and P stoichiometry.

In this study, soils from different landforms, including a basin, slope, and plateau, were sampled to investigate the spatial variance of the ecological stoichiometric characteristics of soil C, N, and P under different rocky desertification grades in the karst graben basin. In addition, other soil properties, especially pH, Mg, and Ca concentrations, were also determined to reveal the influencing geochemical factors for soil C, N, and P stoichiometric ratios.

2. Material and Methods

2.1. Study Area

The study site was located in Mengzi county, Hani-Yi Autonomous Prefecture of Honghe, Yunnan Province, China (Figure 1). It is characterized by a typical karst landscape and the topography is

dominated by mountains and basins. Rocky desertification is usually distributed in mountainous areas with a large elevation difference and steep slopes, which results in gradient effects of water, energy, and other factors, and then forms the vertical changes in climate, biology, soil, and so on [21]. The development degree of rocky desertification in the graben basin area is restricted by geological-climatic conditions, resulting in the formation of the eco-environmental characteristics of the basin with thicker soil cover, shallow hills in the basin, slopes around the basin, and plateau areas where rocks are exposed and rocky desertification is serious [5]. According to the characteristics of the Mengzi karst graben basin, soil samples were collected along the basin, slope, and plateau (Figure 1). The annual average temperature of the basin, slope, and plateau is 19.0, 15.6, and 13.7 °C, respectively, and the annual rainfall of the basin, slope, and plateau is 663, 575, and 1027 mm, respectively [22].

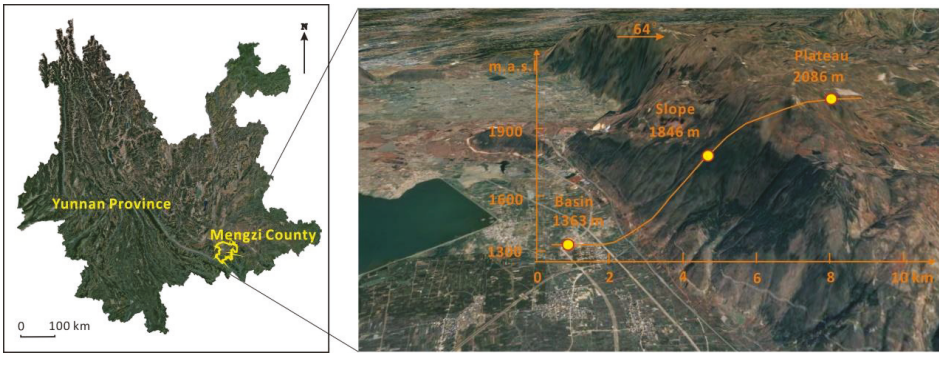

Figure 1. The location of the study area.

2.2. Soil Sampling

The classification of the severity of rocky desertification referred to the method of Jiang et al. (2014) [2], which has been classified into four categories according to the rock exposure rate in China: (1) No rocky desertification with a rock exposure rate <30% of the land; (2) LRD (light rocky desertification with a rock exposure rate ranging from 30% to 50%); (3) MRD (moderate rocky desertification with a rock exposure rate ranging from 50% to 70%); and (4) SRD (severe rocky desertification with a rock exposure rate >70%).

Soil samples were collected from different geomorphic sites, including the basin, slope, and plateau. Different rocky desertification grades, including LRD, MRD, and SRD, were selected in the same landform. The details of the sampling sites, including the vegetation and rocky desertification, are shown in Table 1 and Figure S2.

Table 1. Basic information of the study area and sampling sites.

Location	Latitude and Longitude	Altitude (m)	Rocky Desertification and Vegetation
Basin	103°23′47″ E, 23°28′22″ N	1363	LRD: *Eucalyptus* forest with short planting years and single community structure. The rock bareness rate was ~35%. MRD: Herbs, dominated by Miscanthus. The rock bareness rate was ~55%. SRD: Herbs, herb of Spanishneedles (*Bidens bipinnata* Linn.) and Canadian fleabane (*Conyza canadensis* (Linn.) Cronq.) was dominant specie. The rock bareness rate was >70%.
Slope	103°26′13″ E, 23°27′43″ N	1846	LRD: Artificially planted cypress forests, with high canopy density. The rock bareness rate was ~30%. MRD: Shrub, domained by Purpus Priver (*Ligustrum quihoui* Carr.) and Euphorbiae Pekinensis Radix (*Euphorbia pekinensis* Rupr). The rock bareness rate was ~50% SRD: Ferns are the main species. The rock bareness rate was >70%.
Plateau	103°27′09″ E, 23°27′08″ N	2086	LRD: Forest, the main vegetation types are *Ligustrum quihoui* Carr. and Chinese mugwort (*Artemisia argyi* H. Lév.) and Vaniot. The rock bareness rate was ~30%. MRD: the main vegetation types are Miscanthus. The rock bareness rate was ~50%. SRD: Herbs, domained by Miscanthus with a small amount of *Conyza canadensis* (Linn.) Cronq. The rock bareness rate was >70%.

LRD represents light rocky desertification; MRD represents moderate rocky desertification and SRD represents severe rocky desertification.

At least three representative plots were sampled from the LRD, MRD, and SRD area under the same landform position, resulting in 51 soil samples. The distance between sites was beyond 100 m under the same rocky desertification grade. At each site, 5 plots (1 m × 1 m) were randomly chosen at 20 m intervals. Soils were obtained from the 0 to 15 cm layer after litter removal in each plot and all subsamples were mixed into one composite sample for each site. Fresh soil was passed through a 2 mm sieve, and stones and roots were removed to improve soil homogeneity and were air-dried for measurement of the soil's basic properties and nutrient element concentrations.

2.3. Methods

Soil pH was determined at a 1:2.5 (w:v) soil:water ratio by a DMP-2 mV/pH detector (Quark Ltd., Nanjing, China). SOC was measured using the $K_2Cr_2O_7$-H_2SO_4 oxidation method; total N concentration was measured with the Semi-Micro Kjeldahl method; total P (TP) was determined using $HClO_4$–H_2SO_4 digestion followed by a Mo–Sb colorimetric assay; and total potassium (TK) concentration was measured with the HF-HClO4 flame photometric method [23,24]. Available P (AvP) was determined by the $NaHCO_3$-extraction method [25]. Soil Ca, Mg, copper (Cu), iron (Fe), manganese (Mn), and zinc (Zn) were extracted by HNO_3-HF-$HClO_4$ and analyzed by Inductively Coupled Plasma-Atomic Emission Spectrometry (ICP-AES). Three replicates were performed for each soil sample.

2.4. Data Analysis

Soil nutrient stoichiometry was reported as a molar ratio because it could accurately reflect the amount of elements in the soil [19,26]. The SOC, TN, TP, and AvP concentrations (g/kg) were transformed to mol/kg. The C:N, C:P, C:AvP, N:P, and N:AvP ratios of each soil sample were then calculated as molar ratios (atomic ratios) using SOC:TN, SOC:TP, SOC:AvP, TN:TP, and TN:AvP data, respectively.

Multiple comparisons were conducted by the Duncan method when the variance was homogeneous or the T2 Tamhane test when the variance was not homogeneous. The correlations between the stoichiometric characteristics and the environmental factors studied were analyzed by the Pearson correlation test.

3. Results

3.1. General Patterns of Soil C, N, and P in the Karst Graben Basin

In total, the average values of the C:N, C:P, and N:P ratios in the studied region were lower than those in China. However, both C:AvP and N:AvP were far higher than those in China (Table 2).

Table 2. Soil C, N, and P molar ratios in the karst graben basin.

Landform	C:N	C:P	N:P	C:AvP	N:AvP
Basin	13.4 ± 3.5 a	65.8 ± 18.6 a	5.0 ± 1.3 a	42,429 ± 28,020 a	3292 ± 2181 a
Slope	15.4 ± 3.2 b	116.0 ± 26.2 b	7.8 ± 2.6 b	81,067 ± 36,628 b	5600 ± 3079 b
Plateau	13.2 ± 1.7 a	96.3 ± 39.9 b	7.2 ± 2.5 b	46,285 ± 37,982 a	3399 ± 2589 a
Average	13.6 ± 2.6	92.6 ± 37.3	6.8 ± 2.5	51,516 ± 37,650	3762 ± 2682
China [27]	14.4 ± 0.4	136 ± 11	9.3 ± 0.7	15,810 ± 1832	1114 ± 115

SOC represents soil organic carbon; TN represents total nitrogen; TP represents total phosphorus; AvP represents available phosphorus; C:N represents the molar ratio of SOC:TN; C:P represents the molar ratio of SOC:TP; N:P represents the molar ratio of TN:TP. C:AvP represents the molar ratio of SOC:AvP; N:AvP represents the molar ratio of TN:AvP. Identical letters indicate no significant differences in the average values among soils under different landforms at the 0.05 level.

Both SOC and TN concentrations in the basin were significantly lower than those in the slope and plateau, but no significant differences were found between the slope and plateau ($p < 0.05$, Figure 2). Soil TP concentration in the plateau was significantly higher than that in the slope, but the differences in soil TP concentration between the basin and slope and between the slope and plateau was not significant ($p > 0.05$).

The soil C:N ratio in the basin was significantly lower than that in the slope, while there was no significant difference between the basin and plateau ($p < 0.05$). Both the soil C:P and N:P ratios in the basin were much lower than those in the slope and plateau ($p < 0.05$), while no significant differences were found in the slope and plateau ($p > 0.05$, Figure 2).

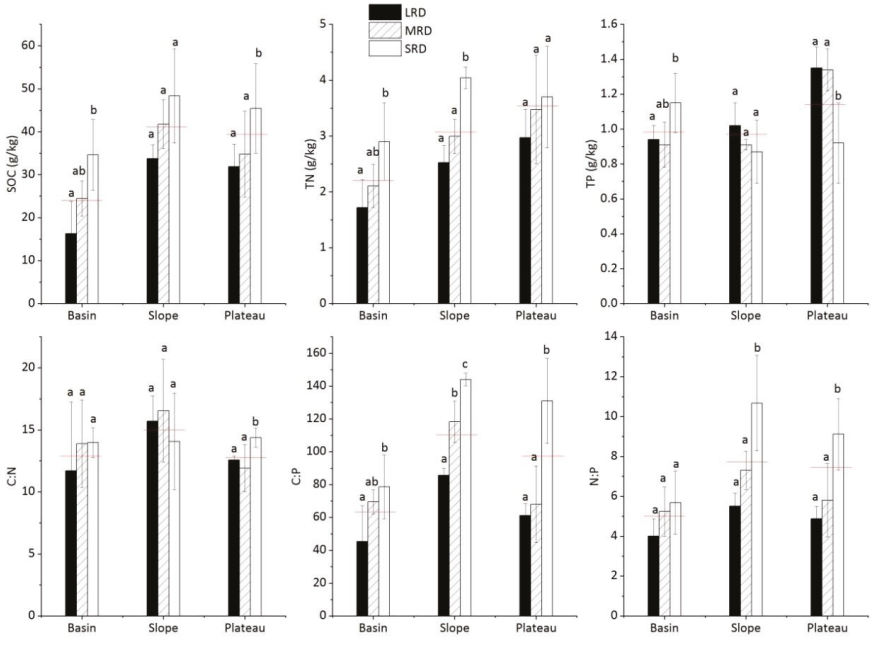

Figure 2. Soil nutrient concentrations and their stoichiometry. The red short line indicates the average value of different rocky desertification degrees in the same geomorphological location. SOC represents soil organic carbon; TN represents total nitrogen; TP represents total phosphorus; C:N represents the molar ratio of SOC:TN; C:P represents the molar ratio of SOC:TP; N:P represents the molar ratio of TN:TP. LRD represents light rocky desertification; MRD represents moderate rocky desertification and SRD represents severe rocky desertification. Identical letters indicate no significant differences in the average values among soils under different rocky desertification in the same landform at the 0.05 level.

3.2. Soil Nutrient Concentrations and their Stoichiometry under Different Rocky Desertification

Both SOC and TN concentrations increased with the aggravation of rocky desertification among the three landforms, while the TP concentration decreased with the aggravation of rocky desertification in the slope and plateau and there was no obvious regularity with the aggravation of rocky desertification in the basin (Figure 2).

The C:N ratios had no consistent regularity with the aggravation of rocky desertification among the three landforms, and there were no significant differences among rocky desertification in the same landform. The C:P and N:P ratios increased with the aggravation of rocky desertification among the three landforms.

3.3. Correlations among Geochemical Variables and C, N, and P Stoichiometry

The correlation between both of SOC and TN and Ca was significant under the condition of zero-order or with the pH value as the controlling factor. There was a simple negative correlation between the Ca and AvP concentration (zero-order in Figure 3). However, the Pearson correlation coefficient between the Ca and AvP concentration decreased significantly when pH was the controlling factor. Soil pH was positively correlated with SOC and TN (zero-order), but under the condition that Ca was the controlling factor, the partial correlation between both of SOC and TN and pH was significantly negative. Hence, Ca was the core element affecting SOC and TN concentrations. Although there was a negative partial correlation between Mg and SOC and TN when Ca was the controlling factor, the correlation between Mg and the stoichiometry of C, N, and P was not significant.

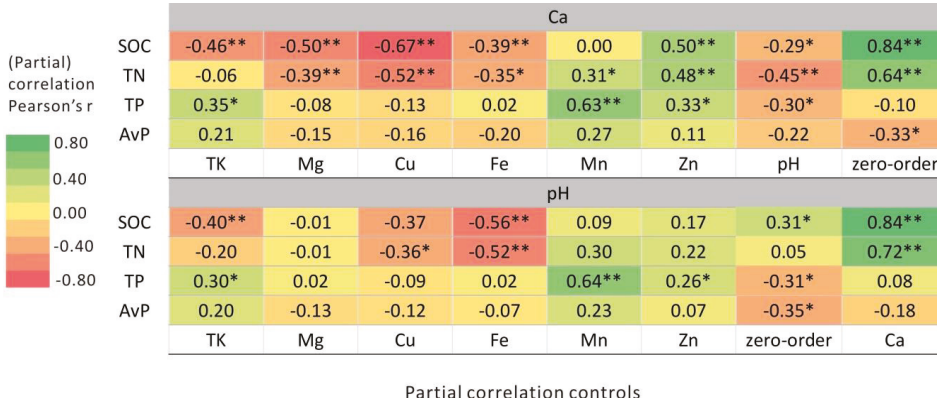

Figure 3. Partial correlation between C, N, and P and geochemical variables. Ca, Mg, Cu, Fe, Mn and Zn represents calcium, magnesium, copper, iron, manganese, and zinc respectively; TK represents total potassium; The color and numbers shown indicate the strength and sign of the correlation. No change in color between controlled and zero-order = no dependency; increase/decrease of color intensity = gain of /loss of correlation. Significance levels are denoted as follows: *, $p < 0.05$; **, $p < 0.01$.

Undoubtedly, both Ca and pH directly influenced the C, N, and P stoichiometry (Figure 4 and zero-order correlations in Figure 5). Both Ca and pH were positively correlated with C:N and C:P ($p < 0.01$). However, the relationship between Ca and N:P was extremely significant and positive ($p < 0.01$), while the correlation between pH and N:P was not significant ($p > 0.05$). Similarly, the correlations between Ca and C:AvP, Ca and N:AvP, and pH and C:AvP were very significant ($p < 0.01$). A significant positive correlation was found between pH and N:AvP ($p < 0.05$).

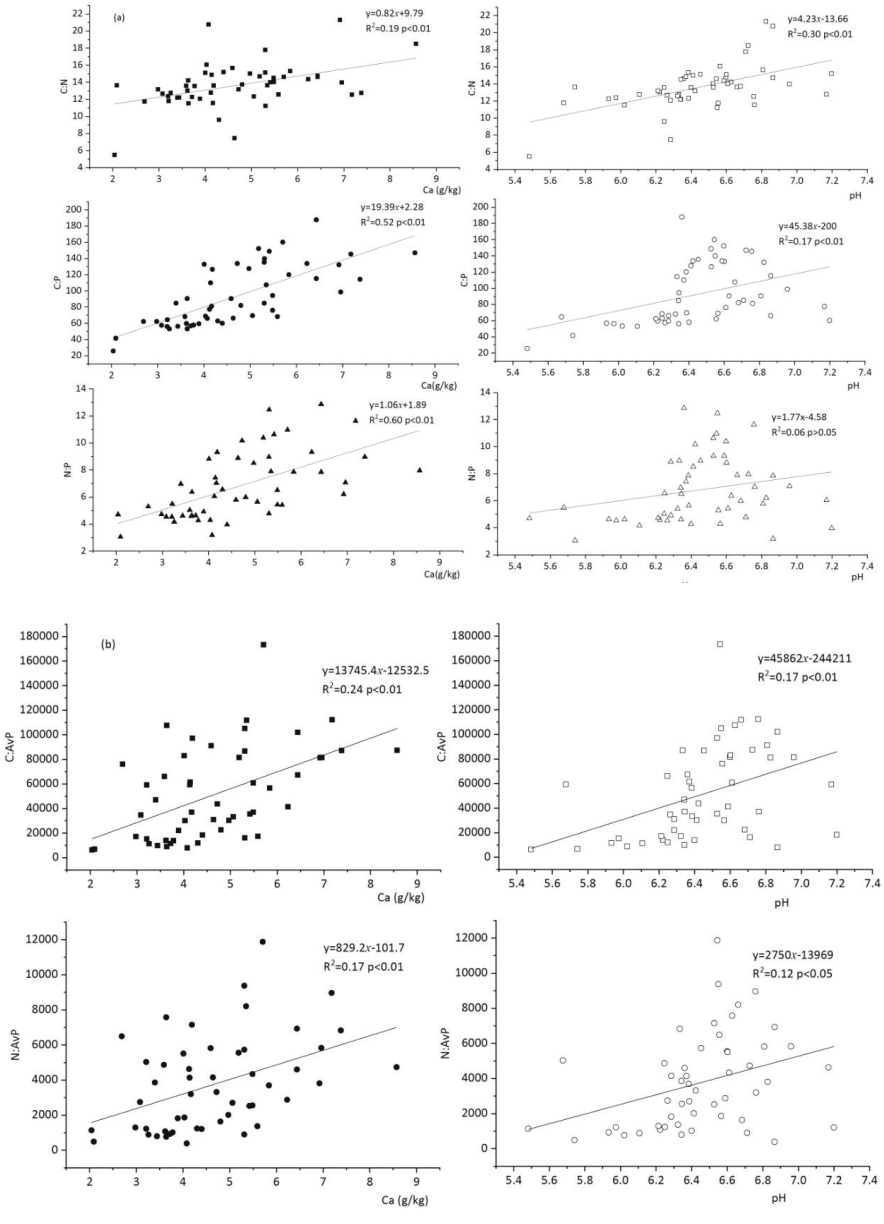

Figure 4. The relationship between Ca, pH, and C, N, and P stoichiometry. (**a**): The relationship between Ca, pH, and C:N, C:P and N:P; (**b**): The relationship between Ca, pH, and C:AvP, N:AvP.

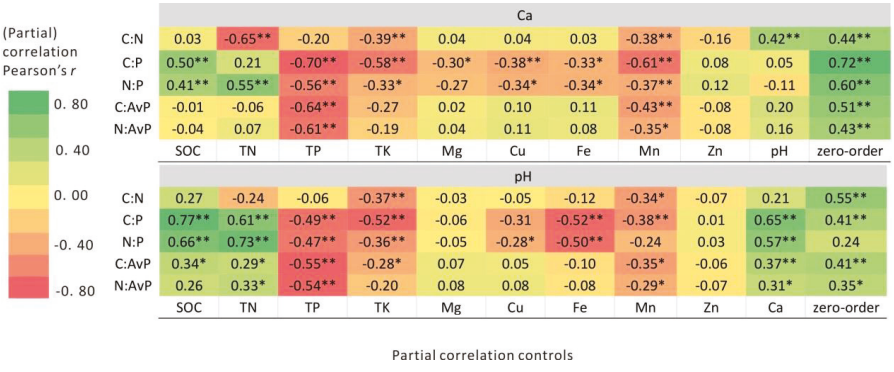

Figure 5. Partial correlation between C, N, and P stoichiometry and geochemical variables. Significance levels are denoted as follows: *, $p < 0.05$; **, $p < 0.01$.

4. Discussion

4.1. Spatial Pattern of Eco-Stoichiometric Characteristics of C, N, and P and Analysis of Influencing Factors

It has been widely accepted that SOC in calcareous soils in the karst region of Southwest China is significantly higher than that in other zonal soils in the same latitude [28,29], which is mainly attributed to the shallow soil layer, high bareness rate, and low soil quantity in the karst area [16]. Most researchers also found that an increased SOC concentration is closely related to the geological background of Ca-rich and pH-alkaline soils in the karst area [30–33]. Calcium in different forms plays an important role in SOC protection through a chemical bonding mechanism and chemical structure stability [34–38]. In this study, Ca was positively correlated with SOC concentration (Figure 3), indicating the important role of Ca in maintaining the SOC pool. Furthermore, SOC and TN had a significant positive correlation, suggesting the co-evolution process of the C and N cycle in calcareous soil. However, the P pool was not basically affected by the changes in the C and N pools, which resulted in the weak correlation between soil TP and SOC and TN. This indicates that P is mainly derived from the weathering release of soil minerals, rather than from the short-term biological cycle in this study [39]. Soil C:N, C:P, and N:P in the studied region were all lower than the average value of China, but the values of C:AvP and N:AvP were much higher than the average value of China (Table 1), which may be attributed to a high total P concentration but low AvP concentration in the karst soil [40].

The spatial distribution of C:N in the studied area is relatively stable, and no significant difference was found among the three rocky desertification lands in different geomorphological locations, suggesting that the vegetation type and rocky desertification degree have little significant effect on the C:N ratio. This was in agreement with a previous result that the C:N ratio was relatively stable and was insignificantly affected by climate, although C and N concentrations had great spatial variability [38,39]. Previous studies found that soil C:P and N:P ratios decreased with increasing disturbance, because the loss of soil C and N pools was faster than the P pool. However, in this study, N:P and C:P ratios increased with the aggravation of rocky desertification, more noticeably in the severe rocky desertification rock region with strong disturbance. Possibly, this could be attributed to increased SOC and TN concentrations with the aggravation of rocky desertification but the soil P concentration at a relatively stable level (Figure 2). Some studies found that soil physical and chemical properties do not always deteriorate with an increasing rocky desertification grade, but the degradation process initially decreases and improves after a certain stage [16,40,41]. This may be related to the "aggregation effect" of bare rocks in a rocky desertification environment [16], which refers to bare rock aggregated nutrients and the karst process from atmospheric subsidence into the surrounding soil. With the grade of rocky desertification, the aggregation effect of bare rock increases gradually. In the intensive rocky desertification environment, this aggregation effect becomes more obvious, coupled with the

weakening of soil erosion, and subsequently results in the improvement of soil nutrients and physical properties, such as SOC, TN, and Ca.

4.2. Soil Ca and pH Controls on Soil C, N, and P Stoichiometry

Due to high Ca concentrations, calcareous soils developed by carbonate bedrock are characterized by high pH [42]. Soil pH can affect the forms and transformation of C, N, and P elements in the soil by changing the geochemical environment and microbial abundance, community, and activity. In addition, soil with a high Ca concentration in rock desertification areas has become the most important environmental factor affecting the local plant physiological characteristics and distribution [1]. In this study, although the correlations between pH and C, N, and P stoichiometry were highly significant (zero-order correlations in Figure 5), the Pearson correlation coefficients between pH and C:P, N:P, C:AvP, and N:AvP decreased significantly when Ca was used as a control variable (Figure 5). In sharp contrast, both zero-order correlations and the Pearson correlations between Ca and C, N, and P stoichiometry were highly significant, when pH was used as a control variable (Figure 5).

Calcium greatly impacted soil C, N, and P stoichiometry in this study. The dominant role of Ca in soil C, N, and P stoichiometry is intriguing, and Ca can supply several possible alternative explanations. Firstly, Ca is the necessary metabolic component of microbial growth, and fungal and bacterial heterotrophs may access and accumulate root Ca to form oxalates, which can be used to maintain microbial metabolism under unfavorable soil conditions [43]. Similar results were reported that Ca-rich species exhibited more rapid decomposition [44]. Secondly, Ca can combine with humus to form Ca humate, which is difficult to mineralize and decompose [28], and thereby lowers the active organic matter.

5. Conclusions

In this work, we analyzed the C, N, and P stoichiometry under different rocky desertification grades from a basin, slope, and plateau in the karst graben basin. Our results showed that the influence of the rocky desertification degree on soil C:N was not significant in the same landform, but soil C:P and N:P increased with the increase of rocky desertification, which was attributed to increased SOC and TN concentrations in the same geomorphic location along with the intensification of rocky desertification, while the difference of P concentration in the same geomorphic location was not significant. This indicates that the soil quality is not deteriorating with the aggravation of rocky desertification, but has a trend of improvement. In addition, we also found that the correlations between pH and C, N, and P stoichiometry decreased significantly when Ca was used as a control variable. In sharp contrast, the correlations between Ca and C, N, and P stoichiometry were highly significant no matter whether pH was used as a control variable, indicating the important role of Ca in soil C, N, and P stoichiometry in karst graben basins. This result provides expanded guidance on the practice of ecological restoration and agricultural cultivation in karst rocky desertification regi ns. Forexample, when conducting ecological restoration of rocky desertification in karst graben basins, we should consider not only the impacts of altitude and vertical climate, but also the tolerance of species to Ca. Selecting suitable species according to local conditions are of great significance for the promotion of ecological restoration in rocky desertification areas.

Supplementary Materials: The following are available online at http://www.mdpi.com/1999-4907/10/7/601/s1, Figure S1: Agricultural planting patterns in rocky desertification areas, Figure S2: Vegetation and rocky desertification in three sampling sites.

Author Contributions: Conceptualization, T.Z.; writing—original draft preparation, H.Y.; investigation, P.Z. and Q.L.; writing—review and editing, T.Z. and J.C.

Funding: This study was supported by the National Key Research and Development Program of China (No. 2016YFC0502501), Guangxi Natural Science Foundation (2017GXNSFAA198153) and Guangxi Scientific Research and Technology Development Project (Guikeneng 1598023-1).

Acknowledgments: Special thanks to the anonymous referees for their valuable comments and suggestions. We also thank Junbing Pu, Manfu Hou, and his team for assistance with collecting soil samples and surveying plant diversity at sampling points.

Conflicts of Interest: The authors declare no conflict of interest.

References

1. Wei, X.; Deng, X.; Xiang, W.; Lei, P.; Ouyang, S.; Wen, H.; Chen, L. Calcium content and high calcium adaptation of plants in karst areas of southwestern Hunan, China. *Biogeosciences* **2018**, *15*, 2991–3002. [CrossRef]
2. Jiang, Z.; Lian, Y.; Qin, X. Rocky desertification in Southwest China: Impacts, causes, and restoration. *Earth Sci. Rev.* **2014**, *132*, 1–12. [CrossRef]
3. Yuan, D.X. Rock desertification in the subtropical Karst of South China. *Z. Geomorphol.* **1997**, *108*, 81–90.
4. Li, Q.; Pu, J.B.; Huang, N.; Du, H.M.; Qi, X.K.; Wang, L.; Yang, H. A research approach for ecological, environmental and geological differentiation of rocky desertification and its driving mechanism in karst graben basin. *Adv. Earth Sci.* **2017**, *32*, 899–907. (In Chinese)
5. Cao, J.H.; Deng, Y.; Yang, H.; Pu, J.B.; Zhu, T.B.; Lan, F.N.; Huang, F.; Liang, J.H. Rocky desertification evolution, treatment technology and demonstration in Karst faulted basins, Southwest China. *Acta Ecol. Sin.* **2016**, *36*, 7103–7108. (In Chinese)
6. Müller, M.; Oelmann, Y.; Schickhoff, U.; Böhner, J.; Scholten, T. Himalayan treeline soil and foliar C:N:P stoichiometry indicate nutrient shortage with elevation. *Geoderma* **2017**, *291*, 21–32. [CrossRef]
7. Hu, C.; Li, F.; Xie, Y.H.; Deng, Z.M.; Chen, X.S. Soil carbon, nitrogen, and phosphorus stoichiometry of three dominant plant communities distributed along a small-scale elevation gradient in the East Dongting Lake. *Phys. Chem. Earth* **2018**, *103*, 28–34. [CrossRef]
8. Mooney, H.A.; Vitousek, P.M.; Matson, P.A. Exchange of Materials Between Terrestrial Ecosystems and the Atmosphere. *Science* **1987**, *238*, 926. [CrossRef]
9. Mooshammer, M.; Hofhansl, F.; Frank, A.H.; Wanek, W.; Hämmerle, I.; Leitner, S.; Schnecker, J.; Wild, B.; Watzka, M.; Keiblinger, K.M.; et al. Decoupling of microbial carbon, nitrogen, and phosphorus cycling in response to extreme temperature events. *Sci. Adv.* **2017**, *3*, e1602781. [CrossRef]
10. Finzi, A.C.; Austin, A.T.; Cleland, E.E.; Frey, S.D.; Houlton, B.Z.; Wallenstein, M.D. Responses and feedbacks of coupled biogeochemical cycles to climate change: Examples from terrestrial ecosystems. *Front. Ecol. Environ.* **2011**, *9*, 61–67. [CrossRef]
11. Jacques Agra Bezerra da Silva, Y.; Williams Araújo do Nascimento, C.; Jacques Agra Bezerra da Silva, Y.; Miranda Biondi, C.; Cordeiro Atanázio Cruz Silva, C.M. Rare Earth Element Concentrations in Brazilian Benchmark Soils. *Rev. Bras. Ciênc. Solo.* **2016**, *40*, 1–13.
12. Wang, S.Q.; Yu, G.R. Ecological stoichiometry characteristics of ecosystem carbon, nitrogen and phosphorus elements. *Acta Ecol. Sin.* **2008**, *28*, 3937–3947. (In Chinese)
13. Li, Y.B.; Shao, J.A.; Yang, H.; Bai, X.Y. The relations between land use and karst rocky desertification in a typical karst area, China. *Environ. Geol.* **2009**, *57*, 621–627. [CrossRef]
14. Luo, G.J.; Li, Y.B.; Wang, S.J.; Cheng, A.Y.; Dan, W.L. Comparison of ecological significance of landscape diversity changes in karst mountains: A case study of 4 typical karst area in Guizhou Province. *Acta Ecol. Sin.* **2011**, *31*, 3882–3889. (In Chinese)
15. Song, T.Q.; Peng, W.X.; Du, H.; Wang, K.L.; Zeng, F.P. Occurrence, spatial-temporal dynamics and regulation strategies of karst rocky desertification in southwest China. *Acta Ecol. Sin.* **2014**, *34*, 5328–5341. (In Chinese)
16. Sheng, M.Y.; Liu, Y.; Xiong, K.N. Response of soil physical-chemical properties to rocky desertification succession in South China Karst. *Acta Ecol. Sin.* **2013**, *33*, 6303–6313. (In Chinese) [CrossRef]
17. Liu, F.; Wang, S.J.; Liu, Y.S.; He, T.B.; Luo, H.B.; Long, J. Changes of soil quality in the process of karst rocky desertification and evaluation of impact on ecological environment. *Acta Ecol. Sin.* **2005**, *25*, 639–644. (In Chinese)
18. Pang, D.; Wang, G.; Li, G.; Sun, Y.; Liu, Y.; Zhou, J. Ecological Stoichiometric Characteristics of Two Typical Plantations in the Karst Ecosystem of Southwestern China. *Forests* **2018**, *9*, 56. [CrossRef]
19. Tian, H.; Chen, G.; Zhang, C.; Melillo, J.M.; Hall, C.A.S. Pattern and variation of C:N:P ratios in China's soils: A synthesis of observational data. *Biogeochemistry* **2010**, *98*, 139–151. [CrossRef]

20. Alfaro, M.R.; Nascimento, C.W.A.; Biondi, C.M.; Silva, Y.J.A.B.; Accioly, A.M.; Montero, A.; Ugarte, O.M.; Estevez, J. Rare-earth-element geochemistry in soils developed in different geological settings of Cuba. *Catena* **2018**, *162*, 317–324. [CrossRef]
21. Li, G.P. Progress and propects in research of mountain meteorogy in China during the past 25 years. *Adv. Meteorol. Sci. Technol.* **2016**, *6*, 115–122. (In Chinese)
22. Wang, S.N.; Pu, J.B.; Li, J.H.; Zhang, T.; Huo, W.J.; Yuan, D.X. Climatic chararacteristics under the influence of basin-mountain coupled topography and its influence on the ecological restoration of rocky desertification in a Mengzi karst graben basin, Southwest China. *Carsol. Sin.* **2019**, *38*, 50–59. (In Chinese)
23. Tyler, G.L.; Olsson, T. Conditions related to solubility of rare and minor elements in forest soils. *J. Plant Nutr. Soil Sci.* **2002**, *165*, 594–601. [CrossRef]
24. Bao, S.D. *Soil Agricultural Chemistry Analysis*; China Agricultural Publishing House: Beijing, China, 2000. (In Chinese)
25. Olsen, S.R. *Estimation of Available Phosphorus in Soils by Extraction with Sodium Bicarbonate*; United States Department of Agriculture: Washington, DC, USA, 1954.
26. Cleveland, C.; Liptzin, D. C:N:P stoichiometry in soil: Is there a "Redfield ratio" for the microbial biomass? *Biogeochemistry* **2007**, *85*, 235–252. [CrossRef]
27. Wei, F.S.; Chen, J.S.; Wu, Y.Y.; Zheng, C.J. Study on the background contents on elements of soils in China. *Chin. J. Environ. Sci.* **1991**, *12*, 12–19.
28. Zhu, T.; Zeng, S.; Qin, H.; Zhou, K.; Yang, H.; Lan, F.; Huang, F.; Cao, J.; Müller, C. Low nitrate retention capacity in calcareous soil under woodland in the karst region of southwestern China. *Soil Biol. Biochem.* **2016**, *97*, 99–101. [CrossRef]
29. Yang, H.; Zhang, L.K.; Yu, S.; Cao, J.H. Effects of different land-uses on the features of water-stable aggregates in karst and clasolite areas in Maocun, Guilin. *Carsol. Sin.* **2012**, *31*, 265–271. (In Chinese)
30. Hu, L.N.; Su, Y.R.; He, X.Y.; Li, Y.; Li, L.; Wang, Y.H.; Wu, J.S. The speciation and content of calcium in karst soils, and its effects on soil organic carbon in karst region of Southwest China. *Sci. Agric. Sin.* **2012**, *45*, 1946–1953.
31. Cao, J.H.; Yuan, D.X.; Pan, G.X. Some soil features in karst ecosystem. *Adv. Earth Sci.* **2003**, *18*, 37–44. (In Chinese)
32. Duan, Z.F.; Fu, W.L.; Zen, X.J.; Du, F.Z. Correlation between soil organic carbon and water-stable aggregate in karst area-A case study in Zhongliangshan karst valley, Chongqing. *Carsol. Sin.* **2009**, *28*, 75–79. (In Chinese)
33. Yang, H.; Zhang, L.K.; Cao, J.H.; Yu, S. Comparison of mineralization and chemical structure of the soil organic carbon under different land uses in Maocun karst area, Guilin. *Carsol. Sin.* **2011**, *30*, 410–416. (In Chinese)
34. Shen, Y.; Fu, W.L.; Lan, J.C.; Cheng, H.; Zhang, S.Q.; Wu, L.Z. Distribution characteristics of soil particulate organic carbon and mineral-associated organic carbon of different land use in karst mountain. *Res. Soil Water Conserv.* **2012**, *19*, 1–6.
35. Chen, X.B.; He, X.Y.; Hu, Y.J.; Su, Y.R. Characteristics and mechanisms of soil organic carbon accumulation and stability in typical karst ecosystems. *Res. Agric. Mod.* **2018**, *39*, 907–915. (In Chinese)
36. Yang, H.; Liang, Y.; Xu, J.M.; Cao, J.H. Research progress of the relationship between soil calcium and soil organic carbon in karst area. *Guangxi Sci.* **2018**, *25*, 505–514. (In Chinese)
37. Yang, H.; Chen, J.R.; Liang, J.H.; Cao, J.H. Preliminary study on the relationship between soil organic carbon and pH value and calcium species in Yaji karst region, Giulin. *Geol. Rev.* **2017**, *63*, 1117–1126. (In Chinese)
38. Yang, H.; Cao, J.H.; Sun, L.; Luan, H.N.; Hou, Y.L. Fractions and distribution of inorganic phosphorus in different land use types of karst area. *J. Soil Water Conserv.* **2010**, *24*, 135–140. (In Chinese)
39. Wen, J.; Ji, H.; Sun, N.; Tao, H.; Du, B.; Hui, D.; Liu, C. Imbalanced plant stoichiometry at contrasting geologic-derived phosphorus sites in subtropics: The role of microelements and plant functional group. *Plant Soil* **2018**, *430*, 113–125. [CrossRef]
40. Yang, H.; Zhu, T.B.; Wang, X.H.; Pu, J.B.; Li, J.H.; Zhang, T.; Cao, J.H. Soil element contents of typical small watershed in the plateau area of karst fault basin, Yunnan. *Ecol. Environ. Sci.* **2018**, *27*, 859–865. (In Chinese)
41. Sheng, M.Y.; Xiong, K.N.; Cui, G.Y.; Liu, Y. Plant diversity and soil physical-chemical properties in karst rocky desertification ecosystem of Guizhou, China. *Acta Ecol. Sin.* **2015**, *35*, 434–448. (In Chinese)
42. Bárcenas-Moreno, G.; Rousk, J.; Bååth, E. Fungal and bacterial recolonisation of acid and alkaline forest soils following artificial heat treatments. *Soil Biol. Biochem.* **2011**, *43*, 1023–1033. [CrossRef]

43. Grabovich, M.Y.D.G.; Churikova, V.V.; Churikov, S.N.; Korovina, T.I. Mechanisms of synthesis and utilization of oxalate inclusions in the colorless sulfur bacterium Macromonas bipunctata. *Mikrobiology* **1995**, *64*, 630–636.
44. Silver, W.L.; Miya, R.K. Global patterns in root decomposition: Comparisons of climate and litter quality effects. *Oecologia* **2001**, *129*, 407–419. [CrossRef]

forests

MDPI

Article

Differential Responses and Controls of Soil CO_2 and N_2O Fluxes to Experimental Warming and Nitrogen Fertilization in a Subalpine Coniferous Spruce (*Picea asperata* Mast.) Plantation Forest

Dandan Li [1], Qing Liu [1,*], Huajun Yin [1], Yiqi Luo [2] and Dafeng Hui [3]

[1] Key Laboratory of Mountain Ecological Restoration and Bioresource Utilization & Ecological Restoration Biodiversity Conservation Key Laboratory of Sichuan Province, Chengdu Institute of Biology, Chinese Academy of Sciences, Chengdu 610041, China; ddli1984@hotmail.com (D.L.); yinhj@cib.ac.cn (H.Y.)
[2] Department of Biological Sciences, Northern Arizona University, Flagstaff, AZ 86001, USA; Yiqi.Luo@nau.edu
[3] Department of Biological Sciences, Tennessee State University, Nashville, TN 37209, USA; dhui@tnstate.edu
* Correspondence: liuqing@cib.ac.cn

Received: 13 August 2019; Accepted: 15 September 2019; Published: 17 September 2019

Abstract: Emissions of greenhouse gases (GHG) such as CO_2 and N_2O from soils are affected by many factors such as climate change, soil carbon content, and soil nutrient conditions. However, the response patterns and controls of soil CO_2 and N_2O fluxes to global warming and nitrogen (N) fertilization are still not clear in subalpine forests. To address this issue, we conducted an eight-year field experiment with warming and N fertilization treatments in a subalpine coniferous spruce (*Picea asperata* Mast.) plantation forest in China. Soil CO_2 and N_2O fluxes were measured using a static chamber method, and soils were sampled to analyze soil carbon and N contents, soil microbial substrate utilization (MSU) patterns, and microbial functional diversity. Results showed that the mean annual CO_2 and N_2O fluxes were 36.04 ± 3.77 mg C m^{-2} h^{-1} and 0.51 ± 0.11 μg N m^{-2} h^{-1}, respectively. Soil CO_2 flux was only affected by warming while soil N_2O flux was significantly enhanced by N fertilization and its interaction with warming. Warming enhanced dissolve organic carbon (DOC) and MSU, reduced soil organic carbon (SOC) and microbial biomass carbon (MBC), and constrained the microbial metabolic activity and microbial functional diversity, resulting in a decrease in soil CO_2 emission. The analysis of structural equation model indicated that MSU had dominant direct negative effect on soil CO_2 flux but had direct positive effect on soil N_2O flux. DOC and MBC had indirect positive effects on soil CO_2 flux while soil NH_4^+-N had direct negative effect on soil CO_2 and N_2O fluxes. This study revealed different response patterns and controlling factors of soil CO_2 and N_2O fluxes in the subalpine plantation forest, and highlighted the importance of soil microbial contributions to GHG fluxes under climate warming and N deposition.

Keywords: warming; nitrogen; greenhouse gas; soil characteristics; microbial properties

1. Introduction

Due to fossil fuel combustion and land use change, global air temperature has been increasing over the past decades [1]. The Qinghai–Tibet Plateau region (QTP) of China is experiencing a larger increase in temperature than other regions with an increasing rate of 0.2 °C per decade [2]. Accompanied with climate warming, nitrogen (N) deposition is increasing in many places on the Earth [3]. China has the third highest rate of nitrogen deposition, followed by North America and Western Europe due to the industrialization and intensive agricultural activities [3,4]. Additionally, in the QTP region, N deposition continues to increase. The climate warming and N deposition are likely to have significant

impacts on greenhouse gases (GHG) emissions in QTP ecosystems because the high-latitude regions are very sensitive to global change with large soil C pool, low inorganic N availability, and higher temperature sensitivity [3].

Carbon dioxide (CO_2) and nitrous oxide (N_2O) are two important GHGs, which contribute to about 60% and 6% of the global warming potential, respectively [2,5]. Many studies have investigated the effects of warming and N deposition on soil GHG fluxes, but large uncertainties still remain. For example, some studies found that warming leads to increase in soil CO_2 emission because it accelerates the decomposition of soil organic C (SOC) [6], but others reported that warming decreases or has no effect on soil CO_2 emission due to the loss of SOC in a long-term warming experiment [7]. Climate warming generally increases soil N_2O flux by enhancing decomposition and N mineralization [8,9], however, it may not influence soil N_2O flux or decrease it depending on the soil conditions [10]. Studies on the effect of N fertilization or deposition on GHG fluxes also showed various results. For example, Jassal et al. [11] found that the N application increases soil CO_2 and N_2O emissions in the first year, but shifts to soil N_2O uptake has no effect on soil CO_2 emission in the second year. Geng et al. [12] reported that the N addition at a low rate of 10 kg N ha^{-1} $year^{-1}$ significantly stimulated soil CO_2 emission, whereas the high rate of N addition (140 kg N ha^{-1} $year^{-1}$) significantly inhibits soil CO_2 emission in a temperate mixed forest.

The different responses of soil CO_2 and N_2O fluxes to global warming and N fertilization in different environments could be determined by soil physical–chemical properties such as soil temperature, soil inorganic nitrogen availability, and soil carbon content [13,14]. One study showed that soil CO_2 flux is positively related to soil dissolve organic carbon (DOC) and NO_3^--N, and soil N_2O flux is positively correlated with soil NH_4^+-N [14]. Another study found that soil CO_2 efflux is positively correlated with soil NH_4^+-N and negatively with soil NO_3^--N [12]. Thus, any changes in these soil properties caused by warming and N fertilization could have different impacts on GHG fluxes [15]. Indeed, Geng et al. [12] found high N addition enhances soil NO_3^--N and inhibits soil CO_2 emission, while low N addition does not affect soil NO_3^--N but stimulates soil CO_2 emission. Seo et al. [16] found warming increases the labile C pool, causes a loss of soil C, and increases soil CO_2 emission. Yin et al. [7] reported that warming decreases SOC and decreases soil CO_2 emission.

The influences of warming and N deposition on soil microbial activity and composition may have significant impacts on soil CO_2 and N_2O fluxes. Soil microorganisms are the major drivers in the biogeochemical processes such as soil C decomposition and N mineralization [17,18]. Any changes in soil microbial diversity and community structure may alter the C and N cycling [17]. For instance, the fungi to bacteria ratio is negatively correlated to soil N mineralization [19]. Furthermore, soil microorganisms can be affected by multiply factors such as climate, soil physical, and chemical properties, and substrate quantity and quality [20,21]. Several studies reported that soil microbial community structure and diversity are strongly impacted by warming and N fertilization, and play an important role on controlling soil CO_2 and N_2O fluxes [17,22,23]. However, convincing data about the direct link of soil GHG fluxes and soil microbial characteristics under warming and N fertilization are still scarce.

The subalpine and alpine forest ecosystems in Eastern Tibetan Plateau, located at the high latitude of the transition zone from the QTP to Sichuan basin, constitute the second largest biome in China and are the main forest ecosystems in southwest China [24]. Spruce (*Picea asperata* Mast.) is the dominant tree species of the plantation, which is the major forest ecosystem in this region after deforestation in the 1950s. Past studies on climate warming and N fertilization in forests in this region mostly focused on the soil C pool and N pool and associated processes [7,25,26]. Although soil GHG fluxes are highly related to the soil C and N pool, these data are not directly reflecting the GHG magnitude. Direct evidence of variations of the responses of soil CO_2 and N_2O fluxes and their controls is needed.

We took advantage of an eight-year field experiment with warming and N fertilization in subalpine spruce plantation forest, and measured soil CO_2 and N_2O fluxes over one year using the static chamber method. We also analyzed soil C and N contents, microbial substrate utilization patterns, and microbial

functional diversity using BIOLOG microplates. We aimed to quantify the magnitude of soil CO_2, N_2O fluxes in the plantation forest and the effects of climate warming and applying N fertilization on the gas fluxes, and reveal influential factors that control soil CO_2 and N_2O fluxes.

2. Materials and Methods

2.1. Experimental Site

The experimental site is located at the Maoxian Ecological Station of the Chinese Academy of Sciences, Sichuan Province, China (31°41′ N, 103°53′ E, 1820 m a.s.l.). The site is in a subalpine canyon zone at the transition region from Qinghai–Tibet Plateau (QTP) to Sichuan basin, with the mean annual temperature, total annual precipitation, and evaporation of 8.9 °C, 920 mm, and 796 mm, respectively. The experiment started in March 2007 with warming and N fertilization treatments and ended in 2015. Soil CO_2 and N_2O fluxes were measured for one year from 14 June 2014 to 25 June 2015, eight years after the treatments were applied.

2.2. Experimental Set-Up and Design

To avoid the potential effects of soil heterogeneity on soil GHG fluxes, we collected the top 50 cm soil from a nearby spruce plantation forest and replaced the indigenous soil in all plots. In March 2007, 40 healthy four-year-old seedlings of spruce were randomly planted in each plot (2 m × 2 m). The seedlings were collected from a local nursery. The experiment included four treatments: Control, warming, N fertilization, and warming and N fertilization. A randomized block design with four replicates (blocks) was used in this study. Artificial warming and N application started in April 2007 and continued to the end of the experiment. The heating method were described in detail in published papers of our research team [27,28]. Ammonium nitrate solution (25 g N m^{-2} $year^{-1}$) was added weekly to the soil surface of fertilization treatment. The equivalent amount of water was added to the other four pairs of plots for unfertilized treatments. In order to eliminate the potential effects of difference in soil water on soil processes between the warmed and un-warmed plots, the warmed plots were watered as frequently as needed and were monitored with a hand-held probe (IMKO, Ettlingen, Germany).

2.3. Microclimate Measurements

Air temperature (20 cm above soil surface) and soil temperature (5 cm depth) were measured using the DS1923G temperature sensor with iButton data loggers (Maxim/Dallas Semiconductor Inc., Dallas, TX, USA) at 60 min intervals. The warming effect decreased with the trees growth and plant coverage. The monthly air temperature in the warmed plots was increased by an average of 2.1, 1.9, 0.3 °C in 2007, 2011, and 2014, respectively. The monthly soil temperature in the warmed plots was increased by an average of 2.6, 3.6, and 0.6 °C in 2007, 2011, and in 2014, respectively.

2.4. Soil CO_2 and N_2O Fluxes Measurements

Soil CO_2 and N_2O fluxes were measured monthly using the static chamber method and gas chromatography technique from 14 June 2014 to 25 June 2015 according to Cai et al. [29]. One PVC tube base with a groove outside but without top and bottom (20 cm inside diameter, and 15 cm height) was inserted into a 10 cm-depth soil in each plot. The removable chamber with a small silicon-sealed bent for gas sampling and a port for measuring chamber temperature at the top of the chamber (without bottom, 21 cm in diameter and 30 cm in height) was placed into the PVC tube base during sampling and removed afterwards. Litter and plants were removed around the tube base before fixing it and four replicates were set in each treatment.

Samples were taken between 10:00 a.m. and 1:00 p.m. in order to minimize diurnal variation in fluxes. Each time, four air samples of each chamber were manually pulled into 100 mL pre-evacuated gas collecting bags (made in Dalian, China) at 0, 15, 30, and 45 min after enclosure of the chamber, and

were taken to the laboratory for analysis using gas chromatography (Agilent 7890A, Santa Clara, CA, USA) within two weeks. Air temperature inside the chamber was measured with a mercury-in-glass thermometer at the time of gas sampling. Soil temperature and moisture were measured outside of each chamber with the DS1923G temperature sensor with iButton data loggers (Maxim/Dallas Semiconductor Inc., Dallas, TX, USA).

Soil CO_2 and N_2O fluxes were calculated as the slope of linear regression between gases concentration and time with an average chamber temperature [30]. All the coefficients of the linear regression (r^2) were greater than 0.80 in this study. Flux was calculated as:

$$\mathrm{F} = \frac{dc}{dt} \times \frac{\mathrm{p}}{0.082\mathrm{T}} \times \mathrm{M} \times \frac{\mathrm{V}}{\mathrm{A}} \quad (1)$$

where F is the gas flux (μg N m^{-2} h^{-1} for N_2O and mg C m^{-2} h^{-1} for CO_2), $\frac{dc}{dt}$ is the rate of change in gas concentration inside the chamber, p is barometric pressure at temperature T (atm), T is the air temperature inside the chamber in K, M is the molecular weight of the gas, 0.082 is the universal gas constant, V is the chamber volume (m^3) and A is the chamber area (m^2).

2.5. Soil Samples and Analysis

Soil samples (n = 4) in each treatment were collected in August and November of 2014, and February and May of 2015. At each sampling date, we took five topsoil (0–15 cm) cores (2.5 cm diameter) close to each chamber and then combined into one composite sample. Soil samples were sieved through 2 mm mesh to remove visible living plant and rock, stored in an icebox at 4 °C, and delivered to the laboratory for analysis.

Soil organic C (SOC) was determined using the $K_2Cr_2O_7$-H_2SO_4 wet digestion method [31]. After digestion with $K_2Cr_2O_7$-H_2SO_4, $FeSO_4$ was used to titrate the remaining $K_2Cr_2O_7$ in the digestion solution and SOC was calculated based on the consumptions of the $K_2Cr_2O_7$. The dissolve organic C (DOC) was measured using the $K_2Cr_2O_7$-H_2SO_4 wet digestion method after extracted by deionized water [32]. Total soil N (TN) was determined by semi-micro Kjeldahl digestion using Se, $CuSO_4$, and K_2SO_4 as catalysts [33]. Soil ammonium (NH_4^+), nitrate (NO_3^-), and nitrite (NO_2^-)-N concentrations were determined using Auto Analyzer 3 (AA3, Bran Luebbe, Norderstedt, Germany) after being extracted with 2 M KCl solution (soil:water = 1:5) for 1 h [34]. Microbial biomass C (MBC) and N (MBN) concentrations were measured with the chloroform fumigation extraction method [35]. MBC and MBN were calculated as the difference between the C and N concentrations extracted with 2 M K_2SO_4 solution of the fumigated and non-fumigated soil, respectively, and then divided an efficiency factor K = 0.45. All the concentrations were calculated based on soil dry weight.

Microbial substrate utilization (MSU) patterns were analyzed using BIOLOG ECO plates (Biolog, Inc., Hayward, CA, USA). Equivalent to 1.0 g dry soil from each fresh sample was first added into 99 mL distilled autoclaved water and was shaken for 20 min to ensure that all the fungal spores are well mixed. Then, the soil solutions were settled for 30 min at 4 °C to remove suspended clay particles. 150 μL supernatant was transferred to the plates and then was incubated at 25 °C for up to 168 h. The OD values (absorbance at 590 nm and 750 nm, respectively) were measured at each 24 h from 48 to 168 h with a microtiter-plate reader (Biolog GenIII Microstation, Biolog company, Hayward, CA, USA). The OD value at 590 nm subtracting the OD value at 750 nm, and then the difference in the control was subtracted from each well's OD to correct for background activity. To minimize the effects of different inoculation densities, data from the 96 h reading were normalized by h dividing the absorbency of each well by the average absorbency for the whole plate (average well color development, AWCD) [17]. AWCD reflect the metabolic activity of soil microbes. Moreover, the Shannon diversity index (H) and diversity index (U) were calculated to represent the diversity and uniformity of the microbial communities.

$$H = -\sum p_i ln p_i \quad (2)$$

$$U = \sqrt{\left(n_i^2\right)} \quad (3)$$

where $p_i = \frac{OD(i,j,t)}{\sum OD(i,j,t)}$; and $n_{i=OD(i,j,t)}$

2.6. Data Analysis

The exponential model was used to determine the sensitivity of soil GHG fluxes to soil temperature (T):

$$F = ae^{bT} \quad (4)$$

where F is the GHG flux, a is the value of flux at 0 °C, and b is the sensitivity of flux to temperature.

The flux sensitivity to temperature (Q_{10}) was calculated as:

$$Q_{10} = e^{10b} \quad (5)$$

The cumulative global warming potential (GWP, kg CO_2 hm^{-2}) was calculated by adding cumulative soil CO_2 flux, and the cumulative GWP from N_2O (cumulative N_2O flux multiplied by 298) [36].

The repeated measure-ANOVA was used to analyze the effects of warming and N fertilization on soil CO_2 and N_2O fluxes. A three-way analysis of variance (ANOVA) was used to test the effects of warming, N fertilization, and sample time (season) on TOC, DOC, TN, inorganic N, AWCD, H, and U. The ECO plates contained 31 types of carbon substrates. The microbial substrates utilization patterns were analyzed to identify the effects of treatments and soil environment factors such as soil water, temperature, soil DOC, SOC, and inorganic nitrogen using Canonical Correspondence Analysis (CCA) in the CANOCO 4.5 software (Microcomputer Power, Ithaca, NY, USA).

Structural equation modelling (SEM) was performed to determine the relative importance of soil variables to soil CO_2 and N_2O fluxes using the Amos 24.0 software package (IBM, New York, NY, USA). We first tested the relationships between the CO_2 and N_2O fluxes and soil properties before the SEM analysis. If the correlation was significant, that variable was put into the SEM. As microbial substrate utilization patterns included 31 types of carbon source utilization, we selected the significant correlations of the carbon source utilization with soil CO_2 and N_2O fluxes, and then used the Principal Component Analysis (PCA) to create a multivariate functional index. The best-fit model was derived using maximum likelihood and a chi-square test (χ^2), P-values, df, and root mean square errors of approximation (RSMEA) were used to evaluate model fitting.

3. Results

3.1. Soil Carbon, Nitrogen and Microbial Properties

Warming significantly increased soil NO_3^--N, NO_2^--N, DOC, and the ratio of MBC/MBN, but decreased TN, SOC, MBC, and MBN (Table 1). Nitrogen fertilization significantly increased soil NO_3^--N, TN, TOC, and the ratio of MBC/MBN, but decreased soil NO_2^--N, DOC, MBC, and MBN. The metabolic activity of soil microbes measured as the average absorbency for the whole BIOLOG ECO plate (AWCD), the Shannon diversity index (H), and uniformity index (U) varied seasonally (Table 1). Warming decreased AWCD and U. Nitrogen fertilization alone had no effect on AWCD and U but significantly affected these variables with warming. The CCA analysis identified 21 substrates that were the most important variables in separating plots along the environmental axes among the 31 carbon substrates (Figure 1). Most of these MSU patterns were correlated with temperature, soil DOC, and soil water. The correlation coefficient were 0.68, 0.72, −0.72 in CCA1 and −0.62, −0.18, 0.32 in CCA2 for temperature, soil DOC, and soil water, respectively.

Table 1. Factorial ANOVA results (p-values) of the effects of season, warming, nitrogen fertilization, as well as their interactions on the soil properties and microbial function diversity. MBC: Microbial biomass C, MBN: Microbial biomass N, SOC: Soil organic C, DOC: Dissolved organic C, TN: Total N, AWCD: Average well color development, H: Shannon diversity index, U: Uniformity.

Treatments	NO_3^--N	NH_4^+-N	NO_2^--N	TN	SOC	DOC	MBC	MBN	MBC/MBN	AWCD	H	U
Season (S)	<0.001	<0.001	<0.001	<0.001	<0.001	<0.001	<0.001	<0.001	<0.001	0.001	<0.001	0.010
Warming (W)	<0.001	0.756	<0.001	<0.001	<0.001	<0.001	<0.001	<0.001	<0.001	0.009	0.461	0.006
Nitrogen (N)	<0.001	0.103	<0.001	0.009	<0.001	<0.001	<0.001	<0.001	<0.001	0.237	0.953	0.276
S × W	<0.001	0.322	<0.001	<0.001	<0.001	<0.001	<0.001	<0.001	<0.001	<0.001	0.032	<0.001
S × N	<0.001	0.008	0.040	0.365	<0.001	<0.001	<0.001	<0.001	<0.001	0.002	0.013	0.006
W ×N	0.565	0.011	0.059	0.015	<0.001	0.002	0.003	<0.001	<0.001	0.016	0.115	0.032
S × W × N	<0.001	0.209	<0.001	0.080	<0.001	<0.001	<0.001	<0.001	<0.001	0.001	0.002	0.004

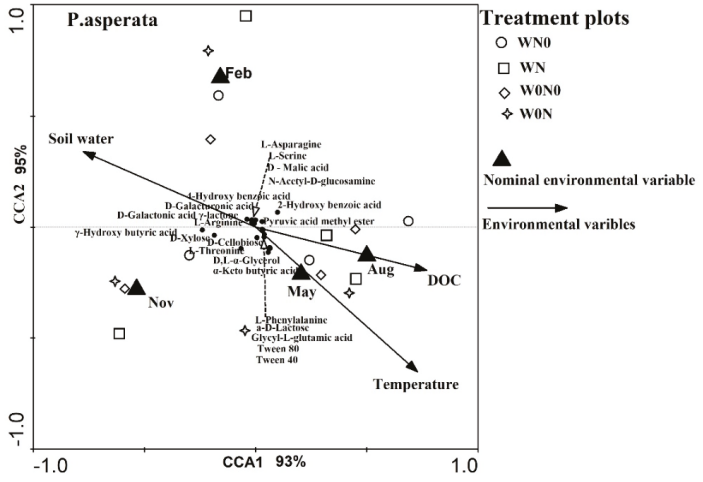

Figure 1. Canonical correspondence analysis (CCA) ordination biplot of treatment plot scores, Biolog substrates, and significant environmental variables. Arrows indicate the direction and relative importance (arrow length) of the environmental variable. Substrates with approximate correlation coefficient >0.20 to the environmental variables are labelled. W_0N_0: Ambient temperature without nitrogen fertilization; W_0N: Ambient temperature with nitrogen fertilization; WN0: Warming without nitrogen fertilization; WN: Warming with nitrogen fertilization. Environmental variables in CCA1 and CCA2 explain 93% and 95%, respectively.

3.2. Soil CO_2 and N_2O Fluxes

The highest soil CO_2 and N_2O fluxes occurred in August and the lowest in January (Figure 2). The mean annual CO_2 and N_2O fluxes were 36.04 ± 3.77 mg C m^{-2} h^{-1} and 0.51 ± 0.11 μg N m^{-2} h^{-1}, respectively (Table 2). Compared to the control (W_0N_0), the annual soil CO_2 flux was slightly decreased in the WN_0 and WN treatments but was increased by 27.8% in the W_0N treatment. Annual soil N_2O flux was increased by 8.2 times and 3.0 times in the W_0N and WN treatments. Soil CO_2 flux was mainly affected by warming, while soil N_2O flux was mainly affected by N fertilization and its interaction with warming. The cumulative GWP from CO_2 and N_2O were 9984 ± 321 and 20.31 ± 3.02 kg CO_2 hm^{-2}, respectively (Table 2).

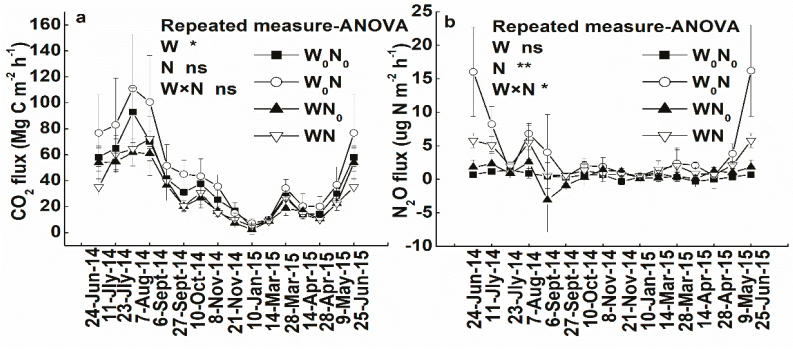

Figure 2. Seasonal changes of soil CO_2 (**a**) and N_2O fluxes (**b**) affected by warming and nitrogen fertilization. W_0N_0: Ambient temperature without nitrogen fertilization; W_0N: Ambient temperature with nitrogen fertilization; WN_0: Warming without nitrogen fertilization; WN: Warming with nitrogen fertilization.

Table 2. Mean annual fluxes of CO_2 (mg m^{-2} h^{-1}), N_2O (μg N m^{-2} h^{-1}) (means + SE) and the cumulative global warming potential (GWP) from CO_2 and N_2O fluxes (kg CO_2 hm^{-2} $year^{-1}$) as affected by treatments.

Variables	Treatment	CO_2	N_2O
Fluxes	W_0N_0	36.04 ± 3.77 ^{ab}	0.51 ± 0.11 ^{a}
	WN_0	27.90 ± 3.14 ^{a}	0.65 ± 0.27 ^{a}
	W_0N	46.08 ± 5.39 ^{b}	4.68 ± 1.61 ^{b}
	WN	29.07 ± 3.29 ^{a}	2.02 ± 0.32 ^{b}
GWP	W_0N_0	9984 ± 321 ^{ab}	20.31 ± 3.02 ^{a}
	WN_0	7800 ± 844 ^{a}	25.63 ± 10.33 ^{a}
	W_0N	12748 ± 2110 ^{b}	208.8 ± 56.37 ^{b}
	WN	8002 ± 282 ^{a}	79.88 ± 8.90 ^{b}
ANOVA (F values)	Warming	8.97 *	4.52
	N fertilization	1.64	17.47 **
	Warming * N fertilization	1.27	5.34 *

Different lowercase letters represent significant differences ($p < 0.05$) between the treatments analyzed by least-significant difference (LSD). Significant * $p < 0.05$, ** $p < 0.01$, *** $p < 0.001$.

3.3. Relationship between the Soil CO_2 and N_2O Fluxes and Environmental Factors

Soil CO_2 and N_2O fluxes increased exponentially with soil temperature across all treatments (Figure 3). The Q_{10} values for CO_2 flux were not significantly different among the control, W_0N, and WN_0 treatments, while Q_{10} in the WN treatment was increased to 5.54 compared to the control (3.94). The Q_{10} values for soil N_2O flux was increased by N fertilization without warming but was decreased by N fertilization with warming.

Soil CO_2 flux was positively correlated with soil MBC, DOC and the microbial substrates utilization, and negatively correlated with soil NH_4^+-N. Soil N_2O flux was positively correlated with the MSU and negatively correlated with soil NH_4^+-N (Figure 3).

3.4. Contributions of Soil Variables to Soil CO_2 and N_2O Fluxes

To quantify the relative importance of the different controlling factors on soil CO_2 and N_2O fluxes, two structural equation modellings (SEMs) were constructed based on the known relationships between soil CO_2 and N_2O fluxes and their key drivers in soil. The SEM showed a better fit to our hypothesized causal relationships ($\chi^2 = 2.82$, $p = 0.59$, RMSEA) = 0.000, Figure 4a; $\chi^2 = 0.81$, $p = 0.94$, RMSEA = 0.000, Figure 4b). The models accounted for 63% and 22% of the variance of soil CO_2 and N_2O fluxes, respectively. Microbial substrates utilization patterns had dominant direct negative effect on soil CO_2 flux and positive effect on N_2O (Figure 5). Soil NH_4^+-N had negative effects on soil CO_2 and N_2O fluxes. DOC and MBC had indirect positive effects on soil CO_2. In addition, soil NO_3^--N and NO_2^--N had indirect effects on soil N_2O.

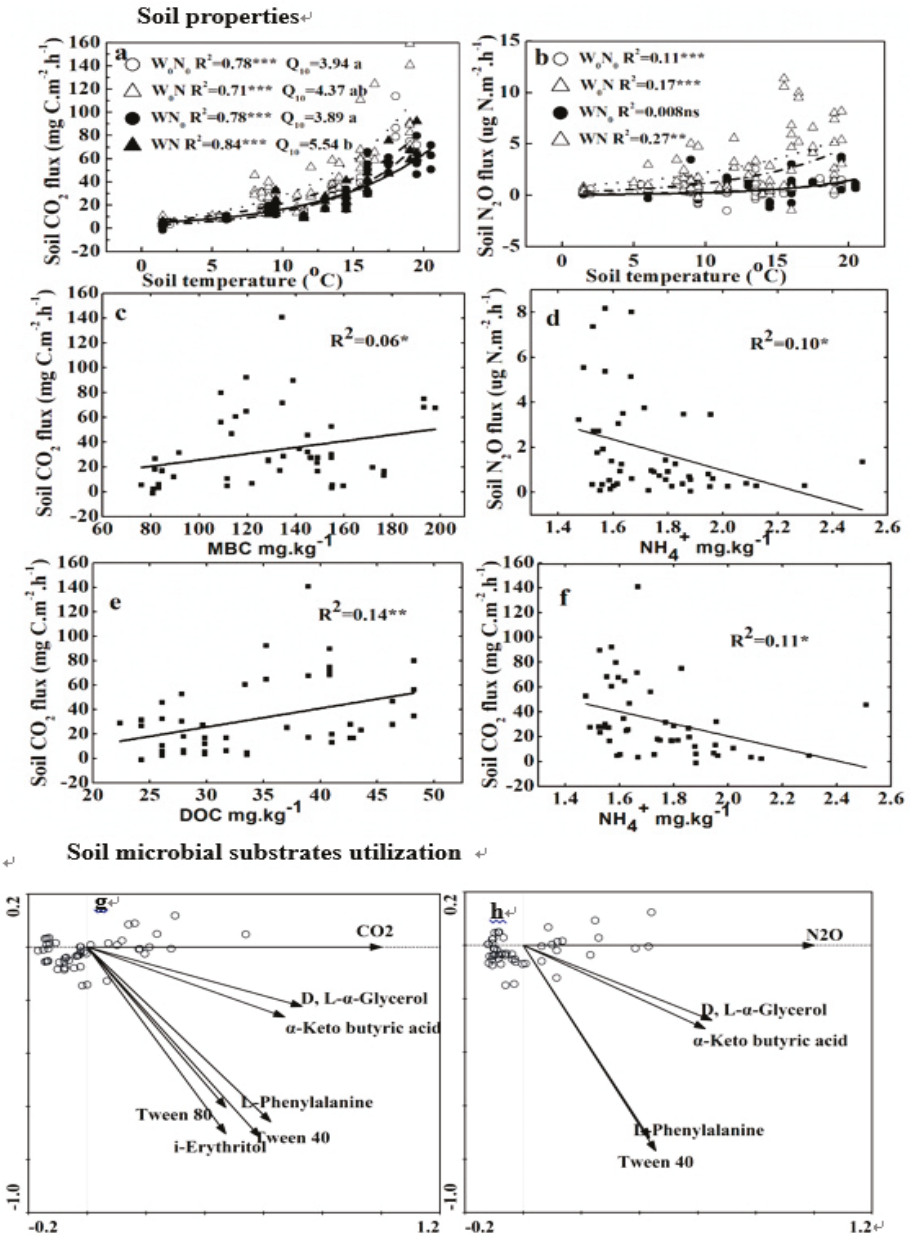

Figure 3. Relationships between the fluxes of soil CO_2 and soil temperature (**a**), MBC (**c**), DOC (**e**), soil NH_4^+ (**f**) and soil microbial substrates utilization (**g**), and between the fluxes of soil N_2O and soil temperature (**b**), soil NH_4^+ (**d**), and carbon utilization of microbial communities (**h**) in the different treatments. Q_{10} values with different lowercase letters indicate significant difference at $p < 0.05$. W_0N_0: Ambient temperature without nitrogen fertilization; W_0N: Ambient temperature with nitrogen fertilization; WN_0: Warming without nitrogen fertilization; WN: Warming with nitrogen fertilization. Different lowercase letters in Figure 3a represent significant differences ($p < 0.05$) between the treatments using least square difference (LSD) method. Significant * $p < 0.05$, ** $p < 0.01$, *** $p < 0.001$.

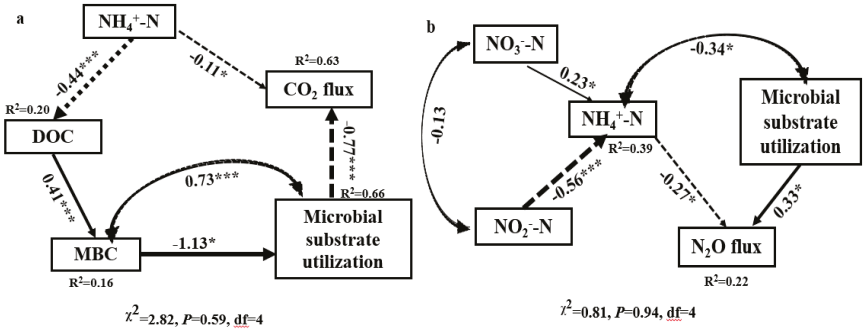

Figure 4. Result of structural equation modelling (SEM) to assess the direct and indirect effects of soil carbon, nitrogen, and microbial properties on soil CO_2 (**a**) and N_2O fluxes (**b**). Single-headed arrows indicate the hypothesized direction of causation. Double-headed arrows represent covariance between related variables. Arrow width is proportional to the strength of the relationship. The numbers adjacent to arrows are standardized path coefficient, which reflect the effect size of the relationship. R^2 value represent the proportion of variance explained for each endogenous variable. Significant * $p < 0.05$, ** $p < 0.01$, *** $p < 0.001$.

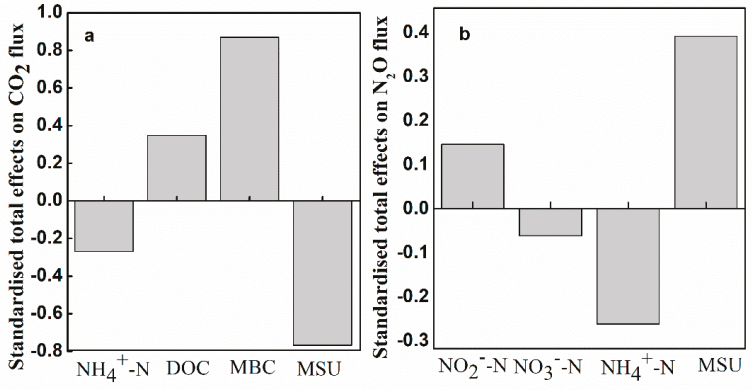

Figure 5. Standardized total effects of soil variables on soil CO_2 (**a**) and N_2O fluxes (**b**) derived from structural equation modelling (SEM). MSU: Microbial substrate utilizations; DOC: Dissolved organic C; MBC: Microbial biomass C.

4. Discussion

4.1. Effects of Warming and Nitrogen Fertilization on Soil CO_2 Flux

We found that warming decreased soil CO_2 flux, while the N fertilization and its interaction with warming had no significant effect on soil CO_2 flux (Figure 2a, Table 2). These results were quite different to some previous studies. For example, Zou et al. [5] and Xu et al. [37] found warming increases soil CO_2 flux in spruce forests, and the effect of N fertilization on soil CO_2 flux varied in forest plantations [12,38,39]. These differences were a consequence of the different soil properties and experimental conditions among these sites, as the interactions among climate, soil organisms, and vegetation, and the duration of experiment could influence soil CO_2 flux [40].

Carbon quality and quantity could regulate the responses of soil CO_2 flux to temperature. The decrease in soil respiration could be due to the consuming of labile C [41,42]. In this study, the experimental plots were filled with forest soil and spruce seedlings were planted in the plots. There was very limited C input compared to the forest plantation with mature trees. Consequently, the CO_2

emission could be restricted by less carbon in the soil [7]. Indeed, SOC and MBC at the site were lower after eight years of warming, although soil DOC was enhanced in this study. Bossio et al. [43] also found similar results. Although SEM analysis showed that soil DOC had a positive effect on soil CO_2 emission, the decreases in MBC had larger effect on soil CO_2 emission than the increases in DOC (Figures 4a and 5a). Overall, warming decreased soil CO_2 emission.

Climate warming and N fertilization studies have mostly focused on the changes of microbial processes (respiration and N mineralization) [25,26]. Few studies have investigated the direct link of soil microbial community with soil CO_2 flux. In this study, we found that microbial substrate utilization patterns had a direct negative effect on soil CO_2 flux (Figures 4a and 5a). This result suggested that there is an association of soil microbial community composition with the response of soil CO_2 flux to warming and N fertilization, as different microbial communities had different sole substrate utilization patterns in the BIOLOG ECO-plate analysis [44]. The CCA analysis further showed that the MSU patterns were positively correlated with soil DOC and soil temperature in the CCA1 although they had contrast effects in the CCA2 (Figure 3). It suggested that climate warming could enhance the activity of the microbial community and the DOC, then reduce the quantity of SOC, and finally decrease soil CO_2 emission. A similar result was reported by Walker et al. [43] who found that permanent warming accelerates microbial activity and causes more carbon loss from soil, and the soil carbon loss in return reduces soil microbial biomass and constrains the influence of microbes on the ecosystem. In this study, warming decreased the microbial metabolic activity represented by AWCD and uniformity of microbial community. The result further suggested that warming induced a shift of microbial community structure from bacteria to fungi. Since fungi have lower growth rates than bacteria on BIOLOG plates, higher fungal dominance may have lower color development rate, resulting in lower AWCD [17]. Consistently, the higher ratio of MBC/MBN in the warmed plots indicated that warming enhanced the fungi as the microbial biomass C/N ratio has been used as an indicator of changes in microbial community structure [45]. Since fungi have greater C assimilation efficiency compared to bacteria, warming decreased the CO_2 release [17,46]. These findings highlighted the important contribution of soil microbial community to soil CO_2 emission.

Moreover, soil carbon quality and quantity and microbes, soil N had a significant effect on soil CO_2 flux. Previous studies showed that the soil N availability affects the soil C turnover by modifying microbial composition and activity or through its limitation on plant growth [47,48]. With sufficient C supply, an increase in N availability could stimulate the microbial activity, and accelerate SOC mineralization [49]. In this study, there was relatively a lack of soil C and no effect on microbial community induced by N fertilization. As a result, N fertilization did not affect the soil CO_2 flux. One surprising finding was that soil NH_4^+-N had a negative effect on soil CO_2 flux in this study (Figure 4a). The positive effect of soil NH_4^+ on soil CO_2 flux had been reported in temperate and subtropical forests [12,50]. The difference between our study and the previous studies may be attributed to the following two reasons. One reason was that spruce prefers to absorb soil NO_3^--N than soil NH_4^+-N [51]. As NH_4^+ was strongly absorbed and held to cation exchange sites of SOC and clay minerals, it would lead to declines in labile C compounds and increases in complex C compounds [50,52]. Thus, soil NH_4^+ had a negative effect on soil DOC as shown in the SEM (Figure 4a). The second reason was that soil NH_4^+ had a negative relationship with the microbial substrate utilization (Figure 4), tended to inhibit soil microbial activity and community composition, and resulted in a decrease in the decomposition of SOC [50]. Therefore, soil NH_4^+ had a negative effect on soil CO_2 flux in this study.

4.2. Effects of Warming and Nitrogen Fertilization on Soil N_2O Flux

Previous studies showed strong positive correlations between soil temperature and N_2O emission in temperate forests [53,54], but quite weak correlations in tropical forests [55,56]. In this study, we found that the soil N_2O emission was slightly positively correlated with the soil temperature and warming did not significantly affect soil N_2O flux in the subalpine plantation forest. However, applying N fertilization had a positive effect on soil N_2O emission. These results suggested that the soil N

condition rather than the temperature controls soil N_2O emission. Consistent with our study, other studies also found that soil N_2O emission increased with N addition in forests [57,58]. The reasons could be that high NO_3^- deposition provided additional N for denitrification and thus increased soil N_2O emission. In this study, the fertilizer as NH_4NO_3 was added into the soil and resulted in an increase in soil NO_3^-, but the SEM indicated that the soil NH_4^+ and NO_2^- were the key factors controlling soil N_2O emission and soil NO_3^- had little effect on soil N_2O. Furthermore, N fertilization had no effect on soil NH_4^+ and decreased soil NO_2^- which may result from enhanced nitrification of soil NH_4^+ and denitrification of soil NO_2^- by nitrifier. The resulting increase in soil N_2O emission, with the depletion of soil NH_4^+, was probably not due to plant uptake as spruce prefers to uptake soil NO_3^- than NH_4^+ [51]. In theory, inorganic N, as the substrate for nitrification and denitrification processes, should be positively correlated with soil N_2O emission regardless of N forms [14,57]. However, more soil NH_4^+ decreased the soil DOC (Figure 4a) and inhibited the soil microbiomes activity (Figure 4b). Since soil N_2O emission was positively correlated with soil CO_2 flux, soil NH_4^+ had the negative effect on soil N_2O emission.

Soil microbe is another factor controlling soil N_2O emission (Figure 4b). The analysis of SEM showed that the soil microbial substrate utilization pattern had a positive effect on soil N_2O emission, which provided direct information that the soil microbial activity controls the soil N_2O emission under global change. Several previous studies showed that climate change can impact N transformations and N_2O emissions via indirect effects on the abundance of different microbial populations and microbial community structure [9,59]. For instance, Cantarel et al. [9] showed a stronger correlation of N_2O fluxes with the soil denitrification activity and the nirK denitrifiers community. In this study, the method of the BIOLOG ECO plates identified soil microbial community and functional diversity mainly through carbon substrates, which may not be sensitive to N addition and may not directly reflect N transformation. Thus, MSU patterns was not affected by N fertilization in this study. Future study is needed to determine the relative importance of the specific microbial activities in nitrification and denitrification.

Furthermore, N condition and microbes, many other soil environmental factors such as soil moisture and soil pH may influence soil N_2O emission [60]. In this study, soil moisture was not influenced by treatments as plots were monitored and watered as frequently as needed to eliminate the effects of soil moisture induced by warming. Seasonal variation of soil N_2O flux could be influenced by soil moisture change. Soil pH varied slightly seasonally and among different treatments, and might not have a large influence on soil N_2O emission. In addition, soil moisture and soil pH mainly affect the soil N availability and soil microbial activity and then indirectly influence soil N_2O emission [60]. Thus, soil N condition and soil microbes were the main factors controlling soil N_2O emission.

5. Conclusions

Eight years after continuous warming and N fertilization in a subalpine spruce plantation forest, we found that soil CO_2 flux was decreased by warming while soil N_2O flux was significantly increased by N fertilization and its interaction with warming. Warming enhanced the DOC and MSU pattern, reduced SOC and MBC, and further constrained the metabolic potential of soil microbes, uniformity index of microbial communities, and finally resulted in a decrease in soil CO_2 emission. For soil N_2O emission, the MSU pattern and soil NO_2^- had positive effects on soil N_2O flux, while the soil NH_4^+ had a negative effect on soil N_2O emission. Both for soil CO_2 flux and N_2O flux, the microbes played a more important role than other factors. This study revealed different response patterns and controls of soil CO_2 and N_2O fluxes in the subalpine plantation forest under climate warming and N deposition, and further highlighted the important contributions of soil microbes to GHG fluxes.

Author Contributions: Conceptualization, D.L. and Q.L.; Methodology, H.Y.; Software, Y.L.; Validation, D.L., Q.L., H.Y., Y.L., and D.H.; Formal analysis, Y.L. and D.H.; Investigation, D.L. and H.Y.; Resources, Q.L.; Data curation, D.L.; Writing—original draft preparation, D.L.; Writing—review and editing, D.L., Q.L., and D.H; Supervision, H.Y.; Project administration, D.L.; Funding acquisition, D.L. and Q.L.

Funding: This research was funded by the National Key R&D Program of China, 2017YFC0505002 and the China Scholarship Council, CSC201804910053.

Acknowledgments: We would like to express our gratitude to the Maoxian Ecological Station of the Chinese Academy of Sciences, Sichuan Province, China, who gave permission to conduct the experiment in this study.

Conflicts of Interest: The authors declare no conflict of interest.

References

1. Trenberth, K.E. Stronger evidence of human influences on climate—The 2001 IPCC assessment. *Environment* **2001**, *43*, 8–19. [CrossRef]
2. IPCC. *Climate Change 2013: The Physical Science Basis*; Cambridge University Press: Cambridge, UK; New York, NY, USA, 2013.
3. Chen, X.P.; Wang, G.X.; Zhang, T.; Mao, T.X.; Wei, D.; Hu, Z.Y.; Song, C.L. Effects of warming and nitrogen fertilization on GHG flux in the permafrost region of an alpine meadow. *Atmos. Environ.* **2017**, *157*, 111–124. [CrossRef]
4. Galloway, J.N.; Cowling, E.B. Reactive nitrogen and the world: 200 years of change. *Ambio* **2002**, *31*, 64–71. [CrossRef]
5. Zou, J.L.; Tobin, B.; Luo, Y.Q.; Osborne, B. Differential responses of soil CO_2 and N_2O fluxes to experimental warming. *Agric. For. Meteorol.* **2018**, *259*, 11–22. [CrossRef]
6. Wu, Z.T.; Dijkstra, P.; Koch, G.W.; Penuelas, J.; Hungate, B.A. Responses of terrestrial ecosystems to temperature and precipitation change: A meta-analysis of experimental manipulation. *Glob. Chang. Biol.* **2011**, *17*, 927–942. [CrossRef]
7. Yin, H.J.; Xiao, J.; Li, Y.F.; Chen, Z.; Cheng, X.Y.; Zhao, C.Z.; Liu, Q. Warming effects on root morphological and physiological traits: The potential consequences on soil C dynamics as altered root exudation. *Agric. For. Meteorol.* **2013**, *180*, 287–296. [CrossRef]
8. Bijoor, N.S.; Czimczik, C.I.; Pataki, D.E.; Billings, S.A. Effects of temperature and fertilization on nitrogen cycling and community composition of an urban lawn. *Glob. Chang. Biol.* **2008**, *14*, 2119–2131. [CrossRef]
9. Cantarel, A.A.M.; Bloor, J.M.G.; Pommier, T.; Guillaumaud, N.; Moirot, C.; Soussana, J.F.; Poly, F. Four years of experimental climate change modifies the microbial drivers of N_2O fluxes in an upland grassland ecosystem. *Glob. Chang. Biol.* **2012**, *18*, 2520–2531. [CrossRef]
10. Hu, Y.G.; Chang, X.F.; Lin, X.W.; Wang, Y.F.; Wang, S.P.; Duan, J.C.; Zhang, Z.H.; Yang, X.X.; Luo, C.Y.; Xu, G.P.; et al. Effects of warming and grazing on N_2O fluxes in an alpine meadow ecosystem on the Tibetan plateau. *Soil Biol. Biochem.* **2010**, *42*, 944–952. [CrossRef]
11. Jassal, R.S.; Black, T.A.; Trofymow, J.A.; Roy, R.; Nesic, Z. Soil CO_2 and N_2O flux dynamics in a nitrogen-fertilized Pacific Northwest Douglas-fir stand. *Geoderma* **2010**, *157*, 118–125. [CrossRef]
12. Geng, J.; Cheng, S.L.; Fang, H.J.; Yu, G.R.; Li, X.Y.; Si, G.Y.; He, S.; Yu, G.X. Soil nitrate accumulation explains the nonlinear responses of soil CO_2 and CH4 fluxes to nitrogen addition in a temperate needle-broadleaved mixed forest. *Ecol. Indic.* **2017**, *79*, 28–36. [CrossRef]
13. Huang, R.; Wang, Y.; Liu, J.; Li, J.; Xu, G.; Luo, M.; Xu, C.; Ci, E.; Gao, M. Variation in N_2O emission and N_2O related microbial functional genes in straw- and biochar-amended and non-amended soils. *Appl. Soil Ecol.* **2019**, *137*, 57–68. [CrossRef]
14. Zhang, J.J.; Peng, C.H.; Zhu, Q.A.; Xue, W.; Shen, Y.; Yang, Y.Z.; Shi, G.H.; Shi, S.W.; Wang, M. Temperature sensitivity of soil carbon dioxide and nitrous oxide emissions in mountain forest and meadow ecosystems in China. *Atmos. Environ.* **2016**, *142*, 340–350. [CrossRef]
15. Shrestha, R.K.; Strahm, B.D.; Sucre, E.B. Greenhouse gas emissions in response to nitrogen fertilization in managed forest ecosystems. *New For.* **2015**, *46*, 167–193. [CrossRef]
16. Seo, J.; Jang, I.; Jung, J.Y.; Lee, Y.K.; Kang, H. Warming and increased precipitation enhance phenol oxidase activity in soil while warming induces drought stress in vegetation of an Arctic ecosystem. *Geoderma* **2015**, *259*, 347–353. [CrossRef]
17. Zhang, W.; Parker, K.M.; Luo, Y.; Wan, S.; Wallace, L.L.; Hu, S. Soil microbial responses to experimental warming and clipping in a tallgrass prairie. *Glob. Chang. Biol.* **2005**, *11*, 266–277. [CrossRef]

18. Qin, H.L.; Xing, X.Y.; Tang, Y.F.; Hou, H.J.; Yang, J.; Shen, R.; Zhang, W.Z.; Liu, Y.; Wei, W.X. Linking soil N_2O emissions with soil microbial community abundance and structure related to nitrogen cycle in two acid forest soils. *Plant Soil* **2019**, *435*, 95–109. [CrossRef]
19. Hogberg, P.; Hogberg, M.N.; Gottlicher, S.G.; Betson, N.R.; Keel, S.G.; Metcalfe, D.B.; Campbell, C.; Schindlbacher, A.; Hurry, V.; Lundmark, T.; et al. High temporal resolution tracing of photosynthate carbon from the tree canopy to forest soil microorganisms. *New Phytol.* **2008**, *177*, 220–228. [CrossRef]
20. Djukic, I.; Zehetner, F.; Watzinger, A.; Horacek, M.; Gerzabek, M.H. In situ carbon turnover dynamics and the role of soil microorganisms therein: A climate warming study in an Alpine ecosystem. *FEMS Microbiol. Ecol.* **2013**, *83*, 112–124. [CrossRef]
21. Gholz, H.L.; Wedin, D.A.; Smitherman, S.M.; Harmon, M.E.; Parton, W.J. Long-term dynamics of pine and hardwood litter in contrasting environments: Toward a global model of decomposition. *Glob. Chang. Biol.* **2000**, *6*, 751–765. [CrossRef]
22. Wang, Y.S.; Cheng, S.L.; Fang, H.J.; Yu, G.R.; Yang, X.M.; Xu, M.J.; Dang, X.S.; Li, L.S.; Wang, L. Relationships between ammonia-oxidizing communities, soil methane uptake and nitrous oxide fluxes in a subtropical plantation soil with nitrogen enrichment. *Eur. J. Soil Biol.* **2016**, *73*, 84–92. [CrossRef]
23. Martins, C.S.C.; Macdonald, C.A.; Anderson, I.C.; Singh, B.K. Feedback responses of soil greenhouse gas emissions to climate change are modulated by soil characteristics in dryland ecosystems. *Soil Biol. Biochem.* **2016**, *100*, 21–32. [CrossRef]
24. Xu, Z.F.; Yin, H.J.; Xiong, P.; Wan, C.; Liu, Q. Short-term responses of Picea asperata seedlings of different ages grown in two contrasting forest ecosystems to experimental warming. *Environ. Exp. Bot.* **2012**, *77*, 1–11. [CrossRef]
25. Zhao, C.; Zhu, L.; Liang, J.; Yin, H.; Yin, C.; Li, D.; Zhang, N.; Liu, Q. Effects of experimental warming and nitrogen fertilization on soil microbial communities and processes of two subalpine coniferous species in Eastern Tibetan Plateau, China. *Plant Soil* **2014**, *382*, 189–201. [CrossRef]
26. Yin, H.J.; Li, Y.F.; Xiao, J.; Xu, Z.F.; Cheng, X.Y.; Liu, Q. Enhanced root exudation stimulates soil nitrogen transformations in a subalpine coniferous forest under experimental warming. *Glob. Chang. Biol.* **2013**, *19*, 2158–2167. [CrossRef]
27. Zhang, Z.L.; Qiao, M.F.; Li, D.D.; Yin, H.J.; Liu, Q. Do warming-induced changes in quantity and stoichiometry of root exudation promote soil N transformations via stimulation of soil nitrifiers, denitrifiers and ammonifiers? *Eur. J. Soil Biol.* **2016**, *74*, 60–68. [CrossRef]
28. Yin, H.J.; Chen, Z.; Liu, Q. Effects of experimental warming on soil N transformations of two coniferous species, Eastern Tibetan Plateau, China. *Soil Biol. Biochem.* **2012**, *50*, 77–84. [CrossRef]
29. Cai, Y.J.; Wang, X.D.; Tian, L.L.; Zhao, H.; Lu, X.Y.; Yan, Y. The impact of excretal returns from yak and Tibetan sheep dung on nitrous oxide emissions in an alpine steppe on the Qinghai-Tibetan Plateau. *Soil Biol. Biochem.* **2014**, *76*, 90–99. [CrossRef]
30. Liu, H.; Zhao, P.; Lu, P.; Wang, Y.S.; Lin, Y.B.; Rao, X.Q. Greenhouse gas fluxes from soils of different land-use types in a hilly area of South China. *Agric. Ecosyst. Environ.* **2008**, *124*, 125–135. [CrossRef]
31. Walkley, A.; Black, L.A. An examination of the Dgtjareff method for determining soil organic matter, and a proposed modification of the chromic acid titration method. *Soil Sci.* **1934**, *37*, 29–38. [CrossRef]
32. Li, Y.Q.; Qing, Y.X.; Lyu, M.K.; Chen, S.D.; Yang, Z.J.; Lin, C.F.; Yang, Y.S. Effects of artificial warming on different soil organic carbon and nitrogen pools in a subtropical plantation. *Soil Biol. Biochem.* **2018**, *124*, 161–167. [CrossRef]
33. Cohen, J.B. *Practical Organic Chemistry*; Macmillan Collection Library: London, UK, 1910.
34. Maynard, D.G.; Kalra, Y.P. Nitrate and exchangeable ammonium nitrogen. In *Soil Sampling and Methods of Analysis*; Carter, M.R., Ed.; Lewis: Edmonton, AB, Canada, 1993.
35. Vance, E.D.; Brookes, P.C.; Jenkinson, D.S. An Extraction Method for Measuring Soil Microbial Biomass-C. *Soil Biol. Biochem.* **1987**, *19*, 703–707. [CrossRef]
36. Dijkstra, F.A.; Morgan, J.A.; Follett, R.F.; Lecain, D.R. Climate change reduces the net sink of CH4 and N_2O in a semiarid grassland. *Glob. Chang. Biol.* **2013**, *19*, 1816–1826. [CrossRef]
37. Xu, Z.F.; Wan, C.A.; Xiong, P.; Tang, Z.; Hu, R.; Cao, G.; Liu, Q. Initial responses of soil CO_2 efflux and C, N pools to experimental warming in two contrasting forest ecosystems, Eastern Tibetan Plateau, China. *Plant Soil* **2010**, *336*, 183–195. [CrossRef]

38. Zhang, J.J.; Li, Y.F.; Chang, S.X.; Qin, H.; Fu, S.L.; Jiang, P.K. Understory management and fertilization affected soil greenhouse gas emissions and labile organic carbon pools in a Chinese chestnut plantation. *For. Ecol. Manag.* **2015**, *337*, 126–134. [CrossRef]
39. Deng, Q.; Zhou, G.; Liu, J.; Liu, S.; Duan, H.; Zhang, D. Responses of soil respiration to elevated carbon dioxide and nitrogen addition in young subtropical forest ecosystems in China. *Biogeosciences* **2010**, *7*, 315–328. [CrossRef]
40. Barrena, I.; Menéndez, S.; Duñabeitia, M.; Merino, P.; Stange, C.F.; Spott, O.; González-Murua, C.; Estavillo, J.M. Greenhouse gas fluxes (CO_2, N_2O and CH_4) from forest soils in the Basque Country: Comparison of different tree species and growth stages. *For. Ecol. Manag.* **2013**, *310*, 600–611. [CrossRef]
41. Luo, Y.Q.; Wan, S.Q.; Hui, D.F.; Wallace, L.L. Acclimatization of soil respiration to warming in a tall grass prairie. *Nature* **2001**, *413*, 622–625. [CrossRef]
42. Oechel, W.C.; Vourlitis, G.L.; Hastings, S.J.; Zulueta, R.C.; Hinzman, L.; Kane, D. Acclimation of ecosystem CO_2 exchange in the Alaskan Arctic in response to decadal climate warming. *Nature* **2000**, *406*, 978–981. [CrossRef]
43. Walker, T.W.N.; Kaiser, C.; Strasser, F.; Herbold, C.W.; Leblans, N.I.W.; Woebken, D.; Janssens, I.A.; Sigurdsson, B.D.; Richter, A. Microbial temperature sensitivity and biomass change explain soil carbon loss with warming. *Nat. Clim. Chang.* **2018**, *8*. [CrossRef]
44. Bossio, D.A.; Scow, K.M. Impact of Carbon and Flooding on the Metabolic Diversity of Microbial Communities in Soils. *Appl. Environ. Microb.* **1995**, *61*, 4043–4050.
45. Paul, E.A.; Clark, F.E. *Soil Microbiology and Biochemistry*; Academic Press: San Diego, CA, USA, 1989.
46. Sakamoto, K.; Oba, Y. Effect of Fungal to Bacterial Biomass Ratio on the Relationship between CO_2 Evolution and Total Soil Microbial Biomass. *Biol. Fert. Soils* **1994**, *17*, 39–44. [CrossRef]
47. Chen, R.R.; Senbayram, M.; Blagodatsky, S.; Myachina, O.; Dittert, K.; Lin, X.G.; Blagodatskaya, E.; Kuzyakov, Y. Soil C and N availability determine the priming effect: Microbial N mining and stoichiometric decomposition theories. *Glob. Chang. Biol.* **2014**, *20*, 2356–2367. [CrossRef]
48. Fisk, M.; Santangelo, S.; Minick, K. Carbon mineralization is promoted by phosphorus and reduced by nitrogen addition in the organic horizon of northern hardwood forests. *Soil Biol. Biochem.* **2015**, *81*, 212–218. [CrossRef]
49. Qiu, Q.Y.; Wu, L.F.; Ouyang, Z.; Li, B.B.; Xu, Y.Y.; Wu, S.S.; Gregorich, E.G. Priming effect of maize residue and urea N on soil organic matter changes with time. *Appl. Soil Ecol.* **2016**, *100*, 65–74. [CrossRef]
50. Wang, Y.S.; Cheng, S.L.; Fang, H.J.; Yu, G.R.; Xu, X.F.; Xu, M.J.; Wang, L.; Li, X.Y.; Si, G.Y.; Geng, J.; et al. Contrasting effects of ammonium and nitrate inputs on soil CO_2 emission in a subtropical coniferous plantation of southern China. *Biol. Fert. Soils* **2015**, *51*, 815–825. [CrossRef]
51. TingTing, Z.; ZILiang, Z.; Na, L.; YuanShuang, Y.; DongHui, Z.; Qin, L.; HuaJun, Y. Differential uptakes of different forms of soil nitrogen among major tree species in subalpine coniferous forests of western Sichuan, China. *Chin. J. Plant Ecol.* **2017**, *41*, 1051–1059.
52. Fang, H.J.; Cheng, S.L.; Yu, G.R.; Xu, M.J.; Wang, Y.S.; Li, L.S.; Dang, X.S.; Wang, L.; Li, Y.N. Experimental nitrogen deposition alters the quantity and quality of soil dissolved organic carbon in an alpine meadow on the Qinghai-Tibetan Plateau. *Appl. Soil Ecol.* **2014**, *81*, 1–11. [CrossRef]
53. Schindlbacher, A.; Zechmeister-Boltenstern, S.; Butterbach-Bahl, K. Effects of soil moisture and temperature on NO, NO_2, and N_2O emissions from European forest soils. *J. Geophys. Res.-Atmos.* **2004**, *109*. [CrossRef]
54. Wu, X.; Bruggemann, N.; Gasche, R.; Shen, Z.Y.; Wolf, B.; Butterbach-Bahl, K. Environmental controls over soil-atmosphere exchange of N_2O, NO, and CO_2 in a temperate Norway spruce forest. *Glob. Biogeochem. Cycles* **2010**, *24*, 45. [CrossRef]
55. Kiese, R.; Butterbach-Bahl, K. N_2O and CO_2 emissions from three different tropical forest sites in the wet tropics of Queensland, Australia. *Soil Biol. Biochem.* **2002**, *34*, 975–987. [CrossRef]
56. Werner, C.; Kiese, R.; Butterbach-Bahl, K. Soil-atmosphere exchange of N_2O, CH_4, and CO_2 and controlling environmental factors for tropical rain forest sites in western Kenya. *J. Geophys. Res.-Atmos.* **2007**, *112*, 71. [CrossRef]
57. Yan, J.H.; Zhang, W.; Wang, K.Y.; Qin, F.; Wang, W.T.; Dai, H.T.; Li, P.X. Responses of CO_2, N_2O and CH4 fluxes between atmosphere and forest soil to changes in multiple environmental conditions. *Glob. Chang. Biol.* **2014**, *20*, 300–312. [CrossRef]

58. Venterea, R.T.; Groffman, P.M.; Verchot, L.V.; Magill, A.H.; Aber, J.D.; Steudler, P.A. Nitrogen oxide gas emissions from temperate forest soils receiving long-term nitrogen inputs. *Glob. Chang. Biol.* **2003**, *9*, 346–357. [CrossRef]
59. Barnard, R.; Leadley, P.W.; Hungate, B.A. Global change, nitrification, and denitrification: A review. *Glob. Biogeochem. Cycles* **2005**, *19*, 152. [CrossRef]
60. Signor, D.; Cerri, C.E.P. Nitrous oxide emissions in agricultural soils: A review. *Pesq. Agropec. Trop.* **2013**, *43*, 322–338. [CrossRef]

forests

MDPI

Article

Nitrogen Addition Affects Soil Respiration Primarily through Changes in Microbial Community Structure and Biomass in a Subtropical Natural Forest

Jiacong Zhou [1,2], Xiaofei Liu [1,2], Jinsheng Xie [1,2,3], Maokui Lyu [1,2], Yong Zheng [1,2], Zhangtian You [1,2], Yuexin Fan [1,2], Chengfang Lin [1,2,3], Guangshui Chen [1,2,3], Yuehmin Chen [1,2,3,*] and Yusheng Yang [1,2,3]

1 State Key Laboratory for Subtropical Mountain Ecology of the Ministry of Science and Technology and Fujian Province, Fujian Normal University, Fuzhou 350007, China; zhoujiacong522@163.com (J.Z.); xfliu@fjnu.edu.cn (X.L.); jshxie@163.com (J.X.); 228lmk@163.com (M.L.); 18059046619@163.com (Y.Z.); allentime@126.com (Z.Y.); yxfan@fjnu.edu.cn (Y.F.); Tonylcf99@163.com (C.L.); gschen@fjnu.edu.cn (G.C.); geoyys@fjnu.edu.cn (Y.Y.)

2 School of Geographical Sciences, Fujian Normal University, Fuzhou 350007, China

3 Institute of Geography, Fujian Normal University, Fuzhou 350007, China

* Correspondence: ymchen@fjnu.edu.cn; Tel.: +86-591-83465013; Fax: +86-591-83465397

Received: 31 March 2019; Accepted: 19 May 2019; Published: 20 May 2019

Abstract: Forest soil respiration plays an important role in global carbon (C) cycling. Owing to the high degree of C and nitrogen (N) cycle coupling, N deposition rates may greatly influence forest soil respiration, and possibly even global C cycling. Soil microbes play a crucial role in regulating the biosphere–atmosphere C exchange; however, how microbes respond to N addition remains uncertain. To better understand this process, the experiment was performed in the *Castanopsis kawakamii* Hayata Nature Reserve, in the subtropical zone of China. Treatments involved applying different levels of N (0, 40, and 80 kg ha^{-2} $year^{-1}$) over a three-year period (January 2013–December 2015) to explore how soil physicochemical properties, respiration rate, phospholipid fatty acid (PLFA) concentration, and solid state ^{13}C nuclear magnetic resonance responded to various N addition rate. Results showed that high levels of N addition significantly decreased soil respiration; however, low levels of N addition significantly increased soil respiration. High levels of N reduced soil pH and enhanced P and C co-limitation of microorganisms, leading to significant reductions in total PLFA and changes in the structure of microbial communities. Significant linear relationships were observed between annual cumulative respiration and the concentration of microbial biomass (total PLFA, gram-positive bacteria (G^+), gram-negative bacteria (G^-), total bacteria, and fungi) and the microbial community structure (G^+: G^- ratio). Taken together, increasing N deposition changed microbial community structure and suppressed microbial biomass, ultimately leading to recalcitrant C accumulation and soil C emissions decrease in subtropical forest.

Keywords: N addition; soil respiration; microbe; subtropical forest

1. Introduction

Anthropogenic reactive nitrogen (N) production originated primarily from agricultural activities, fossil fuel combustion, and the growing popularity of biofuels, and has increased three- to five-fold over the past century [1]. By 2050, N deposition is projected to reach 200 Tg N $year^{-1}$, especially in forest ecosystems [1,2]. Approximately twice as much C is stored in soils compared to that in the atmosphere. Soil respiration (*Rs*) is the primary pathway through which C is released from the soil system into the atmosphere [3]. Thus, even minor changes in *Rs* would have significant effects on C

cycling. Given the nature of the relationship between the C and N cycles, which are highly coupled in terrestrial ecosystems [4,5], it is likely that increasing N deposition will greatly influence *Rs*.

N addition affects *Rs* through regulating forest productivity, microbial biomass, and activities that are directly related to CO_2 production [6]. Meta-analyses have revealed that N addition can increase aboveground and belowground plant growth by 29% and 35.5%, respectively [7,8]. Additionally, N addition reduced microbial biomass by 20% at the global scale [9]. However, how *Rs* responds to rapid N addition remains unclear and previous results have been inconclusive, including acceleration [10], deceleration [11], and no change [9,12]. The conclusions mentioned above are largely dependent on N-limited regions and there is a lack of subtropical studies. Subtropical systems have high rates of CO_2 exchange [13] and relatively high levels of available N in forest soils. Sun et al. [14] suggested that the main factor driving the reduction in *Rs* is different in N-enriched (microbe-mediated) and N-limited (plant-mediated) forests. However, Lee and Jose [15] also found that fine root production is the main factor affecting *Rs* in tropical forests. In our previous study, N addition promoted root biomass to utilize higher levels of P (Figure S1) [16]; however, the microbial response has not yet been described.

Large uncertainties exist in terms of belowground C cycling because soil C dynamics are often regulated by complicated microbial processes. N addition directly increases soil N availability and promotes substrate utilization for microbial decomposition [17–19]. However, co-limitation with other elements, such as P, may occur in subtropical forests. Moreover, N addition could elicit changes in the availability of substrates, which could accentuate C limitation of soil microbes. Although N addition increased the quantity of litter input to the soil [7,8], the quality of soil organic matter (SOM) may decline via increasing lignin content in litter and polymerization of polyphenols [20–22]. Furthermore, chronic N addition could enhance nitrification rates, increase inorganic N concentration, and leach base cations, eventually causing soil acidification to accompany an increase in Al^{3+}, Mn^{2+}, and Fe^{3+} [23,24], thereby suppressing microbial activity. Therefore, the magnitude of these processes determines the direction of *Rs* in response to N addition.

Previous studies have shown that the response of microbial activity to N addition gradients is not linear, with the highest levels of microbial activity occurring at moderate N concentration, and decreasing as N levels increase [25–27]. This tendency was observed not only in *Rs* but also in forest respiration, ectomycorrhizal fungal sporocarp production, and fungal mineralization [28–30]. Different magnitudes of N addition may have different effects on *Rs*.

In our study, we performed a manipulative experiment designed to test the effects of N addition on soil CO_2 emissions in a subtropical forest. The response factors assessed consisted of *Rs* rates, soil microbial biomass, microbial community structure, and soil C structure. Investigating the responses of *Rs* and microbial traits (biomass and community structure) to N addition is critical to develop our understanding of C cycling in subtropical forests. Hence, we hypothesized that: (1) changes in *Rs* would coincide with changes in microbial traits; (2) the effects of N addition on *Rs* are mainly mediated by microbial traits, rather than roots.

2. Materials and Methods

2.1. Study Site

The experiment was carried out in the *Castanopsis kawakamii* Hayata Nature Reserve, which is in central Fujian Province, China (117°28′ E, 26°11′ N), over an almost three-year period (January 2013–December 2015). The study site was composed of an approximately 200-year-old undisturbed mixed stand dominated by *Castanopsis carlesii* Hayata and *Schima superba* Gardn. et Champ., with other less abundant species. Stand density and canopy coverage were approximately 1955 trees ha^{-1} and 89%, respectively.

The climate is classified as a subtropical monsoon, with mean annual precipitation of 1552 mm, 2141 mm, and 2025 mm in 2013, 2014, and 2015, respectively. It has distinct seasons, with most

rain falling between March and August. Mean annual temperature, potential evapotranspiration, and relative humidity in this region were 18.7 °C, 1585 mm, and 79%, respectively [31]. Regional soils are Oxisols, formed from sandstone (based on the United States Department of Agriculture Soil Taxonomy), and are about 30–70 cm deep [32].

2.2. Experimental Design

Three N addition treatments (with four replicates each) were established in this forest, consisting of 0 kg ha^{-2} $year^{-1}$ (control, CT), 40 kg ha^{-2} $year^{-1}$ (low N, LN), and 80 kg ha^{-2} $year^{-1}$ (high N, HN). Treatment levels were based on known background atmospheric N deposition rates in subtropical regions of China (18–53 kg ha^{-2} $year^{-1}$), with an average deposition rate of ~40 kg ha^{-2} $year^{-1}$ [33]. A total of 12 plots (20 m × 20 m) were established, each surrounded by a 10-m wide buffer zone and unshielded from natural atmospheric N deposition. The plots and treatments were set randomly. Beginning in November 2012, a solution of ammonium nitrate (NH_4NO_3), and 20 L of deionized water was distributed monthly below the canopy with a backpack sprayer, totaling 12 applications of equal volume annually, and an equivalent volume of deionized water was sprayed on the control plots.

2.3. Soil Sample Collection

Five soil cores were collected from each subplot with a 3.5-cm-diameter corer in January 2016. We removed the surface litterfall and collected soil samples from the A horizon (0–10 cm). Soil cores were then kept in portable refrigerated box until being processed in the laboratory. After removal of plant roots and stones, soil samples were sieved through a 2-mm mesh and stored at 4 °C prior to the analysis of inorganic N, dissolved organic C, and N and microbial phospholipid fatty acid (PLFA) content. Part of the soil was air-dried for measuring its pH. The remaining soil was air-dried and ground (<150 μm) for determination of total C and total N.

2.4. Soil Respiration Rate Measurement

Soil respiration rate (R_s) was measured using an automated CO_2 efflux system (LI-8100, LI-COR Inc., Lincoln, NE, USA). Eight polyvinyl chloride (PVC) collars (diameter: 20 cm; height: 10 cm) were fixed in each plot in August 2011. Living plants inside the collars were removed and kept for almost 1.5 years to minimize disruption. Soil respiration was assessed once every two weeks over the course of the experimental period. Measurements were taken between 09:00 and 12:00, as soil flux over these hours has been shown to represent the mean of the whole day [34]. Soil temperatures and moisture were simultaneously monitored using a hand-held long-stem thermometer (Model SK-250WP, Sato Keiryoki Mfg. Co. Ltd, Tokyo, Japan) and a time-domain reflectometer (TDR) (Model TDR300, Spectrum Technologies Inc., Plainfield, IL, USA), respectively. The data of monthly soil temperature and annual moisture during study period are shown in Figures S2 and S3.

To examine the effects of N addition rate on R_s in sub/tropical forests, data were obtained from 15 peer-reviewed articles (Table S4) by searching Web of Science. The searched key words were combinations of, "nitrogen (N) addition," "nitrogen (N) deposition," "soil respiration," "subtropical forest" and "tropical forest". Data were selected based on the following criteria: (1) from a field study (data from incubation studies were excluded); (2) from control and simulated N addition treatments in multifactorial studies. Response ratios of R_s to N addition rate (RRs) were calculated using the following equation:

$$RRs = \ln (R_T/R_C) \quad (1)$$

where R_T is the treatment mean and R_C is the control mean. Here, $RRs > 0$ means N addition increased soil respiration; $RRs = 0$, means N addition has no effect on soil respiration; $RRs < 0$ means N addition reduced soil respiration.

2.5. Phospholipid Fatty Acid Analysis

The soil microbial community was characterized using a phospholipid fatty acid (PLFA) analysis, as previously described by Wan et al. [35]. In brief, a solvent consisting of a 2:1:0.8 mixture of methanol (CH_3OH), chloroform ($CHCl_3$), and phosphate buffer (pH 7.4) was used to extract 10 g of freeze-dried soil by shaking for 2 h. The samples were centrifuged at 3500 g for 10 min, and then the supernatant was transferred to a new tube. The remaining soil was re-extracted as described above. The extracted solvents from both steps were combined and then evaporated to 1 mL under N_2 gas. Then, neutral glycolipids, glycolipids-, and polar lipids were separated over a silicon hydroxide column eluted with chloroform, acetone, and methanol, respectively. Polar lipids were methylated to form fatty acid methyl esters (FAMEs) by subjecting them to 0.2 M methanolic KOH. Individual FAMEs were identified by Hewlett Packard 5890 gas chromatography, equipped with a 6890 series injector, a flame ionization detector, and an Ultra 2 capillary column (25 m × 0.2 mm inner diameter, film thickness, 0.33 μm) based on their retention times and in combination with the MIDI Sherlock Microbial Identification System (MIDI Inc., Newark, DE, USA).

Although more than 70 PLFAs, ranging from C_{10}–C_{24}, were identified in this experiment, only the 23 PLFAs found to be consistently present in each sample were included in the analysis. PLFAs identified as being derived from gram-positive bacteria (G^+) included i14:0, i15:0, a15:0, i16:0, i17:0, and a17:0, whereas those identified as being derived from gram-negative bacteria (G^-) included 16:1ω9c, 16:1ω7c, cy17:0, 18:1ω7c, 18:1ω5c, and cy19:0 [36,37]. The sum of the PLFAs from G^+ and G^- bacteria was used to as a measure of total bacteria, and those of 10Me16:0, 10Me17:0, and 10Me18:0 were selected to measure actinomycetes. We selected 18:2ω6c and 18:1ω9c as fungi markers [38]. The PLFAs 14:0, 15:0, 16:0, 16:1ω5c, 17:0, and 18:0 were detected in both bacteria and fungi; thus, they were used to assess the unclassified markers [39–41]. The sum of all selected phospholipids was used to estimate the total microbial biomass and for the analysis of microbial community structure. The G^+:G^- ratio was used to estimate the G^+ to G^- bacterial biomass (G^+:G^-), and the fungal: bacterial PLFA ratio was used to estimate the ratio of fungi to bacteria (F:B).

2.6. Solid-State ^{13}C Nuclear Magnetic Resonance Spectroscopy Analysis

Soil samples for solid state ^{13}C cross polarization magic angle spinning (CP-MAS) nuclear magnetic resonance (NMR) analysis were repeatedly treated with 2% hydrofluoric acid, then rinsed with deionized water, freeze-dried, and ground into powder [42]. The powdered samples were packed into 4-mm zirconium rotors. Solid state ^{13}C NMR spectra were acquired on a 500 MHz Bruker BioSpin Avance III spectrometer (Bruker BioSpin, Rheinstetten, Germany) equipped with a 4-mm probe. The parameters used to obtain the spectra consisted of a 13 kHz spinning rate, 1 ms ramp-CP contact time, 1 s recycle delay, and 4096 scans. Glycine was used as the external reference for chemical shift. NMR spectra were processed using a zero filling factor of 2 and 75 Hz line broadening. The NMR spectra were divided into seven regions representing the different chemical environments of the ^{13}C nucleus (Table S1). The ratios were calculated using percentage intensity values as follows [43,44]:

$$\text{A/O-A ratio} = \text{alkyl C/O} - \text{alkyl C} \quad (2)$$

$$\text{aromaticity} = \text{aromatic C}/(\text{alkyl C} + \text{methoxyl and N-alkyl C} + \text{O-alkyl C} + \text{Di-O-alkyl} + \text{phenolic C} + \text{aromatic C}) \quad (3)$$

2.7. Additional Soil Analysis

Soil inorganic N was treated with 2 M KCl and analyzed using a Continuous Flow Analytic System (Skalar san++, Skalar, Breda, Netherlands); soil organic C (SOC) and total N (TN) were determined with an elemental analyzer (Elementar Vario EL III, Elementar, Langenselbold, Germany). Dissolved organic C (DOC) and N (DON) were extracted from 10 g of field-moist soil by mixing the soil with 40 mL deionized water at 20 °C and shaking for 30 min, then filtering the supernatant through a 0.45-μm

filter membrane [45]. Soil pH was determined with a pH meter (STARTER 300, OHAUS, Pine Brook, NJ, USA) in a 1:2.5 soil: water solution. Soil moisture content was measured gravimetrically by drying for 48 h at 105 °C.

2.8. Statistical Analyses

Daily cumulative respiration (R_c) was calculated from R_s as follows:

$$R_c\ (\text{g C m}^{-2}\ \text{d}^{-1}) = R_s\ (\mu\text{mol m}^{-2}\ \text{s}^{-1}) \times 3600\ (\text{s h}^{-1}) \times 24\ (\text{h d}^{-1}) \times 12/1{,}000{,}000\ (\text{g mol}^{-1}) \quad (4)$$

Soil respiration was measured every two weeks with a total of 24 samplings/year. Annual cumulative respiration was calculated by daily R_c multiplied by the number of sampling interval days. Equation used was as follows:

$$\textit{Annual cumulative respiration} = \sum_{i=1}^{24} \text{daily } R_c\ (\text{i})\ \times 15 \quad (5)$$

The relationship between the R_s and soil temperatures was performed using following widely exponential regression model [46]:

$$R_s = \text{ae}^{\text{bt}} \quad (6)$$

where R_s is the soil respiration rate, t is the soil temperature at 5 cm depth, a and b are the model coefficients.

The apparent temperature sensitively (Q_{10}) was calculated as follows:

$$Q_{10} = \text{e}^{10\text{b}} \quad (7)$$

All statistical analyses were performed using SPSS v.21.0 (SPSS Inc., Chicago, IL, USA). All response variables were tested for normality and homoscedasticity prior to statistical analyses, and data were log-transformed when the assumptions were not met (DON, ammonium nitrogen [NH_4^+-N]). One-way analysis of variance (ANOVA) with the Tukey's HSD test was used to evaluate the differences in soil physicochemical properties, annual cumulative respiration, Q_{10}, and PLFA in response to different N-addition treatments. Linear regression model analyses were conducted to explore the relationships among PLFA and annual cumulative respiration.

3. Results

3.1. Response of Soil Physicochemical Properties to N Deposition

No significant differences in SOC, TN, ammonium N (NH_4^+-N), or nitrate N (NO_3^--N) were detected after three years of N deposition (Table 1). Soil pH decreased with increasing N, with pH significantly reduced (by 0.13 units) in the HN treatment. Soil DOC was significantly higher in the LN treatment, and soil DON increased with higher N addition, with levels in the HN treatment being significantly higher than those in the CT and LN treatments.

Table 1. Effects of N deposition on soil physicochemical properties.

Properties	CT	LN	HN	Contrast Test
SOC ($g \cdot kg^{-1}$)	36.61(7.47)	39.18(13.03)	33.32(7.99)	0.709
Total N ($g \cdot kg^{-1}$)	2.67(0.27)	2.70(0.53)	2.54(0.32)	0.838
pH	4.08(0.06)a	3.97(0.09)ab	3.95(0.09)b	0.096
NH_4^+-N ($mg \cdot kg^{-1}$)	10.79(2.50)	7.21(0.96)	9.57(4.21)	0.053
NO_3^--N ($mg \cdot kg^{-1}$)	1.37(0.32)	1.62(0.53)	1.59(0.57)	0.070
DOC ($mg \cdot kg^{-1}$)	41.93(12.36)b	66.80(3.43)a	39.88(8.03)b	0.003
DON ($mg \cdot kg^{-1}$)	49.95(5.32)b	58.66(6.98)b	132.32(12.93)a	<0.001

The different letters indicate significant differences between treatments at $p < 0.05$. Contrast test (ANOVA) was conducted between N treatments and the controls. Values are expressed as (mean ± standard deviation; $n = 4$). CT: control treatments; LN: low N; HN: high N; SOC: soil organic carbon; TN: total N; NH_4^+-N: ammonium N; NO_3^--N: nitrate N; DOC: dissolved organic carbon; DON: dissolved organic N.

3.2. Response of Soil Respiration Rate and Temperature Sensitivity to N Addition

Monthly dynamics of *Rs* rate showed a strong seasonal pattern, with the highest rate observed in July–August and the lowest in January–February for all treatments (Figure 1). Annual cumulative *Rs* in the LN treatment was 15.62%, 19.16%, and 23.29% higher than in the CT treatment in 2013, 2014, and 2015, respectively, while annual cumulative *Rs* in the HN treatment was 11.86% and 16.68% lower relative to the CT treatment in 2014 and 2015, respectively (Figure 2). However, during the period of 2013 to 2015, the sensitivities of *Rs* to soil temperature were not significantly different among N-addition treatments (Table 2 and Table S2).

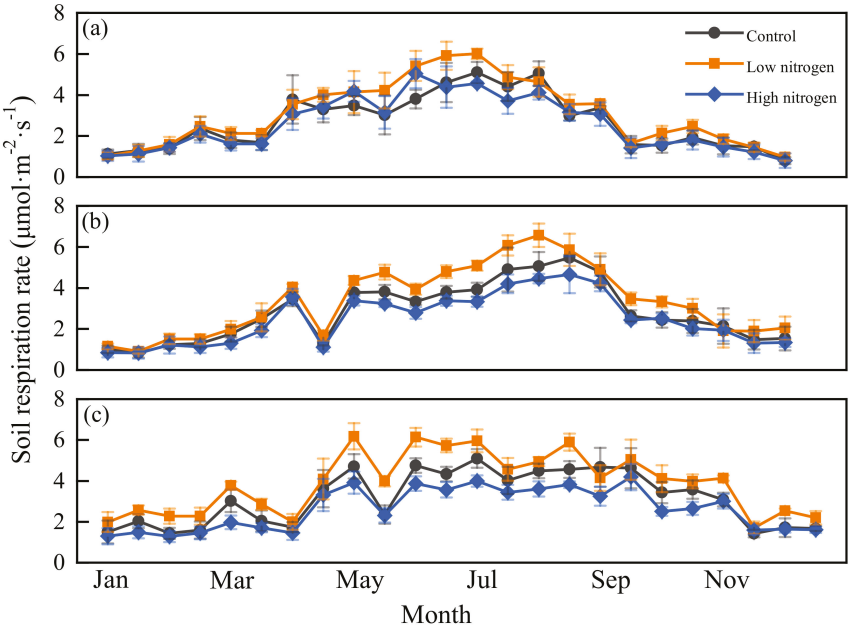

Figure 1. Monthly dynamics of soil respiration rate under different N treatments in 2013 (**a**), 2014 (**b**), and 2015 (**c**). Error bars represent standard deviation ($n = 4$).

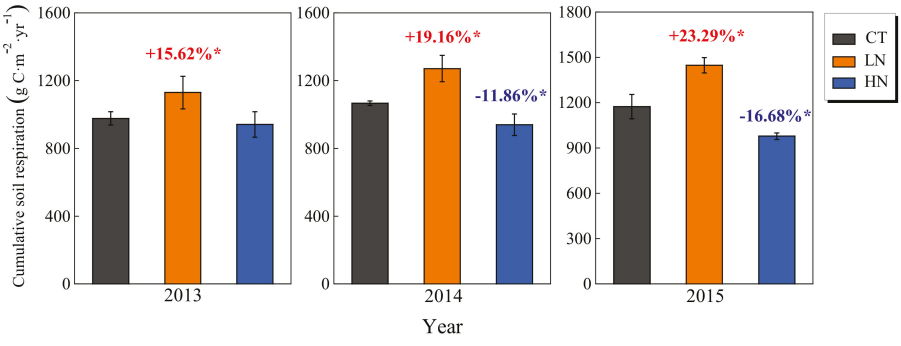

Figure 2. Annual cumulative soil respiration under different N treatments for the period of 2013–2015. * indicates statistically significant difference at $p < 0.05$.

Table 2. The soil respiration sensitivities to soil temperature for the period of 2013–2015.

Treatments	Q_{10}
CT	2.07(0.11)
LN	2.09(0.36)
HN	2.00(0.12)

3.3. Response of Microbial Community to N Addition

The concentrations of G^+, G^-, fungi, and total PLFA were significantly decreased in the HN treatment, but no significant differences were observed for any of the PLFA between the LN and CT treatments (Figure 3; Table S3). The ratio of G^+: G^- was significantly higher in the HN treatment than in the CT treatment (1.5 and 1.1, respectively), but no significant difference in F:B ratio was observed among the treatments.

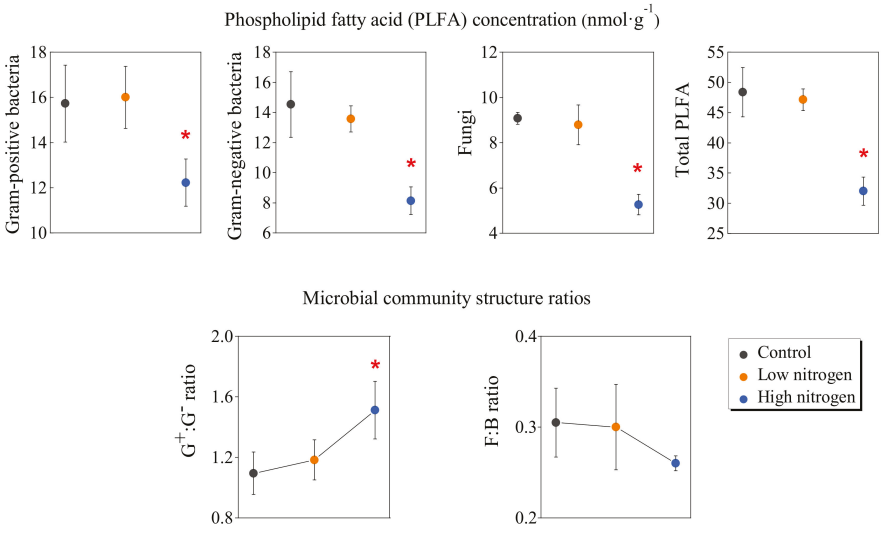

Figure 3. Phospholipid fatty acid (PLFA) concentrations and microbial community structure ratios under different N addition treatments. Error bars represent standard deviation ($n = 4$). * indicates significant difference between the treatment and control at $p < 0.05$.

3.4. Response of Soil Chemical Characteristics to N Addition

The most dominant component was the alkyl C region (Figure 4; Table S1). Alkyl C, aromatic C, phenolic C, and carboxyl/carbonyl C exhibited major differences in the HN treatment. Thus, differences in these chemical shift regions caused a 9% reduction in A/O-A and a 5% increase in aromaticity.

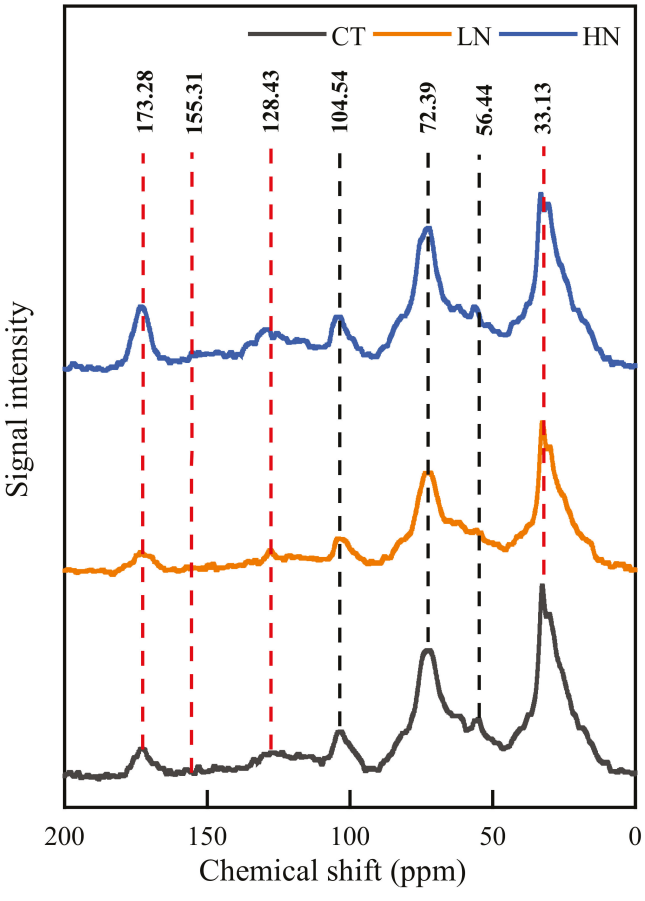

Figure 4. Solid-state ^{13}C nuclear magnetic resonance spectra of soil under different N addition treatments. The red dashed line indicates changes in the chemical shift regions.

3.5. Correlation between Annual Cumulative Soil Respiration and Microbial Biomass, Root Biomass and Microbial Community Structure Ratio

Significant linear relationships were found between annual cumulative *Rs* and the concentration of microbial biomass (total PLFA, G^+, G^-, total bacteria, and fungi) and the G^+: G^- ratio according to linear regression. However, neither root biomass nor the F:B ratio was significantly correlated with annual cumulative *Rs* in 2015 (Figure 5).

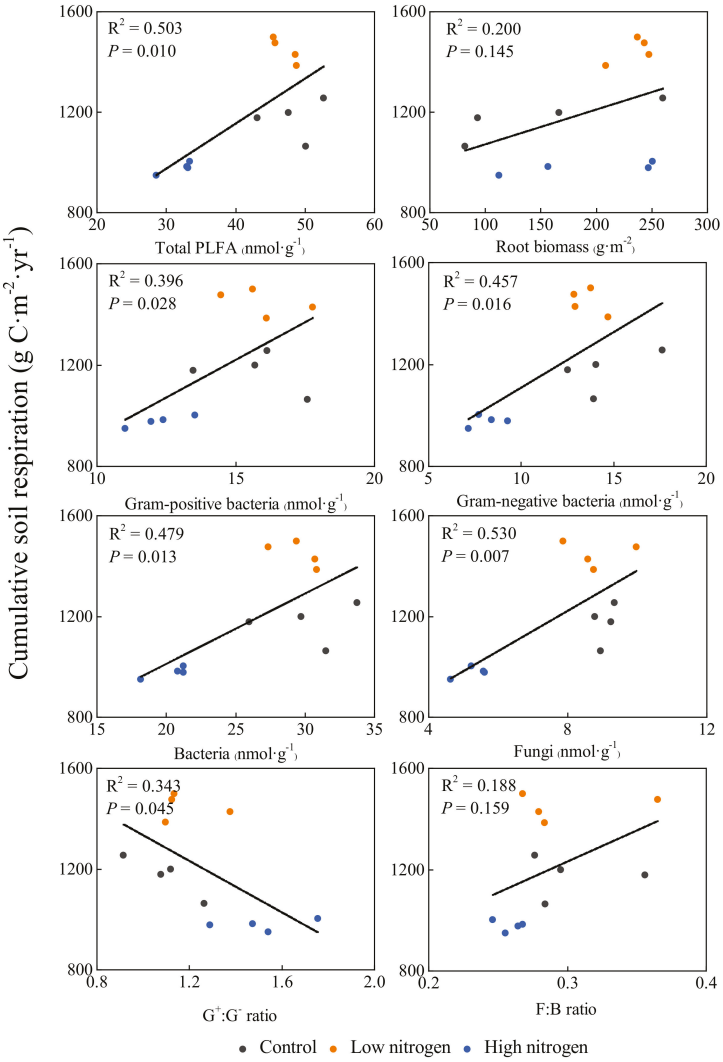

Figure 5. Linear relationships between annual cumulative respiration in 2015 and concentrations of PLFA, microbial community structure ratios, and root biomass.

4. Discussion

4.1. Effects of N Addition on Soil Respiration

Nitrogen deposition did not affect the seasonal patterns of *Rs* rates, with the highest rate observed in July–August and the lowest in January–February (Figure 1). This seasonal pattern has been reported in previous studies and can be ascribed to differences in mean temperature [47,48]. N addition induced significant changes in *Rs* rates ($p < 0.05$); however, the different rates of N addition exhibited distinct trends in terms of their effect on *Rs*. This discrepancy in annual cumulative respiration among the treatments continued to diverge over time, which was consistent with results reported by Allison et al. [28], Hasselquist et al. [30], Bowden et al. [48], and Maaroufi et al. [49]. This is because a certain threshold for N addition exists. For instance, in a subtropical Moso bamboo forest ecosystem,

Li et al. [6] found that a N addition rate of 60 kg N ha^{-1} $year^{-1}$ may reflect a N saturation threshold. When N addition rate exceed 60 kg N ha^{-1} $year^{-1}$, N addition still increased *Rs*, but the positive effects diminished. However, in our study, a significant decrease in *Rs* was observed in 2014 and 2015 when N addition rate exceed 60 kg N ha^{-1} $year^{-1}$, possibly because the bamboo plantation was N-limited and had a high demand for N [50], unlike the natural forests examined in previous research.

Previously, there have been six meta-analyses with regard to the effects of N addition on *Rs* [9–12,51,52]. However, these studies paid little attention to subtropical forests owing to the smaller sample sizes reported. With the increasing attention paid to subtropical forests in recent years, several studies have been carried out. We recollected a series of data from 16 study sites (including this study) and defined <60 kg N ha^{-1} $year^{-1}$ as a low N addition rate according to a N saturation threshold of 50–60 kg N ha^{-1} $year^{-1}$ for global aboveground net primary production [53]. We found strong evidence to indicate that N addition significantly reduces *Rs* in subtropical forests as observed in all examined studies (n = 58, p = 0.011; Figure 6, Table S4). However, the magnitude of N addition rate also affected the response of *Rs*, which mainly showed as a high N addition rate reducing *Rs* (n = 37, p = 0.046), while the response of *Rs* to low N addition rate varied (n = 21, p = 0.052). It is noteworthy that N addition rate is a dominant factor affecting soil acidification and total microbial biomass; however, Zhou et al. [54] indicated that the effect of N addition rate was ignored in several of the previous meta-analyses, such as Janssens et al. [11], Treseder [51], and Lu et al. [52]. In particular, in subtropical forest ecosystems, rapid N addition exacerbates the loss of NO_3^- combined base cations (K^+, Na^+, Ca^{2+}, and Mg^{2+}) through leaching, which in turn causes nutrient cations to be lost at a faster rate than minerals can be replenished [55]. A lack of base cations can be harmful to vegetative and microbial growth in subtropical forest ecosystems [56,57] leading to lower *Rs*.

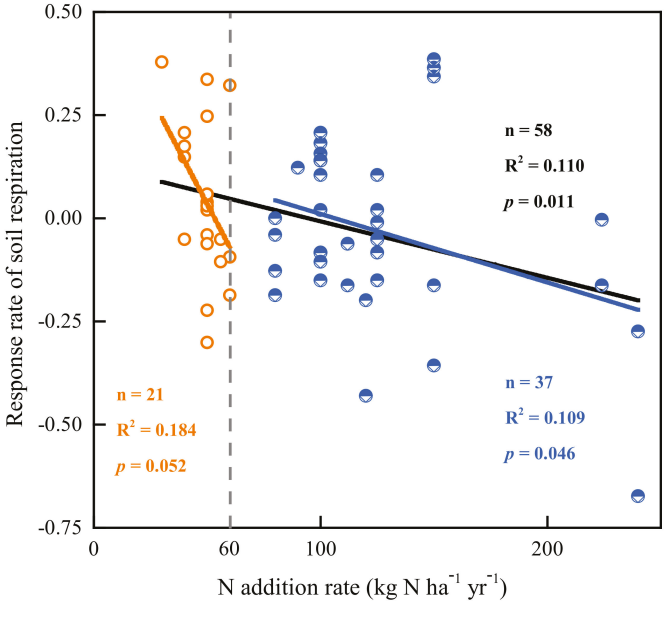

Figure 6. Linear relationship between N addition rate and response ratios of soil respiration (*RRs*) in subtropical systems of the present study and other regions of the world. Orange hollow points indicate relatively low N addition (N addition rate < 60 kg N ha^{-1} $year^{-1}$); blue points indicate relatively high N addition (N addition rate > 60 kg N ha^{-1} $year^{-1}$); orange line indicates linear regression between relatively low N addition rate and *RRs*; blue line indicates linear regression between relatively high N addition rate and *RRs*; black line indicates linear regression between N addition rate and *RRs*.

In our control treatment, the Q_{10} value (2.07) was similar to that reported from a subtropical rehabilitated forest (2.1) [58], but lower than those from a subtropical disturbed forest (2.3) [58], a Moso bamboo forest (2.29) [6], a sweetgum forest (2.73) [59], and a larch forest (3.24) [14] across the temperate zone. This is in line with the observations of Wang et al. [60], in which Q_{10} showed a positive relationship with latitude in forest ecosystems. In addition, the C:N ratio is a dominant factor for regulating Q_{10}, owing to the shift from C limitation to nutrient limitation with increasing latitude [60,61]. This result may support the microbial N mining theory, which suggests that microbes decompose more SOM to obtain sufficient N at high temperature in high latitude forests with low N availability [62].

4.2. Microbial Community and Carbon Structure under N Addition

In accordance with our first hypothesis, we found that the HN treatment reduced the concentration of bacteria, fungi, actinomycetes, and unclassified biomarkers (Figure 3; Table S3), leading to a significant reduction in total PLFA. Both incubation and field studies have definitively shown that *Rs* and microbial biomass are consistently suppressed following N addition [11,51,63]. However, a recent meta-analysis by Zhou et al. [54] revealed that a decrease in microbial biomass is not always associated with N addition suppressing microbial activity. Interestingly, the companion study reported that the C:N:P stoichiometry in microbial biomass was significantly altered in the HN treatments and enhanced microbial P limitation [32]. Additionally, high N addition significantly reduced soil pH. Therefore, these results collectively demonstrate that high N addition inhibits microbial growth.

Ramirez et al. [63] suggested that understanding how N addition induces change in soil microbial communities is imperative for better understanding soil C storage dynamics. High availability of N could alter the microbial process of SOC that is controlled by the microbial community [64,65]. In our study, the HN treatments not only inhibited microbial biomass but also shifted microbial composition (increased G^+:G^- ratio). The two different groups of Gram-stained bacteria, classified by their cell wall compositions, have been shown to differ in their preferences regarding substrate conditions and living strategies in a changing environment [66]. G^+ are well-adapted to low SOM substrates, while G^- prefer conditions with high organic matter availability [67,68]. Increase in the G^+:G^- ratio under the high N addition treatment not only indicated a low quality substrate but also an acclimation of microbes to changes in substrate and nutrient availability.

Undoubtedly, the inhibition in microbial biomass and shift in soil microbial community structure affected the soil C structure, to an extent. The results of the solid state ^{13}C NMR spectroscopy analysis showed that the relative proportions of aromatic C and phenolic C, which originate from lignin and amino acids of peptides [43,69], increased under the HN treatment (Figure 4; Table S1). Wang et al. [65] also observed that lignin-derived phenols accumulated in soil with long-term N addition (22 years). There are two plausible reasons for this observation. First, that N addition significantly increased the lignin content of the plant and litter [21], leading to lower substrate decomposition rates with higher lignin content [70]. Second, phenolic compounds are highly resistant to degradation, being susceptible only to a handful of fungal species that are more efficient at lignin decomposition [71]. Thus, non-preferred microbial substrates would accumulate under high N addition.

4.3. Correlation between Soil Respiration and Microbial Biomass, Root Biomass, and Microbial Community Structure Ratio under N Addition

A significant correlation was observed between microbial traits (biomass and community structure) and cumulative *Rs* rather than root biomass (Figure 5). These results supported our second hypothesis, that microbial traits are primary factors affecting *Rs* under N addition, which is to say that the decrease in *Rs* is mainly due to microbes. A reasonable explanation is that microbes may be subject to co-limiting factors in subtropical forests, such as C and P, rather than N [65,72,73]. This pattern of *Rs* under N addition is different in N limited ecosystems, which have often been reported to increase *Rs* via root products and biomass [74]. Importantly, heterotrophic respiration dominates *Rs* (almost

72%) [75], and the positive relationships were observed between root/fine root biomass and autotrophic respiration [15,76] and microbial biomass and heterotrophic respiration [77]. Additionally, N addition significantly increased root biomass (Figure S1) and decreased microbial biomass, which collectively suggested that heterotrophic respiration may have decreased even further under N addition.

Decreasing microbial biomass is always accompanied by decreasing microbial diversity [78]. Microbial diversity is a vital determinant of ecological function that cannot be obtained using the PLFA method [79]. Thus, it is necessary to employ nucleic-acid-based methods to link microbial diversity to function. In this study, N addition inhibited microbial biomass and shifted microbial community structure, which disrupted the microbial process of SOM, leading to a decrease in *Rs* and an increase in recalcitrant C accumulation, but was also beneficial to an increase in forest soil C sequestration. However, nutrient release from microbial decomposition will slow down as SOC storage increases. Especially in natural forests without intensive management practices (such as fertilization), shifts in biogeochemical cycling will alter the productivity of ecosystems.

5. Conclusions

The effects of N addition on *Rs* are subject to an N saturation threshold, which triggered low N addition to increase *Rs* and high N addition to decrease *Rs* in the subtropical *C. carlesii* forest investigated. High N addition increased P limitation and decreased pH. Additionally, high N addition led to recalcitrant C accumulation, restricting microbial utilization. These processes collectively reduced the total PLFA concentration and shifted microbial community structure (G^+: G^- ratio). Our results suggest that microbial traits are dominant factors affecting *Rs*. As such, additional research on the transformations in soil microbial traits in response to increasing rates of N deposition may provide further insights into soil C emission dynamics in subtropical forests.

Supplementary Materials: The following are available online at http://www.mdpi.com/1999-4907/10/5/435/s1, Figure S1. Changes in root biomass under different N addition treatments. Values are means ± standard error ($n = 4$). * indicates statistically significant differences at $p < 0.05$. CT: control, LN: low nitrogen, HN: high nitrogen, Figure S2. Monthly soil temperature dynamics in 2013 (a), 2014 (b), and 2015 (c), Figure S3. Soil moisture under N addition from 2013 to 2015, Table S1. Relative carbon (C) distribution (%) in different chemical shift regions in ^{13}C cross-polarization magic-angle spinning of soil under different nitrogen addition treatments, Table S2. The exponential relationship between soil CO_2 emission rate and soil temperature in each subplots under different nitrogen addition treatments, Table S3 Effects of N addition on the phospholipid fatty acid biomarker concentration (nmol g^{-1} soil). Error bars represent standard deviation ($n = 4$). The different letters indicate significant differences between treatments at $p < 0.05$. G^+: gram-positive bacteria; G^-: gram-negative bacteria; Bacteria: sum of G^+ and G^-; Unclassified: unclassified biomarkers; ACT: actinomycetes; Total: total PLFA, Table S4 Characteristics of 16 studies site. RRs: Response ratio of soil respiration.

Author Contributions: Conceptualization, J.Z., X.L., Y.C. and Y.Y.; Formal analysis, J.X.; Funding acquisition, Y.C. and Y.Y.; Investigation, J.Z., X.L., M.L., Y.Z. and Z.Y.; Methodology, J.X., M.L., Y.Z., Z.Y., Y.F., C.L. and G.C.; Supervision, Y.C. and Y.Y.; Writing—original draft, J.Z.; Writing—review & editing, J.Z. and Y.C.

Funding: This research was funded in part through the National Natural Science Foundation of China (No. U1505233, No. 31670620) and the National Key Basic Research Program of China (973 Program) (No. 2014CB954003).

Acknowledgments: We would like to thank Wei Zheng, Yuhuang Ji and Guoyu Li for their help in field work and laboratory analyses.

Conflicts of Interest: The authors declare no conflict of interest.

References

1. Galloway, J.N.; Townsend, A.R.; Erisman, J.W.; Bekunda, M.; Cai, Z.; Freney, J.R.; Martinelli, L.A.; Seitzinger, S.P.; Sutton, M.A. Transformation of the nitrogen cycle: Recent trends, questions, and potential solutions. *Science* **2008**, *320*, 889–892. [CrossRef]
2. Sutton, M.A.; Nemitz, E.; Erisman, J.W.; Beier, C.; Bahl, K.B.; Cellier, P.; de Vries, W.; Cotrufo, F.; Skiba, U.; Di Marco, C.; et al. Challenges in quantifying biosphere-atmosphere exchange of nitrogen species. *Environ. Pollut.* **2007**, *150*, 125–139. [CrossRef] [PubMed]

3. Bond-Lamberty, B.; Thomson, A. Temperature-associated increases in the global soil respiration record. *Nature* **2010**, *464*, 579–582. [CrossRef]
4. Tateno, M.; Chapin, F.S. The logic of carbon and nitrogen interactions in terrestrial ecosystems. *Am. Nat.* **1997**, *149*, 723–744. [CrossRef]
5. Cleveland, C.C.; Liptzin, D. C:N:P stoichiometry in soil: Is there a "Redfield ratio" for the microbial biomass? *Biochemistry* **2007**, *85*, 235–252. [CrossRef]
6. Li, Q.; Song, X.; Chang, S.X.; Peng, C.; Xiao, W.; Zhang, J.; Xiang, W.; Li, Y.; Wang, W. Nitrogen depositions increase soil respiration and decrease temperature sensitivity in a Moso bamboo forest. *Agric. For. Meteorol.* **2019**, *268*, 48–54. [CrossRef]
7. Lebauer, D.S.; Treseder, K.K. Nitrogen limitation of net primary productivity in terrestrial ecosystems is globally distributed. *Ecology* **2008**, *89*, 371–379. [CrossRef]
8. Xia, J.; Wan, S. Global response patterns of terrestrial plant species to nitrogen addition. *New Phytol.* **2008**, *179*, 428–439. [CrossRef]
9. Liu, L.; Greaver, T.L. A global perspective on belowground carbon dynamics under nitrogen enrichment. *Ecol. Lett.* **2010**, *13*, 819–828. [CrossRef] [PubMed]
10. Zhou, L.; Zhou, X.; Zhang, B.; Lu, M.; Luo, Y.; Liu, L.; Li, B. Different responses of soil respiration and its components to nitrogen addition among biomes: a meta-analysis. *Glob. Chang. Biol.* **2014**, *20*, 2332–2343. [CrossRef]
11. Janssens, I.A.; Dieleman, W.; Luyssaert, S.; Subke, J.A.; Reichstein, M.; Ceulemans, R.; Ciais, P.; Dolman, A.J.; Grace, J.; Matteucci, G. Reduction of forest soil respiration in response to nitrogen deposition. *Nat. Geosci.* **2010**, *3*, 315–322. [CrossRef]
12. Yue, K.; Peng, Y.; Peng, C.; Yang, W.; Peng, X.; Wu, F. Stimulation of terrestrial ecosystem carbon storage by nitrogen addition: a meta-analysis. *Sci. Rep.* **2016**, *6*, 19895. [CrossRef] [PubMed]
13. Townsend, A.R.; Cleveland, C.C.; Houlton, B.Z.; Alden, C.B.; White, J.W.C. Multi-element regulation of the tropical forest carbon cycle. *Front. Ecol. Environ.* **2011**, *9*, 9–17. [CrossRef]
14. Sun, Z.; Liu, L.; Ma, Y.; Yin, G.; Zhao, C.; Zhang, Y.; Piao, S. The effect of nitrogen addition on soil respiration from a nitrogen-limited forest soil. *Agric. For. Meteorol.* **2014**, *197*, 103–110. [CrossRef]
15. Lee, K.H.; Jose, S. Soil respiration, fine root production, and microbial biomass in cottonwood and loblolly pine plantations along a nitrogen fertilization gradient. *For. Ecol. Manag.* **2003**, *185*, 263–273. [CrossRef]
16. Fan, Y.; Zhong, X.; Lin, F.; Liu, C.; Yang, L.; Wang, M.; Chen, G.; Chen, Y.; Yang, Y. Responses of soil phosphorus fractions after nitrogen addition in a subtropical forest ecosystem: Insights from decreased Fe and Al oxides and increased plant roots. *Geoderma* **2019**, *337*, 246–255. [CrossRef]
17. Vivanco, L.; Austin, A.T. Intrinsic effects of species on leaf litter and root decomposition: A comparison of temperate grasses from North and South America. *Oecologia* **2006**, *150*, 97–107. [CrossRef]
18. Parton, W.; Silver, W.L.; Burke, I.C.; Grassens, L.; Harmon, M.E.; Currie, W.S.; King, J.Y.; Adair, E.C.; Brandt, L.A.; Hart, S.C. Global-Scale Similarities in Nitrogen Release Patterns during Long-Term Decomposition. *Science* **2007**, *315*, 361. [CrossRef]
19. Schimel, J.P.; Weintraub, M.N. The implication of exoenzyme activity on microbial carbon and nitrogen limitation in soil: a theoretical model. *Soil Biol. Biochem.* **2003**, *35*, 549–563. [CrossRef]
20. Wu, N.; Filley, T.R.; Bai, E.; Han, S.; Jiang, P. Incipient changes of lignin and substituted fatty acids under N addition in a Chinese forest soil. *Org. Geochem.* **2015**, *79*, 14–20. [CrossRef]
21. Liu, J.; Wu, N.; Wang, H.; Sun, J.; Peng, B.; Jiang, P.; Bai, E. Nitrogen addition affects chemical compositions of plant tissues, litter and soil organic matter. *Ecology* **2016**, *97*, 1796–1806. [CrossRef]
22. Haider, K.; Martin, J.P. Synthesis and Transformation of Phenolic Compounds by Epicoccum nigrum in Relation to Humic Acid Formation1. *Soil Sci. Soc. Am. J.* **1967**, *31*, 766. [CrossRef]
23. Bouwman, A.F.; van Vuuren, D.P.; Derwent, R.G.; Posch, M. A global analysis of acidification and eutrophication of terrestrial ecosystems. *Water Air Soil Pollut.* **2002**, *141*, 349–382. [CrossRef]
24. Tian, D.; Niu, S. A global analysis of soil acidification caused by nitrogen addition. *Environ. Res. Lett.* **2015**, *10*, 024019. [CrossRef]
25. Enrique, A.G.; Bruno, C.; Christopher, A.; Virgile, C.; Stéven, C. Effects of nitrogen availability on microbial activities, densities and functional diversities involved in the degradation of a Mediterranean evergreen oak litter (*Quercus ilex* L.). *Soil Biol. Biochem.* **2008**, *40*, 1654–1661. [CrossRef]

26. Zhang, N.; Wan, S.; Li, L.; Bi, J.; Zhao, M.; Ma, K. Impacts of urea N addition on soil microbial community in a semi-arid temperate steppe in northern China. *Plant Soil* **2008**, *311*, 19–28. [CrossRef]
27. Zhou, X.; Zhang, Y.; Downing, A. Non-linear response of microbial activity across a gradient of nitrogen addition to a soil from the Gurbantunggut Desert, northwestern China. *Soil Biol. Biochem.* **2012**, *47*, 67–77. [CrossRef]
28. Allison, S.D.; LeBauer, D.S.; Ofrecio, M.R.; Reyes, R.; Ta, A.M.; Tran, T.M. Low levels of nitrogen addition stimulate decomposition by boreal forest fungi. *Soil Biol. Biochem.* **2009**, *41*, 293–302. [CrossRef]
29. Ouyang, X.; Zhou, G.; Huang, Z.; Zhou, C.; Li, J.; Shi, J.; Zhang, D. Effect of N and P addition on soil organic C potential mineralization in forest soils in South China. *J. Environ. Sci.* **2008**, *20*, 1082–1089. [CrossRef]
30. Hasselquist, N.J.; Metcalfe, D.B.; Högberg, P. Contrasting effects of low and high nitrogen additions on soil CO2flux components and ectomycorrhizal fungal sporocarp production in a boreal forest. *Glob. Chang. Biol.* **2012**, *18*, 3596–3605. [CrossRef]
31. Liu, X.; Yang, Z.; Lin, C.; Giardina, C.P.; Xiong, D.; Lin, W.; Chen, S.; Xu, C.; Chen, G.; Xie, J. Will nitrogen deposition mitigate warming-increased soil respiration in a young subtropical plantation? *Agric. For. Meteorol.* **2017**, *246*, 78–85. [CrossRef]
32. Fan, Y.; Lin, F.; Yang, L.; Zhong, X.; Wang, M.; Zhou, J.; Chen, Y.; Yang, Y. Decreased soil organic P fraction associated with ectomycorrhizal fungal activity to meet increased P demand under N application in a subtropical forest ecosystem. *Biol. Fertil. Soils* **2017**, *54*, 149–161. [CrossRef]
33. Liu, X.; Lei, D.; Mo, J.; Du, E.; Shen, J.; Lu, X.; Ying, Z.; Zhou, X.; He, C.; Zhang, F. Nitrogen deposition and its ecological impact in China: An overview. *Environ. Pollut.* **2011**, *159*, 2251–2264. [CrossRef]
34. Sheng, H.; Yang, Y.; Yang, Z.; Chen, G.; Xie, J.; Guo, J.; Zou, S. The dynamic response of soil respiration to land-use changes in subtropical China. *Glob. Chang. Biolog.* **2010**, *16*, 1107–1121. [CrossRef]
35. Wan, X.; Huang, Z.; He, Z.; Yu, Z.; Wang, M.; Davis, M.R.; Yang, Y. Soil C:N ratio is the major determinant of soil microbial community structure in subtropical coniferous and broadleaf forest plantations. *Plant Soil* **2015**, *387*, 103–116. [CrossRef]
36. Frostegård, Å.; Tunlid, A.; Bååth, E. Use and misuse of PLFA measurements in soils. *Soil Biol. Biochem.* **2011**, *43*, 1621–1625. [CrossRef]
37. Ushio, M.; Balser, T.C.; Kitayama, K. Effects of condensed tannins in conifer leaves on the composition and activity of the soil microbial community in a tropical montane forest. *Plant Soil* **2013**, *365*, 157–170. [CrossRef]
38. Swallow, M.; Quideau, S.A.; MacKenzie, M.D.; Kishchuk, B.E. Microbial community structure and function: The effect of silvicultural burning and topographic variability in northern Alberta. *Soil Biol. Biochem.* **2009**, *41*, 770–777. [CrossRef]
39. Olsson, P.A. Signature fatty acids provide tools for determination of the distribution and interactions of mycorrhizal fungi in soil. *Fems Microbiol. Ecol.* **1999**, *29*, 303–310. [CrossRef]
40. Fierer, N.; Schimel, J.P.; Holden, P.A. Variations in microbial community composition through two soil depth profiles. *Soil Biol. Biochem.* **2003**, *35*, 167–176. [CrossRef]
41. Tornberg, K.; Bååth, E.; Olsson, S. Fungal growth and effects of different wood decomposing fungi on the indigenous bacterial community of polluted and unpolluted soils. *Biol. Fertil. Soils* **2003**, *37*, 190–197.
42. Skjemstad, J.O.; Clarke, P.; Taylor, J.A.; Oades, J.M.; Newman, R.H. The removal of magnetic materials from surface soils—A solid state 13 C CP/MAS NMR study. *Aus. J. Soil Res.* **1994**, *32*, 1215–1229. [CrossRef]
43. Preston, C.M.; Nault, J.R.; Trofymow, J.A. Chemical Changes During 6 Years of Decomposition of 11 Litters in Some Canadian Forest Sites. Part 2. ^{13}C Abundance, Solid-State ^{13}C NMR Spectroscopy and the Meaning of "Lignin". *Ecosystems* **2009**, *12*, 1078–1102. [CrossRef]
44. Dai, K.O.H.; Johnson, C.E.; Driscoll, C.T. Organic matter chemistry and dynamics in clear-cut and unmanaged hardwood forest ecosystems. *Biogeochemistry* **2001**, *54*, 51–83. [CrossRef]
45. Jones, D.L.; Willett, V.B. Experimental evaluation of methods to quantify dissolved organic nitrogen (DON) and dissolved organic carbon (DOC) in soil. *Soil Biol. Biochem.* **2006**, *38*, 991–999. [CrossRef]
46. Lloyd, J.; Taylor, J.A. On the Temperature Dependence of Soil Respiration. *Funct. Ecol.* **1994**, *8*, 315–323. [CrossRef]
47. Zhang, X.J.; Hui, X.U.; Chen, G.X. Major factors controlling nitrous oxide emission and methane uptake from forest soil. *J. For. Res.* **2001**, *12*, 239–242.

48. Bowden, R.D.; Davidson, E.; Savage, K.; Arabia, C.; Steudler, P. Chronic nitrogen additions reduce total soil respiration and microbial respiration in temperate forest soils at the Harvard Forest. *For. Ecol. Manag.* **2004**, *196*, 43–56. [CrossRef]
49. Maaroufi, N.I.; Nordin, A.; Hasselquist, N.J.; Bach, L.H.; Palmqvist, K.; Gundale, M.J. Anthropogenic nitrogen deposition enhances carbon sequestration in boreal soils. *Glob. Chang. Biol.* **2015**, *21*, 3169–3180. [CrossRef]
50. Song, X.; Gu, H.; Wang, M.; Zhou, G.; Li, Q. Management practices regulate the response of Moso bamboo foliar stoichiometry to nitrogen deposition. *Sci. Rep.* **2016**, *6*, 24107. [CrossRef]
51. Treseder, K.K. Nitrogen additions and microbial biomass: A meta-analysis of ecosystem studies. *Ecol. Lett.* **2008**, *11*, 1111–1120. [CrossRef] [PubMed]
52. Lu, M.; Zhou, X.; Luo, Y.; Yang, Y.; Fang, C.; Chen, J.; Li, B. Minor stimulation of soil carbon storage by nitrogen addition: A meta-analysis. *Agric. Ecosyst. Environ.* **2011**, *140*, 234–244. [CrossRef]
53. Tian, D.; Hong, W.; Jian, S.; Niu, S. Global evidence on nitrogen saturation of terrestrial ecosystem net primary productivity. *Environ. Res. Lett.* **2016**, *11*, 024012. [CrossRef]
54. Zhou, Z.; Wang, C.; Zheng, M.; Jiang, L.; Luo, Y. Patterns and mechanisms of responses by soil microbial communities to nitrogen addition. *Soil Biol. Biochem.* **2017**, *115*, 433–441. [CrossRef]
55. Driscoll, C.T.; Driscoll, K.M.; Mitchell, M.J.; Raynal, D.J. Effects of acidic deposition on forest and aquatic ecosystems in New York State. *Environ. Pollut.* **2003**, *123*, 327–336. [CrossRef]
56. Mo, J.; Li, D.; Gundersen, P. Seedling growth response of two tropical tree species to nitrogen deposition in southern China. *Eur. J. For. Res.* **2008**, *127*, 275–283. [CrossRef]
57. Lu, X.; Mao, Q.; Gilliam, F.S.; Luo, Y.; Mo, J. Nitrogen deposition contributes to soil acidification in tropical ecosystems. *Glob. Chang. Biol.* **2014**, *20*, 3790–3801. [CrossRef] [PubMed]
58. Mo, J.; Zhang, W.; Zhu, W.; Fang, Y.; Li, D.; Zhao, P. Response of soil respiration to simulated N deposition in a disturbed and a rehabilitated tropical forest in southern China. *Plant Soil* **2007**, *296*, 125–135. [CrossRef]
59. Liu, Q.; Edwards, N.T.; Post, W.M.; Gu, L.; Ledford, J.; Lenhart, S. Temperature-independent diel variation in soil respiration observed from a temperate deciduous forest. *Glob. Chang. Biol.* **2006**, *12*, 2136–2145. [CrossRef]
60. Wang, Q.K.; Zhao, X.C.; Chen, L.C.; Yang, Q.P.; Chen, S.; Zhang, W.D. Global synthesis of temperature sensitivity of soil organic carbon decomposition: Latitudinal patterns and mechanisms. *Funct. Ecol.* **2019**, *33*, 514–523. [CrossRef]
61. Liu, Y.; He, N.P.; Zhu, J.X.; Xu, L.; Yu, G.R.; Niu, S.L.; Sun, X.M.; Wen, X.F. Regional variation in the temperature sensitivity of soil organic matter decomposition in China's forests and grasslands. *Glob. Chang. Biol.* **2017**, *23*, 3393–3402. [CrossRef]
62. Chen, R.; Senbayram, M.; Blagodatsky, S.; Myachina, O.; Dittert, K.; Lin, X.; Blagodatskaya, E.; Kuzyakov, Y. Soil C and N availability determine the priming effect: microbial N mining and stoichiometric decomposition theories. *Glob. Chang. Biol.* **2014**, *20*, 2356–2367. [CrossRef]
63. Ramirez, K.S.; Craine, J.M.; Fierer, N. Consistent effects of nitrogen amendments on soil microbial communities and processes across biomes. *Glob. Chang. Biol.* **2012**, *18*, 1918–1927. [CrossRef]
64. Fatemi, F.R.; Fernandez, I.J.; Simon, K.S.; Dail, D.B. Nitrogen and phosphorus regulation of soil enzyme activities in acid forest soils. *Soil Biol. Biochem.* **2016**, *98*, 171–179. [CrossRef]
65. Wang, J.J.; Bowden, R.D.; Lajtha, K.; Washko, S.E.; Wurzbacher, S.J.; Simpson, M.J. Long-term nitrogen addition suppresses microbial degradation, enhances soil carbon storage, and alters the molecular composition of soil organic matter. *Biogeochemistry* **2019**, *142*, 299–313. [CrossRef]
66. Feng, X.; Simpson, M.J. Temperature and substrate controls on microbial phospholipid fatty acid composition during incubation of grassland soils contrasting in organic matter quality. *Soil Biol. Biochem.* **2009**, *41*, 804–812. [CrossRef]
67. Griffiths, B.S.; Ritz, K.; Ebblewhite, N.; Dobson, G. Soil microbial community structure: effects of substrate loading rates. *Soil Biol. Biochem.* **1999**, *31*, 145–153. [CrossRef]
68. Kramer, C.; Gleixner, G. Variable use of plant- and soil-derived carbon by microorganisms in agricultural soils. *Soil Biol. Biochem.* **2006**, *38*, 3267–3278. [CrossRef]
69. Baldock, J.A.; Oades, J.M.; Waters, A.G.; Peng, X.; Vassallo, A.M.; Wilson, M.A. Aspects of the Chemical Structure of Soil Organic Materials as Revealed by Solid-State ^{13}CNMR Spectroscopy. *Biogeochemistry* **1992**, *16*, 1–42. [CrossRef]
70. Knorr, M.; Frey, S.D.; Curtis, P.S. Nitrogen Additions and Litter Decomposition: A Meta-Analysis. *Ecology* **2005**, *86*, 3252–3257. [CrossRef]

71. Frey, S.D.; Ollinger, S.; Nadelhoffer, K.; Bowden, R.; Brzostek, E.; Burton, A.; Caldwell, B.A.; Crow, S.; Goodale, C.L.; Grandy, A.S.; et al. Chronic nitrogen additions suppress decomposition and sequester soil carbon in temperate forests. *Biogeochemistry* **2014**, *121*, 305–316. [CrossRef]
72. Berg, M.P.; Kniese, J.P.; Zoomer, R.; Verhoef, H.A. Long-term decomposition of successive organic strata in a nitrogen saturated Scots pine forest soil. *For. Ecol. Manag.* **1998**, *107*, 159–172. [CrossRef]
73. Davidson, E.A.; Sabá, R.T. Nitrogen and phosphorus limitation of biomass growth in a tropical secondary forest. *Ecol. Appl.* **2004**, *14*, 150–163. [CrossRef]
74. Zeng, W.; Chen, J.; Liu, H.; Wang, W. Soil respiration and its autotrophic and heterotrophic components in response to nitrogen addition among different degraded temperate grasslands. *Soil Biol. Biochem.* **2018**, *124*, 255–265. [CrossRef]
75. Chambers, J.Q.; Tribuzy, E.S.; Toledo, L.C.; Crispim, B.F.; Higuchi, N.; dos Santos, J.; Araujo, A.C.; Kruijt, B.; Nobre, A.D.; Trumbore, S.E. Respiration from a tropical forest ecosystem: Partitioning of sources and low carbon use efficiency. *Ecol. Appl.* **2004**, *14*, S72–S88. [CrossRef]
76. Zhu, J.; Yan, Q.; Fan, A.N.; Yang, K.; Hu, Z. The role of environmental, root, and microbial biomass characteristics in soil respiration in temperate secondary forests of Northeast China. *Trees* **2009**, *23*, 189–196. [CrossRef]
77. Iqbal, J.; Hu, R.; Feng, M.; Lin, S.; Malghani, S.; Ali, I.M. Microbial biomass, and dissolved organic carbon and nitrogen strongly affect soil respiration in different land uses: A case study at Three Gorges Reservoir Area, South China. Agric. *Ecosyst. Environ.* **2010**, *137*, 294–307. [CrossRef]
78. Wang, C.; Liu, D.; Bai, E. Decreasing soil microbial diversity is associated with decreasing microbial biomass under nitrogen addition. *Soil Biol. Biochem.* **2018**, *120*, 126–133. [CrossRef]
79. Philippot, L.; Spor, A.; Henault, C.; Bru, D.; Bizouard, F.; Jones, C.M.; Sarr, A.; Maron, P.A. Loss in microbial diversity affects nitrogen cycling in soil. *Int. Soc. Microb. Ecol.* **2013**, *7*, 1609–1619.

forests

MDPI

Article

The Influence of Land Use Patterns on Soil Bacterial Community Structure in the Karst Graben Basin of Yunnan Province, China

Jiangmei Qiu [1,2,3], Jianhua Cao [2,3], Gaoyong Lan [2,3], Yueming Liang [2,3], Hua Wang [2,3] and Qiang Li [2,3,*]

1 College of Environmental Science and Engineering, Guilin University of Technology, Guilin 541004, China; 15676217735@163.com

2 Key Laboratory of Karst Dynamics, MNR & GZAR, Institute of Karst Geology, Chinese Academy of Geological Sciences, Guilin 541004, China; jhcaogl@karst.ac.cn (J.C.); langaoyong@karst.ac.cn (G.L.); lym@karst.ac.cn (Y.L.); wanghua@karst.ac.cn (H.W.)

3 International Research Center on Karst under the Auspices of UNESCO, Guilin 541004, China

* Correspondence: liqiang@karst.ac.cn

Received: 21 November 2019; Accepted: 30 December 2019; Published: 31 December 2019

Abstract: Land use patterns can change the structure of soil bacterial communities. However, there are few studies on the effects of land use patterns coupled with soil depth on soil bacterial communities in the karst graben basin of Yunnan province, China. Consequently, to reveal the structure of the soil bacterial community at different soil depths across land use changes in the graben basins of the Yunnan plateau, the relationship between soil bacterial communities and soil physicochemical properties was investigated for a given area containing woodland, shrubland, and grassland in Yunnan province by using next-generation sequencing technologies coupled with soil physicochemical analysis. Our results indicated that the total phosphorus (TP), available potassium (AK), exchangeable magnesium (E-Mg), and electrical conductivity (EC) in the grassland were significantly higher than those in the woodland and shrubland, yet the total nitrogen (TN) and soil organic carbon (SOC) in the woodland were higher than those in the shrubland and grassland. *Proteobacteria*, *Verrucomicrobia*, and *Acidobacteria* were the dominant bacteria, and their relative abundances were different in the three land use types. SOC, TN, and AK were the most important factors affecting soil bacterial communities. Land use exerts strong effects on the soil bacterial community structure in the soil's surface layer, and the effects of land use attenuation decrease with soil depth. The nutrient content of the soil surface layer was higher than that of the deep layer, which was more suitable for the survival and reproduction of bacteria in the surface layer.

Keywords: karst graben basin; land use pattern; bacterial community; next-generation sequencing

1. Introduction

The karst graben basin in the East Yunnan plateau is a special geomorphological formation due to the rifts of the plateau, which were uplifted at the same time [1,2]. This area is also the main area of the "two barriers and three belts" for China's national ecological security. However, due to deforestation of this area over the past several decades, the karst ecosystem has seriously degenerated, thereby affecting soil quality, soil fertility, and ecological conditions, and resulting in abandoned bare land. To fight against this environmental problem, the "Green for Grain" program, or the Natural Forest Protection Project, was launched by the Chinese government in this region [3–5]. Accordingly, the size of the degenerated areas has shrunk with the revegetation process. However, little is known about how vegetation restoration types affect the soil bacterial community's structure in the karst graben basin.

Vegetation restoration can affect soil microorganism communities, which can regulate the soil's biogeochemical cycles and affect the stability of the soil's ecosystem [6–8]. Although many studies have discussed soil microbial community structures with land use pattern changes worldwide, there are few studies on the influence of land use patterns on the soil bacterial community's structure in karst graben basins. For example, Suleiman et al. compared the bacterial community in the original forest-covered area and grassland for eight years and found that the main bacterial community composition showed little difference [9]. Song et al. found that the number and composition of the soil microbial population in the karst peak-cluster depression were different in farmland, grassland, scrubland, forest plantation, secondary forest, and primary forest [10]. Ederson et al. found that there were significant differences in the community composition among crops, pastures, and agroforestry, as well as young secondary forest (up to 5 years old), old secondary forest (5 to 30 years old), and primary forest sites [11]. To better explore the influence of land use patterns on the soil bacterial community structure in the Luxi county in the Yunnan karst graben basin, the woodland, shrubland, and grassland in a given karst area were selected. Our objectives were to (i) gain insight into the difference of soil bacterial community structure with land use changes, (ii) inquire into the effects of land use patterns with soil depth, and (iii) identify the key factors in determining soil bacterial communities. Our findings provide a basis for understanding the influence of land use patterns on soil bacterial community structures in the karst graben basin of Yunnan province, China.

2. Materials and Methods

2.1. Study Sites

Luxi county (103°30′–104°03′ E, 24°15′–24°46′ N) is located in the north Honghe Hani and Yi Autonomous Prefecture in Yunnan province in the subtropical monsoon climate zone, which is rainy in summer and dry in winter. The rainy season extends from May to October, and the dry season runs from March to April. The average annual precipitation is 2026.5 mm. The average annual temperature is 16.3 °C. Moreover, the rocky desertification in Luxi country is serious.

2.2. Soil Sample Collection

Sampling occurred between the wet and dry season, January 2018. Three 20 × 20 m plots were established for each land use pattern. The minimum distance between plots was 400 m to avoid pseudoreplication. Soil samples were collected from the surface soil (0–10 cm), named the A layer, and the other samples were taken from the deep layer (10–20 cm), named B layer, with a split tube auger 5 cm in diameter. At each plot, six soil cores were selected in an S-shaped pattern to form one soil sample. A total of 18 soil samples from woodland (WL), shrubland (SL), and grassland (GL) were collected. Soil samples were named according to the soil sampling sites (such as SL) and soil layer (A: 0–10 cm) in that particular order (e.g., SLA). The three land use patterns were continuously managed for 15 years. All soil samples were transported to the laboratory immediately after collection in sterile plastic bags on dry ice and divided into two uniform portions. One portion was stored at −80 °C for DNA analysis, and the other part was air dried for physicochemical analysis.

2.3. Physicochemical Analysis

Soil moisture content (moisture), soil temperature (T), and EC were measured in situ by soil three-parameter tachometers (Delta-T Devices Ltd., Moisture Meter type HH2, UK). Soil organic carbon (SOC) was determined by wet digestion using the H_2SO_4 and $K_2Cr_2O_7$ method [12]. Total phosphorus (TP) was determined using the molybdenum blue colorimetric method following $HClO_4$ digestion [13]. Available potassium (AK) was extracted with ammonium acetate and analyzed using a flame photometer [14]. Total nitrogen (TN) was determined by an element analyzer [15]. Soil pH was determined by a 1:5 (m:V) soil/water ratio and measured by a corrected desktop pH meter of Maitre-Toledo S470-B Seven Excellence [16]. Exchangeable calcium (E-Ca)

and exchangeable magnesium (E-Mg) were determined by ammonium acetate exchange-atomic absorption spectrophotometry [17].

2.4. DNA Extraction

DNA was extracted using the Powersoil DNA Isolation Kit (Mobio Laboratories, Inc., Carlsbad, CA, USA). For next-generation sequencing, the V3–V4 region of 16S rRNA genes was amplified using PCR primers 338F (ACTCCTACGGGAGGCAGCA) and 806R (GGACTACHVGGGTWTCTA AT). The PCR products targeting the V3–V4 region of the 16S rRNA genes were purified by using the TIANquick Maxi Purification Kit (TIANGEN Biotech (Beijing) Co., Ltd., China). Then, 16S rRNA gene sequencing was performed on the Illumina HiSeq 2500 platform (Illumina Inc., San Diego, CA, USA) at the MAGIENE (Guangzhou, China).

2.5. Bioinformatic Analysis and Statistical Analysis

According to the barcode sequence, the sequencing data were divided into different sample data, and the barcode sequence was truncated. After splicing each sample with FLASH 1.2.11 software [18], the Cutadapt 1.9.1 software was employed to truncate the sequence of PCR amplified primers and remove fragments (less than 200 bp) [19]. Using the SILVA SSURef 123 NR database as the reference database, chimeric sequences were removed by the UCHIME 4.2 software [20,21]. Afterwards, the processed sequences were clustered with the UCLUST 1.2.22 software in operational taxonomic units (OTUs) according to sequences with more than a 97% similarity, and the OTUs were classified by the UCLUST 1.2.22 software alignment against the most recent SILVA (123) database [22]. The QIIME 1.9.1 software was used to perform an alpha diversity (Chao1, Simpson, Shannon, and Observed OTUs) and beta diversity test on the OTU table [23].

SPSS 25 software (SPSS Inc., Chicago, IL, USA) for a one-way ANOVA was used to analyze the difference soil physicochemical properties and bacterial community structure and diversity in different land use patterns [24]. The least significant difference method was used for multiple comparisons, and the Pearson correlation coefficient method was used for a correlation analysis. The Origin 8.5 software was used to map the abundance of bacterial communities at the phyla level. The OTUs whose numbers were more than 0.5% of the total OTUs were defined as the dominant OTUs. RStudio 3.0.3 software was used to draw the heat map of the dominant OTUs and perform a distance-based redundancy analysis (db-RDA) between the soil bacteria and soil physicochemical parameters [25]. The similarity of the OTUs among samples was analyzed by using the Bray–Curtis and weighted UniFrac distance algorithm of principal coordinate analysis (PCoA) [26]. The network maps of dominant OTUs and soil physicochemical factors were drawn via the Gephi 0.9.2 software [27].

3. Results

3.1. Soil Physicochemical Parameters with Land Use Changes

It can be seen that the soil's physicochemical properties were different in the woodland, shrubland, and grassland (Table 1). The TP, AK, E-Mg, EC, and T in grassland were higher than those in the woodland and shrubland. The TN and SOC in the woodland were higher than those in the shrubland and grassland. Moreover, the soil physicochemical properties, except for some physicochemical properties in woodland, decreased by increasing soil depth.

Table 1. The soil physicochemical properties in different land use patterns.

Name	Land Use Pattern	TP	TN	SOC	AK	pH	Moisture	T	EC	E-Ca	E-Mg
		(g/kg)	(g/kg)	(g/kg)	(g/kg)		(%)	(°C)	(ms.m^{-1})	(cmol/kg)	(cmol/kg)
WLA	woodland	0.828 ± 0.020 ab	5.09 ± 0.24 a	61.00 ± 1.96 a	128.47 ± 5.78 b	6.21 ± 0.11 b	37.47 ± 5.04 a	8.60 ± 0.21 c	68.33 ± 4.10 b	5.14 ± 1.15 a	26.82 ± 0.65 c
SLA	Shrubland	0.734 ± 0.025 b	4.11 ± 0.16 b	47.00 ± 2.5 b	124.03 ± 14.05 b	6.72 ± 0.09 a	42.85 ± 2.56 a	11.60 ± 1.12 b	64.33 ± 2.03 b	6.91 ± 0.09 a	36.18 ± 3.48 b
GLA	Grassland	0.941 ± 0.059 a	2.97 ± 0.14 c	33.00 ± 1.47 c	262.17 ± 44.37 a	6.68 ± 0.08 a	40.00 ± 1.42 a	16.53 ± 0.74 a	84.67 ± 2.03 a	6.87 ± 0.08 a	51.56 ± 2.32 a
WLB	woodland	0.640 ± 0.037 a	3.16 ± 0.49 a	35.79 ± 5.32 a	40.40 ± 2.14 b	6.46 ± 0.10 a	36.53 ± 2.98 a	9.37 ± 0.09 c	70.33 ± 6.64 ab	6.64 ± 0.11 a	29.21 ± 0.28 c
SLB	Shrubland	0.595 ± 0.025 a	2.32 ± 0.12 a	24.53 ± 2.13 ab	38.40 ± 3.98 b	6.66 ± 0.08 a	33.07 ± 1.91 a	10.97 ± 0.33 b	56.00 ± 3.00 b	6.85 ± 0.08 a	34.20 ± 1.02 b
GLB	Grassland	0.762 ± 0.084 a	2.34 ± 0.37 a	20.46 ± 3.71 b	127.27 ± 15.21 a	6.55 ± 0.03 a	32.70 ± 1.16 a	12.77 ± 0.34 a	79.33 ± 5.70 a	6.73 ± 0.03 a	39.82 ± 1.05 a

Note: A = 0–10 cm (A layer), B = 10–20 cm (B layer); data are the means ± standard error (means ± SE); different lowercase letters (a, b and c) in the same column represent a significant difference from the different sample points in the same soil layer ($p < 0.05$). TP: total phosphorous, TN: total nitrogen, SOC: soil organic carbon, AK: available potassium, T: temperature, EC: electrical conductivity, E-Ca: exchangeable calcium, E-Mg: exchangeable magnesium.

3.2. Soil Bacterial Community Structure and Diversity

The dominant phyla were different in the three land use types, as well as in the A and B layers, as seen in Figure 1. There were 13 dominant phyla in the A layer (Figure 1a). *Proteobacteria*, *Verrucomicrobia*, and *Acidobacteria* were the most abundant dominant bacteria. The total proportions of the three dominant bacteria in the A layer were woodland (80.22%), shrubland (80.07%), and grassland (59.52%); the *Verrucomicrobia* in grassland were significantly fewer than those in the woodland and shrubland; *Acidobacteria*, *Actinobacteria*, *Bacteroidetes*, and *Chloroflexi* in grassland were significantly higher than those in woodland and shrubland (Table S1). In the B layer, the total proportions of the three most abundant dominant bacteria were woodland (78.61%), shrubland (67.14%), and grassland (56.03%). Among the three different land use patterns, the composition and proportions of the other dominant phyla were different but not significant.

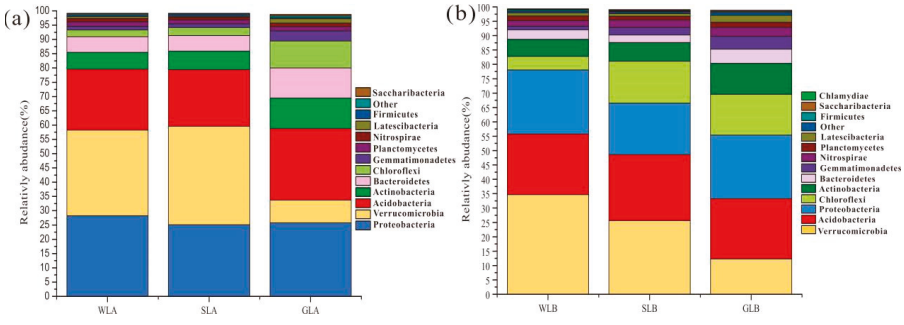

Figure 1. Comparison of the average quantitative contribution of the sequences affiliated with different bacterial phyla from the A layer (**a**) and B layer (**b**). Sequences not classified under any known phylum are included as unassigned bacteria. In each soil sample, the bacterial phylum with relative frequency of less than 1% is included as others.

Moreover, the heat map clearly shows the distribution of the dominant OTUs (Figure 2). In the A layer (Figure 2a), OTU 410 (DA101 soil group) and OTU 24 (*Candidatus Solibacter*) were the dominant OTUs for the woodland; OTUs 238 and 30 (*Candidatus Solibacter*), OTUs 28 and 124 (*Sphingomonas*), OTUs 49, 69, and 27 (subgroup 6), and OTUs 58, 368, 26, and 47 (RB41) were the dominant OTUs for grassland; and OTUs 1, 31, 2312, 9, and 823 (DA101 soil group), and OTU 12 (*Acidobacteria*) were the dominant OTUs for shrubland. In the B layer (Figure 2b), OTUs 163, 823, 2, 1, and 772 (DA101 soil group), and OTUs 10 and 2858 (*Acidobacteriaceae*) were the dominant OTUs in shrubland. OTUs 65 and 16 (0319-6A21) and OTUs 53 and 11 (*Acidobacteriaceae*) were the dominant OTUs in woodland. OTU 21 (*Candidatus Xiphinematobacter*), OTU 71 (*Gemmatimonadaceae*), and OTU 54 (*Pedomicrobium*) were the dominant OTUs in grassland.

The alpha diversities of the soil bacterial communities were different between the three land use types. In the A layer, except for the Simpson index, the alpha diversity indices from grassland were significantly higher than those from shrubland and woodland ($p < 0.05$), as listed in Table 2. Moreover, there was no significant difference between shrubland and woodland ($p > 0.05$). In the B layer, the alpha diversity indices of the three land use patterns were not significantly different, except for the Simpson index. The alpha diversities decreased with an increase in soil depth, except for the Simpson index.

To investigate the effects of land use type and soil depth on soil bacterial communities, we examined the beta diversity (Figure 3). The shrubland and woodland can be accurately clustered together, which shows the similarity of their bacterial communities' compositions. Compared with the A layer, the points in the B layer were more dispersed.

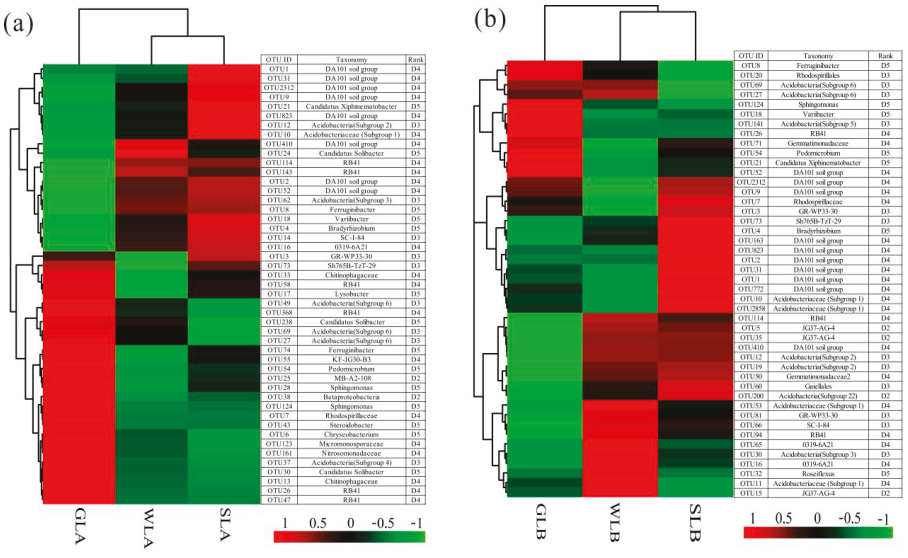

Figure 2. Heat map illustrating the mean relative frequency of the 47 most abundant operational taxonomic units (OTUs) with abundances >0.5% in the A layer with different land uses (**a**). Heat map illustrating the mean relative frequency of the 45 most abundant OTUs with abundances >0.5% in the B layer with different land uses (**b**). Taxonomic assignment of the OTUs is provided at the lowest level of classification possible according to the SILVA 123 database (D1: phylum, D2: class, D3: order, D4: family, and D5: genus).

Table 2. Alpha diversities of the soil bacterial communities with different land use patterns.

Name	Land Use Pattern	Chao1	Shannon	Simpson	Observed OTUs
WLA	Woodland	1656 ± 69 b	8.01 ± 0.23 b	0.985 ± 0.004 a	1162 ± 45 b
SLA	Shrubland	1640 ± 70 b	7.69 ± 0.17 b	0.977 ± 0.004 b	1103 ± 48 b
GLA	Grassland	1935 ± 75 a	8.85 ± 0.10 a	0.993 ± 0.001 a	1409 ± 25 a
WLB	Woodland	1582 ± 89 a	7.80 ± 0.31 a	0.981 ± 0.005 b	1115 ± 67 a
SLB	Shrubland	1565 ± 62 a	7.70 ± 0.07 a	0.982 ± 0.002 a	1030 ± 24 a
GLB	Grassland	1693 ± 119 a	8.54 ± 0.37 a	0.993 ± 0.003 a	1212 ± 106 a

Note: A = 0–10 cm (A layer), B = 10–20 cm (B layer); data are the means ± standard error (means ± SE). Different lowercase letters (a and b) in the same column represent a significant difference from the different sample points in the same soil layer ($p < 0.05$).

3.3. The Relationship between Soil Physicochemical Parameters and Soil Bacteria

To assess the influence of land uses on bacterial community composition, we performed a db-RDA on the dominant bacterial phyla. According to the db-RDA plot and Spearman's correlations between the soil physicochemical parameters and dominant phyla in the land use types, the first two axes accounted for 2.86% of the variability of the bacterial community structure in the A layer. Further, the bacterial communities were positively correlated with six soil physicochemical properties (including SOC, TN, TP, AK, EC, and T) (Figure 4a). *Verrucomicrobia* were negatively correlated with TP, T, E-Mg, AK, and EC, and positively correlated with TN and SOC. *Acidobacteria* were positively correlated with EC, T, and E-Mg; *Actinobacteria* were positively correlated with AK, EC, T, and E-Mg; *Bacteroidetes* were positively correlated with E-Mg, AK, and EC; *Chloroflexi* were positively correlated with T, E-Mg, TP, AK, and EC; and *Actinobacteria*, *Bacteroidetes*, and *Chloroflexi* were negatively correlated with TN and SOC (Figure 5). In the B layer, db-RDA showed that the first two axes accounted for 2.86% of the variability of the bacterial community structure, and bacterial communities were positively

correlated with SOC, TN, AK, and T (Figure 4b). *Verrucomicrobia* were positively correlated with SOC and negatively correlated with AK, T, and E-Mg. *Acidobacteria* were negatively correlated with TP; *Chloroflexi* were negatively correlated with TN and SOC, and positively correlated with T and E-Mg; *Actinobacteria* were positively correlated with AK, TP, T, E-Mg, and EC; and *Bacteroidetes* were positively correlated with AK and TP (Figure 5).

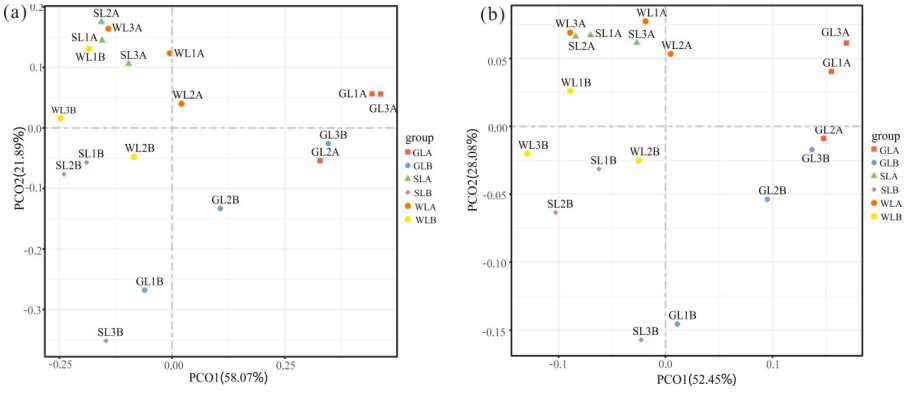

Figure 3. Principal coordinate analysis (PCoA) plots of soil microbial community structures based on the Bray–Curtis and weighted UniFrac results under different land use types in the Yunnan karst graben basin. Bray–Curtis (**a**); weighted UniFrac (**b**).

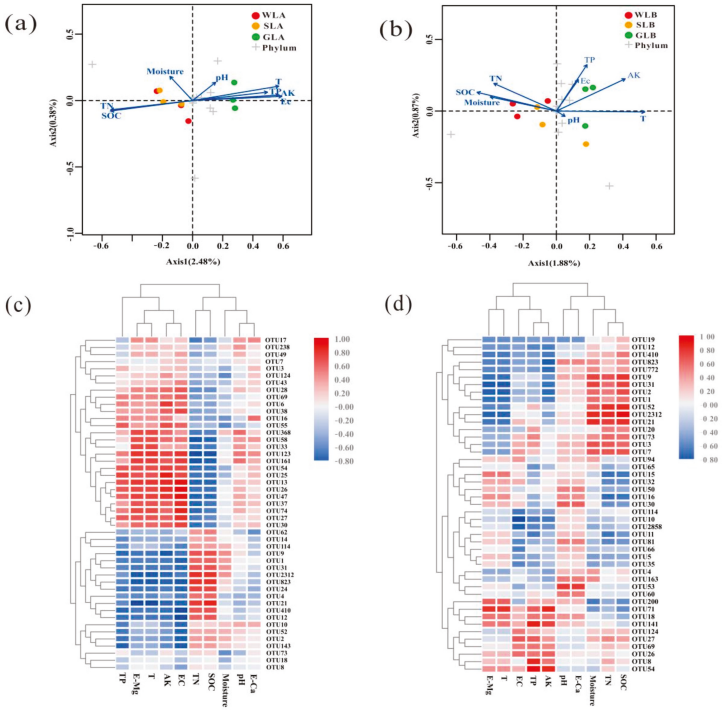

Figure 4. *Cont*.

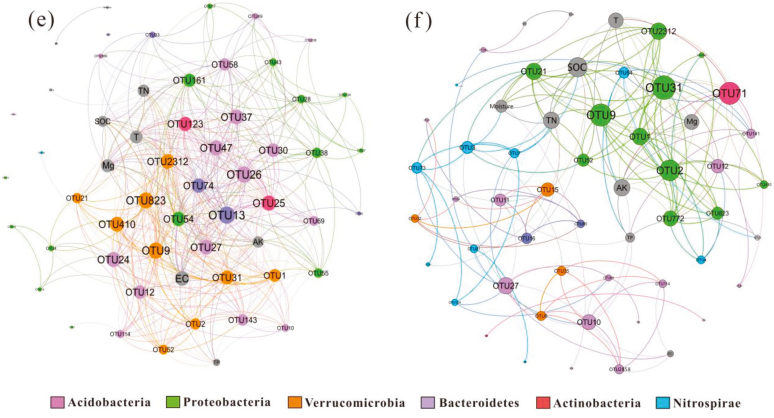

Figure 4. Distance-based redundancy analysis (db-RDA) plots revealing the relationship between the dominant phyla (mean relative frequency >1%) and soil physicochemical parameters in the surface layer (**a**) and deep layer (**b**). Heat map representing the relationship between the soil physicochemical parameters and the most abundant OTUs with abundances >0.5% in the surface layer (**c**) and deep layer (**d**). The networks revealing the co-occurring bacterial OTUs and soil properties in the surface layer (**e**) and deep layer (**f**). The co-occurring networks are colored at the phylum level, and the size of each node is proportional to the number of connections.

A Layer	TP	TN	SOC	AK	pH	T	Moistrue	EC	E-Ca	E-Mg
Proteobacteria	-0.150	0.214	0.283	-0.144	-0.546	-0.395	-0.746*	-0.103	-0.176	-0.395
Verrucomicrobia	-0.691*	0.757*	0.748*	-0.801**	-0.157	-0.775*	0.309	-0.819**	-0.161	-0.775*
Acidobacteria	0.558	-0.611	-0.540	0.565	0.171	0.674*	-0.068	0.777*	-0.089	0.674*
Actinobacteria	0.596	-0.860**	-0.864**	0.820**	0.41	0.830**	-0.132	0.820**	0.327	0.830**
Bacteroidetes	0.666	-0.683*	-0.757*	0.900**	0.114	0.753*	-0.265	0.823**	0.133	0.753*
Chloroflexi	0.739*	-0.776*	-0.816**	0.738*	0.441	0.902**	0.098	0.742*	0.274	0.902**
Planctomycetes	-0.348	0.135	0.254	-0.350	-0.311	-0.180	-0.420	-0.064	-0.439	-0.180
B Layer	**TP**	**TN**	**SOC**	**AK**	**PH**	**T**	**Moisture**	**EC**	**E-Ca**	**E-Mg**
Verrucomicrobia	-0.366	0.581	0.753*	-0.723*	-0.034	-0.845**	0.660	-0.259	-0.028	-0.845**
Acidobacteria	-0.725*	-0.612	-0.423	-0.356	-0.284	0.006	-0.540	-0.568	-0.279	0.006
Proteobacteria	0.472	0.219	0.169	0.354	-0.29	-0.134	0.095	0.503	-0.299	-0.134
Chloroflexi	-0.211	-0.700*	-0.750*	0.193	0.18	0.683*	-0.617	-0.139	0.180	0.683*
Actinobacteria	0.678*	-0.195	-0.406	0.843**	0.239	0.683*	-0.112	0.669*	0.234	0.683*
Bacteroidetes	0.953**	0.437	0.186	0.706	-0.066	0.259	-0.073	0.268	-0.070	0.259
Nitrospirae	-0.386	-0.764*	-0.748*	0.056	0.158	0.534	-0.279	0.143	0.155	0.534
Planctomycetes	0.884**	0.392	0.173	0.641	-0.29	0.153	-0.152	0.251	-0.298	0.153

Figure 5. Spearman's correlations showing the relationship between the soil physicochemical parameters and dominant phyla in the three land use types. Significance levels are denoted as follows: $p < 0.05$ (*) and $p < 0.01$ (**).

Heat maps showed that TP, T, E-Mg, AK, EC, TN, and SOC were significantly correlated with most of the dominant OTUs, whereas pH and E-Ca were significantly correlated with some OTUs (Figure 4c,d). In the A layer, OTUs 26, 47, 58, and 368 (RB41); OTUs 27 and 49 (subgroup 6); and OTUs 30 and 238 (*Candidatus Solibacter*) of *Acidobacteria* were significantly correlated with TP, T, E-Mg, AK, and EC (Figure 4c). Moreover, OTUs 28 and 124 (*Sphingomonas*), OTU 17 (*Lysobacter*), OTU 54 (*Pedomicrobium*), and OTU 43 (*Steroidobacter*) of *Proteobacteria* were also significantly correlated with TP, T, E-Mg, AK, and EC (Figure 4c). In the A layer, OTUs 1, 2, 9, 31, 52, 410, 823, and 2312 (DA101 soil group) and OTUs 114 and 143 (RB41) of *Verrucomicrobia* and *Acidobacteria* were significantly correlated with SOC and TN

(Figure 4c). In the B layer, OTU 26 (RB41) and OTUs 27 and 69 (subgroup 6) of *Acidobacteria* were significantly correlated with TP, T, E-Mg, AK, and EC (Figure 4d), and OTUs 1, 2, 9, 31, 52, 410, 772, 823, and 2312 (DA101 soil group) of *Verrucomicrobia* were significantly correlated with SOC and TN (Figure 4d), as confirmed by their significant relationships in Tables S2 and S3. Although representing the relationship between soil physicochemical parameters and despite the observation that the most abundant OTUs were different in the three land uses, these tables, on the whole, show a certain regularity (Figure 4c,d and Figure S1). The OTU co-occurrence patterns and the relationships among soil bacterial communities and physicochemical parameters were also investigated. Overall, the ecological networks were markedly different among the bacterial groups at different soil depths. This network was comprised of highly connected genera and soil physicochemical properties, thereby forming a "small world" topology. The nodes in the network were assigned to 11 bacterial phyla (Figure 4e,f). Among these, three phyla (*Proteobacteria*, *Acidobacteria*, and *Verrucomicrobia*) were widely distributed, accounting for over 60% of all nodes. In the surface layer, OTUs 26, 47, and 58 (RB41) and OTUs 1, 2, 9, 31, 410, 823, and 2312 (DA101 soil group) of *Acidobacteria* and *Verrucomicrobia* were keystone taxa (Figure 4e). In the deep layer, OTUs 1, 2, 9, and 2312 of *Acidobacteria* were keystone taxa (Figure 4f). This study indicates that these OTUs may play key roles in maintaining the structure and function of soil bacterial communities. It can be seen that EC, E-Mg, SOC, AK, T, and TN were the most important soil physicochemical factors affecting the bacterial community composition in the A layer, whereas SOC, AK, E-Mg, and TN were the most important factors in the B layer. The networks of competition and cooperation were more complex among bacteria in the surface layer than those in the deep layer. The correlation between bacterial communities and soil physicochemical properties decreased with an increase of soil depth (Figure 4c–f).

4. Discussion

4.1. The Characteristics of the Soil Physicochemical Properties

Land use patterns determine the surface vegetation and soil management method, which in turn result in a difference between soil physicochemical properties [28,29]. In our study, TP, AK, E-Mg, EC, and the moisture in grassland were significantly higher than those in the woodland and shrubland. However, the TN and SOC in woodland were significantly higher than those in shrubland and grassland. It is well known that microorganisms are intimately involved in rock weathering and could use these elements as electron acceptors and nutrients [30]. Consequently, grassland, during the early stages of vegetation succession under the influence of microorganisms on rock weathering, had a high concentration of AK, E-Mg, and TP compared with shrubland and woodland. However, due to the deficient root systems and lower amount of litter in grassland, the SOC and TN were low in the grassland. Moreover, SOC and TN are elements of soil fertility and are closely related to ecosystem stability, environmental protection, and land use [31,32]. Compared with grassland, the litter in woodland was high, and the root system was dense. Moreover, TN and SOC were also positively correlated. Therefore, the contents of TN and SOC in woodland were higher than those in shrubland and grassland. Further, soil nutrient contents decreased gradually with increasing soil depth because the soil's surface layer was the humus layer with rich litter, high nutrient content, a well-developed plant root system, good ventilation, and positive hydrothermal conditions [33–36].

4.2. Distribution of Bacterial Diversity Compositions

Bacterial communities from different land use types and different soil depths were highly diverse. In our study, soil bacterial diversity indices from grassland in the A layer and B layer were significantly higher than those in shrubland and woodland ($p < 0.05$). The diversity indices of soil bacterial communities in the three land use types decreased with increasing soil depth, which was consistent with the changes in soil physicochemical properties. Plant community richness usually increases during late successive stages. Moreover, increased plant community richness can significantly alter soil

bacterial community composition and is negatively correlated with bacterial diversity [37]. An increased plant community can supply a diverse array of resources to the soil, thereby promoting coevolutionary niche differentiation and favoring nonantagonistic microbial communities in which antagonism plays little role in maintaining soil community diversity [38]. The decrease in bacterial diversity with increasing soil depth is due to the reduction in the nutrient substrates for bacteria [39]. This is consistent with the expected depth patterns of soil bacterial diversity found in other studies [40,41].

Beta diversity was used to describe the similarities and differences in community structure. The PCoA distance showed a pronounced influence of land use changes on soil bacterial community structure. In our study, bacterial communities from grassland were significantly different from those in woodland and shrubland. This shows that the rate of species replacement between grassland and shrubland was relatively fast, possibly due to the lack of soil nutrients in grassland and increased competition during successive stages, which intensifies the species replacement between communities [42].

4.3. Relationships of Bacterial Communities with Basic Soil Parameters

Soil physicochemical properties determine the living environment of bacteria, which affect soil bacterial communities [43]. Soil bacteria play an extremely important role in organic matter decomposition, soil nutrient cycling, and ecological environment improvement [44,45]. Changes in bacterial community compositions led us to evaluate the extent of different land uses. Then, in our study, 33 dominant phyla were found in the 18 soil samples. *Proteobacteria*, *Verrucomicrobia*, and *Acrobacteria* were the most abundant dominant soil bacteria from the three land use patterns. These phyla have also been found in different relative proportions in other ecosystems worldwide [46,47], suggesting that they may play a fundamental role in these environments.

Proteobacteria showed no significant difference in the three land use patterns, yet their proportion in surface soil (26.61%) was significantly higher than that in deep soil (20.95%), which could be related to their copiotrophic living attributes. *Proteobacteria* belong to aerobic heterotrophic and facultative trophic bacteria [48,49], which are able to live in soils with high organic matter content. As a result, with an increase in soil depth, the soil nutrients decreased, and the abundance of *Proteobacteria* decreased. *Proteobacteria* were not significantly correlated with other physicochemical factors, except for soil moisture (Figure 5). At the same soil depth, the difference in moisture among the three land use patterns was not significant, and the other physicochemical factors had no significant effect on the distribution of *Proteobacteria* because *Proteobacteria* contain many subgroups with different habits, which are distributed in different niches. The *Proteobacteria's* structure is stable, and its anti-interference ability is strong. In the surface layer, OTUs from *Proteobacteria* were more prevalent in grassland (Figure 2a), and most of the OTUs were significantly correlated with TP, AK, E-Mg, EC, and T (Figure 4c). In the deep layer, *Proteobacteria* were not significantly different in their land use (Figure 2b). Further, the OTUs were not significantly correlated with the soil's physicochemical properties (Figure 4d). These bacterial structural differences reflect the prominent changes in particular groups. The heat map revealed that the distribution of OTUs was strongly affected by different land uses and soil depths, and soil nutrients appear to determine the distribution and frequency of OTUs (Figure 4c,d). Among the most frequent *Proteobacterial* OTUs, six were classified at the genus level (*Variibacter*, *Bradyrhizobium*, *Pedomicrobium*, *Steroidobacter*, *Sphingomonas*, *Lysobacter*). Interestingly, some taxonomically related OTUs from land use, such as *Proteobacteria*-related OTUs (28 and 124, classified as part of the *Sphingomonas* group), exhibited similar occurrence patterns. Some recent advances have demonstrated that *Sphingomonas* have unique abilities in degrading refractory contaminants, serving as bacterial antagonists to phytopathogenic fungi [50]. The genus *Bradyrhizobium* (OTU 4) is one of several genera of nitrogen-fixing bacteria, which play an important role in agricultural productivity and global nitrogen cycling. Previous reports have found that *Bradyrhizobium* are dominant in forest soil [51]. However, in our study, *Bradyrhizobium* were found to be dominant in shrubland and woodland environments.

Verrucomicrobia were the most widely distributed and diverse phylum of bacteria in soil habitats [49]. The proportion of *Verrucomicrobia* in grassland was significantly lower than that in woodland and shrubland at different soil depths. *Verrucomicrobia* were distributed in various soil and aquatic habitats, including environments with poor nutrition, eutrophication, extreme pollution, and man-made habitats [52,53]. *Verrucomicrobia* may be more adaptable to oligotrophic environments in soils [54], which are widely distributed in rhizosphere and aggregate soils. They can use a variety of carbon compounds and may be closely related to the carbon cycle [55]. Our study found that *Verrucomicrobia* were significantly positively correlated with TN and SOC (Figure 5), and significantly negatively correlated with TP, AK, EC, and E-Mg. Because the grassland had more soil nutrients, the proportion of *Verrucomicrobia* in grassland was significantly smaller than that in woodland and shrubland. Moreover, it was found that there was a striking increase in verrucomicrobial abundances at different soil depths (Figure 1). The slow growth rate of *Verrucomicrobia* may allow them to exploit the sparse resources in subsurface soil [56]. In different soil layers, OTUs from *Verrucomicrobia* were enriched in the shrubland (Figure 2a,b). Moreover, most OTUs from *Verrucomicrobia* were significantly correlated with TN and SOC (Figure 4c,d). Among the most frequent *Verrucomicrobia* OTUs, only one (OTU 21) was classified at the genus level (*Candidatus Xiphinematobacter*). Previous studies exposed the difficulty of classifying *Verrucomicrobia* because the portion of culturable bacteria within the *Verrucomicrobia* is quite low [57].

Acidobacteria were widespread in all types of soils with high richness [58]. In the A layer, *Acidobacteria* were significantly positively correlated with EC and E-Mg (Figure 5). The proportion of *Acidobacteria* in grassland was significantly higher than that in woodland and shrubland. In the B layer, *Acidobacteria* had a significantly negative correlation with TP (Figure 5), though the proportion of *Acidobacteria* in the three land use patterns was not significantly different. Moreover, the dominant genera from *Acidobacteria* were the *Blastocatella* (OTU 37) and *Candidatus Solibacter* OTUs (21, 30, and 238). In the surface layer, OTUs from *Acidobacteria* were prevalent in the three land uses, reflecting the high adaptability of this group. In the deep layer, OTUs from *Acidobacteria* were more frequent in grassland and shrubland. In addition, most OTUs were significantly correlated with TP, AK, E-Mg, EC, and moisture. Accordingly, each abundant *Acidobacteria* OTU prevailed in a different niche, reflecting the high adaptability of this group. *Acidobacteria* are acidophilic bacteria, which can decompose animal and plant residues and cellulose to form organic carbon [59]. Consequently, they are more suitable for living in a low organic carbon environment. Our study found that *Acidobacteria* were negatively correlated with TOC. Moreover, there was more litter on the soil's surface, making the surface more suitable for the survival of *Acidobacteria*.

5. Conclusions

Proteobacteria, *Verrucomicrobia*, and *Acidobacteria* were the dominant bacteria, but the abundance of bacterial communities was different. *Verrucomicrobia* were significantly positively correlated with TN and SOC and significantly negatively correlated with TP, AK, EC, and E-Mg. *Acidobacteria* were significantly correlated with EC, E-Mg, and TP. Different land use patterns have significant effects on the soil's physicochemical properties. TP, AK, E-Mg, and EC in the grassland were significantly higher than those in the woodland and shrubland. TN and SOC in the woodland were higher than those in the shrubland and grassland. The soil physicochemical properties decreased with increasing soil depth, and SOC, TN, and AK were the most important physicochemical properties affecting the composition of the bacterial community. The diversity of bacterial communities in the three land use types decreased with an increase of soil depth, which was consistent with the trend of soil physicochemical properties. Different land use patterns and soil depths have significant effects on bacterial communities. Land use shapes strong effects in the soil's bacterial community structure on the soil's surface layer, and the effects of land use attenuation decrease with soil depth. Compared with deep soil, surface soil contains more nutrients that are more suitable for the growth and reproduction of bacteria. Our study provides a basis for understanding the influence of land use patterns and soil

depths on the bacterial community structure in the karst graben basin of Yunnan province, China. Selecting a suitable land use according to the soil bacterial community structure of karst graben basins has great significance. We should also consider the impacts of soil bacterial communities on land use at different soil depths.

Supplementary Materials: The following are available online at http://www.mdpi.com/1999-4907/11/1/51/s1: Table S1: Abundance of dominant phyla in the three land use types. Table S2: Spearman's correlations showing the relationship between soil physicochemical parameters and dominant OTUs in the A layer. Table S3: Spearman's correlations showing the relationship between the soil physicochemical parameters and dominant OTUs in the B layer. Figure S1: Heat map representing the relationship between the soil physicochemical parameters and the most abundant OTUs with abundances >0.5% of the three land uses in different soil layers: woodland in the surface layer (**a**), shrubland in the surface layer (**b**), grassland in the surface layer (**c**), woodland in the deep layer (**d**), shrubland in the deep layer (**e**), and grassland in the deep layer (**f**).

Author Contributions: J.Q. organized the available literature and data, and subsequently developed the original draft of the manuscript. G.L., Y.L., and H.W. collected the soil samples. Q.L. planned and designed the research. Q.L. and J.C. developed the original concept for the project, co-authored the proposal to fund the research, and edited all subsequent drafts of the manuscript. All authors have read and agreed to the published version of the manuscript.

Funding: Project supported by the National Key Research and Development Program of China "Ecological, environmental and geological differentiation of rocky desertification and its driving mechanism in the karst graben basin" (No. 2016YFC0502501).

Conflicts of Interest: The authors declare no conflict of interest.

References

1. Yao, L.S. The formation mechanism and model of faulted karst basins in Yunnan province. *Carsol. Sin.* **1984**, *3*, 48–55. (In Chinese)
2. Wang, Y.; Zhang, H.; Zhang, G.; Wang, B.; Peng, S.H.; He, R.S.; Zhou, C.Q. Zoning of environmental geology and functions in karst fault-depression basins. *Carsol. Sin.* **2017**, *36*, 283–295. [CrossRef]
3. Deng, L.; Zhou, P.; Guan, S.; Li, R. Effects of the grain-for-green program on soil erosion in China. *Int. J. Sediment. Res.* **2012**, *27*, 120–127. [CrossRef]
4. Yang, J. Yunnan Natural Forest Resources Conservation Project Phase II Started in an All-round Way. *Yunnan For.* **2011**, *32*, 24. (In Chinese)
5. Bai, C.L. Deepening Reform and Accelerating Development Creating a New Situation of Natural Forest Protection Project Construction in Yunnan Province. *Yunnan For.* **2007**, *28*, 4–7. (In Chinese)
6. Xu, H.J.; Wang, X.H.; Li, H.; Yao, H.Y.; Su, J.Q.; Zhu, Y.G. Biochar impacts soil microbial community composition and nitrogen cycling in an acidic soil planted with rape. *Environ. Sci. Technol.* **2014**, *48*, 9391–9399. [CrossRef]
7. Zhang, Y.; Du, B.H.; Jin, Z.G.; Li, Z.H.; Song, H.N.; Ding, Y.Q. Analysis of bacterial communities in rhizosphere soil of healthy and diseased cotton (*Gossypium* sp.) at different plant growth stages. *Plant. Soil* **2011**, *339*, 447–455. [CrossRef]
8. McCann, K.S. The diversity-stability debate. *Nature* **2000**, *405*, 228–233. [CrossRef]
9. Suleiman, A.K.A.; Manoeli, L.; Boldo, J.T.; Pereira, M.G.; Roesch, L.F.W. Shifts in soil bacterial community after eight years of land-use change. *Syst. Appl. Microbiol.* **2013**, *36*, 137–144. [CrossRef]
10. Song, M.; Zou, D.S.; Du, H.; Peng, W.X.; Zeng, F.P.; Tan, Q.J.; Fan, F.J. Characteristics of soil microbial populations in depressions between karst hills under different land use patterns. *Chin. J. Appl. Ecol.* **2013**, *24*, 2471–2478. [CrossRef]
11. Edarson, D.C.J.; Terence, L.M.; James, M.T.; Fatima, M.D.S.M. Changes in land use alter the structure of bacterial communities in Western Amazon soils. *ISME J.* **2009**, *3*, 1004–1011. [CrossRef]
12. Bremner, J.M.; Jenkinson, D.S. Determination of organic carbon in soil. I. Oxidation by dichromate of organic matter in soil and plant materials. *Eur. J. Soil Sci.* **2010**, *11*, 394–402. [CrossRef]
13. Parkinson, J.A.; Allen, S.E. A wet oxidation procedure suitable for determination of nitrogen and mineral nutrients in biological material. Commun. *Soil Sci. Plant Anal.* **1975**, *6*, 1–11. [CrossRef]
14. Carson, P.L. Recommended potassium test. In *Recommended Chemical Soil Test Procedures for the North Central Region*; Dahnke, W.C., Ed.; North Dakota Agricultural Experiment Station: Fargo, ND, USA, 1980; Volume 499, pp. 17–18.

15. Wilke, B.M. Determination of chemical and physical soil properties. In *Monitoring and Assessing Soil Bioremediation*; Springer: Heidelberg/Berlin, Germany, 2005. [CrossRef]
16. Li, Q.; Hu, Q.; Zhang, C.; Müller, W.E.G.; Schröder, H.C.; Li, Z. The effect of toxicity of heavy metals contained in tailing sands on the organic carbon metabolic activity of soil microorganisms from different land use types in the karst region. *Environ. Earth Sci.* **2015**, *74*, 6747–6756. [CrossRef]
17. Chan, C.O.; Yang, X.D.; Fu, Y.; Feng, Z.L.; Sha, L.Q.; Peter, C.; Zou, X.M. 16S rRNA gene analyses of bacterial community structures in the soils of evergreen broad-leaved forests in south-west China. *FEMS Microbiol. Ecol.* **2006**, *58*, 247–259. [CrossRef]
18. Magoč, T.; Salzberg, S.L. FLASH: Fast length adjustment of short reads to improve genome assemblies. *Bioinformatics* **2011**, *27*, 2957–2963. [CrossRef]
19. Martin, M. Cutadapt removes adapter sequences from high-throughput sequencing reads. *EMBnet. J.* **2011**, *17*, 10–12. [CrossRef]
20. Quast, C.; Pruesse, E.; Yilmaz, P.; Gerken, J.; Schweer, T.; Yarza, P.; Peplies, J.; Glöckner, F.O. The SILVA ribosomal RNA gene database project: Improved data processing and web-based tools. *Nucl. Acids Res.* **2013**, *41*, D590–D596. [CrossRef]
21. Edgar, R.C.; Haas, B.J.; Clemente, J.C.; Quince, C.; Knight, R. UCHIME improves sensitivity and speed of chimera detection. *Bioinformatics* **2011**, *27*, 2194–2200. [CrossRef]
22. Edgar, R.C. Search and clustering orders of magnitude faster than BLAST. *Bioinformatics* **2010**, *26*, 2460–2461. [CrossRef]
23. Caporaso, J.G.; Kuczynski, J.; Stombaugh, J.; Bittinger, K.; Bushman, F.D.; Costello, E.K.; Fierer, N.; Goodrich, J.K.; Gordon, J.I.; Huttley, G.A.; et al. QIIME allows analysis of highthroughput community sequencing data. *Nat. Methods* **2010**, *7*, 335–336. [CrossRef] [PubMed]
24. Zuur, A.F.; Ieno, E.N.; Smith, G.M. *Analysing Ecological Data*; Springer: New York, NY, USA, 2007.
25. R Core Team. *R: A Language and Environment for Statistical Computing*; R Foundation for Statistical Computing: Vienna, Austria, 2014; Available online: http://www.R-project.org/ (accessed on 15 July 2019).
26. Anderson, M.J.; Willis, T.J. Canonical analysis of principal coordinates: A useful method of constrained ordination for ecology. *Ecology* **2003**, *84*, 511–525. [CrossRef]
27. Bastian, M.; Heymann, S.; Gephi, M.J. An open source software for exploring and manipulating networks. In Proceedings of the Third International Conference on Weblogs and Social Media, ICWSM 2009, San Jose, CA, USA, 17–20 May 2009. [CrossRef]
28. Oberson, A.; Friesen, D.K.; Rao, I.M.; Bühler, S.; Frossard, E. Phosphorus Transformations in an Oxisol under contrasting land-use systems: The role of the soil microbial biomass. *Plant Soil* **2001**, *237*, 197–210. [CrossRef]
29. Batlle-Aguilar, J.; Brovelli, A.; Porporato, A.; Barry, D.A. Modelling soil carbon and nitrogen cycles during land use change-A review. *Agron. Sustain. Dev.* **2011**, *31*, 251–274. [CrossRef]
30. Liu, Y.P.; Lu, M.X.; Zhang, X.W.; Sun, Q.B.; Liu, R.L.; Lian, B. Shift of the microbial communities from exposed sandstone rocks to forest soils during pedogenesis. *Int. Biodeter. Biodegr.* **2019**, *140*, 21–28. [CrossRef]
31. Huang, X.F.; Zhou, Y.C.; Zhang, Z.M. Distribution characteristics of soil organic carbon under different land use in a karst rocky desertification area. *J. Soil Water Conserv.* **2017**, *31*, 215–221. [CrossRef]
32. Tong, J.H.; Hu, Y.C.; Du, Z.L.; Zou, Y.Q.; Li, Y.Y. Effects of land use change on soil organic carbon and total nitrogen storage in karst immigration regions of Guanxi Province, China. *Chin. J. Appl. Ecol.* **2018**, *29*, 2890–2896. [CrossRef]
33. Li, L.; Qin, F.C.; Jiang, L.N.; Yao, X.L. Vertical distribution of soil organic carbon content and its influenceing factors in Aaohan, Chifeng. *Acta Ecol. Sin.* **2019**, *39*, 345–354. [CrossRef]
34. Chaplot, V.; Bouahom, B.; Valentin, C. Soil organic carbon stocks in Laos: Spatial variations and controlling factors. *Glob. Chang. Biol.* **2010**, *16*, 1380–1393. [CrossRef]
35. Kuang, W.N.; Qian, J.Q.; Ma, Q.; Liu, Z.M. Vertical distribution of soil organic carbon content and its relation to root distribution in five desert shrub communities. *Chin. J. Ecol.* **2016**, *35*, 275–281. [CrossRef]
36. Wang, D.; Geng, Z.C.; She, D.; He, W.X.; Hou, L. Soil organic carbon storage and vertical distribution of carbon and nitrogen across different forest types in the Qinling Mountains. *Acta Ecol. Sin.* **2015**, *35*, 5421–5429. [CrossRef]
37. Daniel, C.S.; Matthew, G.B.; James, M.B.; Linda, L.K. Plant community richness and microbial interactions structure bacterial communities in soil. *Ecology* **2015**, *96*, 134–142. [CrossRef]
38. Kinkel, L.L.; Bakker, M.G.; Schlatter, D.C. A coevolutionary framework for managing disease-suppressive soils. *Annu. Rev. Phytopathol.* **2011**, *49*, 47–67. [CrossRef] [PubMed]

39. Zhang, C.; Li, J.; Wang, J.; Liua, G.B.; Wang, G.L.; Guo, L.; Peng, S.Z. Decreased temporary turnover of bacterial communities along soil depth gradient during a 35-year grazing exclusion period in a semiarid grassland. *Geoderma* **2019**, *351*, 49–58. [CrossRef]
40. He, S.B.; Guo, L.X.; Niu, M.Y.; Miao, F.H.; Jiao, S.; Hu, T.M.; Long, M.X. Ecological diversity and cooccurrence patterns of bacterial community through soil profile in response to long-term switchgrass cultivation. *Sci. Rep.* **2017**, *3608*, 7. [CrossRef]
41. Cheng, J.M.; Guanghua Jing, G.H.; Wei, L.; Jing, Z.B. Long-term grazing exclusion effects on vegetation characteristics, soil properties and bacterial communities in the semiarid grasslands of China. *Ecol. Eng.* **2016**, *97*, 170–178. [CrossRef]
42. Wang, S.X.; Wang, X.A.; Guo, H. Change patterns of β-diversity in the succession process of plant communities on Loess Plateau of Northwest China. *Chin. J. Ecol.* **2013**, *32*, 1135–1140. [CrossRef]
43. Tian, Q.; Taniguchi, T.; Shi, W.Y.; Li, G.Q.; Yamanaka, N.; Du, S. Land-use types and soil chemical properties influence soil microbial communities in the semiarid Loess Plateau region in China. *Sci. Rep.* **2017**, *7*, 45289. [CrossRef]
44. Bru, D.; Ramette, A.; Saby, N.P.A.; Dequiedt, S.; Ranjard, L.; Jolivet, C.; Arrouays, D.; Philippot, L. Determinants of the distribution of nitrogen-cycling microbial communities at the landscape scale. *ISME J.* **2011**, *5*, 532–542. [CrossRef]
45. Adria, L.F.; Craig, C.S.; Donald, L.W.; Christopher, S.; Trevor, J.G.; Michael, J.S. Associations between soil bacterial community structure and nutrient cycling functions in long-term organic farm soils following cover crop and organic fertilizer amendment. *Sci. Total Environ.* **2016**, *566*, 949–959. [CrossRef]
46. Manuel, D.B.; Angela, M.O.; Tess, E.B.; Alberto, B.G.; David, J.E.; Richard, D.B.; Fernando, T.M.; Brajesh, K.S.; Noah, F. A global atlas of the dominant bacteria found in soil. *Science* **2018**, *359*, 320–325. [CrossRef]
47. Zhou, J.; Guan, D.W.; Zhou, B.K.; Zhao, B.S.; Ma, M.C.; Qin, J.; Jiang, X.; Chen, S.F.; Cao, F.M.; Shen, D.L.; et al. Influence of 34-years of fertilization on bacterial communities in an intensively cultivated black soil in northeast China. *Soil Biol. Biochem.* **2015**, *90*, 42–51. [CrossRef]
48. Griffiths, B.S.; Philippot, L. Insights into the resistance and resilience of the soil microbial community. *FEMS Microbiol. Rev.* **2013**, *37*, 112–129. [CrossRef] [PubMed]
49. Anna, K.; Jorge, L.M.R.; Eiko, E.K.; Patrick, S.G.C.; Johannes, A.V.V.; George, A.K. Phylogenetic and metagenomic analysis of *Verrucomicrobia* in former agricultural grassland soil. *FEMS Microbiol. Ecol.* **2010**, *71*, 23–33. [CrossRef]
50. David, C.W.; Susan, D.S.; David, B.R. The genus Sphingomonas: Physiology and ecology. *Curr. Opin. Biotechnol.* **1996**, *7*, 301–306. [CrossRef]
51. David, V.; Kendra, R.M.; Erick, C.; Cameron, R.S.; Steven, J.H.; William, W.M. Non-symbiotic *Bradyrhizobium* ecotypes dominateNorth American forest soils. *ISME J.* **2015**, *9*, 2435–2441. [CrossRef]
52. Heinz, S.; Cheryl, J.; Jamest, S. The phylum *Verrucomicrobia*: A phylogenetically heterogeneous bacterial group. *Prokaryotes* **2006**, *7*, 881–896. [CrossRef]
53. Wagner, M.; Horn, M. The *Planctomycetes*, *Verrucomicrobia*, *Chlamydiae* and sister phyla comprise a superphylum with biotechnological and medical relevance. *Curr. Opin. Biotechnol.* **2006**, *17*, 241–249. [CrossRef]
54. Noll, M.; Diethart, M.; Frenzel, P.; Manigee, D.; Liesack, W. Succession of bacterial community structure and diversity in a paddy soil oxygen gradient. *Environ. Microbiol.* **2005**, *7*, 382–395. [CrossRef]
55. Fierer, N.; Ladau, J.; Clementei, J.C.; Leff, J.W.; Owens, S.M.; Katherine, S.P.; Knight, R.; Gilbert, J.A.; McCulley, R.L. Reconstructing the microbial diversity and function of pre-agricultural tallgrass prairie soils in the United States. *Science* **2013**, *342*, 621–624. [CrossRef]
56. Janssen, P.H.; Yates, P.S.; Grinton, B.E.; Taylor, P.M.; Sait, M. Improved culturability of soil bacteria and isolation in pure culture of novel members of the divisions *Acidobacteria*, *Actinobacteria*, *Proteobacteria*, and *Verrucomicrobia*. *Appl. Environ. Microb.* **2002**, *68*, 2391–2396. [CrossRef]
57. Stefan, S.; Boyke, B.; Cathrin, S.; Peter, S.; Manfred, R.; Brian, J.T.; Hans, P.K. Characterization of the first cultured representative of *Verrucomicrobia* subdivision 5 indicates the proposal of a novel phylum. *ISME J.* **2016**, *10*, 2801–2816. [CrossRef]

58. Wang, P.; Chen, B.; Zhang, H. High throughput sequencing analysis of bacterial communities in soils of a typical Poyang Lake wetland. *Acta Ecol. Sin.* **2017**, *37*, 1650–1658. [CrossRef]
59. Zhang, Y.G.; Cong, J.; Lu, H.; Li, G.L.; Qu, Y.Y.; Su, X.J.; Zhou, J.Z.; Li, D.Q. Community structure and elevational diversity patterns of soil *Acidobacteria*. *J. Environ. Sci.* **2014**, *26*, 171–1724. [CrossRef]

forests

MDPI

Article

Effects of Plum Plantation Ages on Soil Organic Carbon Mineralization in the Karst Rocky Desertification Ecosystem of Southwest China

Hui Yang [1,2], Biqin Mo [1,2], Mengxia Zhou [1,2], Tongbin Zhu [1,2,*] and Jianhua Cao [1,2]

[1] Karst Dynamics Laboratory, Institute of Karst Geology (CAGS), Ministry of Natural Resources (MNR) and Guangxi, Guilin 541004, China; yanghui-kdl@karst.ac.cn (H.Y.); mermaid_yh@126.com (B.M.); mengxia.zhou95@gmail.com (M.Z.); jhcaogl@karst.ac.cn (J.C.)

[2] International Research Centre on Karst, Under the Auspices of United Nations Educational, Scientific and Cultural Organization (UNESCO), Guilin 541004, China

* Correspondence: ztb@karst.ac.cn; Tel.: +86-773-583-7840; Fax: +86-773-583-7845

Received: 30 October 2019; Accepted: 2 December 2019; Published: 4 December 2019

Abstract: Soil organic carbon (SOC) mineralization is closely related to carbon source or sink of terrestrial ecosystem. Understanding SOC mineralization under plum plantation is essential for improving our understanding of SOC responses to land-use change in karst rocky desertification ecosystem. In this study, 2-year, 5-year, and 20-year plum plantations and adjacent abandoned land dominated by herbs were sampled, and a 90-day incubation experiment was conducted to investigate the effect of plum plantations with different ages on SOC mineralization in subtropical China. Results showed that: (1) Plum plantation significantly decreased SOC content compared with abandoned land, but there was no significant difference in SOC content among plum plantations with different ages. Oppositely, the accumulative SOC mineralization (C_t) and potential SOC mineralization (C_0) showed different responses to plum plantation ages. (2) The dynamics of the SOC mineralization were a good fit to a first-order kinetic model. Both C_0 and C_t in calcareous soil of this study was several- to 10-folds lower than other soils in non-karst regions, indicating that SOC in karst regions has higher stability. (3) Correlation analysis revealed that both C_t and C_0 was significantly correlated with soil calcium (Ca), suggesting an important role of Ca in SOC mineralization in karst rocky desertification areas. In conclusion, a Ca-rich geological background controls SOC mineralization in karst rocky desertification areas.

Keywords: calcareous soil; plum plantation ages; organic carbon mineralization; fitting parameters; organic carbon accumulation

1. Introduction

Due to the fragile geological and ecological conditions, rocky desertification widely occurs in the southwest karst region of China [1], which is characterized by serious soil erosion, devoid of vegetation and soil [2]. To effectively prevent rocky desertification, a series of ecological restorations have been carried out to increase the forest cover and to mitigate soil erosion by the Chinese government [3]. Consequently, various land uses, including undisturbed (e.g., grassland and shrub) and man-made (e.g., corn, woodland and fruit crop) ecosystems, have been formed in karst rocky desertification regions. These ecological restoration measures have tremendously affected the physical, chemical, and microbiological properties in soils [4]. Plum plantation is one of the local sustainable development models of characteristic agriculture in karst rocky desertification areas, which can not only effectively restore the ecological environment, but also significantly increase farmers' income in local. In recent years, the planting area of plum trees has been increasing continuously in the process of controlling rocky desertification [5].

Dynamic change of soil organic carbon (SOC) is of great significance to global C cycle and current climate change. The quantity and intensity of carbon dioxide (CO_2; an important greenhouse gas) released by SOC mineralization through microbial decomposition can reflect the quality of soil and evaluate soil carbon emissions into the atmosphere [6,7]. In addition, SOC mineralization is closely related to the maintenance of soil nutrients and the formation of CO_2 [8]. The CO_2 emission rate and its dynamic change process are also important indicators reflecting the change of soil quality. Furthermore, SOC concentration at a particular time is controlled by the balance between C input from litter and C output from SOC mineralization [9]. Investigating the SOC mineralization process is the most effective methods to evaluate C loss or stability [10].

Vegetation type influences the rate of accumulation and mineralization of organic matter in forest soil [11]. Some research proved that C loss from soil respiration depends on stand age. It is low in young, high in intermediate, and low again in old stands [12,13]. Plum is one of the principal tree species in the rocky desertification restoration area in the National Sustainable Development Experiment and Demonstration Zone in Gongcheng county. However, there is less study about SOC storage and SOC mineralization in plum forests in rocky desertification restoration areas. In particular, it is not clear whether plum plantation age is the key factor controlling SOC stability and how other factors influence SOC decomposition dynamics. In addition, calcareous soil developed on carbonate rock is characterized by high pH and Ca materials in a karst region [1], which may lead to the obvious differences in SOC mineralization compared to other soil types. The lack of knowledge regarding SOC mineralization under plum plantation during karst rocky desertification restoration limits the ability to predict how this ecosystem will respond to climate change. We hypothesized that both the karst geological background, especially soil pH and Ca concentrations, and plantation ages may play an important role in controlling SOC mineralization.

Therefore, we measured the distribution and mineralization of organic C in soils collected from plum fields with different plantation ages (2 year, 5 year, and 20 year) and adjacent abandoned land in the karst rocky desertification region of subtropical China. The main objectives of this study were to (1) estimate SOC content, mineralization, and soil nutrients under plum plantations with different stand ages; (2) evaluate the relative importance of soil properties affecting SOC content and mineralization; (3) potentially assess mineralization and decomposition rates of SOC.

2. Materials and Methods

2.1. Study Area

The study site was located in the National Sustainable Development Experiment and Demonstration Zone and also a key area of national rocky desertification control in Gongcheng county, Guilin, Guangxi Zhuang Autonomous Region (110°47′4′′ E, 24°54′35′′ N) (Figure 1), which is a subtropical monsoon climate, with an annual average temperature of 19.7 °C and an annual average precipitation of 1438 mm.

The study area is a hilly and middle-low mountain landform. Its parent material is carboniferous limestone. Karst soil is sparse and drought-prone. Because of long-term human activities, natural vegetation is destroyed and large areas of steep slopes are reclaimed, resulting in surface rock bareness, coupled with thin soil layer, shallow bedrock exposure, storm erosion, and a large number of rocks gradually exposed after soil erosion. Severe rocky desertification occurs (Figure S1).

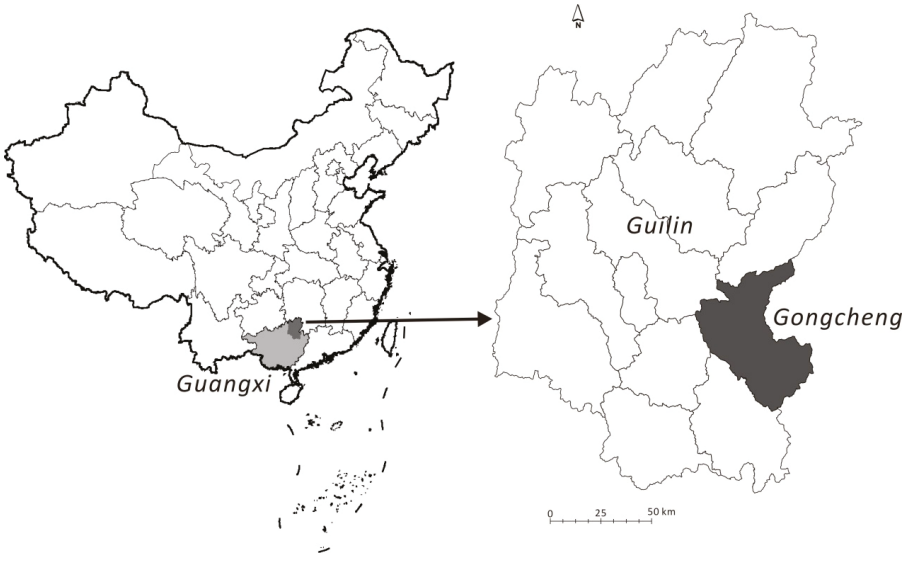

Figure 1. The location of the study area.

2.2. Soil Sampling and Preparation

Soil samples were collected from three plum fields with 2-year, 5-year, and 20-year plantation ages, and abandoned land was used as control. The understory of the plum plantation was dominated by the meda *villosa (Poir.) A. Camus* and *Digitaria sanguinalis (Linn.) Scop.* The dominated plants of the abandoned land were herbs, dominated by *Miscanthus* with a small amount of *Conyza canadensis (Linn.) Cronq*. Fertilizer was applied four times each year, including three times of chemical fertilizer and one time of organic fertilizer. The chemical fertilizer was compound fertilizer (including N 18%, P_2O_5 18%, K_2O 18%). The organic fertilizer was cattle manure (including C 413.8 g kg^{-1}, N 2.7 g kg^{-1}, P_2O_5 1.3 g kg^{-1}, K_2O 6.0 g kg^{-1}). Under each plum tree, an average of 2 kg of chemical fertilizer and 20 kg of organic fertilizer were applied each year. The application rate of N, P_2O_5, and K_2O reached to approximately 250, 100, and 240 kg ha^{-1} $year^{-1}$, respectively.

In November 2015, three representative sites were sampled for plum plantations with different ages and abandoned land as spatial replications, resulting in 12 soil samples. In each site, three 20 m × 20 m plots with similar architecture and growth of plum trees, separated at least 40 m from each other, were randomly selected. Soils of the top 0–10 cm were collected from five quadrats (1 m × 1 m) in each plot; one on each corner and one in the center were mixed to form a composite sample. After removing animal and plant debris and stones, the collected samples were air-dried at room temperature. The composite samples were divided into two parts. One part of the collected sample was passed through a 2-mm sieve to carry out SOC mineralization experiment, and the other part was grinded and passed through a 0.25-mm sieve and homogenized for soil physical and chemical property determination, including pH, SOC, total nitrogen (TN), total phosphorus (TP), total potassium (TK), and calcium (Ca).

2.3. Experiment Design

A laboratory incubation experiment was carried out to determine SOC mineralization. Soil samples were incubated with a constant temperature regime at 20 °C, which was close to the annual mean temperature (19.7 °C) in the sampled area. The incubation temperatures were controlled by digital biochemical incubators (SPX-70B, Hangzhou Julai Instrument Co., Ltd., Hangzhou, China).

Each soil sample (100 g dry), including three repeats, was placed in a 1000 mL incubation jar (Figure S2). The soil moisture content was adjusted to 60% of field capacity prior to incubation. All samples were pre-incubated at 20 °C for 7 days to minimize the burst of respiration due to wetting the dry soils [10]. Then, a 50 mL beaker containing 10 mL of 0.1 mol/L NaOH solution was placed at the bottom of the incubation jar, sealed and capped, and incubated in a 20 °C thermostat in darkness. Three blank controls (no soil addition) were arranged at the same time in order to eliminate the influence of CO_2 in the air when NaOH solution was replaced every time. A total of 39 samples, including 12 soil samples with 3 incubation replicates and 3 blank controls, were used for the incubation experiment. Deionized water was added to the soil twice a week to keep the loss of soil water within 2% [14]. The 50 mL beaker containing 10 mL of 0.1 mol/L NaOH solution was replaced at days 2, 5, 8, 14, 20, 26, 32, 38, 44, 62, 74, and 90. The amount of CO_2 released during incubation can be calculated by titrating residual NaOH with 0.1 mol/L HCl solution.

2.4. Methods

Soil pH was determined at a 1:2.5 (w/v) soil/water ratio by a digital millivolt pH Meter-2 (DMP-2 mV/pH) detector (Quark Ltd., Nanjing, China); SOC was determined using the $K_2Cr_2O_7$–H_2SO_4 volumetric dilution heating method; total nitrogen was determined using the Kjeldahl procedure [15]; total potassium (TK) concentration was determined with the HF–$HClO_4$ flame photometric method; and total phosphorus (TP) was measured using $HClO_4$–H_2SO_4 digestion followed by an Mo–Sb colorimetric assay [1]; soil calcium (Ca) was extracted by HNO_3–HF–$HClO_4$ and analyzed by inductively coupled plasma–atomic emission spectrometry (ICP–AES). Three replicates were performed for each soil sample.

The mineralization of SOC was calculated by the following Equation (1).

$$C_m = C_{HCl} \times (V_0 - V_1) \times 22/0.1 \quad (1)$$

where C_m was the amount of CO_2 release (mg CO_2/kg soil); C_{HCl} was the concentration of hydrochloric acid (mol/l); V_0 was the volume of hydrochloric acid consumed in blank titration (ml); V_1 was the volume of hydrochloric acid consumed in titration of samples (ml); 22 was half of the Molar mass of CO_2 (mol/kg); 0.1 was soil weight (kg).

2.5. Data Analysis

The data was fitted in an exponential model using the data analysis and graphing software (Origin ver. 7.5; Origin Lab Corp., Northampton, MA, USA) to obtain kinetics of SOC mineralization (Equation (2)) [16].

$$C_t = C_0 (1 - e^{-kt}) \quad (2)$$

where C_t was the cumulative mineralization of SOC after t days; C_0 was amount of potential mineralizable SOC (mg/kg); k for constant of mineralization rate of SOC (/day).

The half-turnover period was calculated by Equation (3).

$$T_{1/2} = 1n2/k \quad (3)$$

where $T_{1/2}$ was half the turnover period (day).

The obtained data were statistically analyzed using the analysis Statistical Package Social Science (SPSS ver. 20.0; IBM Corp., Armonk, NY, USA) to compare the analysis of variance. Tukey's honestly significant difference (HSD) was then calculated for indicating the significant differences in soil properties and SOC mineralization ($p < 0.05$). Graphs were plotted using the Origin 7.5 program. The correlations between the SOC mineralization and the soil chemical properties were analyzed by the Pearson correlation test.

3. Results

3.1. Soil Chemical Properties as Affectted by Plantation Age

Compared to abandoned land, plum plantation significantly decreased pH and the contents of SOC and TN ($p < 0.05$) (Table 1), but there was no significant difference among plum plantations with different ages ($p > 0.05$). Although C/N ratios in soils under plum plantation were lower than that under abandoned land, the significant difference was not found between abandoned land and plum plantations. There was no significant difference in TP contents among abandoned land and three plum plantations ($p > 0.05$). The highest TK contents were found in soils under 5-year plum plantation and abandoned land, which were significantly higher than 2-year and 20-year plum plantations. Plum plantation significantly decreased Ca contents compared with abandoned land ($p < 0.05$), with the lowest in soil under 5-year plum plantation.

Table 1. Soil properties under plum plantations with different ages.

	pH	SOC (g/kg)	TN (g/kg)	C/N	TP (g/kg)	TK (g/kg)	Ca (%)
CK	6.60 ± 0.10 ^{a}	22.38 ± 0.53 ^{a}	1.01 ± 0.04 ^{a}	25.97 ± 1.62 ^{a}	0.49 ± 0.08 ^{a}	18.07 ± 0.05 ^{a}	0.97 ± 0.13 ^{a}
2 year	5.31 ± 0.32 ^{b}	11.87 ± 3.18 ^{b}	0.61 ± 0.18 ^{b}	22.83 ± 2.82 ^{a}	0.55 ± 0.25 ^{a}	14.56 ± 0.55 ^{b}	0.54 ± 0.23 ^{b}
5 year	5.91 ± 0.51 ^{c}	10.17 ± 3.28 ^{b}	0.74 ± 0.20 ^{ab}	17.96 ± 8.61 ^{a}	0.44 ± 0.21 ^{a}	19.47 ± 1.68 ^{a}	0.27 ± 0.10 ^{c}
20 year	5.17 ± 0.28 ^{b}	11.70 ± 5.27 ^{b}	0.66 ± 0.27 ^{b}	21.34 ± 6.50 ^{a}	0.63 ± 0.31 ^{a}	15.06 ± 1.25 ^{b}	0.40 ± 0.16 ^{bc}

Note: CK represents abandoned land; 2 year represents plum forest plantation for 2 years; 5 year represents plum forest plantation for 5 years; 20 year represents plum forest plantation for 20 years. SOC represents soil organic carbon; TN represents total nitrogen; C/N represents the molar ratio of soil organic carbon (SOC)/TN; TP represents total phosphorus; TK represents total potassium; Ca represents calcium. Identical letters indicate no significant differences in the average values among soils under different plantation ages at the 0.05 level.

3.2. Mineralization Rate of Soil Organic C under Plum Plantations with Different Ages

Soil organic carbon mineralization rate decreased with incubation time (Figure 2), and accorded with logarithmic function $y = a + b\ln(x)$ (Table 2), indicating that SOC mineralization rate would change b% absolute value when incubation time changed by 1% unit.

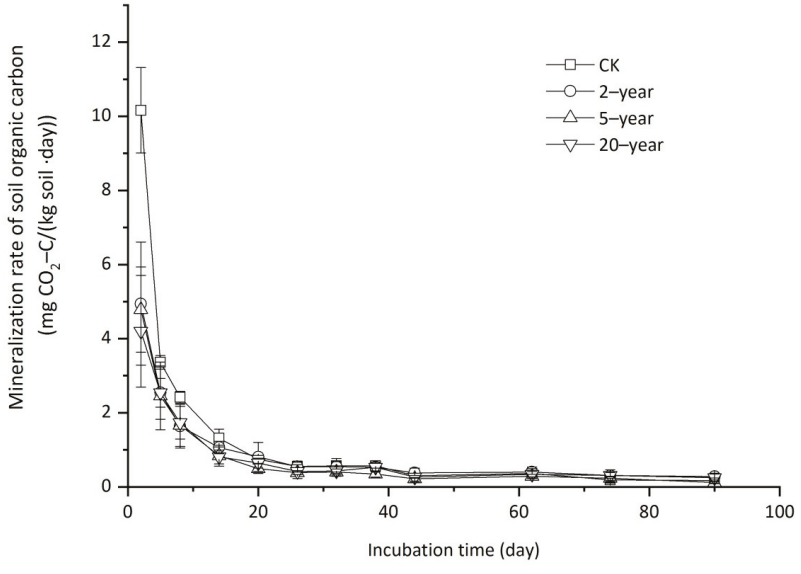

Figure 2. Daily mineralization rate of soil organic carbon.

Table 2. Regression equation of SOC mineralization rate relative to plum plantation age.

Treatment	Regression Equation	R^2
CK	$y = 8.221 - 2.101\ln(x)$	0.734 **
2 year	$y = 4.499 - 1.078\ln(x)$	0.835 **
5 year	$y = 4.736 - 1.085\ln(x)$	0.831 **
20 year	$y = 4.040 - 0.971\ln(x)$	0.853 **

Note: y represents CO_2 production rate; x represents incubation day; ** means significant correlation at 0.01 level.

Based on the decline rate of SOC mineralization (Figure 2), it can be divided into three stages. The first stage (2–14 days) was the early stage of the incubation. The rate of CO_2 production decreased rapidly from the peak (2 days) and changed greatly. There was no significant difference in the mineralization rate of SOC among three planting ages, but it was significantly lower than CK. The second stage (14–62 days) was the medium stage of the incubation, and the rate of CO_2 production declined from a slow stage to a stable stage. The SOC mineralization rate of CK was higher than that in the three planting ages. At the last stage (62–90 days), the SOC mineralization rate of CK began to be lower than that of soils under plum plantations with different ages, and the difference was significant.

3.3. Cumulative Mineralization of Soil Organic Carbon Under Plum Plantations with Different Ages

Carbon mineralization showed a curvilinear relationship with time over the incubation period (starting from 0 to day 90) (Figure 3). Across different plantation ages, cumulative CO_2–C emission varied from 2.29 mg CO_2–C/kg soil (day 2) to 61.17 mg CO_2–C/kg soil (day 90).

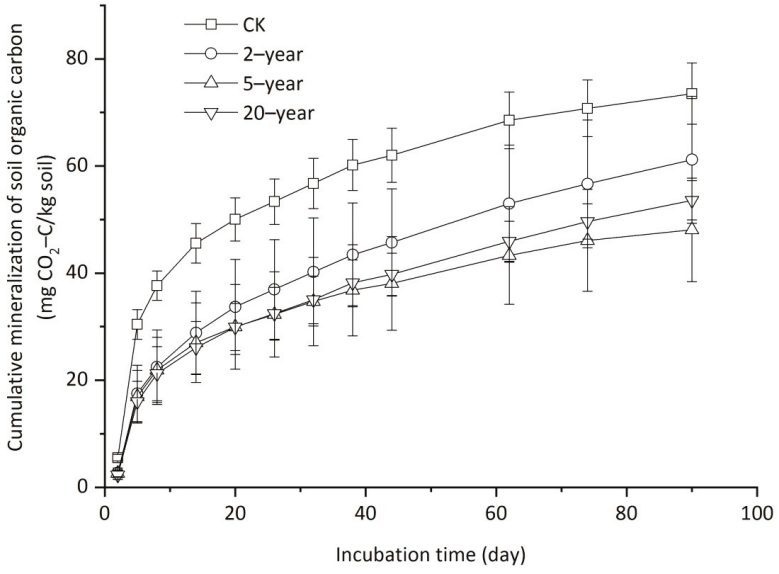

Figure 3. Cumulative mineralization of SOC relative to plum plantation age.

The cumulative release of CO_2 increased with incubation time, but the cumulative release intensity gradually slowed down. During the whole incubation, the cumulative release of CO_2 was higher in CK than that in plum plantations with different ages. The cumulative release of CO_2 was ranked as 2-year, 20-year, and 5-year plantations.

3.4. Parameters of Soil Organic Carbon Mineralization Kinetic Equations Under Plum Plantations with Different Ages

The first-order kinetic equation was used to fit the cumulative mineralization of SOC under plum plantations with different ages, and the fitting results were good ($R^2 > 0.90$). The potential mineralization of SOC (C_0) and constant for SOC mineralization rate (k) estimated from the first-order kinetic equation are shown in Table 3. The values of C_0 ranged from 44.13 (5-year) to 67.10 mg/kg (CK), and it was significant higher in CK than that in plum plantations ($p < 0.05$). The CO_2–C release from mineralization of soil potential organic C, i.e., the turnover rate (k) of bioactive organic carbon pool, ranged from 0.043 (2-year) to 0.079 day^{-1} (CK), and the half-turnover period was 8.80 (CK)–16.1 day (2-year) (Table 3). The values of k for different plum plantation ages showed the same trend with C_0. With increasing plum plantation age, soil potential mineralized C pool decreased, but soil potential mineralized C pool increased slightly after 20-year plum plantation, although the difference was not significant between 5-year and 20-year plum plantations ($p > 0.05$).

Table 3. Cumulative mineralization of SOC after the 90 days of incubation and parameters of its kinetic equations.

Treatment	C_t (mg/kg)	C_0 (mg/kg)	k (/d)	$T_{1/2}$ (d)	C_0/SOC (%)	R^2
CK	73.52 ± 8.43 ^{a}	67.10 ± 7.56 ^{a}	0.079 ± 0.003 ^{a}	8.80	0.30	0.93
2-year	61.17 ± 5.56 ^{b}	57.92 ± 1.33 ^{b}	0.043 ± 0.001 ^{b}	16.1	0.49	0.96
5-year	48.09 ± 3.27 ^{c}	44.13 ± 5.71 ^{c}	0.060 ± 0.001 ^{c}	11.6	0.43	0.93
20-year	53.60 ± 4.11 ^{c}	49.85 ± 2.55 ^{c}	0.046 ± 0.002 ^{b}	15.1	0.43	0.94

Note: C_t represents cumulative mineralization of SOC; C_0 represents amount of potential mineralizable SOC; k represents constant of mineralization rate of SOC; $T_{1/2}$ represents half-turnover period; C_0/SOC represents ratio of potential mineralizable organic carbon to total organic carbon in soil. Values followed by different letters in the same column mean significance at 0.05 level.

3.5. SOC Mineralization as Affected by Chemical Properties

Many environmental factors might influence the mineralization of SOC [17]. Soil organic carbon content was positively correlated with C_t and C_0. Therefore, the difference of SOC mineralization in plum plantations with different ages was mainly due to the difference in SOC content. The proportion of active organic C varies with the content of SOC. Among the many factors, the Ca content and C/N ratio significantly affect SOC mineralization (Table 4). The mineralization rate of SOC was the highest in the abandoned land with the highest Ca content and C/N ratio.

Table 4. Correlations between the C parameters and soil property factors.

	pH	SOC	TN	C/N	TP	TK	Ca
C_t	0.593	0.923 **	0.690	0.974 **	−0.035	−0.079	0.959 **
C_0	0.524	0.883 *	0.621	0.981 **	0.014	−0.159	0.931 **
k	0.986 **	0.823 *	0.983 **	0.423	−0.627	0.741	0.733

* Significant correlation ($p < 0.05$); ** Extremely significant correlation ($p < 0.01$).

4. Discussion

4.1. Effects of Plantation Ages on Soil Chemical Properties

Plum plantation significantly reduced SOC content by about 50% compared with abandoned land, which may be attributed to the changes in agricultural managements (e.g., the clear-cut of forest, tillage and mineral N fertilizer). Except for the direct reduction in litter input to soil, weed control, tillage, and mineral N fertilizer can also stimulate the decomposition of SOC, thereby lowing SOC content. Despite applying large organic fertilizer during plum plantation, it may not counterbalance the negative effect on SOC consumption through litter reduction and agricultural managements. However,

SOC contents did not exhibit the obvious differences among plum plantations with different ages, suggesting that SOC pool is maintained at the relatively stable level once grassland is converted to plum, irrespective of plum plantation years.

The C/N value in the studied soils was relatively stable, and no significant difference was found among plum plantations with different ages. This was in agreement with the previous result that the C/N ratio was relatively stable and was insignificantly affected by climate, although C and N concentrations had great spatial variability [1]. Compared with abandoned land, TP content in soil under plum plantation did not significantly change, which was consistent with a previous study that TP was mainly derived from the weathering release of soil minerals, rather than from the short-term biological cycle in karst rocky desertification areas [1]. Oppositely, potassium sources in soil are mainly derived from potassium minerals and fertilization. With the increase of plum plantation ages, Ca content in soil decreased obviously, which may be because plum trees absorb a lot of Ca as one of the nutrient elements in the process of growth.

4.2. SOC Mineralization and Affecting Factors

In this study, CO_2 production rate is faster in the initial stage of incubation, possibly owing to the priming effect [18]. After pre-incubation, a large number of active organic substances such as sugars and proteins can be effectively decomposed by microorganisms in the initial stage of mineralization [8]. Greater SOC mineralization in abandoned land than plum plantations was often attributed to greater total SOC [19] or greater labile SOC, e.g., dissolved organic carbon (DOC) and microbial biomass C (MBC), which could stimulate the abundance and activity of microorganisms, and subsequently accelerate SOC mineralization [20,21]. With the prolongation of incubation time, the mineralization rate of SOC gradually decreased with decreasing decomposable organic matter. At the later stage of incubation, the organic matter in soil was mainly composed by cellulose and lignin [18], which were difficult to decompose and could not be utilized by microorganisms, resulting in the decline of the mineralization rate of organic carbon. The CO_2 efflux rate in this study showed a similar trend with many research results [8,18,22]. In addition, the relationship between SOC mineralization rate and incubation time was logarithmic function, which was consistent with previous research results [8,23,24].

The cumulative mineralization and mineralization rate of SOC under plum plantations with different ages decreased compared to abandoned land. High CO_2 emissions probably indicate high biological activities in soil [25] and this might take place through microbial exhalation [26], as well as the emissions of CO_2 during organic matter decomposition [27]. Thus, it is no wonder to find out that the efflux rate of CO_2 from the plantation soils was lower than that in abandoned land. The long-term application of chemical fertilizer during plum plantation is not conducive to the formation of soil aggregates. This may exacerbate the microbial growth environment, resulting in the decrease of soil microbial biomass [28]. It may also be that N in fertilizer combines with lignin in soil to form more stable organic compounds [29], which then inhibits the mineralization of SOC. The mechanism of soil characteristics affecting microbial species and activities in plum forests of different ages in karst mountainous areas remains to be further studied.

4.3. Carbon Pool Stability and Factors that Potentially Affect SOC Decomposition

Both cumulative CO_2–C emission and potential mineralizable SOC in calcareous soil of this study was several- to 10-folds lower than that in other soils [8,13,17], similar to the results in soils of karst regions [30], indicating that SOC in karst regions has higher stability. Both Ca and C/N were important factors affecting SOC mineralization in this study. Soil C/N affects the abundance, activity, and community composition of microorganisms [31]. Calcium is the necessary metabolic component of microbial growth, and fungal and bacterial heterotrophs may access and accumulate root Ca to form oxalates, which can be used to maintain microbial metabolism under unfavorable soil conditions. Therefore, it has an important influence on the decomposition of SOC.

5. Conclusions

The amount of SOC mineralization is governed by the net C content in soil. Results of this research showed that mineralization of SOC occurred, but was somewhat several- to 10-folds lower in karst soils, indicating that SOC in karst regions has higher stability. The higher SOC and the consequent higher release of CO_2 in this study may indicate a reversible equilibrated process between decomposition of soil organic matter and buildup of more stable organic components at the same time. The mineralization of SOC under plum plantation is significantly correlated with soil Ca, suggesting an important role of Ca in SOC mineralization in rocky desertification areas. Furthermore, it was also found that agricultural management, e.g., fertilization and weed control under plum forests, may play an important role in SOC mineralization.

Supplementary Materials: The following are available online at http://www.mdpi.com/1999-4907/10/12/1107/s1: Figure S1. Rocky desertification in the study area; Figure S2. The sketch of the incubation device.

Author Contributions: Conceptualization, J.C.; writing—original draft preparation, H.Y.; investigation, B.M. and M.Z.; writing—review and editing, T.Z.

Funding: This study was supported by the National Key Research and Development Program of China (No.2016YFC0502501; No.2017YFC0406104), the Guangxi National Science Foundation (2017GXNSFAA198153) and the Guangxi Scientific Research and Technology Development Project Guikeneng 1598023-1, the CAGS research Fund (YWF201715, 201724), and the program of Hainan Association for Science and Technology Plans to Youth R & D Innovation (QCXM201713).

Acknowledgments: Special thanks to the anonymous referees for their valuable comments and suggestions. The authors also thank Chunlai Zhang and Bing Bai for their help with field work.

Conflicts of Interest: The authors declare no conflicts of interest.

References

1. Yang, H.; Zhang, P.; Zhu, T.; Li, Q.; Cao, J. The characteristics of soil C, N, and P stoichiometric ratios as affected by geological background in a karst graben area, Southwest China. *Forests* **2019**, *10*, 601. [CrossRef]
2. Yuan, D.X. Rock desertification in the subtropical Karst of South China. *Z. Geomorphol.* **1997**, *108*, 81–90.
3. Li, W.H. Degradation and restoration of forest ecosystems in China. *For. Ecol. Manag.* **2004**, *201*, 33–41.
4. Singh, K.; Singh, B.; Singh, R.R. Changes in physico-chemical, microbial and enzymatic activities during restoration of degraded sodic land: Ecological suitability of mixed forest over monoculture plantation. *Catena* **2012**, *96*, 57–67. [CrossRef]
5. Guangxi Daily. Available online: http://www.forestry.gov.cn/main/138/20190613/075621420562132.html (accessed on 13 June 2019).
6. Li, S.J.; Qiu, L.P.; Zhang, X.C. Mineralization of soil organic carbon and its relations with soil physical and chemical properties on the Loess Plateau. *Acta Ecol. Sin.* **2010**, *30*, 1217–1226. (In Chinese)
7. Smith, P. Carbon sequestration in croplands: The potential in Europe and the global context. *Eur. J. Agron.* **2004**, *20*, 229–236. [CrossRef]
8. Guo, Z.; Wang, X.L.; Duan, J.J.; Jiao, K.Q.; Sun, S.S.; Duan, Y.H.; Zhang, Y.R.; Li, Y.; Jiang, T.M. Long-term fertilization and mineralization of soil organic carbon in paddy soil from yellow earth. *Acta Pedol. Sin.* **2018**, *55*, 225–235. (In Chinese)
9. Vesterdal, L.; Elberling, B.; Christiansen, J.R.; Callesen, I.; Schmidt, I.K. Soil respiration and rates of soil carbon turnover differ among six common European tree species. *For. Ecol. Manag.* **2012**, *264*, 185–196. [CrossRef]
10. Huang, J.; Lin, T.C.; Xiong, D.; Yang, Z.; Liu, X.; Chen, G.; Xie, J.; Li, Y.; Yang, Y. Organic carbon mineralization in soils of a natural forest and a forest plantation of southeastern China. *Geoderma* **2019**, *344*, 119–126. [CrossRef]
11. Malý, S.; Fiala, P.; Reininger, D.; Obdržálková, E. The relationships among microbial parameters and the rate of organic matter mineralization in forest soils, as influenced by forest type. *Pedobiologia* **2014**, *57*, 235–244. [CrossRef]
12. Pregitzer, K.S.; Euskirchen, E.S. Carbon cycling and storage in world forests: Biome patterns related to forest age. *Glob. Chang. Biol.* **2004**, *10*, 2052–2077. [CrossRef]

13. Liu, L.; Wang, H.; Dai, W. Characteristics of soil organic carbon mineralization and influence factor analysis of natural Larix olgensis forest at different ages. *J. For. Res.* **2019**, *30*, 1495–1506. [CrossRef]
14. Chen, X.; Tang, J.; Jiang, L.; Li, B.; Chen, J.; Fang, C. Evaluating the impacts of incubation procedures on estimated Q10 values of soil respiration. *Soil Biol. Biochem.* **2010**, *42*, 2282–2288. [CrossRef]
15. Gao, Y.; He, N.; Yu, G.; Chen, W.; Wang, Q. Long-term effects of different land use types on C, N, and P stoichiometry and storage in subtropical ecosystems: A case study in China. *Ecol. Eng.* **2014**, *67*, 171–181. [CrossRef]
16. Stanford, G.; Smith, S.J. Nitrogen mineralization potentials of soils 1. *Soil Sci. Soc. Am. J.* **1972**, *36*, 465–472. [CrossRef]
17. Ahmed, A.A.; Mohamed, H.H.A.; Tamer, M.S.A.; Walid, E.B.; Samira, E.M. Mineralization of organic carbon and nitrogen in semi-arid soils under organic and inorganic fertilization. *Environ. Technol. Innov.* **2018**, *9*, 243–253.
18. Munda, S.; Bhaduri, D.; Mohanty, S.; Chatterjee, D.; Tripathi, R.; Shahid, M.; Kumar, U.; Bhattacharyya, P.; Kumar, A.; Adak, T.; et al. Dynamics of soil organic carbon mineralization and C fractions in paddy soil on application of rice husk biochar. *Biomass Bioenergy* **2018**, *115*, 1–9. [CrossRef]
19. Yang, K.; He, R.; Yang, W.; Li, Z.; Zhuang, L.; Wu, F.; Tan, B.; Liu, Y.; Zhang, L.; Tu, L.; et al. Temperature response of soil carbon decomposition depends strongly on forest management practice and soil layer on the eastern Tibetan Plateau. *Sci. Rep.-UK* **2017**, *7*, 4777. [CrossRef]
20. Wang, J.; Song, C.; Zhang, J.; Wang, L.; Zhu, X.; Shi, F. Temperature sensitivity of soil carbon mineralization and nitrous oxide emission in different ecosystems along a mountain wetland-forest ecotone in the continuous permafrost of Northeast China. *Catena* **2014**, *121*, 110–118. [CrossRef]
21. Chen, Y.; Chen, G.; Robinson, D.; Yang, Z.; Guo, J.; Xie, J.; Fu, S.; Zhou, L.; Yang, Y. Large amounts of easily decomposable carbon stored in subtropical forest subsoil are associated with r-strategy-dominated soil microbes. *Soil Biol. Biochem.* **2016**, *95*, 233–242. [CrossRef]
22. Xiao, D.; Huang, Y.; Feng, S.; Ge, Y.; Zhang, W.; He, X.; Wang, K. Soil organic carbon mineralization with fresh organic substrate and inorganic carbon additions in a red soil is controlled by fungal diversity along a pH gradient. *Geoderma* **2018**, *321*, 79–89. [CrossRef]
23. Li, Z.; Zhang, T.; Chen, B. Dynamics of soluble organic carbon and its relation to mineralization of soil organic carbon. *Acta Pedol. Sin.* **2004**, *41*, 544–552. (In Chinese)
24. Chen, T.; Hao, X.; Du, L.; Lin, B.; Feng, M.; Hu, R.; Gao, J. Effects of long-term fertilization on paddy soil organic carbon mineralization. *Chin. J. Appl. Ecol.* **2008**, *19*, 1494–1500. (In Chinese)
25. Worrell, E.; Price, L.; Martin, N.; Hendriks, C.; Meida, L.O. Carbon dioxide emissions from the global cement industry. *Annu. Rev. Energy Environ.* **2001**, *26*, 303–329. [CrossRef]
26. Davidson, E.A.; Verchot, L.V.; Cattânio, J.H.; Ackerman, I.L.; Carvalho, J.E.M. Effects of soil water content on soil respiration in forests and cattle pastures of eastern Amazonia. *Biogeochemistry* **2000**, *48*, 53–69. [CrossRef]
27. Paustian, K.; Six, J.; Elliott, E.T.; Hunt, H.W. Management options for reducing CO2 emissions from agricultural soils. *Biogeochemistry* **2000**, *48*, 147–163. [CrossRef]
28. Yu, S.; Wang, J.; Gao, Y. Effect of plastic mulching and different fertilization treatments on soil microbial biomass carbon and nitrogen. *J. Shenyang Agric. Univ.* **2006**, *37*, 602–606. (In Chinese)
29. Ågren, G.I.; Bosatta, E.; Magill, A.H. Combining theory and experiment to understand effects of inorganic nitrogen on litter decomposition. *Oecologia* **2001**, *128*, 94–98. [CrossRef]
30. Ci, E.; Mahdi, A.-K.; Wang, L.; Ding, C.; Xie, D. Soil organic carbon mineralization as affected by cyclical temperature fluctuations in a karst region of southwestern China. *Pedosphere* **2015**, *25*, 512–523. [CrossRef]
31. Wang, H.; Fan, Z.; Deng, D. Effects of environmental factors on soil organic carbon mineralization in a pinus sylvestris var. mongolica plantation. *Chin. J. Ecol.* **2008**, *27*, 1469–1475. (In Chinese)

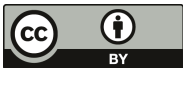

forests

MDPI

Article

Effects of Long-Term Successive Rotations, Clear-Cutting and Stand Age of Prince Rupprecht's larch (*Larix principis-rupprechtii* Mayr) on Soil Quality

Kuangji Zhao [1,2], Timothy J. Fahey [2], Dong Liang [3], Zhongkui Jia [1,*] and Lvyi Ma [1,4]

1 Key Laboratory for Silviculture and Conservation of the Ministry of Education, College of Forestry, Beijing Forestry University, Beijing 100083, China; zhaokuangji@gmail.com (K.Z.); maluyi@bjfu.edu.cn (L.M.)
2 Department of Natural Resources, Cornell University, New York, NY 14853, USA; tjf5@cornell.edu
3 Beijing Hangtian Wanyuan Landscape Environment Greening Engineering Co., Ltd., Beijing 100076, China; deep_spring@163.com
4 National Energy R&D Center for Non-Food Biomass, Beijing Forestry University, Beijing 100083, China
* Correspondence: jiazk@bjfu.edu.cn

Received: 5 August 2019; Accepted: 8 October 2019; Published: 22 October 2019

Abstract: A decline in soil quality is a major factor contributing to the degradation of forest ecological function. Vegetation plays a vital role in maintaining soil quality; however, the influence of plantation length on soil quality remains unclear. In this study, we collected soil samples in Northern China using a space-for-time substitution method. Soil were collected from control grassland; a clear-cutting site; 16-year-old (young, first, and second generation), 28-year-old (immature, first, and second generation), and 44-year-old (mature, first generation) *Larix principis-rupprechtii* Mayr stands in May, July, and September 2016. We measured soil physical and chemical properties, microbial communities, and enzymatic activities. We selected soil bulk density, non-capillary porosity, volume humidity, soil organic carbon and activity of polyphenol oxidase to calculate a soil quality index (SQI) for each site. Our data indicated that clear-cutting greatly decreased soil quality of *Larix principis-rupprechtii* forests but returning the harvesting residues to the forest floor could reduce the negative impact of clear-cutting on soil quality. The soil quality improved significantly by prolonging the cultivation cycle and it took about 39 years for the first-generation forest to restore soil quality to the level of the control plot. Our study confirms that SQI provides a comprehensive measurement of soil quality with the identification of a minimum data set. Comparing SQI with other soil quality indicators would help us to optimize the method for assessing soil quality.

Keywords: soil quality; successive planting; generation; stand age; clear-cutting; *Larix principis-rupprechtii* Mayr

1. Introduction

Soil degradation is a global problem in the 21st century [1]. Declining soil quality leads to the disruption of normal ecosystem functions and a reduction in ecosystem services [2]. From 1950 to 2010, soil ecosystem services were degraded by 60% [3], and accelerated soil degradation was reported to globally affect around 33% of the earth's land surface [4]. One potential cause of soil degradation is plantation forestry since repeated harvest and successive replanting can result in the depletion of soil nutrients [5,6]. The high nutrient demands of some tree species [7,8] may eventually lead to a decrease in soil quality [9]. Therefore, to maintain the productivity of forests, urgent action is needed to assess the impact of successive cultivation of timber forests on soil quality.

The selection of soil quality indicators should be based on the comprehensive evaluation of soil functions and ecological services [10]. Some studies have evaluated soil quality with soil chemistry [11–13], in particular, soil organic carbon (SOC) and nitrogen content [14]. Some other works have assessed soil quality only in terms of biological properties, such as microarthropod communities, without regarding chemical or physical properties or both [15–17]. These studies only reflect the limited aspects of soil quality. Ideally, soil quality indicators should take physical properties, chemical properties, biological communities, enzyme activities, and the interactions among these indicators into account [18]. A more comprehensive and easy-to-understand soil quality index (SQI) has been proposed for quantifying the combined physical, chemical, and biological properties of soil and their response to soil management practices [19].

Soil quality and forest stand management can affect each other [20]. The impact of forest growth on soil quality has been extensively studied in fast-growing plantation forests [6]. However, soil quality changes in successive rotations have been rarely investigated in timber forests with long growth cycles. The contribution of soil quality to ecosystem services is closely linked to forest management activities. In some situations, forest management results in complex interactive effects on soil properties [21]. Many works have evaluated the effects of clear-cutting on soil quality [22–25]; however, few studies have reported the SQI approach by considering forest stand growth (stand age and forest generation), human management (afforestation and clear-cutting), afforestation-stand growth-timber harvest, continuous variation of forest land.

Larix principis-rupprechtii is one of the main afforestation species in China due to its wide ecological plasticity, rapid growth, high-quality wood products, and strong stress resistance. We explored the application of the SQI approach to evaluate the effects of forest plantation management on soil health in Northern China. We quantified a suite of soil properties and evaluated the SQI of a reference grassland and a series of *Larix principis-rupprechtii* forest plantations, including first-generation 16-year-old (young), 28-year-old (immature) and 44-year-old (mature) forests, a clear-cutting site, and second-generation 16-year-old (young) and 28-year-old (immature) forests. The changes in soil quality were investigated by measuring the physical and chemical properties, the microbial communities, and the extracellular enzyme activity of soil. We aimed to advise forest management planning to maintain soil health and sustainability. We expected (1) that the soil quality would improve with an increase in stand age; (2) that the soil quality would decline by the change of successive forest generations; and (3) that clear-cutting would decrease soil quality.

2. Materials and Methods

2.1. Study Area

This experiment was carried out in Saihanba National Forest Park (SNFP), Weichang Manchu and Mongolian Autonomous County, Hebei Province, China (E 116°51′–117°39′, N 42°02′–42°36′). The elevation of the study sites was from 1600 to 1800 m. The area has a semi-arid monsoon climate and is located in the cool temperate zone with a mean annual temperature of −1.5 °C, a maximum annual temperature of 29.7 °C, and a minimum annual temperature of −38.7 °C. The mean annual rainfall is 433 mm, concentrated from June to August. Study sites are characterized as mainly gray forest soils, predominantly consisting of sand, since about 65% of the soils are sand silt. The carbon (C): nitrogen (N) ratio is 8.9 ± 0.3, and the soil parent materials are eluvium, saprolite, and alluvium; the thickness of the surface organic layer of each stand was about 3–8 cm [26]. *Larix principis-rupprechtii* is the dominant tree species in the coniferous forest belt of Northern China [27], and the plantation area accounts for 77.1% of the total plantation area in SNFP.

2.2. Experimental Design and Sampling

The experimental site was originally native grassland dominated by Maianthemum bifolium and Saussurea japonica. A reference grassland plot (abbreviated as CG) represented the sites on

which the forest plantations of *Larix principis* were established. The forest plantations included the first-generation 16-year-old (young, abbreviated as 1G-16YR), 28-year-old (immature, abbreviated as 1G-28YR), and 44-year-old (mature, abbreviated as 1G-44YR) stands; the second-generation 16-year-old (young, abbreviated as 2G-16YR) and 28-year-old (immature, abbreviated as 2G-28YR) stands; and a clear-cutting site (CC) where a mature, i.e., 44-year old, first-generation plantation was harvested in 45 years. The CG plot had never been planted with any trees and had no human disturbance. The 2G-16YR and 2G-28YR were plots where 3-year-old *Larix principis-rupprechtii* seedlings were planted after clear-cutting of mature plantations 13 and 25 years earlier respectively. The woodland was plowed the year before afforestation; in the year of afforestation, the woodland was excavated by a tree planting digger, and the seedlings were planted. The first five years after afforestation, workers used a mower to cut grass in the woodlands. After clear-cutting, we also employed a tracked grab wood machine to remove the timber from the woodland. Unfortunately, no 44-year-old second-generation stands were available in the SNFP. All the sites used in the present study were located in similar soil and landscape.

In May 2015, five 20 m × 20 m quadrats were established in a grid within each of the seven types of plots, totaling 35 plots. More information is provided in Table 1.

Table 1. Stand characteristics of *Larix principis-rupprechtii* plantations of seven types of plots.

Samples	Aspect	Angle of the Slope (°)	Slope Position	Canopy Density	Age (YR)	Altitude (m)	Mean DBH (cm)	Mean Tree Height (m)
Control grassland	North	1°	Above	-	-	1657.50	-	-
1G-16YR	South	3°	Below	0.80	16	1666.20	8.80	9.40
1G-28YR	-		-	0.50	28	1702.40	23.90	15.68
1G-44YR	North	5°	Middle	0.70	44	1712.00	35.50	20.50
Clear-cutting forest land	-		-	-	-	1672.00	-	-
2G-16YR	-		-	0.90	16	1696.00	7.70	6.90
2G-28YR	South	2°	Middle	0.90	28	1692.20	11.00	9.60

Notes: DBH indicates the diameter at breast height.

In May, July, and September 2016, the soils from the top 0–10 cm, 10–20cm and 20–30 cm layers were collected from the study sites in one day. Ten soil cores were collected at randomly selected points from each plot with a 3.6-cm-diameter soil auger, and the samples from different depths at the same location were mixed together as a composite sample, thereby totaling ten composite samples. Stones and roots were removed from the soil samples by hand, and the samples were sieved through 2-mm sieves. Five soil samples were stored at 4 °C to analyze the soil microbial biomass and enzyme activity, and the remaining samples were oven-dried at 105 °C to reach a constant dry weight for chemical analysis.

2.3. Physical Analysis

Soil bulk density (SBD) was determined by the intact core method [28,29], and soil capillary porosity (CP) was subsequently calculated using Equation (1) [30]. Soil non-capillary porosity (NCP) was also assessed by employing Equation (2) [31]. Moreover, Equation (3) was utilized to quantify total soil porosity (TP) based on NCP and CP [32], and soil ventilation (SV) was measured by Equation (4); Equation (5) estimated volume humidity (VH). Soil water content (SWC) and saturated soil water content (SSWC) were also measured according to the gravimetric method [33]. Capillary water capacity (CWC) was characterized by the method of Rowell [34], and field capacity (FC) was analyzed using a pressure plate apparatus [35,36].

$$CP = CWC \times \frac{SBD}{v} \times 100 \quad (1)$$

$$NCP = \frac{SSWC - CWC}{SBD} \quad (2)$$

$$TP = NCP + CP \quad (3)$$

$$SV = VH - TP \quad (4)$$

$$VH = SWC \times SBD \quad (5)$$

where CP (%), CWC (%), SBD (g cm^{-3}), V (cm^3), and NCP (%) represent capillary porosity, capillary water capacity, the soil bulk density, the volume of the soil core, and non-capillary porosity, respectively; SSWC (%), TP (%), SV (%), VH (%), and SWC (%) stand for the saturated soil water content, the soil total porosity, the soil ventilation, volume humidity, and the soil water content, respectively.

2.4. Chemical Analysis

The soil pH was measured in deionized water by a Delta320 pH-meter using a slurry having a soil to water ratio of 2:5 (Mettler-Toledo Instruments, Shanghai Co., Ltd., Shanghai, China). The SOC was also evaluated using Walkley and Black wet oxidation method as outlined in Bao's work [37]. Moreover, the total nitrogen (TN) of the soil was digested by concentrated sulfuric acid (98% H_2SO_4), and the available phosphorus (AP) extracted from soil by employing hydrochloric acid-ammonium fluoride (HCl + NH_4F) was determined by AA3 HR AutoAnalyzer (Seal Analytical Ltd., Southampton, UK). The total potassium (TK) of the soil was extracted using concentrated sulfuric acid (98% H_2SO_4) and measured by Lumina3300 (Aurora Biomed Inc., Vancouver, BC, Canada).

2.5. Microbial Properties

Soil samples for soil microorganism analysis were passed through a 1-mm sieve and stored in a ziplock bag at 4 °C. The soil microbes were assessed using dilution plate counting [38], and five replicates were performed on each sample. Bacteria were cultured in a medium of beef-extracted peptone agar. Actinomycetes and fungi were respectively cultured using a modified Gaussian medium and Martin's agar medium; the culture temperature was 28 °C. The bacteria and actinomycetes were cultured for 3–5 days and the fungi were cultured for 5–7 days.

2.6. Soil Enzyme Activity

The activity of catalase and polyphenol oxidase (PPO) activities were measured by potassium permanganate titration and pyrogallol colorimetry according to Waldrop et al. [39]. Soil urease activity was also assessed by sodium phenol colorimetry according to Kandeler and Gerber [40].

2.7. Statistical Analysis

The SQI was calculated according to Andrews and Carroll [18], and three steps were involved in the elaboration of the quality index: (1) the identification of a minimum data set (MDS), (2) the assignment of a score to each indicator by linear scoring functions, and (3) the data integration into an index.

Three steps were used to identify the MDS. (1) Data screening: one-way analysis of variance (ANOVA) was performed on the physical, chemical, and biological properties and the enzyme activities of the soil. Then, the variables exhibiting significant differences among treatments ($p < 0.05$) were chosen for the next step. (2) Selection of representative variables: the principal component analysis (PCA, see Supplementary Material, Table S1) was performed on the variables chosen from step (1). Only the principal component (PC) explained greater than 5% and eigenvalues ≥ 1 were examined. Within each PC, only the factors weighted with absolute values within 10% of the highest weight were retained for the MDS. (3) Redundancy reduction: multivariate correlation coefficients were used to determine the strength of the relationships among the variables. Highly correlated variables (correlation coefficient > 0.70) were considered redundant and nominated to be eliminated from the data set. To choose variables within the well-correlated groups, we summed the absolute values of the correlation coefficients for these variables. It was assumed that the variable with the highest correlation sum represents the group best. Any uncorrelated, highly weighted variable was considered important and retained in the MDS.

Linear scoring was applied in this study following the approach of Andrews and Carroll [18]. The linear scoring function (Equation (6)) was used to convert the measured values to the scored values as follows [41]:

$$S_{ij} = \frac{V_{ij} - V_{imin}}{V_{imax} - V_{imin}} \quad (6)$$

where S_{ij} is the score of soil variable i of sample j, and V_{ij} represents the observed variable value of sample j; V_{imax} and V_{imin} stand for the highest value of variable i and the lowest value of variable i, respectively. The scores of the indicators in the MDS (Table 2) were integrated into an SQI (Equation (7)) according to the work of Andrews et al. [42], as follows:

$$\mathrm{SQI} = \sum_{i=1}^{n} (S_i \times Q(xi)) \quad (7)$$

where S_i is the score assigned to indicator i, and $Q(xi)$ denotes the scoring result of each soil quality factor; n represents the number of indicators included in the MDS.

Table 2. Soil quality indicator scores (mean ± standard error) for the soil samples taken from the *Larix principis-rupprechtii* plantations.

	CG	1G-16YR	1G-28YR	1G-44YR	CC	2G-16YR	2G-28YR
SBD	0.76 ± 0.04 ^{a}	0.29 ± 0.04 ^{c}	0.36 ± 0.04 ^{bc}	0.49 ± 0.01 ^{b}	0.48 ± 0.04 ^{b}	0.27 ± 0.06 ^{c}	0.28 ± 0.04 ^{c}
NCP	0.48 ± 0.02 ^{b}	0.25 ± 0.11 ^{b}	0.33 ± 0.07 ^{b}	0.75 ± 0.11 ^{a}	0.42 ± 0.03 ^{b}	0.37 ± 0.06 ^{b}	0.44 ± 0.13 ^{b}
VH	0.46 ± 0.05 ^{cd}	0.33 ± 0.09 ^{d}	0.59 ± 0.03 ^{bc}	0.67 ± 0.03 ^{b}	0.90 ± 0.04 ^{a}	0.33 ± 0.03 ^{d}	0.43 ± 0.05 ^{d}
SOC	0.24 ± 0.04 ^{c}	0.39 ± 0.06 ^{bc}	0.43 ± 0.04 ^{b}	0.71 ± 0.09 ^{a}	0.36 ± 0.01 ^{bc}	0.43 ± 0.02 ^{b}	0.47 ± 0.02 ^{b}
PPO	0.47 ± 0.02 ^{bc}	0.43 ± 0.06 ^{c}	0.58 ± 0.09 ^{ab}	0.63 ± 0.02 ^{a}	0.43 ± 0.01 ^{c}	0.25 ± 0.02 ^{d}	0.45 ± 0.01 ^{bc}

Notes: SBD: soil bulk density; NCP: non-capillary porosity; VH: volume humidity; SOC: soil organic carbon; and PPO: polyphenol oxidase. In rows, the values with different letters are significantly different ($p < 0.05$).

One-way analysis of variance (ANOVA) was utilized to judge the significant differences among the physical, chemical, and biological properties of the soil, among the enzyme activity of the soil, and among the SQI of these treatments for the seven types of the forest lands. First, Shapiro-Wilk test and Levene test were used to respectively verify the assumptions of the normality and homogeneity of variance of the data on each variable; Duncan test was then used for a multiple comparison analysis. All the statistics calculation was conducted using PASW Statistics 18 (IBM, Armonk, NY, USA) with the level of significance set at $p < 0.05$. A p-value smaller than 0.05 indicates that the possibility of assumption is greater than 95%, and a p-value less than 0.01 in the following denotes that the possibility of assumption is greater than 99%. All the figures were also generated using Origin 8 (Origin Lab, Northampton, MA, USA).

3. Results

3.1. Soil Physical Properties

3.1.1. Soil Bulk Density

As shown in Figure 1, SBD was significantly higher in CG plot (1.39 g cm^{-3}) among the seven types of plots. After the initial afforestation, the sample SBD dropped significantly, i.e., the SBD of 1G-16YR was 1.12 g cm^{-3}. The SBD of the first-generation forest was enhanced with an increase in stand age. The SBD of the mature forest wood (1.24 g cm^{-3}) was also higher than that of the other stands. Moreover, there was no significant difference in SBD before and after clear-cutting. The SBD of the 2G-16YR plot (1.10 g cm^{-3}) was significantly lower than that of CC plots. The SBD of the second-generation forest still rose with an increase in stand age, but the SBD of CC was significantly dropped by 11.85% compared to CG. In this study, the difference in the SBD of the soils of the seven types of plots was significant ($p < 0.01$).

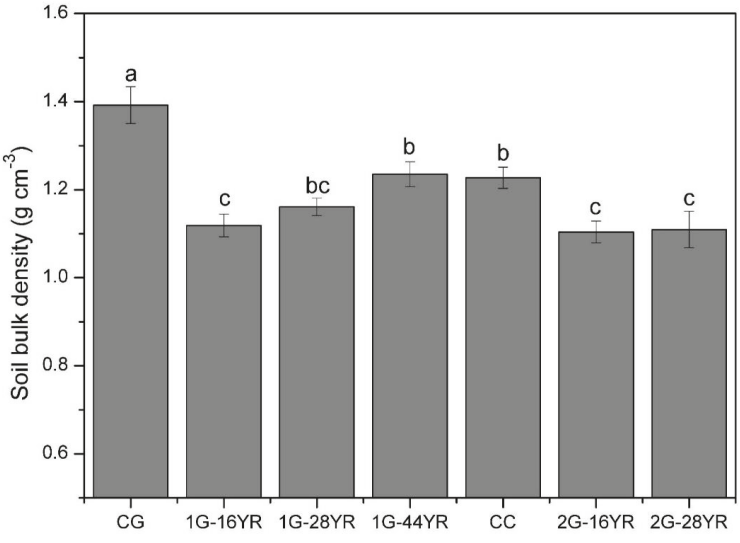

Figure 1. Soil bulk density in the successive *Larix principis-rupprechtii* plantations. CG indicated the control grassland; 1G-16YR indicated the 16-year 1st generation forest; 1G-28YR indicated the 28-year 1st generation forest; 1G-44YR indicated the 44-year 1st generation forest; CC indicated clear-cutting forest; 2G-16YR indicated the 16-year 2nd generation forest, and 2G-28YR indicated the 28-year 2nd generation forest. Soil bulk density (SBD) values with the same letter are not significantly different at $p < 0.05$. Error bars indicate the standard error; $n = 15$.

3.1.2. Soil Porosity

TP and NCP generally improved with a rise in stand age synchronously, and the values (60.73% and 11.99%) in 1G-44YR were higher compared to the other stand types (Figure 2). The TP of 1G-16YR was significantly increased by 9.62% compared with that of CG, but the NCP of 1G-16YR was 20.46% lower than that of CG. The TP and NCP of the samples in the plot were not significantly different before and after the second afforestation ($p > 0.05$). Caused by clear-cutting, NCP fell by 23.61% in the 1G-44YR plot. CP and SV also decreased with the increase of stand age. The values of forest CP (51.72%) and SV (43.61%) appeared in 1G-16YR were higher than those of the other stands. The CP and SV of 1G-16YR were 1.82% and 9.67% higher than that of CG, respectively, whereas the difference was not significant ($p < 0.05$). Also, the CP and SV of 2G-16YR significantly grew respectively by 2.63% and 106.62% compared to that of CC ($p < 0.01$); however, the SV of CC was significantly lower than that of CG by 49.77%. Except for CP ($p = 0.15$), the other soil porosity indicators were significantly different among the seven types of the plots ($p \leq 0.05$).

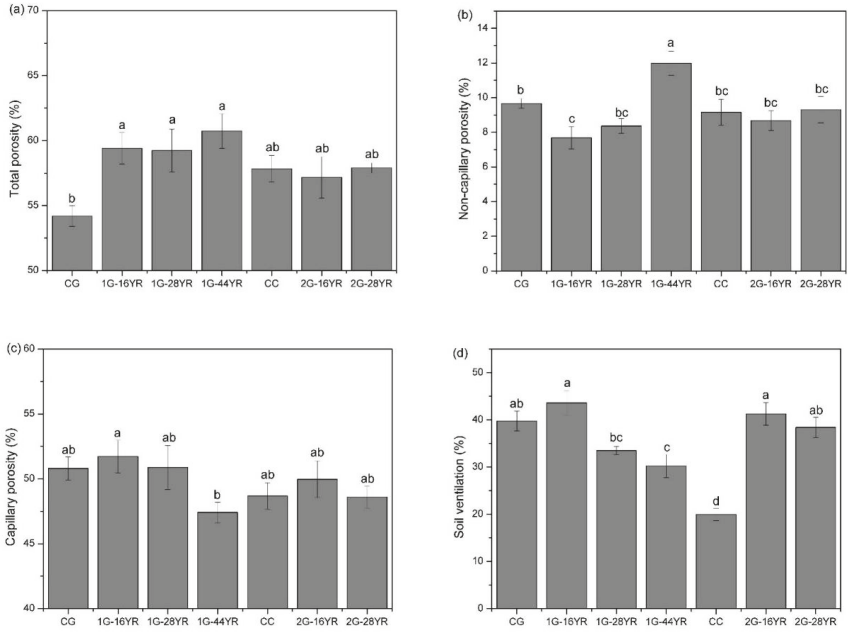

Figure 2. Soil porosity in the successive *Larix principis-rupprechtii* plantations. (**a**) Total porosity; (**b**) Non-capillary porosity; (**c**) Capillary porosity; (**d**) Soil ventilation. CG indicated the control grassland; 1G-16YR indicated the 16-year 1st generation forest; 1G-28YR indicated the 28-year 1st generation forest; 1G-44YR indicated the 44-year 1st generation forest; CC indicated clear-cutting forest; 2G-16YR indicated the 16-year 2nd generation forest, and 2G-28YR indicated the 28-year 2nd generation forest. Soil porosity values with the same letter are not significantly different at $p < 0.05$. Error bars indicate the standard error; $n = 15$.

3.1.3. Soil Water Content

The trend of SWC was the same as VH trend (Figure 3a,e). As stand age rises, a significant decline was seen in SWC and VH after afforestation, but an opposite trend was noticed after clear-cutting. SWC (30.97%) and VH (29.14%) in the CC plots were significantly higher than those of the other stands. The CWC and FC of the first-generation forest dropped with an increase in stand age. Nevertheless, no significant difference was seen in CWC and FC between the two stand ages of the second-generation forest. The values of CWC (46.39%) and FC (44.62%) appeared in 1G-16YR (Figure 3c,d) were higher compared to the other stand types, and CWC and FC were upgraded either by afforestation or by clear-cutting. The value of SSWC was significantly higher in 1G-16YR (49.97%) than in the CC plots (41.76%, Figure 3b). Compared with CG, SWC and VH significantly rose by 78.83% and 82.96% in the CC plots, respectively. Except for SSWC, the soil moisture indices were significantly different among the seven types of the plots ($p < 0.05$).

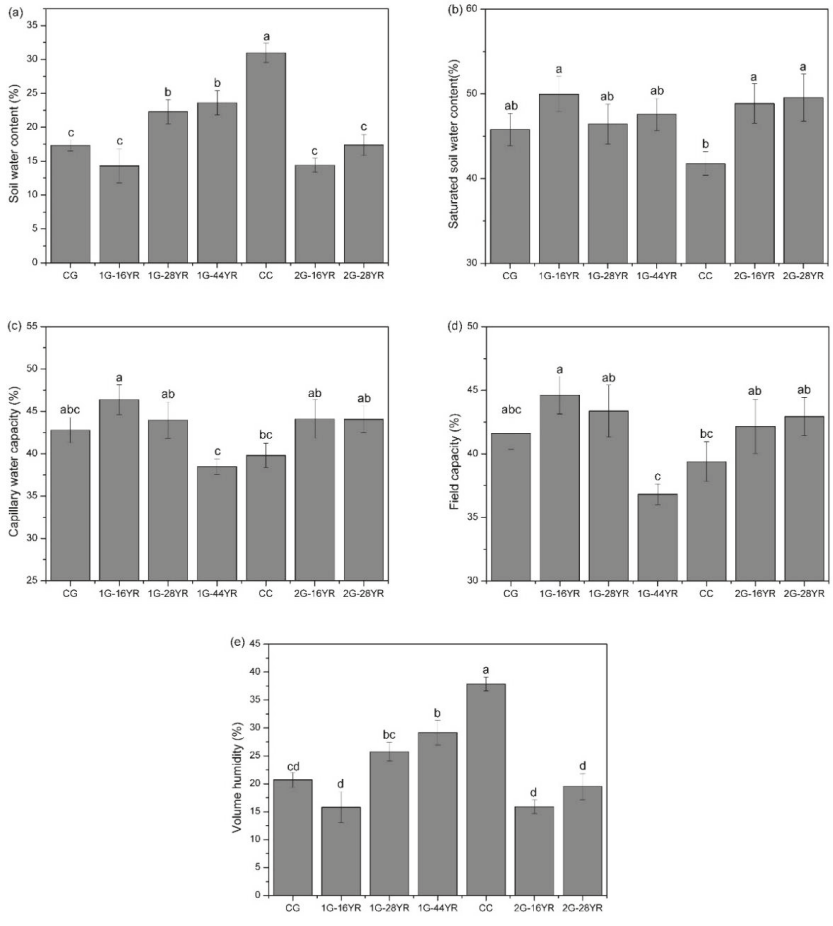

Figure 3. Water in soil in the successive *Larix principis-rupprechtii* plantations. (**a**) Soil water content; (**b**) Saturated soil water content; (**c**) Capillary water capacity; (**d**) Field capacity; (**e**) Volume humidity. CG indicated the control grassland; 1G-16YR indicated the 16-year 1st generation forest; 1G-28YR indicated the 28-year 1st generation forest; 1G-44YR indicated the 44-year 1st generation forest; CC indicated clear-cutting forest; 2G-16YR indicated the 16-year 2nd generation forest and 2G-28YR indicated the 28-year 2nd generation forest. Water in soil values with the same letter are not significantly different at $p < 0.05$. Error bars indicate the standard error; $n = 15$.

3.2. Soil Chemical Properties

3.2.1. Soil pH Value

The pH value of the second-generation forest was significantly higher than that of the first-generation forest (Figure 4); the acidity of the soil was lower in the CG plot (6.36), but the acidity of 1G-16YR (5.64) soil was higher compared to the other stand types. The pH value of the first-generation forest increased as the stand age rose, while the second-generation forest showed an opposite trend. The pH of clear-cut land was also reduced by 1.37%. Moreover, the pH of CC was significantly lower (9.59%) than that of CG. The pH difference among the plots was significant ($p < 0.01$).

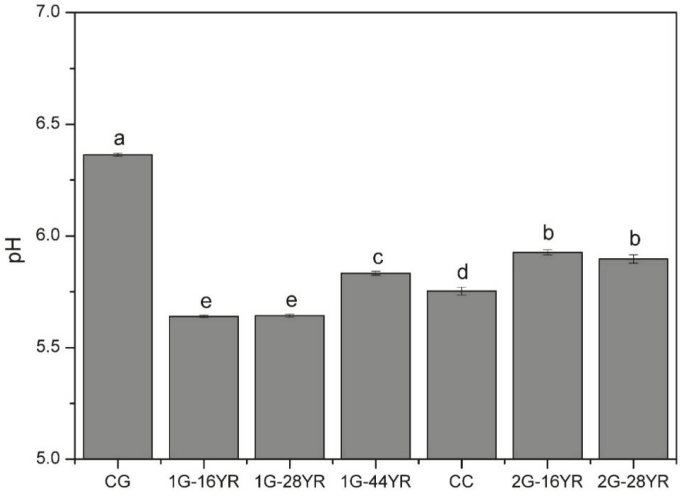

Figure 4. Soil pH value in the successive *Larix principis-rupprechtii* plantations. CG indicated the control grassland; 1G-16YR indicated the 16-year 1st generation forest; 1G-28YR indicated the 28-year 1st generation forest; 1G-44YR indicated the 44-year 1st generation forest; CC indicated clear-cutting forest; 2G-16YR indicated the 16-year 2nd generation forest and 2G-28YR indicated the 28-year 2nd generation forest. The pH value with the same letter is not significantly different at $p < 0.05$. Error bars indicate the standard error; $n = 15$.

3.2.2. Soil Nutrients

SOC, TN, and TK all were enhanced with an increase in stand age unanimously. After clear-cutting, SOC, TN, and TK were reduced by 44.44%, 29.85%, and 16.31%, respectively. Afforestation reduced TN and TK both in the CG plot and the CC plot but increased SOC. The value of SOC in 1G-44YR (84.27 g kg^{-1}) was significantly higher than that of the other stand types. In addition, the values of TN (3.90 g kg^{-1}) and TK (3.02 g kg^{-1}) of the CG plots were remarkably higher compared to the other stand types (Figure 5). However, the TN and TK values of the CC plot were considerably lower than those of CG plot by 44.97% and 23.65%, respectively. Except for AP, the indicators were markedly different among the seven types of plots ($p < 0.01$).

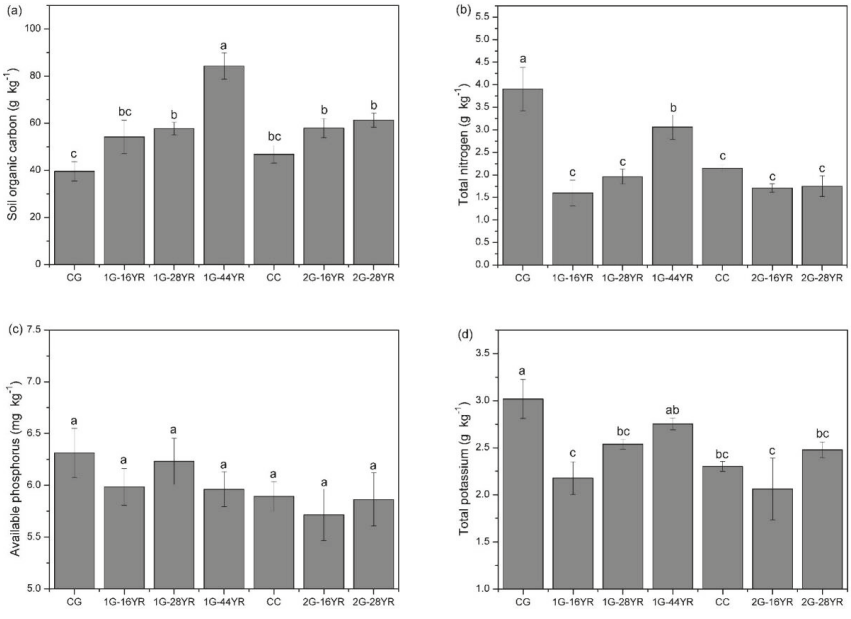

Figure 5. Soil nutrients in the successive *Larix principis-rupprechtii* plantations. (**a**) Soil organic carbon; (**b**) Total nitrogen; (**c**) Available phosphorus; (**d**) Total potassium. CG indicated the control grassland; 1G-16YR indicated the 16-year 1st generation forest; 1G-28YR indicated the 28-year 1st generation forest; 1G-44YR indicated the 44-year 1st generation forest; CC indicated clear-cutting forest; 2G-16YR indicated the 16-year 2nd generation forest and 2G-28YR indicated the 28-year 2nd generation forest. Soil nutrients with the same letter are not significantly different at $p < 0.05$. Error bars indicate the standard error; n=15.

3.3. Soil Biological Properties

3.3.1. Soil Microorganisms

As illustrated in Figure 6, bacteria, actinomycete, and fungi were promoted with the increased stand age. The value of bacteria in 1G-44YR (60.87×10^6 g^{-1}), the value of actinomycete in 2G-28YR (11.70×10^6 g^{-1}), and that of fungi in the CG plots (11.83×10^4 g^{-1}) were higher than their counterparts in the other types of stands. The bacteria of the first-generation forest land were significantly larger than those of the second-generation forest. The value of the bacteria of 1G-16YR was 2.27 times more than that of 2G-16YR, and the bacteria value of 1G-28YR was 1.69 times higher than that of 2G-28YR. Except for fungi ($p = 0.06$), the other indicators were noticeably different among the plots ($p < 0.05$).

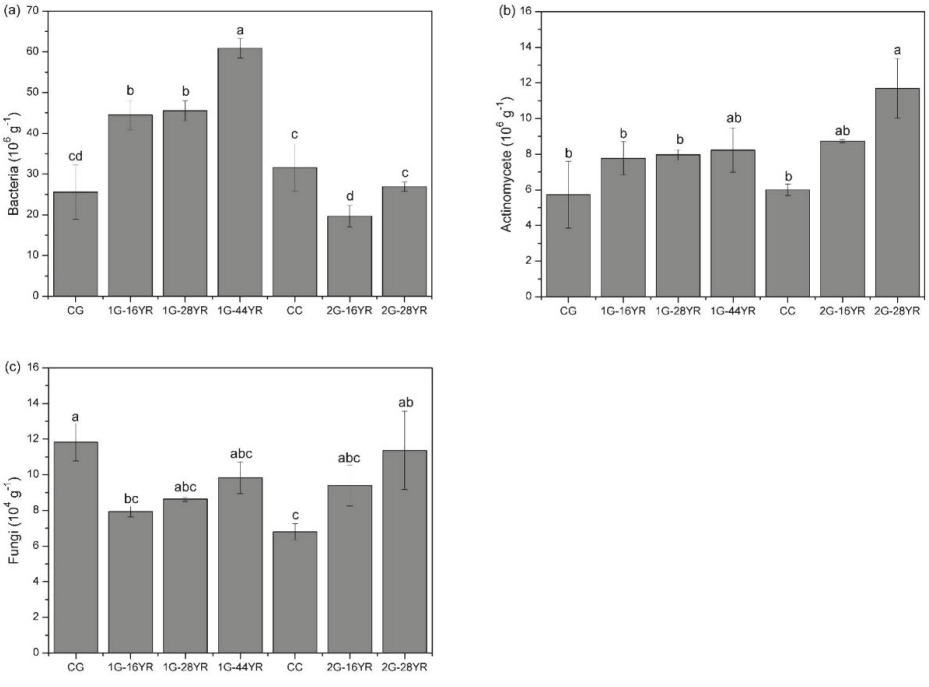

Figure 6. Soil microorganisms in the successive *Larix principis-rupprechtii* plantations. (**a**) Bacteria; (**b**) Actinomycete; (**c**) Fungi. CG indicated the control grassland; 1G-16YR indicated the 16-year 1st generation forest; 1G-28YR indicated the 28-year 1st generation forest; 1G-44YR indicated the 44-year 1st generation forest; CC indicated clear-cutting forest; 2G-16YR indicated the 16-year 2nd generation forest and 2G-28YR indicated the 28-year 2nd generation forest. Soil microorganisms with the same letter are not significantly different at $p < 0.05$. Error bars indicate the standard error; $n = 15$.

3.3.2. Soil Enzyme Activity

The activity of catalase, PPO, and urease was enhanced with the increase of stand age (Figure 7). The catalase value of the CG plot (0.62 mL g^{-1}) and the values of PPO and urease of the 1G-44YR plot (0.44 10^{-2} and 2.67 mg g^{-1}) were higher than those of the other plots. The PPO value of 2G-16YR was significantly decreased by 32.03% compared with that of the CC plot, while the PPO value was considerably reduced by 26.39% due to clear-cutting. Also, clear-cutting markedly dropped urease by 51.94%.

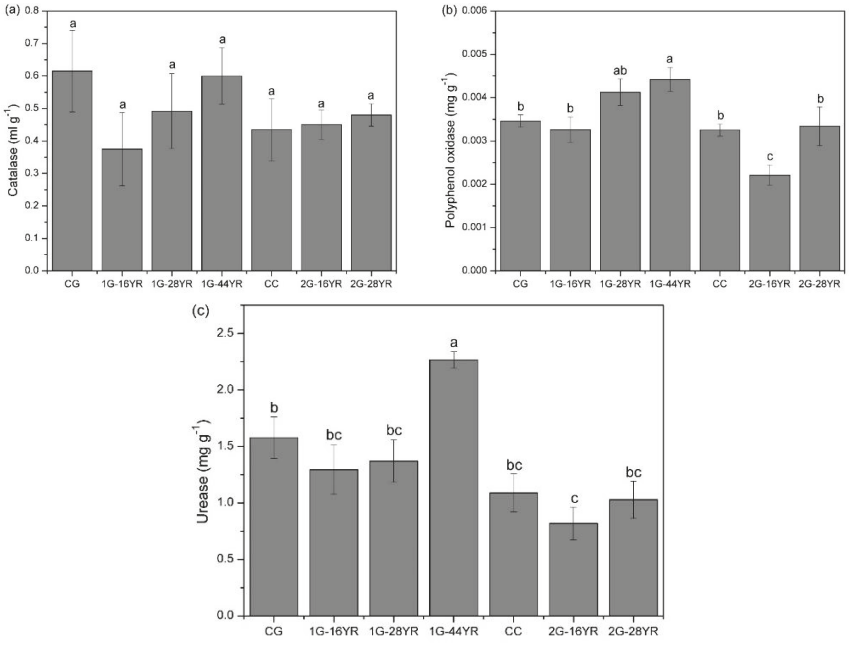

Figure 7. Soil enzyme activities in the successive *Larix principis-rupprechtii* plantations. (**a**) Catalase; (**b**) Polyphenol oxidase; (**c**) Urease. CG indicated the control grassland; 1G-16YR indicated the 16-year 1st generation forest; 1G-28YR indicated the 28-year 1st generation forest; 1G-44YR indicated the 44-year 1st generation forest; CC indicated clear-cutting forest; 2G-16YR indicated the 16-year 2nd generation forest and 2G-28YR indicated the 28-year 2nd generation forest. Soil enzyme activities with the same letter are not significantly different at $p < 0.05$. Error bars indicate the standard error; $n = 15$.

3.4. Soil Quality Index

Soil variables with significant differences among treatments included SBD, TP, NCP, SV, SWC, CWC, FC, VH, pH, SOC, TN, TK, bacteria, actinomycete, PPO, and urease. The first four PC's explained greater than 5% and eigenvalues ≥ 1. The highly weighted variables under the four PC's were SBD, TN, SV, VH, bacteria, PPO, NCP and SOC (see Supplementary Material, Table S1). As illustrated in Figure 8 and Table S2, 1G-44YR had the greatst soil quality; NCP and SOC were not well correlated with the other variables and retained for the MDS. SBD and TN were remarkably correlated; SBD had a higher correlation sum, so it was retained for the MDS. SV and VH were negatively correlated to each other; VH was retained for the MDS by the higher correlation sum. Bacteria and PPO were noticeably correlated; PPO had a higher correlation sum and was retained for the MDS. The variables selected to remain in MDS are SBD, NCP, VH, SOC, and PPO, which are used to calculate SQI.

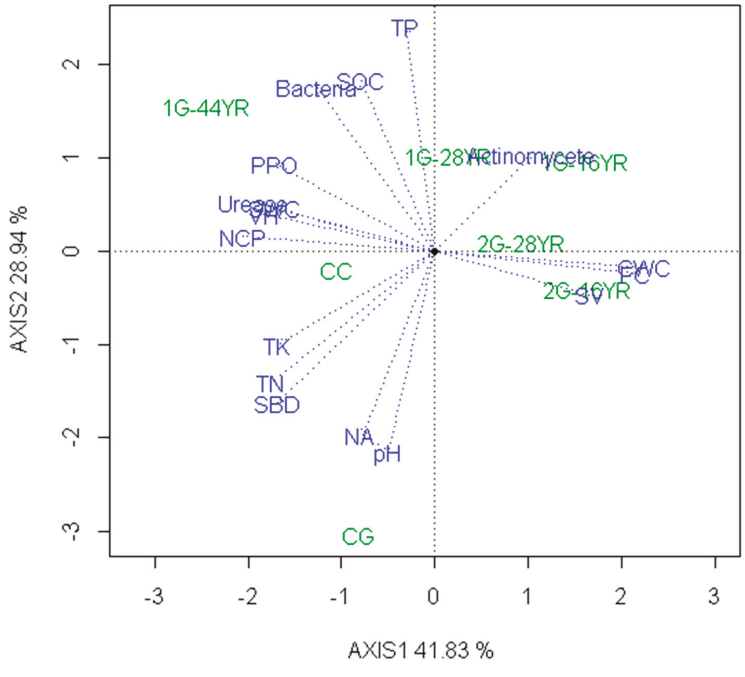

Figure 8. Biplots of soil variables and treatments in PC1 and PC2.

As depicted in Figure 9, the SQI of 1G-44YR (0.66) was significantly larger than that of the other stand types. The SQI of CG (0.47) and that of CC (0.51) were remarkably higher than that of 1G-16YR (0.34) and that of 2G-16YR (0.33) by 38.24% and 54.55%, respectively. After a stand incubation period (compare the 1G-16YR with the 2G-16YR), the SQI was decreased by 2.90%, but the improvement was not significant ($p < 0.05$).

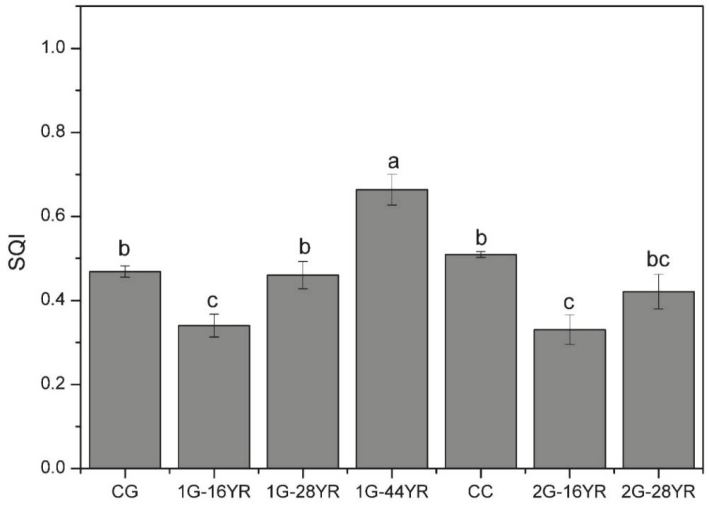

Figure 9. Soil quality index in the successive *Larix principis-rupprechtii* plantations. SQI: soil quality index; CG indicated the control grassland; 1G-16YR indicated the 16-year 1st generation forest; 1G-28YR indicated the 28-year 1st generation forest; 1G-44YR indicated the 44-year 1st generation forest; CC indicated clear-cutting forest; 2G-16YR indicated the 16-year 2nd generation forest and 2G-28YR indicated the 28-year 2nd generation forest. Soil quality indices with the same letter are not significantly different at $p < 0.05$. Error bars indicate the standard error; $n = 15$.

4. Discussion

4.1. Stand Age

Our observations supported our first hypothesis since all the indicators improved with an increase in stand age, except for TP, CP, SV, SSWC, CWC, FC, pH, AP, and catalase. The comprehensive analysis confirmed that the SQI was also significantly increased with an increased stand age. Furthermore, the results of this study are consistent with the work of Lima et al. [43], whereas they are contrary to the results of Zhang et al. [6]; this contrast is attributed to the lower temperature of the studied site, which consequently slowed down the decomposition of soil organic matter. Moreover, tree species are the main factors affecting microbial community activity and changing soil nutrient dynamics [44], and the pine needles of *Larix principis-rupprechtii* returns nutrients to the soil in the form of litter in the non-growth season. The growth rate of *Larix principis-rupprechtii* was slower and the demand for soil nutrients was relatively less. Thus, the cultivation of *Larix principis-rupprechtii* would improve soil quality. This study also stated that the average annual growth of the SQI from 28- to 44-year old was 1.27 times larger than that of the SQI from 16- to 28-year old (Figure 9). The older the forest stand is, the clearer the improvement of the soil quality is. It was speculated that the reason may be as follows: (1) The forest was gradually closed due to the increase of stand age; lower decomposition and soil disturbance reduction were found after the canopy closed [14,45,46]. Also, a high litter mass may contribute to the subsequent increase in SOC stocks in the older stands [47–49]. (2) During the early stages of plant life, nutrient absorption was kept at a high level, whereas litter production was at a low level. However, litter production increased, but nutrient absorption fell as the plant became older [50]. Therefore, extending the cultivation cycle of *Larix principis-rupprechtii* forests is beneficial to improving soil quality.

4.2. Forest Generation

The results also showed that indicators such as SWC, VH, bacteria and PPO dropped by the change of forest generation. According to the comprehensive analysis, increasing forest generation reduced the soil quality in the stand, but the difference was insignificant, which failed to support our second hypothesis. The results of this study are not consistent with the work of Zhang et al. [6] on the soil change of the third and fourth generations of *eucalyptus* forests. It was speculated that Zhang et al. [6] decreased the disturbance of soil afforestation activities by changing the reclamation method the after clear-cutting of the third-generation forest and fertilized forest land to supplement soil nutrients and improve soil quality. In the present study, plowing the forest (creating furrows and ridges) exposed the soil to air during afforestation. The exposure process promoted the loss of mineral components and reduced soil quality. In addition to afforestation activities, clear-cutting also accelerates the decomposition rate of SOC [51,52] and reduces SOC stocks, thereby causing a considerable decline in the soil quality in the forest land [27]. After clear-cutting, the cutting remains were not returned to the forest land, further resulting in a remarkable decrease in the soil quality of the forest land. However, the growth of the first-generation forests for more than 40 years has noticeably enhanced the soil quality. Therefore, an increase in the forest generation did not significantly reduce the soil quality of the forest land. Hence, the main reason for the decline of soil quality was artificial disturbance, including clear-cutting and afforestation. By returning harvesting residues and taking fertilizing measures, the negative effects of human disturbance, such as clear-cutting and afforestation, on the soil quality of forest lands would be reduced; delaying deforestation is also helpful in improving soil quality. Due to the long growth cycle of *Larix principis-rupprechtii* in Northern China, this study only focused on the first- and second-generation forests of *Larix principis-rupprechtii* in Northern China, and the influence of successive rotations on the soil quality should be continuously observed.

4.3. Clear-Cutting

Our observations demonstrated that a decline in the soil quality is caused by the reduction in porosity, microbial quantity except catalase, and the enzyme activity of soil with clear-cutting supporting the third hypothesis. Previous studies have shown that soil quality also declines due to human disturbance such as clear-cutting [6,53]. They are mutually validated by the present study. Deforestation negatively impacts on soil physical properties and leads to the loss of soil nutrients [23], coinciding with our results. Understorey vegetation also provides a better condition for microorganisms and alleviates rainfall-induced erosion and nutrient leaching [54]. After clear-cutting, dragging wood away and cutting residues could destroy the understorey vegetation and litter on soil and could expose a large number of aggregates of soil to air; thus, soil erosion and nutrient leaching occur after heavy rainfalls [55]. Erosion also damages soil structure and influences the circulation of elements, microbial populations, and organic compounds in soil [56,57]. While most litter and harvesting residues were not returned to the forest land, the return of forest nutrients mainly depends on the precipitation leaching and the decomposition of inorganic nutrients by roots, leading to the remarkable inhibition of nutrient cycle in the forest ecosystem and a marked reduction in the efficiency of nutrient cycle [58]. Clear-cutting causes the exposure of ridges to air, the decomposition of organic matter, and the massive loss of soil mineral elements (a maximum loss of N, C, and K+) [24,59–61], which in turn lowers the number of microorganisms and soil enzyme activity, thereby ultimately reducing the soil quality and making the soil more barren [22,25]. Therefore, clear-cutting causes exposure of soil to air and ultimately declines soil quality. In order to alleviate the negative effects of clear-cutting on soil quality, the use of heavy machinery should be minimized during the clear-cutting process, and the disturbance of human activities to forest soil should be lessened as well [62], especially the disturbance to forest soil during the removal of tree stumps. Returning the harvesting residues to the forest land is required to maintain the coverage of litter and understorey vegetation. Thus, the decomposition of the soil organic matters, the soil erosion, the changes in soil structure, and the loss of soil nutrients through drenching would be minimized.

4.4. Forest Cultivation Cycle and Soil Quality Recovery Time

From planting *Larix principis-rupprechtii* seedlings to harvesting wood as a cultivation cycle, the soil quality declined by 2.90% through a forest cultivation cycle. Soil quality declining problems such as exposure of soil to air and nutrient loss are caused by the distribution of land through planting trees. As the soil quality in the growing forests gradually recovers, the forests play a role in improving the soil quality. In this study, due to the use of heavy machinery in the harvesting process and failure to take measures such as returning the cutting leftovers, the forest soil quality was greatly reduced. The studies of Selvaraj et al. [52] also support our results. Since the soil quality gradually improved from 16-year-old to 44-year-old forest stands after planting *Larix principis-rupprechtii,* the change in the stand SQI (Figure 9) presumed that it would take about 39 years for the first-generation forest (calculated by regression analysis, see Supplementary Material, Table S3) and more than 28 years for the second-generation forest to restore soil quality. Therefore, in order to maintain the soil quality, the planting cycle of *Larix principis-rupprechtii* should be longer than 39 years.

SQI is a relatively novel method for soil quality assessment. In this research, five representative variables were selected among 24 soil variables to define the smallest data set, for SQI calculation. It provides a more intelligible and comprehensive measurement for soil quality. In future research, comparsion SQI and other common indicators for soil quality evaluation would be expected for more accurate variables determinating, to further optimize SQI calculation method.

5. Conclusions

The main findings of this study are as follows:

(1) Extending the cultivation cycle of *Larix principis-rupprechtii* forest was beneficial to improving soil quality.
(2) Increasing forest generation did not significantly reduce soil quality.
(3) Clear-cutting could greatly decrease soil quality, and returning the harvesting residues to the forest land may reduce the negative impact of clear-cutting on soil quality.
(4) In order to maintain soil health and achieve sustainable planting, the planting period of *Larix principis-rupprechtii* forests should be more than 39 years.
(5) SQI provided a more intelligible and comprehensive measurement of soil quality with the identification of a minimum data set. Future studies should compare SQI with other soil quality indicators to further optimize SQI calculation method.

To better understand the impacts of successive *Larix principis-rupprechtii* planting on soil quality, more generations of *Larix principis-rupprechtii* plantations should be evaluated.

Supplementary Materials: The following are available online at http://www.mdpi.com/1999-4907/10/10/932/s1, Table S1: Results of the principal components analysis of soil variables, Table S2: Results of the correlation analysis of soil variables, Table S3: Standardized regression coefficients of the generalized linear models (GLMs) used to examine the effects of stand age on SQI for the first-generation *Larix principis-rupprechtii*.

Author Contributions: K.Z.: Data collection, data analysis, and manuscript writing. T.J.F.: Guide the revision of the manuscript. D.L.: Data collection, data analysis. Z.J.: Design of the study and supervision of the scientific experiments and data analysis. L.M.: Supervision of the scientific experiments.

Funding: This research was funded by National Natural Science Foundation of China (31870387) and China Scholarship Council.

Conflicts of Interest: The authors declare no conflicts of interest.

References

1. Lal, R. Restoring Soil Quality to Mitigate Soil Degradation. *Sustainability* **2015**, *7*, 5875–5895. [CrossRef]
2. Lal, R. Soil degradation as a reason for inadequate human nutrition. *Food Sec.* **2009**, *1*, 45–57. [CrossRef]
3. León, J.D.; Osorio, N.W. Role of Litter Turnover in Soil Quality in Tropical Degraded Lands of Colombia. *Sci. World J.* **2014**, *2014*, 693981. [CrossRef] [PubMed]

4. Bini, C. Soil: A precious natural resource. In *Conservation of Natural Resources*; Kudrow, N.J., Ed.; Nova Science Publishers: Hauppauge, NY, USA, 2009; pp. 1–48.
5. Yu, X.B.; Yang, G.Q.; Li, S.K. Study on the changes of soil properties in Eucalyptus plantation under continuous-planting practices. In *Studies on Longterm Productivity Management of Eucalyptus Plantation*; Yu, X.B., Ed.; China Forestry Publishing House: Beijing, China, 2000; pp. 94–103.
6. Zhang, K.; Zheng, H.; Chen, F.L.; Ouyang, Z.Y.; Wang, Y.; Wu, Y.F.; Lan, J.; Fu, M.; Xiang, X.W. Changes in Soil Quality after Converting Pinus to Eucalyptus Plantations in Southern China. *Solid Earth* **2015**, *6*, 115–123. [CrossRef]
7. LeBauer, D.S.; Treseder, K.K. Nitrogen Limitation of Net Primary Productivity in Terrestrial Ecosystems Is Globally Distributed. *Ecology* **2008**, *89*, 371–379. [CrossRef] [PubMed]
8. Laclau, J.P.; Ranger, J.; Goncalves, J.L.D.; Maquere, V.; Krusche, A.V.; M'Bou, A.T.; Nouvellon, Y.; Saint-Andre, L.; Bouillet, J.P.; Piccolo, M.D.; et al. Biogeochemical Cycles of Nutrients in Tropical Eucalyptus Plantations Main Features Shown by Intensive Monitoring in Congo and Brazil. *For. Ecol. Manag.* **2010**, *259*, 1771–1785. [CrossRef]
9. Yu, F.K.; Huang, X.H.; Wang, K.Q.; Duang, C.Q. An overview of ecological degradation and restoration of Eucalyptus plantations. *Chin. J. Eco-Agric.* **2009**, *17*, 393–398. [CrossRef]
10. Bünemann, E.K.; Bongiorno, G.; Bai, Z.; Creamer, R.E.; De Deyn, G.; de Goede, R.; Pulleman, M. Soil quality—A critical review. *Soil Biol. Biochem.* **2018**, *120*, 105–125. [CrossRef]
11. Garay, I.; Pellens, R.; Kindel, A.; Barros, E.; Franco, A.A. Evaluation of soil conditions in fast-growing plantations of Eucalyptus grandis and Acacia mangium in Brazil: A contribution to the study of sustainable land use. *Appl. Soil Ecol.* **2004**, *27*, 177–187. [CrossRef]
12. Muñoz-Rojas, M.; Jordán, A.; Zavala, L.M.; De la Rosa, D.; AbdElmabod, S.K.; Anaya-Romero, M. Organic carbon stocks in Mediterranean soil types under different land uses (Southern Spain). *Solid Earth* **2012**, *3*, 375–386. [CrossRef]
13. Parras-Alcántara, L.; Martín-Carrillo, M.; Lozano-García, B. Impacts of land use change in soil carbon and nitrogen in a Mediterranean agricultural area (Southern Spain). *Solid Earth* **2013**, *4*, 167–177. [CrossRef]
14. Zhang, Y.; Wei, Z.C.; Li, H.T.; Guo, F.T.; Wu, P.F.; Zhou, L.L.; Ma, X.Q. Biochemical quality and accumulation of soil organic matter in an age sequence of *Cunninghamia lanceolata* plantations in southern China. *J. Soils Sediments* **2017**, *17*, 2218–2229. [CrossRef]
15. Filip, Z. International approach to assessing soil quality by ecologically-related biological parameters. *Agric. Ecosyst. Environ.* **2002**, *88*, 169–174. [CrossRef]
16. Parisi, V.; Menta, C.; Gardi, C.; Jacomini, C.; Mozzanica, E. Microarthropod communities as a tool to assess soil quality and biodiversity: A new approach in Italy. *Agric. Ecosyst. Environ.* **2005**, *105*, 323–333. [CrossRef]
17. Ritz, K.; Black, H.I.J.; Campbell, C.D.; Harris, J.A.; Wood, C. Selecting biological indicators for monitoring soils: A framework for balancing scientific and technical opinion to assist policy development. *Ecol. Indic.* **2009**, *9*, 1212–1221. [CrossRef]
18. Andrews, S.S.; Carroll, C.R. Designing a soil quality assessment tool for sustainable agroecosystem management. *Ecol. Appl.* **2001**, *11*, 1573–1585. [CrossRef]
19. Zornoza, R.; Acosta, J.A.; Bastida, F.; Domínguez, S.G.; Toledo, D.M.; Faz, A. Identification of sensitive indicators to assess the interrelationship between soil quality, management practices and human health. *Soil* **2015**, *1*, 173–185. [CrossRef]
20. Gruba, P.; Socha, J.; Pietrzykowski, M.; Pasichnyk, D. Tree species affects the concentration of total mercury (Hg) in forest soils: Evidence from a forest soil inventory in Poland. *Sci. Total Environ.* **2019**, *647*, 141–148. [CrossRef]
21. Bouma, J.; Van Ittersum, M.K.; Stoorvogel, J.J.; Batjes, N.H.; Droogers, P.; Pulleman, M.M. Soil capability: Exploring the functional potentials of soils. *Glob. Soil Secur.* **2017**, 27–44. [CrossRef]
22. Weis, W.; Huber, C.; Gattlein, A. Regeneration of mature Norway spruce stands: Early effects of selective cutting and clear cutting on seepage water quality and soil fertility. *Sci. World J.* **2001**, *1*, 493–499. [CrossRef]
23. Zhou, X.N.; Zhou, Y.; Zhou, C.J.; Wu, Z.L.; Zheng, L.F.; Hu, X.S.; Chen, H.X.; Gan, J.B. Effects of Cutting Intensity on Soil Physical and Chemical Properties in a Mixed Natural Forest in Southeastern China. *Forests* **2015**, *6*, 4495–4509. [CrossRef]
24. Aleksandrowicz-Trzcinska, M.; Drozdowski, S.; Zybura, H. Effect of Mechanical Site Preparation on Features of the Soil in a Clear-Cut Area. *Sylwan* **2018**, *162*, 648–657.

25. Hume, A.M.; Chen, H.Y.H.; Taylor, A.R. Intensive Forest Harvesting Increases Susceptibility of Northern Forest Soils to Carbon, Nitrogen and Phosphorus Loss. *J. Appl. Ecol.* **2018**, *55*, 246–255. [CrossRef]
26. Zhao, K.J.; Zheng, M.X.; Fahey, T.J.; Jia, Z.K.; Ma, Y.L. Vertical gradients and seasonal variations in the stem CO_2 efflux of *Larix principis-rupprechtii* Mayr. *Agric. For. Meteorol.* **2018**, *262*, 71–80. [CrossRef]
27. Yao, Y.T.; Zhang, J.Z.; Hu, J.F. *Larix Principis-Rupprechtii*; Agricultural Science and Technology Press of China: Beijing, China, 2013.
28. McKenzie, N.; Coughlan, K.; Cresswell, H. *Soil Physical Measurement and Interpretation for Land Evaluation*; Csiro Publishing: Collingwood, Australia, 2002; Volume 5.
29. Wu, G.L.; Yang, Z.; Cui, Z.; Liu, Y.; Fang, N.F.; Shi, Z.H. Mixed artificial grasslands with more roots improved mine soil infiltration capacity. *J. Hydrol.* **2016**, *535*, 54–60. [CrossRef]
30. Jiao, F.; Wen, Z.M.; An, S.S. Changes in soil properties across a chronosequence of vegetation restoration on the Loess Plateau of China. *Catena* **2011**, *86*, 110–116. [CrossRef]
31. Huang, C.Y. *Soil Science*; China Agriculture Press: Beijing, China, 2003; pp. 89–92.
32. Hardie, M.; Clothier, B.; Bound, S.; Oliver, G.; Close, D. Does Biochar Influence Soil Physical Properties and Soil Water Availability? *Plant Soil* **2014**, *376*, 347–361. [CrossRef]
33. Clark, M.D.; Gilmour, J.T. The effect of temperature on decomposition at optimum and saturated soil water contents. *Soil Sci. Soc. Am. J.* **1983**, *47*, 927–929. [CrossRef]
34. Rowell, D.L. *Soil Science: Methods and Applications*; Routledge: London, UK, 2014.
35. Cassel, D.K.; Nielsen, D.R. Field capacity and available water capacity. In *Methods of Soil Analysis. Part 1*, 2nd ed.; Klute, A., Ed.; Agron. Monogr. 9. ASA and SSSA: Madison, WI, USA, 1986; pp. 901–926.
36. Givi, J.; Prasher, S.O.; Patel, R.M. Evaluation of pedotransfer functions in predicting the soil water contents at field capacity and wilting point. *Agric. Water Manag.* **2004**, *70*, 83–96. [CrossRef]
37. Bao, S.D. *Soil Agro-Chemical Analysis*; China Agriculture Press: Beijing, China, 2000.
38. Chen, H.K. *Soil Microbiology*; Shanghai Science and Technology Press: Shanghai, China, 1981; pp. 44–45.
39. Waldrop, M.P.; Balser, T.C.; Firestone, M.K. Linking microbial community composition to function in a tropical soil. *Soil Biol. Biochem.* **2000**, *32*, 1837–1846. [CrossRef]
40. Kandeler, E.; Gerber, H. Short-term assay of soil urease activity using colorimetric determination of ammonium. *Biol. Fertil. Soils* **1988**, *6*, 68–72. [CrossRef]
41. Zheng, H.; Ouyang, Z.Y.; Wang, X.K.; Miao, H.; Zhao, T.Q.; Peng, T.B. How different reforestation approaches affect red soil properties in Southern China. *Land Degrad. Dev.* **2005**, *16*, 387–396. [CrossRef]
42. Andrews, S.S.; Karlen, D.L.; Mitchell, J.P. A comparison of soil quality indexing methods for vegetable production systems in Northern California. *Agric. Ecosyst. Environ.* **2002**, *90*, 25–45. [CrossRef]
43. Lima, A.M.; Silva, I.R.; Neves, J.C.; Novais, R.F.; Barros, N.F.; Mendonça, E.S.; Leite, F.P. Soil organic carbon dynamics following afforestation of degraded pastures with eucalyptus in southeastern Brazil. *For. Ecol. Manag.* **2006**, *235*, 219–231. [CrossRef]
44. Lucas-Borja, M.E.; Hedo, J.; Cerdá, A.; Candel-Pérez, D.; Viñegla, B. Unravelling the importance of forest age stand and forest structure driving microbiological soil properties, enzymatic activities and soil nutrients content in Mediterranean Spanish black pine (*Pinus nigra* Ar. ssp. salzmannii) Forest. *Sci. Total Environ.* **2016**, *562*, 145–154. [CrossRef]
45. Mao, R.; Zeng, D.H.; Hu, Y.L.; Li, L.J.; Yang, D. Soil organic carbon and nitrogen stocks in an age-sequence of poplar stands planted on marginal agricultural land in Northeast China. *Plant Soil* **2010**, *332*, 277–287. [CrossRef]
46. Cheng, J.; Lee, X.; Theng, B.K.; Zhang, L.; Fang, B.; Li, F. Biomass accumulation and carbon sequestration in an age-sequence of *Zanthoxylum bungeanum* plantations under the Grain for Green Program in karst regions, Guizhou province. *Agric. For. Meteorol.* **2015**, *203*, 88–95. [CrossRef]
47. Zhou, G.Y.; Liu, S.G.; Li, Z.; Zhang, D.Q.; Tang, X.L.; Zhou, C.Y.; Yan, J.H.; Mo, J.M. Old-Growth Forests Can Accumulate Carbon in Soils. *Science* **2006**, *314*, 1417. [CrossRef]
48. Luyssaert, S.; Schulze, E.D.; Borner, A.; Knohl, A.; Hessenmoller, D.; Law, B.E.; Ciais, P.; Grace, J. Old-growth forests as global carbon sinks. *Nature* **2008**, *455*, 213–215. [CrossRef]
49. Chen, G.S.; Yang, Z.J.; Gao, R.; Xie, J.S.; Guo, J.F.; Huang, Z.Q.; Yang, Y.S. Carbon Storage in a Chronosequence of Chinese Fir Plantations in Southern China. *For. Ecol. Manag.* **2013**, *300*, 68–76. [CrossRef]

50. Xu, D.P. An approach to nutrient balance in tropical and south subtropical short rotation plantations. In *Studies on Long-Term Productivity Management of Eucalyptus Plantation*; Yu, X.B., Ed.; China Forestry Publishing House: Beijing, China, 2000; pp. 27–35.
51. Diochon, A.C.; Kellman, L. Physical fractionation of soil organic matter: Destabilization of deep soil carbon following harvesting of a temperate coniferous forest. *J. Geophys. Res. Biogeosci.* **2009**, *114*, G01016. [CrossRef]
52. Selvaraj, S.; Duraisamy, V.; Huang, Z.J.; Guo, F.T.; Ma, X.Q. Influence of Long-Term Successive Rotations and Stand Age of Chinese Fir (*Cunninghamia lanceolata*) Plantations on Soil Properties. *Geoderma* **2017**, *306*, 127–134. [CrossRef]
53. Jennings, T.N.; Smith, J.E.; Cromack, K.; Sulzman, E.W.; McKay, D.; Caldwell, B.A.; Beldin, S.I. Impact of postfire logging on soil bacterial and fungal communities and soil biogeochemistry in a mixed-conifer forest in central Oregon. *Plant Soil* **2012**, *350*, 393–411. [CrossRef]
54. Yu, X.B.; Chen, Q.B.; Wang, S.M.; Mo, X.Y. Research on land degradation in forest plantation and preventive strategies. In *Studies on Long-Term Productivity Management of Eucalyptus Plantation*; Yu, X.B., Ed.; China Forestry Publishing House: Beijing, China, 2000; pp. 1–7.
55. Zhang, X.; Kirschbaum, M.U.F.; Hou, Z.; Guo, Z. Carbon stock changes in successive rotations of Chinese fir (*Cunninghamia lanceolata* (Lamb.) Hook.) plantations. *For. Ecol. Manag.* **2004**, *202*, 131–147. [CrossRef]
56. Kibblewhite, M.G.; Ritz, K.; Swift, M.J. Soil health in agricultural systems. *Philos. Trans. R. Soc. Lond. Ser. B* **2008**, *363*, 685–701. [CrossRef]
57. Brussaard, L. Ecosystem services provided by the soil biota. In *Soil Ecology and Ecosystem Services*; Wall, D.H., Bardgett, R.D., Behan-Pelletier, V., Herrick, J.E., Jones, H., Ritz, K., Six, J., Strong, D.R., van der Putten, W.H., Eds.; Oxford University Press: Oxford, UK, 2012; pp. 45–58.
58. Zinn, Y.L.; Resck, D.V.; da Silva, J.E. Soil organic carbon as affected by afforestation with Eucalyptus and Pinus in the Cerrado region of Brazil. *For. Ecol. Manag.* **2002**, *166*, 285–294. [CrossRef]
59. Nave, L.E.; Vance, E.D.; Swanston, C.W.; Curtis, P.S. Harvest impacts on soil carbon storage in temperate forests. *For. Ecol. Manag.* **2010**, *259*, 857–866. [CrossRef]
60. Achat, D.L.; Deleuze, C.; Landmann, G.; Pousse, N.; Ranger, J.; Augusto, L. Quantifying consequences of removing harvesting residues on forest soils and tree growth—A meta-analysis. *For. Ecol. Manag.* **2015**, *348*, 124–141. [CrossRef]
61. Thiffault, E.; Hannam, K.D.; Pare, D.; Titus, B.D.; Hazlett, P.W.; Maynard, D.G.; Brais, S. Effects of forest biomass harvesting on soil productivity in boreal and temperate forests—A review. *Environ. Rev.* **2011**, *19*, 278–309. [CrossRef]
62. Cambi, M.; Grigolato, S.; Neri, F.; Picchio, R.; Marchi, E. Effects of forwarder operation on soil physical characteristics: A case study in the Italian alps. *Croat. J. For. Eng.* **2016**, *37*, 233–239.

forests

MDPI

Article

Conversion of Natural Evergreen Broadleaved Forests Decreases Soil Organic Carbon but Increases the Relative Contribution of Microbial Residue in Subtropical China

Liuming Yang [1,2], Silu Chen [1,2], Yan Li [1,2], Quancheng Wang [1,2], Xiaojian Zhong [1,2], Zhijie Yang [1,2], Chengfang Lin [1,2,*] and Yusheng Yang [1,2]

1 School of Geographical Science, Fujian Normal University, Fuzhou 350007, China; yanglm2007@aliyun.com (L.Y.); pgydesj@163.com (S.C.); 15705956185@163.com (Y.L.); wangquancheng0304@126.com (Q.W.); xj.zhong@fjnu.edu.cn (X.Z.); zhijieyang@fjnu.edu.cn (Z.Y.); geoyys@fjnu.edu.cn (Y.Y.)

2 Key Laboratory for Subtropical Mountain Ecology, School of Geographical Sciences, Fujian Normal University, Fuzhou 350007, China

* Correspondence: tonylcf99@fjnu.edu.cn; Tel.: +86-0591-83483731; Fax: +86-0591-83465379

Received: 27 April 2019; Accepted: 28 May 2019; Published: 29 May 2019

Abstract: It has been recognized that land use change affects soil organic carbon (SOC) dynamics and the associated microbial turnover. However, the contribution of microbial residue to SOC storage remains largely unknown in land use change processes. To this end, we adopted a "space for time" approach to examine the dynamics of SOC and amino sugars, which was a biomarker of microbial residue C, in different natural forest conversions. Three typical converted forests were selected: an assisted natural regeneration (ANR) and two coniferous plantations of *Cunninghamia lanceolata* (Lamb.) Hook (Chinese fir) and *Pinus massoniana* Lamb. (pine) each. All of these were developed at the same time after the harvest of an old natural forest and they were used to evaluate the effects of forest conversions with contrasting anthropogenic disturbance on SOC and microbial residue C, along with the natural forest. Natural forest conversion led to an approximately 42% decrease in SOC for ANR with low anthropogenic disturbance, 60% for the Chinese fir plantation, and 64% for the pine plantation. In contrast, the natural forest conversion led to a 32% decrease in the total amino sugars (TAS) for ANR, 43% for the Chinese fir plantation, and 54% for the pine plantation at a soil depth of 0–10 cm. The ratios of TAS to SOC were significantly increased following natural forest conversion, with the highest ratio being observed in the Chinese fir plantation, whereas the ratios of glucosamine to muramic acid (GluN/MurA) were significantly decreased in the two plantations, but not in ANR. The contents of SOC, individual amino sugar, or TAS, and GluN/MurA ratios were consistently higher at a soil depth of 0–10 cm than at 10–20 cm for all of the experimental forests. Redundancy analysis showed that microbial residue C was significantly correlated with SOC, and both were positively correlated with fine root biomass, annual litterfall, and soil available phosphorus. Taken together, our findings demonstrated that microbial residue C accumulation varied with SOC and litter input, and played a more important role in SOC storage following forest conversion to plantations with higher anthropogenic disturbance.

Keywords: soil organic carbon; soil microbial residue; forest conversion; natural forest; assisted natural regeneration; plantation

1. Introduction

The decomposition, transformation, and stabilization of soil organic carbon (SOC) are the consequence of microbial growth and activity, which is a process that is associated with proliferation, metabolism, and mortality of microorganisms. More and more attention has been paid to microbial residue in recent studies, which demonstrated that senesced microbial biomass may play a much greater role in the stabilization of soil C pools than that previously considered [1–4]. It is critical to elucidate the response of soil microbial residue to global change, as well as the underlying mechanisms driving its transformation, to better understand global biogeochemical cycles and improve current global C cycle models [5,6]. There are a number of studies exploring the effects of global change on soil microbial residue. For example, Zhang et al. reported land use effects on amino sugars in soil particle size fractions [7]. Liang and Balser observed that warming and N deposition reduced microbial residue contribution to the soil C pool [8]. To the best of our knowledge, studies investigating the effects of forest conversion on microbial residue contribution to soil C sequestration are lacking.

Space for time substitution is still used as a reasonable method to evaluate the legacy of forest conversion on ecosystem properties. In general, the reestablished forests, such as plantation forests, are taken as experimental units and adjacent native forest as a reference. The forest conversions are usually subjected to different management coupled with anthropogenic disturbances of various intensity, which alter the structure of the forest ecosystem [9–11]. Consequently, changes in forest structure and management practices likely lead to the alteration, not only of input rates and organic matter decomposability, but also of soil moisture and temperature regimes [12,13]. The adaptation of soil microbial abundance, community composition, and activity following these changes can shift the soil biogeochemical cycling processes regulated by microorganisms [14,15], eventually affecting the contribution of microbial residue C to the soil C pool [16].

It is difficult to establish the correlation between living microbial biomass and long-term SOC sequestration [17] or to directly measure C that is bound in microbial residues. Alternatively, amino sugars, which are important microbial residue biomarkers in soil [18,19], can represent the legacy of microbial-derived constituents and be used to estimate the contribution of dead microbial cells to soil organic C pools [20,21]. Glucosamine (GluN), muramic acid (MurA), galactosamine (GalN), and mannosamine (ManN) are the most important amino sugars in soils [22,23]. GluN is predominantly derived from the chitin of fungal cell walls and it is also found in bacterial peptidoglycan [18,24]. MurA is solely derived from bacterial cell walls [19,24]. GalN is generally considered to originate from bacteria [19]. The concentration and ratios of the above amino sugars can be used to evaluate the microbial (bacterial versus fungal) contribution to soil C sequestration [18,20,23,25].

Subtropical forests provide an important contribution to global terrestrial ecosystem C storage [26,27]. In southern China, the majority of natural forests were cleared by the late 1970s and first converted into two coniferous plantations, Chinese fir (*Cunninghamia lanceolata* (Lamb.) Hook) and pine (*Pinus massoniana* Lamb.), to satisfy the high demand for timber, fuel, and other forest products due to rapid human population growth. The conversion not only has a profound effect on the ecosystem C budget [11,28,29], but it also leads to other ecological consequences, such as a loss in species diversity [30–33] and soil erosion [34]. As an alternative to conversion to plantations, forests with assisted natural regeneration (ANR) have been introduced to China for more than five decades [35,36], with the goal of protecting and nurturing mother trees and their seedlings that are inherently present in the area, rather than the establishment of entirely new forest plantations [37]. Our previous study showed that, when compared to monoculture plantations, ANR significantly increased the plant biomass and diversity, and more effectively promoted ecosystem services, including the mitigation of runoff and soil erosion, and the exportation of dissolved organic C [34]. However, the effects of forest conversions on these forest types with various intensities of anthropogenic disturbance to soil C dynamics, and, in particular, that of microbial residue, have rarely been assessed and compared.

In the present study, an ANR forest and two dominant plantations (Chinese fir and pine) with contrasting intensity of anthropogenic disturbance were selected to examine the effects of forest

conversions on the dynamics of soil microbial residues. All of the selected forests were developed from a natural forest clearing in subtropical China, with similar soil properties and forest age. Following the conversion of native forest to plantations or ANR forests, different litter inputs exhibited a remarkable influence on the response of bacterial and fungal groups [38], which possibly resulted in distinct microbial residue retention patterns and different microbial functions during SOC accumulation [39,40]. We hypothesize that (1) soil amino sugar concentrations are lower in all of the converted forests than the native forest, with the lowest concentration in one of the two plantations. Mature and undisturbed ecosystems have a higher ratio of K-strategists to r-strategists than did young and disturbed ecosystems, according to the theory of Odum on ecosystem succession and disturbance [41,42]. Furthermore, a recent meta-analysis showed that converted forests consistently shifted from fungal to bacterial dominance with increasing land degradation [43]. Thus, we hypothesize that (2) natural forest conversion leads to a decrease of fungal relative to the bacterial residue C ratios, and these ratios, in descending order, will be as follows: native forest > ANR > plantations. Previous studies showed that labile C fractions were sensitive indicators of SOC dynamics that resulted from forest conversion [44], whereas microbial residue C was incorporated into the recalcitrant C pool [6], which may not respond equally to environmental change, as does the total soil C. Therefore, we hypothesize that (3) forest conversions increase the ratios of TAS (total amino sugars) to total SOC, with highest ratio in one of the two plantations, because of the entirely new forest establishment, resulting in rapid loss of labile C fractions, whereas a lower ratio than the plantations will occur in the ANR forest.

2. Materials and Methods

2.1. Site Description

This study was conducted in the Chenda Observation Study Site (26°19′55′′ N, 117°36′53′′ E, 300 m a.s.l.) of Sanming Forest Ecosystem and Global Change Research Station in Fujian Province, China. This study site borders the Daiyun Mountains on the southeast and the Wuyi Mountains on the northwest. A typical maritime subtropical monsoon climate characterizes the study site. The mean annual temperature (MAT) is 19.1 °C with low temperatures occurring in January and high temperatures occurring in July. The mean annual relative humidity is 81% and the mean annual precipitation (MAP) is 1750 mm. Approximately 75% of the total precipitation occurs from March to August. The mean annual potential evapotranspiration is 1585 mm. The soil at the study site is formed from granite and is classified as red soil according to the China soil classification system and it is equivalent to Ultisol in the USDA Soil Taxonomy [45]. Soil texture in the natural forest is sandy with sand (2–0.05 mm), silt (0.05–0.002 mm), and clay (<0.002 mm), being 16.4%, 37.3%, and 46.3%, respectively, which does not significantly change after forest conversions. The soil depth exceeds 1.0 m.

The natural forest represents an old-growth, evergreen broadleaved *Castanopsis carlesii* (Hemsl.) forest in mid-subtropical China, which has been protected for more than 200 years, according to the record of local forest management department and it is characterized with high biodiversity, widespread old trees, snags, and downed wood. In addition to *Castanopsis carlesii*, the overstory contained other tree species, such as *Castanopsis kawakamii* Hayata, *Schima superba* Gardner & Champ., *Litsea subcoriacea* Y.C. Yang & P.H. Huang, and *Elaeocarpus decipiens* Hemsl. Two types of regeneration were adopted following the deforestation of the natural *Castanopsis carlesii* forests in 1975. One was natural regeneration, in which only the overstory was harvested and the understory and harvest residue remained. The other was to reestablish entirely new plantations following the forest being clear-cut, slashed, and burned. In 1976, the soil was prepared by digging holes. Afterwards, one-year-old seedlings of *C. lanceolata* or *P. massoniana* were planted at 3000 trees per hectare. The plantations were managed with similar practices, such as weeding and fertilization during the first three years and thinning twice between 10 and 15-years-old. The distances between the selected experimental forests fell within 1 km. Table 1 presents the general characteristics of the forests.

Table 1. Forest characteristics in a natural forest of *Castanopsis carlesii* (Hemsl.) (NF), assisted natural regeneration (ANR) and two plantation forests of *Cunninghamia lanceolata* (Lamb.) Hook (Chinese fir, CF) and *Pinus massoniana* Lamb. (PM).

Variable	NF	ANR	CF	PM
Altitude (m)	315	315	301	303
Slope (°)	35	28	30	35
Canopy coverage (%)	89	90	65	70
Mean tree height (m)	11.9	10.8	18.2	18.4
Mean tree diameter at breast height (cm)	20.0	14.3	15.6	16.3
Stand density (stem ha^{-1})	1955	3788	2858	1500

2.2. Soil Sampling, Litterfall, and Fine Root Biomass Measurements

Three replicate plots (20 m × 50 m) were set up for each forest type, and the distance between plots was kept at 20 m to assess the effects of forest conversion on microbial residue. Soil samples (0–10 cm and 10–20 soil layer) were collected in April 2017; 15 cores (5 cm in diameter) were randomly collected from each plot in a plastic bag as a composite sample. After removing the stones, pebbles, roots, and large pieces of plant residues, the soil was ground and sieved (<2 mm sieve), and then combined, homogenized, and divided into three subsamples. The first samples were kept at 4 °C for the determination of soil enzyme activity and microbial biomass. The second samples were kept at −20 °C and they were freeze-dried at −80 °C, and then ground to pass through a 0.149 mm sieve for the determination of amino sugar. The third soil samples were air dried for analysis of soil physical and chemical properties. Five rectangle litter traps (0.5 m × 1.0 m) with 1 mm nylon mesh were randomly arranged about 0.25 m above the soil surface in each plot. Litterfall was semimonthly collected from October 2010 to September 2016 using the method that was described by Yang et al. [46]. For the fine root sampling, 15 soil cores were randomly taken in each plot with a soil corer (5 cm in diameter) in April of 2017. The thick roots (>2 mm) were carefully removed from the soil samples with forceps and then the soils were wet-sieved with a mesh size of 0.5 mm. The sieved soils were put into a beaker with deionized water at a temperature of 1 °C and repeatedly stirred to float the fine root segments to water surface for collection [47]. The fine roots were placed into an oven at a temperature of 65 °C for 48 h and then weighed.

2.3. Soil Analysis

Soil pH was measured with a soil:water ratio of 1:2.5. SOC and total N were determined while using a CN auto analyzer (Elementar Vario MAX, Germany). For nitrate and ammonium analyses, 5 g of fresh soil from each sample was extracted using a 2 mol/L KCl solution. The solutions were shaken for 40 min. and then filtered for nitrate and ammonium determination while using a continuous flow analyzer (SKALAR San++, Breda, The Netherlands). The soil cation exchange capacity (CEC) was assessed by the ammonium acetate extraction method at pH 7. The soil available phosphorus (P) was detected while using the ion exchange resin method that Sibbesen developed [48].

2.4. Determination of Soil Amino Sugars

Amino sugar content in soils was detected while using the method of Zhang and Amelung [22]. Briefly, the finely ground soil samples (containing approximately 0.3 mg N) were hydrolyzed with 10 mL 6 M HCl at 105 °C for 8 h, and 0.1 mL myo-inositol (internal standard) was added to the hydrolysate solution, which was filtered through a glass fiber membrane filter (0.45 diameter), dried using a rotary evaporator, re-dissolved with deionized water, and then transferred into a 50 mL Teflon tube. The pH of the sample solutions was adjusted to 6.6–6.8 with 1 M KOH and 0.01 M HCl and the samples were then centrifuged. After the solution was freeze-dried, 5 mL methanol was added to dissolve the residues, after which the methanol solution was transferred to a vial and dried with N_2 at

45 °C. Finally, 1 mL deionized water and 0.1 mL recovery standard (*N*-methylglucamine) were added to the residues and freeze-dried.

The freeze-dried residues were dissolved with 0.3 mL derivatization reagent containing 32 mg mL^{-1} hydroxylamine hydrochloride and 40 mg mL^{-1} 4-dimethylamino-pyridine in pyridine-methanol (4:1 *v/v*) were heated at 78 °C for 35 min. in a water bath. After cooling, 1 mL acetic anhydride was added and then reheated to 78 °C for 25 min. Next, 1.5 mL dichloromethane and 1 mL 1 M HCl were added to achieve liquid–liquid separation. After water phase removal, the organic phase was washed three times with 1 mL deionized water. The remaining organic phase was dried by N_2 gas at 45 °C. Finally, 0.2 mL ethyl acetate-hexane (1:1) was added to dissolve the derivative for final analysis. The amino sugar derivatives were separated using an Agilent 6890A gas chromatography (GC, Agilent Tech. Co. Ltd., USA) that was equipped with DB-1 fused silica column (25 m × 0.32 mm × 0.25 mm) with a flame ionization detector. The concentrations of individual amino sugars were quantified based on the internal standard myo-inositol.

2.5. Statistics

Each forest was considered as an experimental unit, and the data were averaged across the three plots from each forest. Due to using pseudo-replication in this study, all of the standard errors were pseudo-replication errors as were mean comparisons. Results must be carefully interpreted and only trends in the data by forest type can be discussed, with an appreciation of the problems of pseudo-replication.

Before analysis, all the variables were checked for normal distribution (Kolmogorov–Smirnov test) and homogeneity (Levene test). One-way ANOVA with Tukey's HSD test was performed to test for differences of litter mass, fine root biomass, soil physicochemical properties, and soil amino sugars among forests. Statistical significance was established at the 5% level, unless otherwise mentioned. Redundancy analysis (RDA) was applied to elucidate the relationships among total amino sugar (TAS), GluN, GalN, MurA, GluN/MurA, GluN/GalN, the proportion of total amino sugar to total C, and the corresponding soil environmental variables (total litterfall, fine root biomass, pH, soil organic C, total N, total P, soil texture) among different forest types. SPSS 18.0 (SPSS, Inc., Chicago, IL, USA) was used for all statistical analyses, except for RDA, which was performed while using CANOCO software for Windows 4.5 (Ithaca, NY, USA). Forward selection was based on Monte Carlo permutation ($n = 999$). Before RDA, we conducted forward selection of the environmental variables that were significantly correlated with variations of amino sugars while using the Monte Carlo permutation test ($p < 0.05$).

3. Results

3.1. Soil Properties

The SOC content was high in the natural forest (51.8 ± 3.0 mg g^{-1}). Following conversion of the natural forest, there was an approximately 42% reduction in SOC for the ANR forest (30.0 ± 2.7 mg g^{-1}), 60% for the Chinese fir plantation (20.9 ± 1.3 mg g^{-1}), and 64% for the pine plantation (18.6 ± 0.9 mg g^{-1}) at 0–10 cm soil layer, with over 50% reductions at the 10–20 cm soil layer for all the converted forests. Similarly, the soil N content was 2.75 ± 0.10 mg g^{-1} at 0–10 cm soil layer in the natural forest, and there was an approximately 30% reduction in the ANR (1.91 ± 0.12 mg g^{-1}) and an approximately 50% decrease in the two plantations (1.13 ± 0.09 and 1.29 ± 0.07 mg g^{-1} for the Chinese fir and pine plantations, respectively) after forest conversions, as well as more than a 50% decrease at the 10–20 cm soil layer for all of the converted forests (Table 2). Soil pH was increased for all of the converted forests (Table 2).

Table 2. Soil properties under four different forest types.

Soil Property	0–10 cm Layer				10–20 cm Layer			
	NF	ANR	PM	CF	NF	ANR	PM	CF
SOC (mg g^{-1})	51.8 ± 3.0 A	30.0 ± 2.7 B	18.6 ± 0.9 C	20.9 ± 1.3 bC	27.0 ± 1.4 a	12.7 ± 0.1 b	10.7 ± 0.5 b	11.7 ± 0.7 b
TN (mg g^{-1})	2.75 ± 0.10 A	1.91 ± 0.12 B	1.13 ± 0.09 C	1.29 ± 0.07 C	1.47 ± 0.03 a	1.06 ± 0.03 b	0.75 ± 0.01 c	0.86 ± 0.05 bc
C/N	18.8 ± 0.6 A	15.6 ± 0.4 B	16.5 ± 1.1 BC	16.2 ± 0.2 C	18.3 ± 0.8 a	12.0 ± 0.3 b	14.3 ± 0.4 b	13.7 ± 0.2 b
CEC (cmol kg^{-1})	15.8 ± 1.7 A	7.1 ± 1.2 B	6.7 ± 0.6 B	6.5 ± 0.5 B	9.8 ± 0.4 a	5.5 ± 0.2 b	5.7 ± 0.3 b	6.0 ± 0.2 b
pH	4.08 ± 0.07 B	4.44 ± 0.09 A	4.47 ± 0.03 A	4.52 ± 0.06 A	4.10 ± 0.03 a	4.28 ± 0.04 ab	4.39 ± 0.02 b	4.35 ± 0.02 b
NH_4^+ (mg kg^{-1})	27.3 ± 0.8 A	26.5 ± 4.7 A	11.6 ± 0.9 B	12.8 ± 1.0 B	12.2 ± 0.2 a	9.6 ± 0.8 b	6.4 ± 0.1 b	6.8 ± 0.2 b
NO_3^- (mg kg^{-1})	0.86 ± 0.09 BC	1.98 ± 0.33 A	0.26 ± 0.03 C	1.38 ± 0.18 AB	1.19 ± 0.04 a	1.14 ± 0.06 a	0.32 ± 0.03 c	0.73 ± 0.05 b
Sand (2–0.05 mm, %)	16.4 ± 2.7 A	15.2 ± 3.1 A	11.1 ± 0.3 A	12.3 ± 0.2 A	16.3 ± 1.1 a	17.5 ± 3.0 a	13.3 ± 0.5 b	16.6 ± 0.5 a
Silt (0.05–0.002 mm, %)	37.3 ± 1.9 A	34.9 ± 1.9 A	39.0 ± 1.6 A	37.5 ± 1.2 A	40.6 ± 1.8 a	36.6 ± 1.8 a	40.8 ± 1.2 a	41.1 ± 0.2 a
Clay (<0.002 mm, %)	46.3 ± 3.3 A	50.0 ± 1.9 A	50.0 ± 1.9 A	50.3 ± 1.4 A	43.1 ± 2.8 a	45.8 ± 1.7 a	45.8 ± 1.7 a	42.4 ± 0.6 a
Available P (mg kg^{-1})	5.47 ± 0.45 A	6.55 ± 0.56 A	2.57 ± 0.52 B	3.46 ± 0.35 B	1.10 ± 0.14 b	1.96 ± 0.20 a	1.17 ± 0.10 b	1.22 ± 0.06 b

The effects were significant at $p < 0.05$; different uppercase letters indicate significant differences at 0–10 cm among different forests, and different lowercase letters indicate significant differences at 10–20 cm among different forests. Values are means ± standard errors ($n = 3$). ANR: Assisted natural regeneration; CEC: cation exchange capacity; CF: Chinese fir forest; NF: Natural forest; PM: *Pinus massoniana* Lamb. forest; SOC: Soil organic carbon; TN: Total nitrogen.

The average annual litterfall from 2011 to 2016 was found to be the highest in the natural forest (8.04 Mg hm^{-2}), followed by the ANR forest (6.15 Mg hm^{-2}), pine plantation (5.03 Mg hm^{-2}), and Chinese fir (4.63 Mg hm^{-2}) plantation. The conversion of the natural forest led to a significant decrease in annual leaf litterfall in the pine and Chinese fir plantations, but not in the ANR, with the lowest annual litterfall observed in the Chinese fir plantation. Similarly, the conversion of the natural forest led to a significant decrease in fine root biomass at the 0–10 cm soil layer in all the converted forests, with the lowest biomass being observed in the pine plantation (Figure 1).

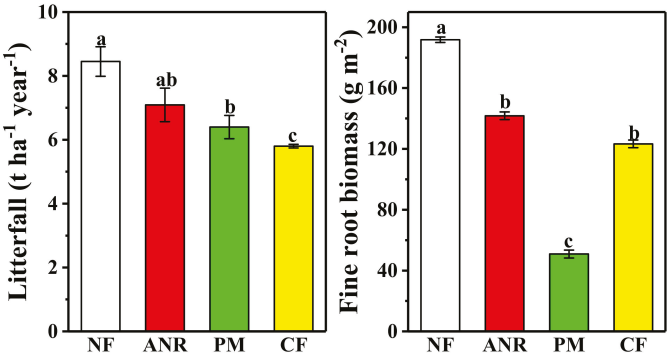

Figure 1. Litterfall and fine root biomass (0–10 cm) under different forest types; different lowercase letters indicate significant differences among the different forests. Values are means ± standard errors (n = 3), Natural forest: NF; Natural regeneration forest: ANR; *Pinus massoniana* Lamb. forest: PM; Chinese fir forest: CF.

3.2. Concentrations of Amino Sugars in the Different Forests

Conversions of natural forest to either ANR forest or plantations led to significant decreases in the concentrations of GluN, MurA, and TAS at the 0–10 cm soil layers, whereas, for GalN, significant decreases were only observed in the pine plantation. The concentration of TAS was high in the natural forest (1850 mg kg^{-1}), which was reduced by 32% in the ANR forest (1250 mg kg^{-1}), by 43% in the Chinese fir plantation (1050 mg kg^{-1}), and by 54% in the pine plantation (850 mg kg^{-1}). All of the individual amino sugar and total amino sugar concentrations were significantly higher at the 0–10 cm than at the 10–20 cm soil layer for all forest types (Figure 2).

In the converted forests, there were significantly higher concentrations of GluN and TAS at the 0–10 cm soil layer in the ANR forest than in the pine plantation, but there were no significant differences in the concentrations of individual amino sugars or TAS at the 10–20 cm soil layers (Figure 2).

3.3. Amino Sugar Biomarker Ratios

Following the conversions of the natural forest, there was an approximately 20% decrease in the GluN/MurA ratios for the two plantations at the 0–10 cm soil layer, but there was no significant decrease at the 10–20 cm soil layer for all the converted forests (Figure 3).

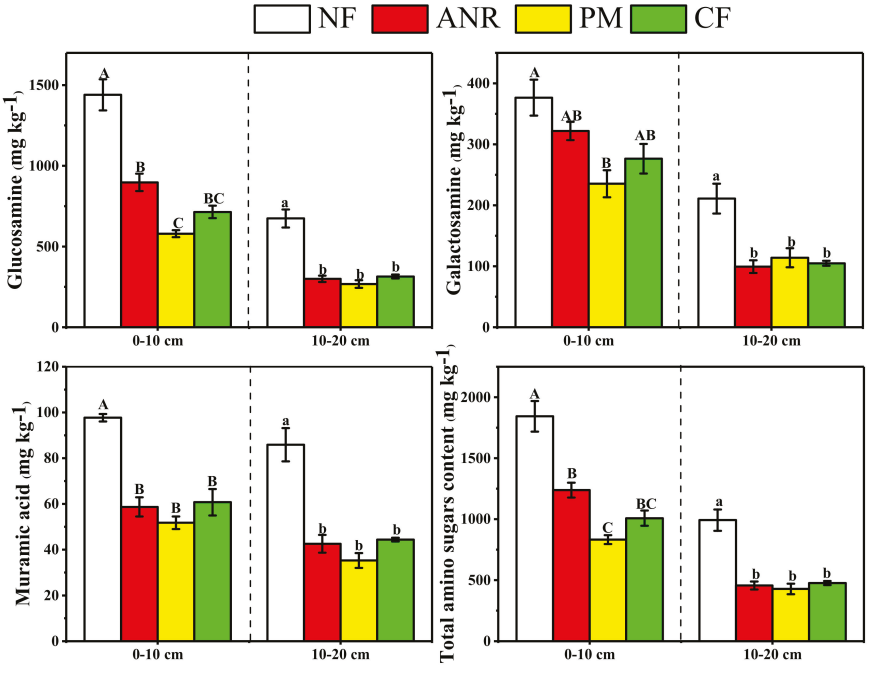

Figure 2. The concentration of soil amino sugars at different soil layers in different forest types; different uppercase letters indicate significant differences at 0–10 cm among the different forests, and different lowercase letters indicate significant differences at 10–20 cm among the different forests. Values are means ± standard errors (n = 3), Natural forest: NF; Natural regeneration forest: ANR; *P. massoniana* forest: PM; Chinese fir forest: CF.

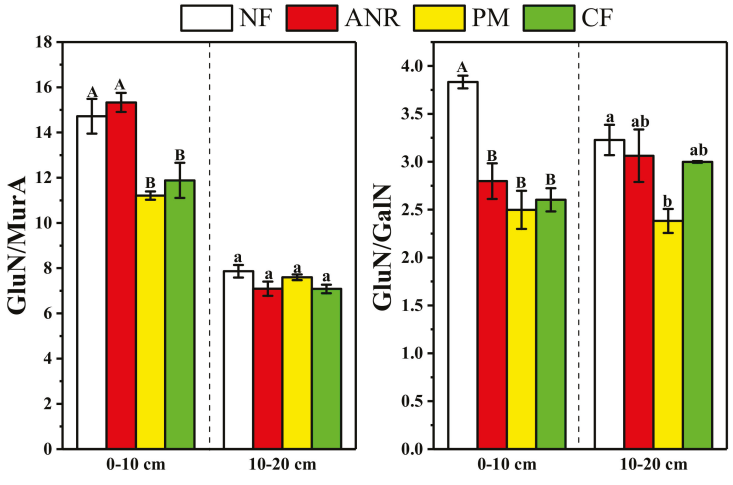

Figure 3. Ratios of glucosamine (GluN) to muramic acid (MurA) or to galactosamine (GalN) at different soil layers in different forest types; different uppercase letters indicate significant differences at 0–10 cm among the different forests, and different lowercase letters indicate significant differences at 10–20 cm among the different forests. Values are means ± standard errors (n = 3), Natural forest: NF; Natural regeneration forest: ANR; *P. massoniana* forest: PM; Chinese fir forest: CF.

Conversions of the natural forest led to significant decreases in the GluN/GalN ratios for all of the converted forest types at the 0–10 cm soil layer. At the 10–20 cm soil layer, the natural forest conversion to pine plantation led to a significant decrease in the GluN/GalN ratio (Figure 3).

3.4. Ratios of TAS to SOC in the Different Forest Type

Conversions of the natural forest led to a significant increase in the ratios of TAS to SOC at the 0–10 cm soil layer, but there was no significant difference among the converted forests. No differences were observed in the ratios of TAS to SOC following conversions of the natural forest at the 10–20 cm soil layer, but there was a significantly higher ratio of TAS to SOC in the pine plantation than in the ANR (Figure 4).

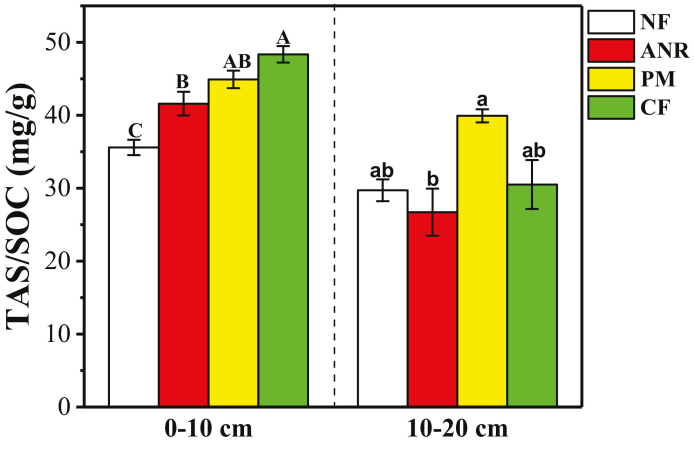

Figure 4. The proportion of total amino sugars to total soil organic carbon (TAS/SOC) in two soil layers under different forest types; different uppercase letters indicate significant differences at 0–10 cm among the different forests, and different lowercase letters indicate significant differences at 10–20 cm among the different forests. Values are means ± standard errors (n = 3), Natural forest: NF; Natural regeneration forest: ANR; *P. massoniana* forest: PM; Chinese fir forest: CF.

3.5. Correlation between Amino Sugars and Soil Properties

Redundancy analysis indicated that the environmental factors explained 87.9% of the variance of soil amino sugars across four different forests, with axis 1 explaining 83.1% and axis 2 explaining 4.8% of the variance (Figure 5). The ordination biplot from RDA was clearly distinguished among the four forests. Forward selection of factors in the RDA ordinations revealed that variations in soil amino sugars were closely related to SOC, fine root biomass, litter fall, and available P.

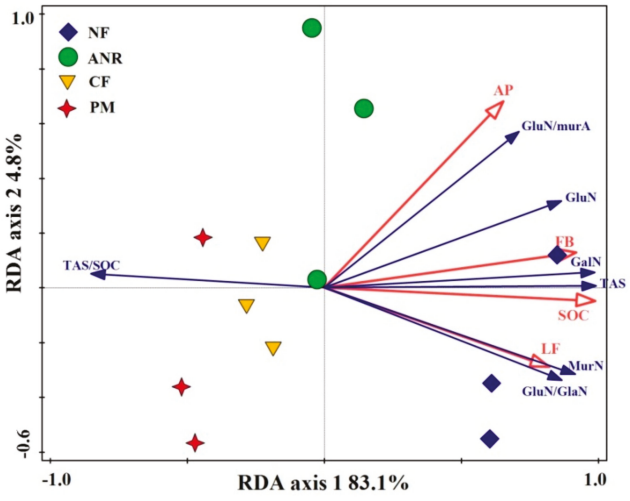

Figure 5. Correlations of soil amino sugar data to soil environmental factors determined by redundancy analysis (RDA). The amino sugar data included glucosamine (GluN), galactosamine (GalN), muramic acid (MurA), total amino sugar (TAS), ratios of glucosamine (GluN) to muramic acid, and proportion of total amimo sugar to SOC (TAS/SOC). AP, available P; SOC, soil organic carbon, FB, fine root biomass, LF, litterfall, Natural forest: NF; Natural regeneration forest: ANR; *P. massoniana* forest: PM; Chinese fir forest: CF.

4. Discussion

4.1. Effects of Natural Forest Conversion on Concentrations of Soil Total C and Amino Sugars

Although a considerable disagreement remains regarding the effects of land-use change on soil C stocks [49], it is generally considered that the preservation of natural old-growth forests may be related to a much higher C sequestration than that by the promotion of forest regrowth in long-term C pools, in particular, in recalcitrant soil organic matter [50–52]. Our previous studies in the subtropics also showed a much higher soil C concentration in the older natural forest than in the secondary forests or plantations [44,53]. Consistent with this finding, in the present study, conversions of old natural forest result in over 40% decreases in soil C concentration in all of the converted forests (Table 1). Replacing old-growth forest by young stands will lead to massive soil C losses to the atmosphere, mainly by reducing the flux into a permanent pool of soil organic matter and by redistributing C between pools with different turnover times because of the disturbance effects of various intensities [54]. The converted forests had experienced several forest management disturbances before our experiment, and the present study showed that natural forest conversion has a profound effect on soil C stocks in the subtropical forest, which cannot be recovered to a pre-harvest level, even after over 40 years of forest regrowth.

We anticipate that forest conversion may affect not only the SOC dynamics, but also the variation of microbial residues, because microbial C residues are regarded as a significant contributor to SOC, owing to their relatively long residence time in soils [19,55–58]. As in hypothesis (1), we observed a generally significant reduction in the concentration of microbial residues, including GluN, GalN, MurA, and TAS, in the converted forests, with the lowest decrease of TAS being observed in the ANR forest and the highest decrease in the pine plantation (Figure 1). These results are consistent with the results of previous studies, which also show that land use and management substantially affected amino sugar concentrations [2,59,60]. High temperature and rainfall, steep slopes, and fragile soil characterize South China. Following natural forest conversion, increases in soil temperature and

erosion due to less forest cover in the initial forest regrowth generally led to accelerated SOC loss in the subtropics [44,61]. In particular, increased and intensive anthropogenic disturbance, such as slash burning and site preparation, contributed to higher SOC reduction in forest plantations [61]. Likewise, these aforementioned factors may also affect microbial residue accumulation in the different forest types, which the redundancy analysis that showed soil amino sugar concentrations were closely correlated with SOC and soil available P was confirmed (Figure 5). Most tropical and subtropical forests occur in highly weathered soil, where the available P is low [62,63]. The soil P availability could influence the activities, biomass, and compositions of soil microbial communities [64–66], which may also explain the amino sugar dynamics during the forest conversions.

Further, Liang et al. reported there was a tree species-specific effect on soil microbial residue accumulation in an old-growth forest ecosystem, with recalcitrant Eastern Hemlock litter making a relatively lower contribution of microbial residue to the total soil C [67]. When compared with the plantations, the ANR forest mostly consisted of broad leaf tree species, which, when compared to coniferous litter, could be conducive to microbial residue retention by increasing soil amino sugars [68]. Correlation analysis showed that soil amino sugar concentrations were positively correlated with fine root biomass and annual leaf litterfall (Figure 5). These factors could again explain the higher GluN, GalN, and TAS in the ANR forest than in the pine plantations (Figure 1). Unexpectedly, the absence of significant differences in all amino sugars was observed between the ANR forest and the Chinese fir plantation in the present study. This could result from the high fine root biomass in the Chinese fir plantations, mainly owing to a higher abundance of herbs and shrubs than those in other two converted forests [69]. The herbs and shrubs are ephemeral, which could lead to high input of fine root litter and eventually contribute to amino sugar accumulation.

The higher concentration of SOC in surface soil than in deeper soil may support more abundant microorganisms [70,71]. Thus, larger amounts of microbial residue accumulated at the 0–10 cm than at 10–20 cm soil depth in each forest that was observed in this study (Table 1). This was consistent with the results of previous studies [68,72,73].

4.2. Amino Sugar Biomarker Ratios

Ratios of GluN/MurA and GluN/GalN are normally used to indicate the contribution of fungal versus bacterial residues to SOC accumulation [20,23,25,57]. Land use change may affect the formation of microbial residues [7]. In this study, forest conversions resulted in dramatic declines in all of the examined amino sugars, including GluN, GalN, and MurA, but at different rates (Figure 1). The decrease of GluN/MurA ratios in the two plantations indicated a slower recovery of fungal communities relative to bacteria following natural forest conversion, which is in agreement with Hedlund et al., who argued that fungi, in particular, mycorrhizal fungi, may have less efficient dispersal and colonizing abilities after vegetation removal [74]. Among the converted forests, although there was no difference in TAS, different GluN/MurA ratios (Figure 2) may reflect the effect of land use intensification on amino sugar partition. Our finding of higher GluN/MurA ratios in the ANR forest indicated that slight anthropogenic disturbance is conducive to the accumulation of fungal derived microbial residue, which is in agreement with our hypothesis (2).

When compared to the 0–10 cm soil depth, at 10–20 cm, there was an approximately 40% decrease in GluN to MurA ratios (Figure 2). The reduction in fungal biomass and residues in subsoil might be related to the accumulation of less decomposed plant residues with an increasing depth. Moritz et al. [75] and Liang and Balser [17] observed similar decreases in the GluN to MurA ratio with depth. These decreases indicated that bacteria are more important in subsoil organic C turnover than are fungi. Fungi are aerobic organisms that typically utilize fresh litter as their preferred C source and generally successfully outcompete bacteria in the surface soils, particularly under acidic conditions [76]. With increasing depth, studies have typically shown a decrease in the relative abundance of fungi [70,75,77].

The absence of a difference in GluN/GalN rather than GluN/MurA ratios between the two soil depths was observed in this study (Figure 3), which is consistent with the result of Liang et al. [66] and

Moritz et al. [75]. Liang et al. argued that GluN/MurA and GluN/GalN indicated different aspects of the relative fungal to bacterial contribution or the relative retention times of various amino sugars in soil C dynamics [67].

4.3. Contribution of TAS to SOC in the Different Forest Types

Microbial residues are important constituents of SOC and they do not always change in the same pattern, as does the SOC dynamics [68]. Our previous studies showed a more pronounced loss of labile C than total SOC following the conversion of natural forest into plantations or secondary forests [44]. The present study shows a significant increase in the ratios of TAS to total SOC at the 0–10 cm soil depth in the converted forest, whereas no significant difference between the natural forest and converted forests occurred for the 10–20 cm soil depth (Figure 3). These results indicate the slower loss of microbial residue C than other soil C fractions following forest conversions, which suggests that microbial residue, as a refractory C, plays an important role in SOC storage, particularly in the surface 0–10 cm soil. Furthermore, lower increases of the TAS to total SOC ratio in the ANR forest than those in the two plantations may reflect that microbial residue is of greater importance in soil storage with the intensity of anthropogenic disturbance. Our findings support hypothesis (3), that forest conversions increase the ratios of microbial residue C to total C, with the highest increase in the two plantations.

We compared the effects of forest conversions that are based on the experiment of three replicate plots in each stand, which is not truly replicated. Therefore, our results should be cautiously interpreted because of an intrinsic error of pseudo-replication [78]. Furthermore, we should be critical of the scope of possible interpretation due to inevitable temporal and spatial heterogeneity derived from space for time substitution. It deserves special notice that all mean comparisons were expected to be a best-case scenario, because the error terms should be larger and mean separations should have a wider difference to allow for a true separation.

5. Conclusions

In the subtropics, natural forest conversions result in dramatic reductions, not only in SOC, but also in microbial residue C, which cannot be recovered, even after more than 40 years of forest regrowth. Microbial residue C accumulation varies with SOC and litter input constrained by forest management with various anthropogenic disturbances. As a recalcitrant C, microbial residue plays an important role in soil C storage following forest conversions. When comparing with tree plantations, natural forest conversion to the ANR forest had a significant effect in maintaining SOC, but not necessarily a significant effect on microbial residue accumulation.

Author Contributions: L.Y., C.L., X.Z. and Y.Y. designed the experiments; S.C., Y.L., Q.W. and L.Y. performed the experiments; C.L., L.Y., Y.Y. and Z.Y. analyzed the data, wrote and revised the paper.

Funding: The research was financially supported by the National Natural Science Foundation of China (No. 31770663, 31300523, 31130013, 31600433, and 31700545).

Acknowledgments: We are grateful to the two anonymous reviewers, whose comments help greatly improve this manuscript. Thanks also go to Jim Nelson for providing valuable comments and doing proofreading on the manuscript.

Conflicts of Interest: The authors declare no conflict of interest.

References

1. Liang, C.; Schimel, J.P.; Jastrow, J.D. The importance of anabolism in microbial control over soil carbon storage. *Nat. Microbiol.* **2017**, *2*, 17105. [CrossRef] [PubMed]
2. Ma, T.; Zhu, S.; Wang, Z.; Chen, D.; Dai, G.; Feng, B.; Su, X.; Hu, H.; Li, K.; Han, W.; et al. Divergent accumulation of microbial necromass and plant lignin components in grassland soils. *Nat. Commun.* **2018**, *9*, 3480. [CrossRef] [PubMed]
3. Liang, C.; Cheng, G.; Wixon, D.L.; Balser, T.C. An Absorbing Markov Chain approach to understanding the microbial role in soil carbon stabilization. *Biogeochemistry* **2011**, *106*, 303–309. [CrossRef]

4. Schimel, J.P.; Schaeffer, S.M. Microbial control over carbon cycling in soil. *Front. Microbiol.* **2012**, *3*, 1–11. [CrossRef]
5. Benner, R. Biosequestration of carbon by heterotrophic microorganisms. *Nat. Rev. Microbiol.* **2011**, *9*, 75. [CrossRef] [PubMed]
6. Liang, C.; Balser, T.C. Microbial production of recalcitrant organic matter in global soils: Implications for productivity and climate policy. *Nat. Rev. Microbiol.* **2011**, *9*, 75. [CrossRef]
7. Zhang, X.; Amelung, W.; Yuan, Y.; Samson-Liebig, S.; Brown, L.; Zech, W. Land-use effects on amino sugars in particle size fractions of an Argiudoll. *Appl. Soil Ecol.* **1999**, *11*, 271–275. [CrossRef]
8. Liang, C.; Balser, T.C. Warming and nitrogen deposition lessen microbial residue contribution to soil carbon pool. *Nat. Commun.* **2012**, *3*, 1222. [CrossRef]
9. Raich, J.W. Effects of Forest Conversion on the Carbon Budget of a Tropical Soil. *Biotropica* **1983**, *15*, 177–184.
10. Piquer-Rodríguez, M.; Torella, S.; Gavier-Pizarro, G.; Volante, J.; Somma, D.; Ginzburg, R.; Kuemmerle, T. Effects of past and future land conversions on forest connectivity in the Argentine Chaco. *Landsc. Ecol.* **2015**, *30*, 817–833.
11. Jandl, R.; Lindner, M.; Vesterdal, L.; Bauwens, B.; Baritz, R.; Hagedorn, F.; Johnson, D.W.; Minkkinen, K.; Byrne, K.A. How strongly can forest management influence soil carbon sequestration? *Geoderma* **2007**, *137*, 253–268. [CrossRef]
12. Post, W.M.; Kwon, K.C. Soil carbon sequestration and land-use change: processes and potential. *Chang. Boil.* **2000**, *6*, 317–327. [CrossRef]
13. Lal, R. Forest soils and carbon sequestration. *For. Ecol. Manag.* **2005**, *220*, 242–258. [CrossRef]
14. Schimel, J.; Balser, T.C.; Wallenstein, M. Microbial stress-response physiology and its implications for ecosystem function. *Ecology* **2007**, *88*, 1386–1394. [CrossRef] [PubMed]
15. Schimel, J. Microbial ecology: Linking omics to biogeochemistry. *Nat. Microbiol.* **2016**, *1*, 15028. [CrossRef] [PubMed]
16. Shao, P.; Liang, C.; Lynch, L.; Xie, H.; Bao, X. Reforestation accelerates soil organic carbon accumulation: Evidence from microbial biomarkers. *Soil Boil. Biochem.* **2019**, *131*, 182–190. [CrossRef]
17. Liang, C.; Balser, T.C. Preferential sequestration of microbial carbon in subsoils of a glacial-landscape toposequence, Dane County, WI, USA. *Geoderma* **2008**, *148*, 113–119. [CrossRef]
18. Joergensen, R.G. Amino sugars as specific indices for fungal and bacterial residues in soil. *Boil. Fertil. Soils* **2018**, *54*, 559–568. [CrossRef]
19. Amelung, W.; Miltner, A.; Zhang, X.; Zech, W. Fate of microbial residues during litter decomposition as affected by minerals. *Soil Sci.* **2001**, *166*, 598–606. [CrossRef]
20. Joergensen, R.G.; Wichern, F. Quantitative assessment of the fungal contribution to microbial tissue in soil. *Soil Boil. Biochem.* **2008**, *40*, 2977–2991. [CrossRef]
21. Reay, M.K.; Knowles, T.D.J.; Jones, D.L.; Evershed, R.P. Development of Alditol Acetate Derivatives for the Determination of 15N-Enriched Amino Sugars by Gas Chromatography–Combustion–Isotope Ratio Mass Spectrometry. *Anal. Chem.* **2019**, *91*, 3397–3404. [CrossRef]
22. Zhang, X.; Amelung, W. Gas chromatographic determination of muramic acid, glucosamine, mannosamine, and galactosamine in soils. *Soil Boil. Biochem.* **1996**, *28*, 1201–1206. [CrossRef]
23. Amelung, W.; Brodowski, S.; Sandhage-Hofmann, A.; Bol, R. Combining Biomarker with Stable Isotope Analyses for Assessing the Transformation and Turnover of Soil Organic Matter. *Adv. Agron.* **2008**, *100*, 155–250.
24. Parsons, J.W. Chemistry and Distribution of Amino Sugars in Soils and Soil Organisms. *Soil Biochem.* **1981**, *5*, 197–227.
25. Guggenberger, G.; Frey, S.D.; Six, J.; Paustian, K.; Elliott, E.T. Bacterial and Fungal Cell-Wall Residues in Conventional and No-Tillage Agroecosystems. *Soil Sci. Soc. J.* **1999**, *63*, 1188–1198. [CrossRef]
26. Pan, Y.; Birdsey, R.A.; Fang, J.; Houghton, R.; Kauppi, P.E.; Kurz, W.A.; Phillips, O.L.; Shvidenko, A.; Lewis, S.L.; Canadell, J.G.; et al. A Large and Persistent Carbon Sink in the World's Forests. *Science* **2011**, *333*, 988–993. [CrossRef] [PubMed]
27. Wang, Y.; Wang, H.; Xu, M.; Ma, Z.; Wang, Z.-L. Soil organic carbon stocks and CO_2 effluxes of native and exotic pine plantations in subtropical China. *CATENA* **2015**, *128*, 167–173. [CrossRef]

28. De Medeiros, E.V.; Duda, G.P.; Dos Santos, L.A.; de Sousa Lima, J.R.; de Almeida-Cortêz, J.S.; Hammecker, C.; Lardy, L.; Cournac, L. Soil organic carbon, microbial biomass and enzyme activities responses to natural regeneration in a tropical dry region in Northeast Brazil. *CATENA* **2017**, *151*, 137–146. [CrossRef]
29. Yang, Y.-S.; Chen, G.-S.; Guo, J.-F.; Xie, J.-S.; Wang, X.-G. Soil respiration and carbon balance in a subtropical native forest and two managed plantations. *Plant Ecol.* **2007**, *193*, 71–84. [CrossRef]
30. Murdiyarso, D.; Van Noordwijk, M.; Wasrin, U.R.; Tomich, T.P.; Gillison, A.N. Environmental benefits and sustainable land-use options in the Jambi transect, Sumatra. *J. Veg. Sci.* **2002**, *13*, 429–438. [CrossRef]
31. Yang, Y.S.; Guo, J.F.; Chen, G.S.; He, Z.M.; Xie, J.S. Effect of slash burning on nutrient removal and soil fertility in Chinese fir and evergreen broadleaved forests of mid-subtropical China. *Pedosphere* **2003**, *13*, 87–96.
32. Tian, D.; Yan, W.; Chen, X.; Deng, X.; Peng, Y.; Kang, W.; Peng, C. Variation in runoff with age of Chinese fir plantations in Central South China. *Hydrol. Process.* **2008**, *22*, 4870–4876. [CrossRef]
33. Chen, G.; Yang, Y.; Yang, Z.; Xie, J.; Guo, J.; Gao, R.; Yin, Y.; Robinson, D. Accelerated soil carbon turnover under tree plantations limits soil carbon storage. *Sci. Rep.* **2016**, *6*, 19693. [CrossRef]
34. Yang, Y.; Wang, L.; Yang, Z.; Xu, C.; Xie, J.; Chen, G.; Lin, C.; Guo, J.; Liu, X.; Xiong, D.; et al. Large Ecosystem service benefits of assisted natural regeneration. *J. Geophys. Res. Biogeosci.* **2018**, *123*, 676–687. [CrossRef]
35. Shono, K.; Cadaweng, E.A.; Durst, P.B. Application of Assisted Natural Regeneration to Restore Degraded Tropical Forestlands. *Restor. Ecol.* **2007**, *15*, 620–626. [CrossRef]
36. Chazdon, R.L.; Guariguata, M.R. Natural regeneration as a tool for large-scale forest restoration in the tropics: prospects and challenges. *Biotropica* **2016**, *48*, 716–730. [CrossRef]
37. Shoo, L.P.; Catterall, C.P. Stimulating Natural Regeneration of Tropical Forest on Degraded Land: Approaches, Outcomes, and Information Gaps. *Restor. Ecol.* **2013**, *21*, 670–677. [CrossRef]
38. Liu, L.; Gundersen, P.; Zhang, T.; Mo, J. Effects of phosphorus addition on soil microbial biomass and community composition in three forest types in tropical China. *Soil Boil. Biochem.* **2012**, *44*, 31–38. [CrossRef]
39. Tang, X.L.; Liu, S.G.; Zhou, G.Y.; Zhang, D.Q.; Zhou, C.Y. Soil-atmospheric exchange of CO_2, CH_4, and N_2O in three subtropical forest ecosystems in southern China. *Glob. Chang. Biol.* **2006**, *12*, 546–560. [CrossRef]
40. Wan, X.; Huang, Z.; He, Z.; Yu, Z.; Wang, M.; Davis, M.R.; Yang, Y. Soil C:N ratio is the major determinant of soil microbial community structure in subtropical coniferous and broadleaf forest plantations. *Plant Soil* **2015**, *387*, 103–116. [CrossRef]
41. Odum, E.P. The Strategy of Ecosystem Development. *Science* **1969**, *164*, 262–270. [CrossRef] [PubMed]
42. Odum, E.P. Trends Expected in Stressed Ecosystems. *BioScience* **1985**, *35*, 419–422. [CrossRef]
43. Zhou, Z.; Wang, C.; Luo, Y. Effects of forest degradation on microbial communities and soil carbon cycling: A global meta-analysis. *Glob. Ecol. Biogeogr.* **2018**, *27*, 110–124. [CrossRef]
44. Yang, Y.; Guo, J.; Chen, G.; Yin, Y.; Gao, R.; Lin, C. Effects of forest conversion on soil labile organic carbon fractions and aggregate stability in subtropical China. *Plant Soil* **2009**, *323*, 153–162. [CrossRef]
45. State Soil Survey Service of China (SSSSC). *China Soil*; China Agricultural Press: Beijing, China, 1998. (In Chinese)
46. Yang, Y.-S.; Chen, G.-S.; Lin, P.; Xie, J.-S.; Guo, J.-F. Fine root distribution, seasonal pattern and production in four plantations compared with a natural forest in Subtropical China. *Ann. For. Sci.* **2004**, *61*, 617–627. [CrossRef]
47. Liu, X.; Yang, Z.; Lin, C.; Giardina, C.P.; Xiong, D.; Lin, W.; Chen, S.; Xu, C.; Chen, G.; Xie, J.; et al. Will nitrogen deposition mitigate warming-increased soil respiration in a young subtropical plantation? *Agric. Meteorol.* **2017**, *246*, 78–85. [CrossRef]
48. Sibbesen, E. An investigation of the anion-exchange resin method for soil phosphate extraction. *Plant Soil* **1978**, *50*, 305–321. [CrossRef]
49. Powers, J.S.; Corre, M.D.; Twine, T.E.; Veldkamp, E. Geographic bias of field observations of soil carbon stocks with tropical land-use changes precludes spatial extrapolation. *Proc. Natl. Acad. Sci. USA* **2011**, *108*, 6318–6322. [CrossRef]
50. Luyssaert, S.; Schulze, E.D.; Börner, A.; Knohl, A.; Hessenmöller, D.; Law, B.E.; Ciais, P.; Grace, J. Old-growth forests as global carbon sinks. *Nature* **2008**, *455*, 213. [CrossRef]
51. Dybala, K.E.; Matzek, V.; Gardali, T.; Seavy, N.E. Carbon sequestration in riparian forests: A global synthesis and meta-analysis. *Glob. Chang. Biol.* **2019**, *25*, 57–67. [CrossRef]
52. Silver, W.L.; Kueppers, L.M.; Lugo, A.E.; Ostertag, R.; Matzek, V. Carbon sequestration and plant community dynamics following reforestation of tropical pasture. *Ecol. Appl.* **2004**, *14*, 1115–1127. [CrossRef]

53. Sheng, H.; Yang, Y.; Yang, Z.; Chen, G.; Xie, J.; Guo, J.; Zou, S. The dynamic response of soil respiration to land-use changes in subtropical China. *Glob. Chang. Boil.* **2010**, *16*, 1107–1121. [CrossRef]
54. Schulze, E.D.; Wirth, C.; Heimann, M. Climate change: Managing forests after Kyoto. *Science* **2000**, *289*, 2058–2059. [CrossRef] [PubMed]
55. Kiem, R.; Kögel-Knabner, I. Contribution of lignin and polysaccharides to the refractory carbon pool in C-depleted arable soils. *Soil Boil. Biochem.* **2003**, *35*, 101–118. [CrossRef]
56. Glaser, B.; Turrión, M.-B.; Alef, K. Amino sugars and muramic acid—biomarkers for soil microbial community structure analysis. *Soil Boil. Biochem.* **2004**, *36*, 399–407. [CrossRef]
57. Throckmorton, H.M.; Bird, J.A.; Monte, N.; Doane, T.; Firestone, M.K.; Horwath, W.R. The soil matrix increases microbial C stabilization in temperate and tropical forest soils. *Biogeochemistry* **2015**, *122*, 35–45. [CrossRef]
58. Keiluweit, M.; Wanzek, T.; Kleber, M.; Nico, P.; Fendorf, S. Anaerobic microsites have an unaccounted role in soil carbon stabilization. *Nat. Commun.* **2017**, *8*, 1771. [CrossRef] [PubMed]
59. Guan, Z.-H.; Li, X.G.; Wang, L.; Mou, X.M.; Kuzyakov, Y. Conversion of Tibetan grasslands to croplands decreases accumulation of microbially synthesized compounds in soil. *Soil Boil. Biochem.* **2018**, *123*, 10–20. [CrossRef]
60. Ye, G.; Lin, Y.; Kuzyakov, Y.; Liu, D.; Luo, J.; Lindsey, S.; Wang, W.; Fan, J.; Ding, W. Manure over crop residues increases soil organic matter but decreases microbial necromass relative contribution in upland Ultisols: Results of a 27-year field experiment. *Soil Biol. Biochem.* **2019**, *134*, 15–24. [CrossRef]
61. Chen, G.-S.; Yang, Y.-S.; Xie, J.-S.; Guo, J.-F.; Gao, R.; Qian, W. Conversion of a natural broad-leafed evergreen forest into pure plantation forests in a subtropical area: Effects on carbon storage. *Ann. For. Sci.* **2005**, *62*, 659–668. [CrossRef]
62. Li, J.; Li, Z.; Wang, F.; Zou, B.; Chen, Y.; Zhao, J.; Mo, Q.; Li, Y.; Li, X.; Xia, H. Effects of nitrogen and phosphorus addition on soil microbial community in a secondary tropical forest of China. *Biol. Fertil. Soils* **2015**, *51*, 207–215. [CrossRef]
63. Turner, B.L.; Brenes-Arguedas, T.; Condit, R. Pervasive phosphorus limitation of tree species but not communities in tropical forests. *Nature* **2018**, *555*, 367–370. [CrossRef] [PubMed]
64. Tang, X.; Placella, S.A.; Daydé, F.; Bernard, L.; Robin, A.; Journet, E.-P.; Justes, E.; Hinsinger, P. Phosphorus availability and microbial community in the rhizosphere of intercropped cereal and legume along a P-fertilizer gradient. *Plant Soil* **2016**, *407*, 119–134. [CrossRef]
65. Cleveland, C.C.; Townsend, A.R.; Schmidt, S.K. Phosphorus Limitation of microbial processes in moist tropical forests: Evidence from short-term laboratory incubations and field studies. *Ecosystems* **2002**, *5*, 680–691. [CrossRef]
66. Treseder, K.K.; Allen, M.F. Direct nitrogen and phosphorus limitation of arbuscular mycorrhizal fungi: a model and field test. *New Phytol.* **2002**, *155*, 507–515. [CrossRef]
67. Liang, C.; Fujinuma, R.; Wei, L.; Balser, T.C. Tree species-specific effects on soil microbial residues in an upper Michigan old-growth forest system. *Forestry* **2007**, *80*, 65–72. [CrossRef]
68. Shao, S.; Zhao, Y.; Zhang, W.; Hu, G.; Xie, H.; Yan, J.; Han, S.; He, H.; Zhang, X. Linkage of microbial residue dynamics with soil organic carbon accumulation during subtropical forest succession. *Soil Boil. Biochem.* **2017**, *114*, 114–120. [CrossRef]
69. Guo, J.; Yang, Z.; Lin, C.; Liu, X.; Chen, G.; Yang, Y. Conversion of a natural evergreen broadleaved forest into coniferous plantations in a subtropical area: effects on composition of soil microbial communities and soil respiration. *Boil. Fertil. Soils* **2016**, *52*, 799–809. [CrossRef]
70. Fierer, N.; Schimel, J.P.; Holden, P.A. Variations in microbial community composition through two soil depth profiles. *Soil Boil. Biochem.* **2003**, *35*, 167–176. [CrossRef]
71. Steenwerth, K.L.; Drenovsky, R.E.; Lambert, J.J.; Kluepfel, D.A.; Scow, K.M.; Smart, D.R. Soil morphology, depth and grapevine root frequency influence microbial communities in a Pinot noir vineyard. *Soil Boil. Biochem.* **2008**, *40*, 1330–1340. [CrossRef]
72. Zhang, B.; Liang, C.; He, H.; Zhang, X. Variations in Soil Microbial Communities and Residues Along an Altitude Gradient on the Northern Slope of Changbai Mountain, China. *PLoS ONE* **2013**, *8*, e66184. [CrossRef] [PubMed]

73. Sradnick, A.; Oltmanns, M.; Raupp, J.; Joergensen, R.G. Microbial residue indices down the soil profile after long-term addition of farmyard manure and mineral fertilizer to a sandy soil. *Geoderma* **2014**, *226*, 79–84. [CrossRef]
74. Hedlund, K.; Griffiths, B.; Christensen, S.; Scheu, S.; Setälä, H.; Tscharntke, T.; Verhoef, H. Trophic interactions in changing landscapes: responses of soil food webs. *Basic Appl. Ecol.* **2004**, *5*, 495–503. [CrossRef]
75. Moritz, L.K.; Liang, C.; Wagai, R.; Kitayama, K.; Balser, T.C. Vertical distribution and pools of microbial residues in tropical forest soils formed from distinct parent materials. *Biogeochemistry* **2009**, *92*, 83–94. [CrossRef]
76. Turrión, M.B.; Glaser, B.; Zech, W. Effects of deforestation on contents and distribution of amino sugars within particle-size fractions of mountain soils. *Boil. Fertil. Soils* **2002**, *35*, 49–53. [CrossRef]
77. Taylor, J.P.; Wilson, B.; Mills, M.S.; Burns, R.G. Comparison of microbial numbers and enzymatic activities in surface soils and subsoils using various techniques. *Soil Boil. Biochem.* **2002**, *34*, 387–401. [CrossRef]
78. Hurlbert, S.H. Pseudoreplication and the Design of Ecological Field Experiments. *Ecol. Monogr.* **1984**, *54*, 187–211. [CrossRef]

forests

MDPI

Article

Evaluation of Forest Conversion Effects on Soil Erosion, Soil Organic Carbon and Total Nitrogen Based on ^{137}Cs Tracer Technique

Xi Zhu [1], Jie Lin [1,*], Qiao Dai [1], Yanying Xu [1] and Haidong Li [2]

[1] Co-Innovation Center for Sustainable Forestry in Southern China of Jiangsu Province, Key Laboratory of Soil and Water Conservation and Ecological Restoration of Jiangsu Province, Nanjing Forestry University, Nanjing 210037, China; 13913410166@163.con (X.Z.); D2313238461@163.com (Q.D.); xyy1414@163.com (Y.X.)

[2] Nanjing Institute of Environmental Sciences, Ministry of Ecology and Environment, Nanjing 210042, China; lhd@nies.org

* Correspondence: jielin@njfu.edu.cn

Received: 8 April 2019; Accepted: 13 May 2019; Published: 20 May 2019

Abstract: Soil erosion can affect the horizontal and the vertical distribution of soil carbon at the landscape scale. The ^{137}Cs tracer technique can overcome the shortcomings of traditional erosion research and has proven to be the best method to study soil erosion. To understand the responses of soil organic carbon and nitrogen to soil erosion and forest conversion in the development of slope economic forests in rocky mountain areas, three representative types of economic forests that were all formed after clear-cutting and afforestation on the basis of CBF (coniferous and broad-leaved mixed forests) were selected: CF (chestnut forests) with small human disturbance intensity, AF (apple forests), and HF (hawthorn forests) with high interference intensity. The results showed that all land use types have significantly eroded since 1950; the average annual loss of soil was 0.79 mm in the CBF, 2.31 mm in the AF, 1.84 mm in the HF, and 0.87 mm in the CF. The results indicated aggravation of soil erosion after the transformation of the CBF into an economic forest. The economic forest management reduced the average carbon storage and accelerated nutrient loss. The better vegetation coverage and litter coverage of CF made them stand out among the three economic forest varieties. Therefore, when developing economic forests, we should select species that can produce litter to ensure as much soil conservation as possible to reduce the risk of soil erosion.

Keywords: land use types; soil organic carbon; soil total nitrogen

1. Introduction

Forest ecosystems play a significant role in climate change mitigation by the uptake of a substantial portion of carbon dioxide (CO_2) from the atmosphere as well as their long-term deposition into biomass and soil [1,2]. Afforestation has proven to be an effective method for increasing C stocks [3–5]. However, the growth of the economy and the population drove up demand for forest products, facilitating forest conversion. Many studies showed that such forest conversion (i.e., forest-for-economic forest) may lead to soil erosion and other ecological problems [6,7]. Similarly, soil erosion—which is a worldwide problem with both social and environmental consequences—has proven to lead to lateral and vertical migration of nutrients [8].

The dynamic research on soil carbon and nitrogen storage and migration has attracted increasingly more scholars' attention worldwide [9–11]. In recent years, scholars have carried out extensive studies on the effects of soil erosion on soil organic carbon in sloping farmland [12–20]. However, few studies have been reported on soil erosion caused by forest transformation and the horizontal migration of soil nutrients. Therefore, it was necessary to systematically study how SOC (soil organic carbon) and TN (total nitrogen) respond to soil erosion after forest conversion.

China has the greatest area of forest plantations on a global scale, consisting of one fourth of the total plantation area [21]. Since the 1960s, the area of forests has rapidly increased to satisfy the ever-growing requirements for wood and other forest products in northeastern China, which has led to a series of serious ecological and environmental problems, such as soil erosion (especially water erosion) [22]. After transforming forests into economic forests, the structure of forests become uniform. Climate, biomass production, and plant distribution can also be totally changed [23–25]. Researchers have found reductions in soil C storage following forest conversion from natural forests to plantations [26,27]. In order to facilitate forest management, shrubs and weeds in forests are often removed. Such a change of vegetation cover can affect both the biological and the chemical properties of the soil, such as belowground C and nutrient storage [28]. Previous studies have also reported that water erosion is a pivotal process that can affect the horizontal migration and the redistribution of SOC and TN [29,30]. However, there have been few reports on how natural forest conversion into economic forests affects soil erosion, SOC, and TN. This is an important environmental issue that has not been well quantified.

Soil erosion caused by man-made, forced interference has received more and more attention [31–35]. Most of these studies made use of traditional RUSLE (revised universal soil loss equation) and evaluated large-scale changes in soil erosion intensity and spatial patterns by remote sensing and GIS. Traditional erosion research methods often miss information such as the soil erosion process and the land use change [36,37], while the ^{137}Cs tracer technology can overcome the shortcomings of traditional erosion research [38]. Under the background of global large-scale nuclear explosion tests in the 1950s and the 1970s, the ^{137}Cs tracer method was developed, and it has been widely used in soil erosion research at different spatial scales around the world since the 1990s [20,39]. This method has the characteristics of simplicity, high quantification degree, low research cost, and reliable results. It has been proven to be the best method to study soil erosion [40].

In this study, the goal was to explore the influence of forest conversion on soil erosion and carbon and nitrogen migration by using ^{137}Cs in order to provide a theoretical basis for the further rational utilization and protection of soil resources and to assist the in-depth study on the regional carbon and nitrogen balance. The specific goals were to answer the following questions: (a) How do the characteristics of soil thickness and nutrient change with forest conversion? (b) How does forest conversion affect the vertical distribution characteristics of soil organic carbon and total nitrogen after forest conversion? (c) How does the storage of SOC and TN change after forest conversion? (d) Through the comparison of the studied forest types, which is the best forest type for conversion? In order to assess how forest conversion into economic forests affects soil erosion as well as SOC and TN, this study chose the study area of the great Wu mountain valley. The basin is situated at the starting point of the Belt Road, Lianyungang, which was originally a coniferous and broad-leaved mixed forest (CBF). However, in the 1970s, the economic forest should have transformed in a short time.

2. Materials and Methods

2.1. Study Sites

Dawu Mountain (35°11′ E, 118°50′ N) is located in the northwest of Ganyu District, Lianyungang, Jiangsu province, Southeast China (Figure 1). It belongs to a warm-temperate maritime monsoon climate with four distinct seasons, an average annual temperature of 13.9 °C, an annual rainfall of 976.6 mm, a frost-free period of 216 days, and average annual sunshine of 2534 h. The soil is a subcategory of coarse-grained brown soil with more sand and gravel in the topsoil. The vegetation is a temperate deciduous broad-leaved forest area dominated by artificial forests, supplemented by a small amount of natural deciduous broad-leaved forests and evergreen coniferous forests, including secondary vegetation such as Masson pine, broad-leaved trees, and arborvitae, and economic trees such as hawthorn and chestnut. Most of the research area was originally planted on the open forestland at the end of the 20th century. By the beginning of the 21st century, part of the plantation forest was in

a state of natural regeneration, and some plantations were transformed into economic forests. In the experimental area, coniferous and broad-leaved mixed forests are the representative stand types of planted forests. The main tree species include *Pinus massoniana* Lamb., *Platycladus orientalis* (L.) Franco, sapling trees, and *Metasequoia glyptostroboides* Hu et W. C. Cheng, and there are herbs and humus layers under the forest. The hawthorn forest, the chestnut forest, and the apple forest are all economic forests that have been transformed by a mixed forest of coniferous and broad-leaved forest in which the surface of the chestnut forest is covered with litter, the surfaces of the hawthorn and the apple forests are exposed, and there are obvious artificial tilling traces. Basic information of different land use types was shown in Table 1.

In July 2016, field sampling was conducted to avoid the influence of topography, landforms, and elevation on the results of the study. Based on field surveys, the same parent material and relative geographical location were selected on the slope according to the principles of typicality and representativeness. According to the principles of typicality and representativeness, three sites, each of which has the same parent material and relatively centralized geographical location, were selected on the sloping land, including the HF (hawthorn forest), the AF (apple forest), the CF (chestnut forest), and the CBF. The three economic forests (HF, AF, and CF) were all formed after clear-cutting and afforestation on the basis of coniferous and broad-leaved mixed forests. The CBF was replanted after the replanting of the woodland. The forest age is approximately 10 years, and the slope is 10°~15°, from which it can be assumed that the soil properties of all the plots were similar before the economic forest regeneration. The CBF is an artificial forest with no interference. The CF is an economic forest with less human interference intensity, while the HF and the AF are economic forests with greater interference intensity.

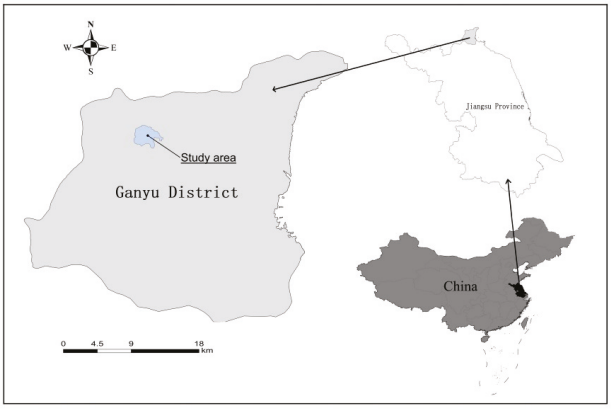

Figure 1. Location of the study site.

2.2. Sampling and Measuring Methods

Using the S-shaped sampling strategy, five sampling points in each sample were placed. The soil samples were collected by 0–10, 10–20, and 20–30 cm, and the same soil samples were mixed into three layered soil samples. At the same time, the soil samples were collected using a 100 cm^3 standard ring knife. In order to determine the content of the nuclide in the soil, the whole sample of the 0–20 cm soil and the spaced 5 cm stratified sample were collected with the diameter of a 5 cm soil drill. After returning to the laboratory, the soil sample collected by the non-earth drills was naturally air-dried, and plant debris, small stones, and organisms were removed. Some of them were kept, as they were found along the natural cracks to form small clusters of approximately 1 cm^3 to classify the aggregates. The other part was milled through a 2 mm sieve and was used for the determination of soil-related properties. After removing the stone weeds, the soil samples used for the determination of isotopes

were naturally air-dried after being ground through a 20-mesh sieve, dried in an oven at 105 °C to a constant weight, cooled to room temperature, and weighed with a precision of 0.001 g (ultimately weighing 300 g).

The physical and the chemical properties of the soil were measured according to the national standard. The soil bulk density was measured by the ring knife method. The pH was measured by an acidity meter. The total nitrogen, carbon, and nitrogen ratio and the ratio of carbon and hydrogen were measured by the element analyzer. The organic carbon content of the soil was oxidized with the potassium dichromate-external heating method. The mechanical composition was measured by a laser particle size analyzer (grading standard: 0.002, 0.05, and 2 mm). The specific surface area of the soil was analyzed using an ASAP2020 automatic surface area and pore size distribution analyzer (Micromeritics Instrument Corp, Atlanta, GA, USA). The soil water-soluble organic carbon was determined by weighing 5 g over a 2 mm screen soil in a 100 mL centrifuge tube, adding 25 mL of water, shaking, centrifuging, and taking the supernatant and filtering with a 0.45 μm microporous membrane to obtain the solution. At last, it was poured into a TOC (total organic carbon) sample tube and measured on a Shimadzu TOC-VCPH automatic analyzer [41]. The test of the nuclide ^{137}Cs used the background gamma spectrometer produced by the ORTEC Company (Dallas, TX, USA) of the United States and the C coaxial high pure germanium probe of the type GEM-40190 of the probe. The measurement time of each sample was 25,000 s, and the specific activity of the soil sample was calculated by a comparison with the standard source.

2.3. Calculation of the Soil ^{137}Cs

In this study, the top of Dawu Mountain was chosen as the background value point because there was no artificial activity on the top of the mountain, and the terrain was flat. The woodland structure i0s dominated by arbors, and the meadows are dominated by *Pinus massoniana*. Through the determination of two background value sampling points, the background value of ^{137}Cs was determined to be 1732.48 Bq/m^2. The ^{137}Cs content in soil was calculated using Formula (1).

$$CPI = \sum_{i=1}^{n} 1000 \times C_i \times Bd_i \times D_i \quad (1)$$

CPI is ^{137}Cs per unit area activity of the sampling point, Bq/m^2; i is the sampling sequence number; n is the sampling layer number; 1000 is the unit correction factor; C_i is the specific activity of ^{137}Cs in the sampling layer i, Bq/kg; Bd_i is the soil bulk density of the sampling layer of layer i, g/cm^3; D_i is the depth of sampling layer I, m.

The soil erosion modulus was calculated using the following models:

$$A(d) = A_{ref}(1 - e^{-\lambda d}) \quad (2)$$

$$h = -\frac{1}{(t-1963)\lambda} \ln[(1 - \frac{Y}{100})] \quad (3)$$

$$Y = 100(A_{ref} - A)/A_{ref} \quad (4)$$

$$E_R = 10000 \times h \times D \quad (5)$$

A(d) is the total area activity of the soil above depth d, Bq/m^2; A_{ref} is the ^{137}Cs area activity background value, Bq/m^2; λ is the profile index of ^{137}Cs depth distribution, cm^{-1}. T is the sampling year; Y is the ^{137}Cs area activity of the measured relative background value reduction percentage, %, D is the soil bulk density, g/cm3; h is the erosion of years of erosion thickness, m/a; E_R is the soil erosion modulus, t/(km^2·a).

2.4. Calculation the Storage and Loss of Soil Carbon and Nitrogen

The xth nutrient density per unit soil area is:

$$D_x = 0.01 \sum_{i=1}^{n} C_i \times d_i \times b_i \quad (6)$$

where D_x is the xth nutrient density (g/m^2); C_i is the xth nutrient content in the soil i layer (g/kg); b_i is the bulk density of the i layer soil (g/cm^3); d_i is the thickness of the i layer of soil (cm).

The absolute loss of the xth nutrient per unit area is:

$$L_X = 10 \times C_X \times D \times h \quad (7)$$

where L_X is the absolute loss of the xth nutrient (t/km^2); C_X is the xth nutrient content in the soil (g/kg); D is the soil bulk density (kg/m^3); h is the average annual loss of the soil thickness (m).

The relative loss rate of soil nutrient per unit area:

$$R = L_X / D_X \quad (8)$$

where R is the relative loss rate of the nth nutrient per unit area (%).

2.5. Data Processing and Analysis

Mean values were calculated for each of the variables, and one-way ANOVA was used to evaluate forest type and soil depth on the measured variables for pairwise comparison. The least significant difference (LSD) test was used for mean comparison of two forest types at the same soil depth and different soil depth in the same forest type at $p < 0.05$. The relationships between the ^{137}Cs and SOC or TN were evaluated by Pearson's correlation analysis. These statistical analyses were completed with the R language (Vienna University: Vienna, Austria) and SPSS 19.0. (SPSS Inc: Chicago, IL, USA). The graphics were plotted with Origin software (Publisher: city, country OriginLab: Northampton, MA, USA).

Table 1. Basic information of different land use types.

Land Use Type	Forest Age (year)	LAI	Litter Thickness (mm)	Slope (°)	Aspect	pH	Soil Bulk Density/g cm^3	Sand/%	Silt%	Clay%
HF	11	2.1	0	15	SE	5.67 ± 0.27	1.42 ± 0.12	30.84 ± 5.05	65.00 ± 5.63	4.16 ± 0.36
CF	13	2.5	1.1	11	SE	5.95 ± 0.34	1.43 ± 0.05	31.57 ± 7.83	64.66 ± 6.66	3.77 ± 0.18
AF	10	2.2	0	13	SE	5.48 ± 0.26	1.47 ± 0.18	41.07 ± 8.65	56.63 ± 4.36	2.29 ± 0.23
CBF	25	3.2	1.3	13	SE	5.67 ± 0.27	1.44 ± 0.12	36.59 ± 7.53	60.21 ± 6.96	3.20 ± 0.41

Note: all data are expressed in mean ± SE (standard error), which were calculated based on three samples. CBF: coniferous and broad-leaved mixed forest; HF: hawthorn forest; AF: apple forest; CF: chestnut forest; LAI: leaf area index.

3. Results

3.1. Characteristics of ^{137}Cs and Annual Erosion Modulus after Forest Conversion.

In comparison with the CBF, the specific activity of $^{\text{the }137}$Cs decreased to 92%, 82%, and 36% at the 0–10 cm soil depth in AF, HF, and CF, respectively (Figure 2A). The CBF had the largest difference between the two soil layers, with the 0–10 cm layer 2.04 times that of the 10–20 cm layer. The specific activities of the ^{137}Cs in CH and CF were 1.28 and 1.06 times greater in 0–10 cm layer compared to the 10–20 cm layer, respectively. The results of the LSD analysis showed that, in the 0–10 cm soil layer, the average ^{137}Cs activity of the soil in CBF was significantly greater than that of the other three land use depths. In the 10–20 cm soil depth, the average ^{137}Cs specific activities in CBF and CF were significantly higher than those in HF and AF.

Compared with the background value, the ^{137}Cs content of all land use types was significantly lower than the background value of 1732.48 Bq·m^2. Among them, CBF decreased the least, which was 68.43% (Table 2). AF decreased the most by 96.50%. The annual soil erosion thickness for different land use types followed the order of AF (2.31 mm) > HF (1.84 mm) > CF (0.87 mm) > CBF (0.79 mm). In comparison with the CBF, the annual soil erosion thickness of AF and HF increased 192% and 133%, respectively (Figure 2B). Moreover, the annual soil erosion thickness significantly differed between the CBF and the economic forests (AF and HF). However, there was no significant difference between CBF and CF. The correlation analysis showed that the ^{137}Cs activity in the soil showed a significant positive correlation with the content of soil organic carbon and total nitrogen ($p < 0.05$) (Table 3).

Table 2. ^{137}Cs loss in different land use types.

Land Use Types	Depth/cm	^{137}Cs Content/Bq·m^{-2}	Percentage ^{137}Cs Loss/%
CBF	0–20	546.92	68.4
HF	0–20	123.88	92.9
AF	0–20	60.60	96.5
CF	0–20	495.89	71.4

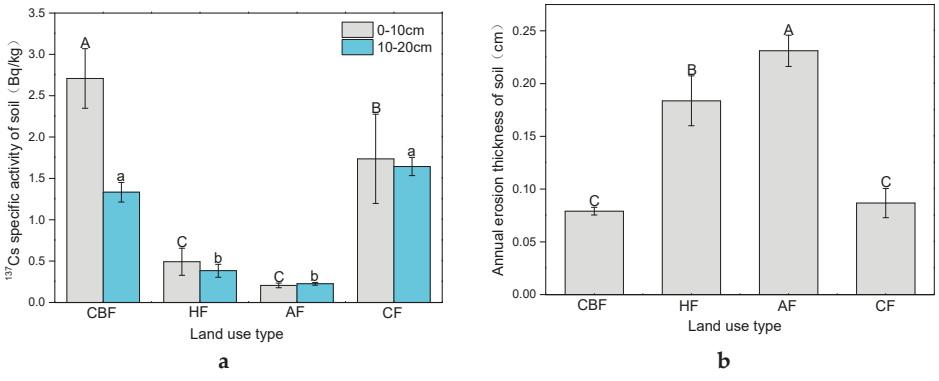

Figure 2. ^{137}Cs levels and the annual loss in soil depth under different land use types. Note: bars represent ± SE of the mean ($n = 3$). Different letters indicate significant differences in the same layer and different land use types ($p < 0.05$). (**a**) represents specific activity of soil ^{137}Cs in each layer with different land use types; (**b**) represents average annual loss thickness of soil in different land use types.

Table 3. Correlation between ^{137}Cs and soil chemical properties.

	TN	TP	TK	SOC	DOC	C/N	C/H
Cor.	0.54 **	−0.18	−0.03	0.56 **	0.11	0.49 *	0.40
P	0.006	0.39	0.99	0.005	0.60	0.02	0.05
N	24	24	24	24	24	24	24

TN: total nitrogen; TP: total phosphorus; TK: total kalium; SOC: soil organic carbon; DOC: dissolved organic carbon; C/N: carbon/ nitrogen; C/H: carbon/hydrogen. * Significant correlation was found at the level of $\alpha = 0.05$ and ** at the level of $\alpha = 0.01$.

3.2. SOC and TN Storage after Forest Conversion

The average SOC and TN storages in the CBF were 3.33 kg/m^2 and 0.36 kg/m^2, respectively, and the economic forest management reduced the SOC storage and the TN storage of the soil (Figure 3). In comparison with the CBF, the SOC storage and the TN storage in AF were the lowest, decreasing by 63.66% and 52.78%. The SOC (TN) storages in HF and CF decreased by 49.25% (38.89%) and 61.26% (50%), respectively. The results of the LSD analysis showed that the SOC and the TN storage in different

land use types did not change significantly with the soil layers. Among three economic forests, the SOC and the TN storage of the CF were significantly greater than those of the other three types of land use ($p < 0.05$). In the 20–30 cm soil layer, the SOC storage of the HF was significantly higher than that of the AF ($p < 0.05$). In the other two layers, there was no significant difference in the SOC storage of the three economic forests.

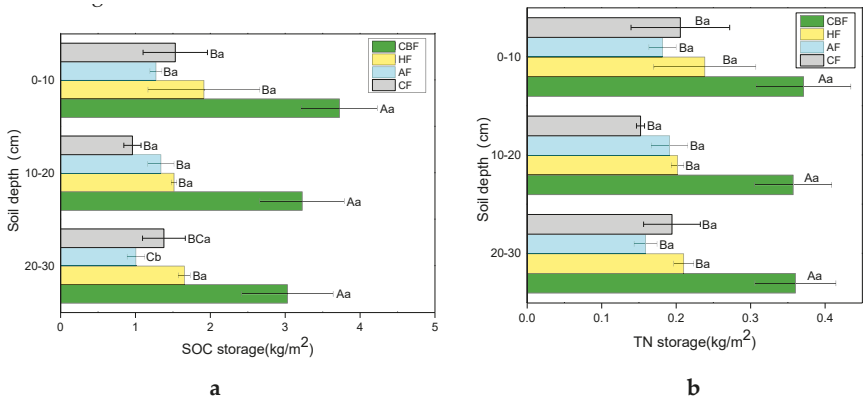

Figure 3. The TN and the SOC stocks under different land use types. Note: bars represent ± SE of the mean ($n = 3$). Different capital letters indicate significant differences of different land use types in the same soil layer, and different lower-case letters indicate significant differences of different soil layers in the same land use types. (**a**,**b**) represent the reserves of organic carbon and nitrogen, respectively.

3.3. SOC and TN Losses after Forest Conversion

The annual loss of topsoil carbon in CBF was 41.37 t/km^2. HF had the most topsoil carbon loss, which was 50.78 t/km^2 (Figure 4A). The results of the LSD analysis showed that the annual loss of topsoil carbon in HF was significantly greater than that in CF. The annual loss of topsoil nitrogen in CBF was 2.95 t/km^2 (Figure 4B). The annual loss of topsoil nitrogen in HF, AF, and CF was 1.51, 1.42, and 0.61 that of CBF, respectively. The LSD analysis results showed that the annual loss of topsoil nitrogen of HF and AF was significantly greater than it was for CF ($p < 0.05$).

As shown in Figure 5A, the annual relative loss rate of SOC in the CBF was 0.41%. The economic forest construction increased the annual carbon soil relative loss rate. In comparison with the CBF, the AF was the largest, being 2.43 times that of the CBF. The annual relative churn rates of HF and CF were 2.36 and 1.49 times that of CBF, respectively. The results of the LSD analysis showed that the rates of the soil carbon loss per year in the soil of HF and AF were significantly greater than that in the CBF soil ($p < 0.05$).

The annual relative loss of TN in the CBF was 0.27%. The construction of economic forests increased the annual relative loss rate of TN. In comparison with the CBF, the AF loss was the largest—2.93 times that of CBF. The HF and the CF were 2.48 times and 1.19 times that of the CBF, respectively. The LSD analysis results showed that the annual rates of TN loss in the HF and the AF were significantly greater than those in the CF and the CBF ($p < 0.05$).

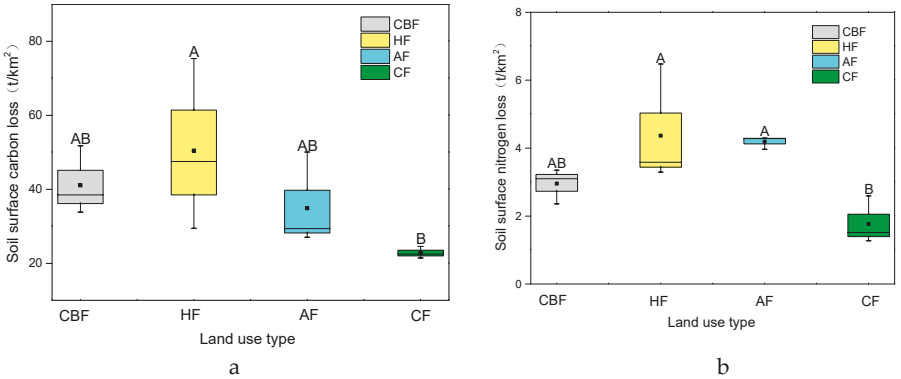

Figure 4. Soil surface carbon and nitrogen loss under different land use types. Note: the boxplot consists of five statistics: minimum, upper quartile, median, lower quartile, and maximum. The center of the boxplot is the median. Bars represent ± SE of the mean (n = 3). Different capital letters indicate that the difference between different land use types of the same soil layer is significant. (**a**,**b**) represent the surface loss of carbon and nitrogen, respectively.

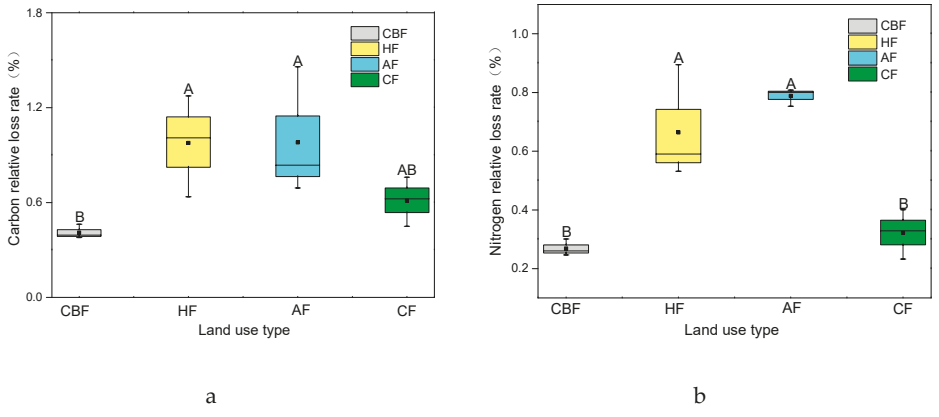

Figure 5. The carbon and nitrogen relative loss rates under different land use types. Note: the boxplot consists of five statistics: minimum, upper quartile, median, lower quartile, and maximum. The center of the boxplot is the median. Bars represent ± SE of the mean (n = 3). Different capital letters indicate that the difference between different land use types of the same soil layer is significant. (**a**,**b**) represent the relative loss of carbon and nitrogen, respectively.

4. Discussion

4.1. Soil Erosion after Forest Conversion

The acquisition of the background value was the key to tracing soil erosion by nuclides [42,43]. The background value of ^{137}Cs can be obtained by the long-term monitoring of radioactive settlement, or it can be determined by selecting the correct reference points [44]. In this study, the background value of ^{137}Cs was 1732.48 Bq/m^2. Similar research on the Yimeng mountain area showed that the background value was 1602 Bq/m^2, which was close to this study [45]. In addition, according to the global simulated nuclear explosion ^{137}Cs background value model of Walling [46], the simulation background value of the study area was 1467 Bq/m^2, which was roughly equivalent to the background value of this study area. This indicates that the measured background value was reliable. Compared

with the background value, all land use types underwent extremely serious soil erosion. It was reported that, in the Ganyu District of Lianyungang City, the high stone content in the soil made it more vulnerable to soil erosion. It has become a key area for soil erosion control [47–49].

The annual soil erosion thickness value of CBF was the lowest, which was 0.79 mm. The soil erosion moduli of AF, HF, and CF were all higher than CBF (Figure 2). The results indicated that CBF conversion to economic forests led to more severe soil erosion. As is shown in Table 1, compared with economic forests, CBF had the largest LAI (leaf area index), which indicated that CBF had high vegetation cover, which was consistent with previous studies. Binkley and Giardina [25] reported that, after being intercepted by canopy, the energy of raindrops was reduced to almost zero when they reached the soil. This explained why the thickness of soil loss in the CBF was the smallest. Among the three types of economic forests, the soil loss thickness of the CF was the smallest. CBF and CF had more litter cover on the surface than HF and AF. (Table 1). It has been reported that good litter cover reduces the ability of rain to wash the surface, which then reduces the loss of soil sediment [50–52]. We can further draw the conclusion that, when forests are converted into economic forests, it is necessary to select trees that can improve vegetation coverage and litter thickness so as to effectively reduce soil erosion. In this study, it was found that CF could better reduce soil erosion, which can be applied to the forestry construction in this area. However, in other areas, where environmental conditions may be different, the benefits of chestnut forests may not be realized. Therefore, more suitable tree species need to be selected according to local conditions. The potential benefits of chestnut forests observed in this study may depend more on the depth of litter in the study site. The abundance of litter depends not only on the defoliation but also on the management of forests in a variety of ways to maintain litter. Therefore, in addition to selecting suitable species for soil and water conservation, proper forest management is particularly important.

The annual soil erosion thickness was AF > HF > CF > CBF (Figure 2 A). The change trend was the same as the specific surface area of soil (Figure 6). The BET (Brunner Emmett Tellermethod) specific surface area of the soils increased with the management of the economic forests. Among them, AF increased by 43.46%, while HF and CF increased by 20.09% and 5.61%, respectively. The specific surface area of soil is an important indicator of soil quality and an intuitive expression of land use at a micro-scale [53–55]. The specific surface area contains abundant information, such as material migration, tillage methods, parent material structure, and so on. An increase in the specific surface area of an economic forest can increase the soil porosity and the macroaggregate content. Therefore, both water holding capacity and anti-erosion ability of soil are weakened. This is consistent with the conclusions of our research. Conversion into economic forests and improper management will aggravate soil erosion.

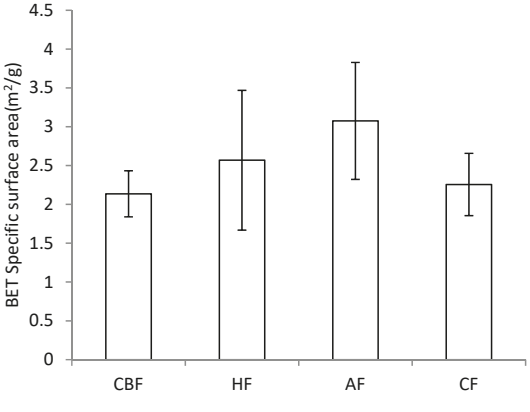

Figure 6. Soil pore structure under different land use patterns.

4.2. The Contact of Erosion and SOC and TN

The order of average SOC and TN storage was CBF > HF > CF > AF (Figure 3). This result indicated that the economic forest management reduced the SOC storage and the TN storage of the soil. It has been reported that the forest conversion can directly or indirectly affect many processes in the carbon–nitrogen biogeochemical cycle of ecosystems [55], such as changing the input and the degradation of organic matter and the physical protection of carbon and nitrogen by aggregates [56]. In addition, the SOC storage in the CBF decreased obviously as the soil layer deepened, which was consistent with the conclusions of related research done by Ma W et al. [7].

The results showed that the order of annual loss of SOC in the soil surface was HF > CBF > AF > CF (Figure 4). The reasons for this were two-fold. On one hand, erosion caused the absolute loss of nutrients. As was shown in Table 3, ^{137}Cs had a significant correlation with SOC. It was reported that the redistribution of soil carbon and nitrogen under soil erosion was generally divided into two aspects—lateral migration and vertical migration [57–59]. Water was the main cause of soil erosion, which was accompanied by the whole process of soil particle dispersion, migration, and deposition. Soil carbon and nitrogen, as important parts of the soil, were usually lost in both sediment-bound and runoff-dissolved states during erosion [60,61]. On the other hand, when the soil itself carried a high content of organic carbon, the absolute loss of nutrients was high. SOC content in CF and CBF was relatively rich in itself. When soil erosion was milder, there was a high absolute loss rate.

Compared with the absolute loss, the annual relative loss rate of soil carbon and nitrogen could better show the overall situation of soil carbon and nitrogen under different land use types, which was an effective index for characterizing the soil quality degradation [62]. The results showed that the relative loss rate of the CBF was significantly smaller than those of the AF and the HF, which were similar to the soil layer loss thickness distribution. This indicated that the soil carbon and the nitrogen loss in the AF and the HF were serious and should have been strengthened to reduce the soil erosion and the loss of nutrients as well as to improve the soil quality [63]. In addition, it was found that the rate of soil carbon loss per year under different land use types was obviously greater than that of soil nitrogen relative loss. This was consistent with relevant studies [64].

The correlation analysis showed that the ^{137}Cs activity in the soil showed a significant positive correlation with the content of soil organic carbon and total nitrogen (Table 3), which indicated that the contents of soil carbon and nitrogen under different land use modes in the area were closely related to soil erosion. This was consistent with earlier reports by Cheng J X et al. [65,66].

5. Conclusions and Deficiencies

The results showed that the conversion of coniferous broad-leaved mixed forests into the economic forests aggravated soil erosion. The average annual soil loss thickness of CBF was 0.79 mm, while those of AF, HF, and CF were 2.31 mm, 1.84 mm, and 0.87 mm, respectively. Economic forest management reduced the average carbon storage of soil, and the ranges from big to small were AF, CF, and HF by 63.66%, 61.26%, and 49.25%, respectively. The soil erosion process directly leads to the loss of soil carbon and nitrogen, which has a negative impact on the development of local agriculture and forestry. In the process of practical application, we should pay attention when forests are converted into economic forests, as it is necessary to select trees that can improve vegetation coverage and litter thickness in order to effectively reduce soil erosion. However, there are still some problems and shortcomings in this paper, such as the relative contribution rate of soil erosion and land use change to soil carbon and nitrogen loss, which could not be concluded from the existing data and will be more detailed in future experiments.

Author Contributions: Data interpretation, Y.X.; Data analysis, X.Z.; Manuscript drafting, X.Z.; Research design, Q.D.; Manuscript revision, J.L. Basic structure of this thesis, H.L.

Funding: This research was supported by National Natural Science Foundation of China (No. 31870600), Nation Key R&D program of China (2017YFC0505505), Priority Academic Program Development of Jiangsu Higher Education Institutions (PAPD).

Conflicts of Interest: The authors declare no conflict of interest.

References

1. Sun, Y.; Gu, L.; Dickinson, R.E.; Norby, R.J.; Pallardy, S.G.; Hoffman, F.M. Impact of mesophyll diffusion on estimated global land CO_2 fertilization. *Proc. Natl. Acad. Sci. USA* **2014**, *111*, 15774–15779. [CrossRef] [PubMed]
2. Tharammal, T.; Bala, G.; Narayanappa, D.; Nemani, R. Potential roles of CO_2 fertilization, nitrogen deposition, climate change, and land use and land cover change on the global terrestrial carbon uptake in the twenty-first century. *Clim. Dyn.* **2018**, *52*, 1–14. [CrossRef]
3. Li, D.; Niu, S.; Luo, Y. Global patterns of the dynamics of soil carbon and nitrogen stocks following afforestation: A meta-analysis. *New Phytol.* **2012**, *195*, 172–181. [CrossRef]
4. Vilén, T.; Cienciala, E.; Schelhaas, M.J.; Verkerk, P.J.; Lindner, M.; Peltola, H. Increasing carbon sinks in European forests: Effects of afforestation and changes in mean growing stock volume. *Forestry* **2016**, *89*, 82–90. [CrossRef]
5. Lebenya, R.M.; Huyssteen, C.W.V.; Preez, C.C.D. Change in soil organic carbon and nitrogen stocks eight years after conversion of sub-humid grassland to Pinus and Eucalyptus forestry. *Soil Res.* **2018**, *56*, 318. [CrossRef]
6. Jiang, W.; Yang, S.; Yang, X.; Ning, G. Negative impacts of afforestation and economic forestry on the Chinese Loess Plateau and proposed solutions. *Quat. Int.* **2016**, *399*, 165–173. [CrossRef]
7. Ma, W.; Li, Z.; Ding, K.; Huang, B.; Nie, X.; Lu, Y.; Xiao, H. Soil erosion, organic carbon and nitrogen dynamics in planted forests: A case study in a hilly catchment of Hunan Province, China. *Soil Tillage Res.* **2016**, *155*, 69–77. [CrossRef]
8. Gómez, J.A.; Campos, M.; Guzmán, G.; Castillollanque, F.; Vanwalleghem, T.; Lora, Á.; Giráldez, J.V. Soil erosion control, plant diversity, and arthropod communities under heterogeneous cover crops in an olive orchard. *Environ. Sci. Pollut. Res. Int.* **2017**, *25*, 1–13. [CrossRef]
9. Jian, S.; Li, J.; Ji, C.; Wang, G.; Mayes, M.A.; Dzantor, K.E.; Hui, D.; Luo, Y. Soil extracellular enzyme activities, soil carbon and nitrogen storage under nitrogen fertilization: A meta-analysis. *Soil Biol. Biochem.* **2016**, *101*, 32–43. [CrossRef]
10. Gentsch, N.; Mikutta, R.; Alves, R.J.E.; Barta, J.; Gittel, A.; Hugelius, G.; Kuhry, P.; Lashchinskiy, N.; Palmtag, J.; Richter, A. Storage and transformation of organic matter fractions in cryoturbated permafrost soils across the Siberian Arctic. *Biogeosciences* **2015**, *12*, 2697–2743. [CrossRef]
11. Murty, D.; Kirschbaum, M.U.F.; Mcmurtrie, R.E.; Mcgilvray, H. Does conversion of forest to agricultural land change soil carbon and nitrogen? a review of the literature. *Glob. Chang. Biol.* **2010**, *8*, 105–123. [CrossRef]
12. Fang, H.Y.; Sheng, M.L.; Sun, L.Y.; Cai, Q.G. [Using 137Cs and 210Pb(ex) to trace the impact of soil erosion on soil organic carbon at a slope farmland in the black soil region]. *Ying Yong Sheng Tai Xue Bao* **2013**, *24*, 1856–1862.
13. Nie, X.J.; Zhao, T.Q.; Qiao, X.N. Impacts of soil erosion on organic carbon and nutrient dynamics in an alpine grassland soil. *Soil Sci. Plant Nutr.* **2013**, *59*, 660–668. [CrossRef]
14. Zhao, P.; Sheng, L.; Wang, E.; Chen, X.; Deng, J.; Zhao, Y. Tillage erosion and its effect on spatial variations of soil organic carbon in the black soil region of China. *Soil Tillage Res.* **2018**, *178*, 72–81. [CrossRef]
15. Borrelli, P.; Paustian, K.; Panagos, P.; Jones, A.; Schütt, B.; Lugato, E. Effect of Good Agricultural and Environmental Conditions on erosion and soil organic carbon balance: A national case study. *Land Use Policy* **2016**, *50*, 408–421. [CrossRef]
16. Li, Y.; Zhang, Q.W.; Reicosky, D.C.; Lindstrom, M.J.; Bai, L.Y.; Li, L. Changes in soil organic carbon induced by tillage and water erosion on a steep cultivated hillslope in the Chinese Loess Plateau from 1898–1954 and 1954–1998. *J. Geophys. Res. Biogeosci.* **2015**, *112*, 531–532. [CrossRef]
17. Maïga-Yaleu, S.; Guiguemde, I.; Yacouba, H.; Karambiri, H.; Ribolzi, O.; Bary, A.; Ouedraogo, R.; Chaplot, V. Soil crusting impact on soil organic carbon losses by water erosion. *Catena* **2013**, *107*, 26–34. [CrossRef]
18. Dialynas, Y.G.; Bastola, S.; Bras, R.L.; Marin-Spiotta, E.; Silver, W.L.; Arnone, E.; Noto, L.V. Impact of hydrologically driven hillslope erosion and landslide occurrence on soil organic carbon dynamics in tropical watersheds. *Water Resour. Res.* **2016**, *52*, 8895–8919. [CrossRef]

19. Janeau, J.L.; Gillard, L.C.; Grellier, S.; Jouquet, P.; Le, T.P.Q.; Luu, T.N.M.; Ngo, Q.A.; Orange, D.; Pham, D.R.; Tran, D.T. Soil erosion, dissolved organic carbon and nutrient losses under different land use systems in a small catchment in northern Vietnam. *Agric. Water Manag.* **2014**, *146*, 314–323. [CrossRef]
20. Zhang, J.H.; Wang, Y.; Li, F.C. Soil organic carbon and nitrogen losses due to soil erosion and cropping in a sloping terrace landscape. *Soil Res.* **2015**, *53*, 87–96. [CrossRef]
21. Rogowski, A.S.; Tamura, T. Movement of 137Cs by Runoff, Erosion and Infiltration on the Alluvial Captina Silt Loam. *Health Phys.* **1963**, *11*, 1333–1340. [CrossRef]
22. Ge, F.L.; Zhang, J.H.; Su, Z.A.; Nie, X.J. Response of changes in soil nutrients to soil erosion on a purple soil of cultivated sloping land. *Acta Ecol. Sin.* **2007**, *27*, 459–463. [CrossRef]
23. Zhuang, J.Y.; Zhang, J.C.; Yang, Y.; Zhang, B.; Li, J. Effect of forest shelter-belt as a regional climate improver along the old course of the Yellow River, China. *Agrofor. Syst.* **2016**, *91*, 1–9. [CrossRef]
24. Hartanto, H.; Prabhu, R.; Ase, W.; Asdak, C. Factors affecting runoff and soil erosion: Plot-level soil loss monitoring for assessing sustainability of forest management. *For. Ecol. Manag.* **2003**, *180*, 361–374. [CrossRef]
25. Dan, B.; Giardina, C. Why do Tree Species Affect Soils? The Warp and Woof of Tree-soil Interactions. *Biogeochemistry* **1998**, *42*, 89–106.
26. Scott, N.A.; Tate, K.R.; Ross, D.J.; Parshotam, A. Processes influencing soil carbon storage following afforestation of pasture with Pinus radiata at different stocking densities in New Zealand. *Soil Res.* **2006**, *44*, 85–96. [CrossRef]
27. Lü, M.; Xie, J.; Chao, W.; Guo, J.; Wang, M.; Liu, X.; Chen, Y.; Chen, G.; Yang, Y. Forest conversion stimulated deep soil C losses and decreased C recalcitrance through priming effect in subtropical China. *Biol. Fertil. Soils* **2015**, *51*, 857–867. [CrossRef]
28. Lord, W.J.; Vlach, E. Responses of Peach Trees to Herbicides, Mulch, Mowing, and Cultivation. *Weed Sci.* **1973**, *21*, 227–229.
29. Zhang, X.; Li, Z.; Tang, Z.; Zeng, G.; Huang, J.; Guo, W.; Chen, X.; Hirsh, A. Effects of water erosion on the redistribution of soil organic carbon in the hilly red soil region of southern China. *Geomorphology* **2013**, *197*, 137–144. [CrossRef]
30. Wright, A.C. A model of the redistribution of disaggregated soil particles by rainsplash. *Earth Surf. Process. Landf.* **2010**, *12*, 583–596. [CrossRef]
31. Kateb, H.E.; Zhang, H.; Zhang, P.; Mosandl, R. Soil erosion and surface runoff on different vegetation covers and slope gradients: A field experiment in Southern Shaanxi Province, China. *Catena* **2013**, *105*, 1–10. [CrossRef]
32. Wei, L.; Zhang, B.; Wang, M. Effects of antecedent soil moisture on runoff and soil erosion in alley cropping systems. *Agric. Water Manag.* **2007**, *94*, 54–62. [CrossRef]
33. Zhang, Z.; Liu, S.; Dong, S. Ecological Security Assessment of Yuan River Watershed Based on Landscape Pattern and Soil Erosion. *Procedia Environ. Sci.* **2010**, *2*, 613–618. [CrossRef]
34. Vieira, D.C.S.; Fernández, C.; Vega, J.A.; Keizer, J.J. Does soil burn severity affect the post-fire runoff and interrill erosion response? A review based on meta-analysis of field rainfall simulation data. *J. Hydrol.* **2015**, *523*, 452–464. [CrossRef]
35. Klaminder, J.; Yoo, K.; Giesler, R. Soil carbon accumulation in the dry tundra: Important role played by precipitation. *J. Geophys. Res. Biogeosci.* **2009**, *114*, 126. [CrossRef]
36. Solaimani, K.; Modallaldoust, S.; Lotfi, S. Investigation of land use changes on soil erosion process using geographical information system. *Int. J. Environ. Sci. Technol.* **2009**, *6*, 415–424. [CrossRef]
37. Cotler, H.; Ortega-Larrocea, M.P. Effects of land use on soil erosion in a tropical dry forest ecosystem, Chamela watershed, Mexico. *Catena* **2006**, *65*, 107–117. [CrossRef]
38. Rodway-Dyer, S.J.; Walling, D.E. The use of 137Cs to establish longer-term soil erosion rates on footpaths in the UK. *J. Environ. Manag.* **2010**, *91*, 1952–1962. [CrossRef] [PubMed]
39. Mabit, L.; Klik, A.; Benmansour, M.; Toloza, A.; Geisler, A.; Gerstmann, U.C. Assessment of erosion and deposition rates within an Austrian agricultural watershed by combining 137Cs, 210Pbex and conventional measurements. *Geoderma* **2009**, *150*, 231–239. [CrossRef]
40. Sheng, L.; Lobb, D.A.; Kachanoski, R.G.; Mcconkey, B.G. Comparing the use of the traditional and repeated-sampling-approach of the 137 Cs technique in soil erosion estimation. *Geoderma* **2011**, *160*, 324–335.

41. Zhang, G.; Weiliang, G.U.; Shulan, J.I.; Liu, Z.; Peng, Y.; Wang, Z. Preparation of polyelectrolyte multilayer membranes by dynamic layer-by-layer process for pervaporation separation of alcohol/water mixtures. *J. Membr. Sci.* **2006**, *280*, 727–733. [CrossRef]
42. Silva, J.; Mello, J.W.V.; Abrahão, W.A.P.; Fontes, M.P.F.; Junior, L.S.; Ferreira, V.P.; Taddei, M.H.T.; Rocha, O.F.; Gilkes, R.J.; Prakongkep, N. Multi-element background for trace elements and radionuclides in soil from Minas Gerais State, Brazil. In Proceedings of the 19th World Congress of Soil Science: Soil Solutions for a Changing World, Brisbane, Australia, 1–6 August 2010; Symposium 3.5.2 Risk Assessment and Risk Based Remediation 2010; pp. 40–43.
43. Gosman, A.; Blažíček, J. Study of the diffusion of trace elements and radionuclides in soils. *J. Radioanal. Nucl. Chem.* **1994**, *182*, 179–191. [CrossRef]
44. Lu, J.G.; Huang, Y.; Li, F.; Wang, L.; Li, S.; Hsia, Y. The investigation of 137Cs and 90Sr background radiation levels in soil and plant around Tianwan NPP, China. *J. Environ. Radioact.* **2006**, *90*, 89–99. [CrossRef]
45. Zhang, M.L.; Yang, H.; Xu, C.A.; Yang, J.D.; Liu, X.H. A preliminary study on soil erosion in Yimeng mountainous area using Cs tracer. *Acta Pedol. Sin.* **2010**, *47*, 408–414.
46. Walling, D.E.; He, Q.; Blake, W. Use of 7Be and 137Cs measurements to document short- and medium-term rates of water-induced soil erosion on agricultural land. *Water Resour. Res.* **1999**, *35*, 3865–3874. [CrossRef]
47. Estifanos, A. Assessment Of Micro-Watershed Vulnerability For Soil Erosion In Ribb Watershed Using GIS And Remote Sensing. Ph.D. Thesis, Mekelle University, Mekelle, Ethiopia, 2014.
48. Jain, S.; Goel, M.K. Assessing the vulnerability to soil erosion of the Ukai Dam catchments using remote sensing and GIS. *Int. Assoc. Sci. Hydrol. Bull.* **2002**, *47*, 31–40. [CrossRef]
49. Zhao, Y.; Wang, E.; Cruse, R.M.; Chen, X. Characterization of seasonal freeze-thaw and potential impacts on soil erosion in northeast China. *Can. J. Soil Sci.* **2012**, *92*, 567–571. [CrossRef]
50. Clarke, P.J.; Prior, L.D.; French, B.J.; Vincent, B.; Knox, K.J.E.; Bowman, D.M.J.S. Using a rainforest-flame forest mosaic to test the hypothesis that leaf and litter fuel flammability is under natural selection. *Oecologia* **2014**, *176*, 1123–1133. [CrossRef]
51. Pan, C.; Wang, Q.; Ruan, X.; Li, Z. Biological Activity and Quantification of Potential Autotoxins from the Leaves of Picea Schrenkiana. *Chin. J. Plant Ecol.* **2009**, *27*, 245–262.
52. Pagel-Wieder, S.; Fischer, W.R. Short communication Estimation of the specific surface area of soil particles by adsorption of polyvinylalcohol in aqueous suspension. *J. Plant Nutr. Soil Sci.* **2015**, *164*, 441–443. [CrossRef]
53. Dolinar, B. Prediction of the soil-water characteristic curve based on the specific surface area of fine-grained soils. *Bull. Eng. Geol. Environ.* **2015**, *74*, 697–703. [CrossRef]
54. Dunjo, G.; Pardini, G.; Gispert, M. The role of land use-land cover on runoff generation and sediment yield at a microplot scale, in a small Mediterranean catchment. *J. Arid Environ.* **2004**, *57*, 239–256. [CrossRef]
55. Fang, Y.; Gundersen, P.; Vogt, R.D.; Koba, K.; Chen, F.; Xi, Y.C.; Yoh, M. Atmospheric deposition and leaching of nitrogen in Chinese forest ecosystems. *J. For. Res.* **2011**, *16*, 341–350. [CrossRef]
56. Koch, J.A.; Makeschin, F. Carbon and nitrogen dynamics in topsoils along forest conversion sequences in the Ore Mountains and the Saxonian lowland, Germany. *Eur. J. For. Res.* **2004**, *123*, 189–201. [CrossRef]
57. Wu, J.; Huang, J.; Liu, D.; Li, J.; Zhang, J.; Wang, H. Effect of 26 Years of Intensively Managed Carya cathayensis Stands on Soil Organic Carbon and Fertility. *Sci. World J.* **2014**, *2014*, 1–6.
58. Feng, W.; Zheng, S.; Jiang, J.; Xia, J.; Liang, J.; Zhou, J.; Luo, Y. Methodological uncertainty in estimating carbon turnover times of soil fractions. *Soil Biol. Biochem.* **2016**, *100*, 118–124. [CrossRef]
59. Guo, X.; Meng, M.; Zhang, J.; Chen, H.Y.H. Vegetation change impacts on soil organic carbon chemical composition in subtropical forests. *Sci. Rep.* **2016**, *6*, 29607. [CrossRef]
60. Chen, C.Y.; Hou, H.P.; Qiang, L.; Ping, Z.; Zhang, Z.Y.; Dong, Z.Q.; Ming, Z. Effects of planting density on photosynthetic characteristics and changes of carbon and nitrogen in leaf of different corn hybrids. *Acta Agron. Sin.* **2010**, *36*, 871–878. [CrossRef]
61. Abbasi, M.K.; Tahir, M.M.; Sabir, N.; Khurshid, M. Impact of the addition of different plant residues on nitrogen mineralization–immobilization turnover and carbon content of a soil incubated under laboratory conditions. *Solid Earth* **2015**, *6*, 197–205. [CrossRef]
62. Moldan, F.; Kjønaas, O.J.; Stuanes, A.O.; Wright, R.F. Increased nitrogen in runoff and soil following 13 years of experimentally increased nitrogen deposition to a coniferous-forested catchment at Gårdsjön, Sweden. *Environ. Pollut.* **2006**, *144*, 610–620. [CrossRef]

63. Wang, Y.; Fu, B.; Lü, Y.; Chen, L. Effects of vegetation restoration on soil organic carbon sequestration at multiple scales in semi-arid Loess Plateau, China. *Catena* **2011**, *85*, 58–66. [CrossRef]
64. Yuan, D.H.; Wang, Z.Q.; Chen, X.; Guo, X.B.; Zhang, R.L. Losses of nitrogen and phosphorus under different land use patterns in small red soil watershed. *Acta Ecol. Sin.* **2003**, *23*, 188–198.
65. Conant, R.T.; Paustian, K. Spatial variability of soil organic carbon in grasslands: Implications for detecting change at different scales. *Environ. Pollut.* **2002**, *116*, S127–S135. [CrossRef]
66. Dong, J.; Yang, D.Y.; Zhou, B.; Xu, Q.M. Study on Soil Erosion Rates in the Three Gorges Reservoir Area Using ~(137)Cs Tracing Method. *J. Soil Water Conserv.* **2006**, *20*, 1–5.

forests

MDPI

Article

Forest Soil Profile Inversion and Mixing Change the Vertical Stratification of Soil CO_2 Concentration without Altering Soil Surface CO_2 Flux

Xiaoling Wang [1,2], Shenglei Fu [2,3], Jianxiong Li [1], Xiaoming Zou [4], Weixin Zhang [2,3], Hanping Xia [2], Yongbiao Lin [2], Qian Tian [2] and Lixia Zhou [2,*]

1 Guangdong Key Laboratory of Animal Conservation and Resource Utilization, Guangdong Public Laboratory of Wild Animal Conservation and Utilization, Guangdong Institute of Applied Biological Resources, Guangzhou 510260, China; wangxl@giabr.gd.cn (X.W.); ljx196208@126.com (J.L.)

2 Key Laboratory of Vegetation Restoration and Management of Degraded Ecosystems, South China Botanical Garden, Chinese Academy of Sciences, Guangzhou 510650, China; sfu@scbg.ac.cn (S.F.); weixinzhang@139.com (W.Z.); xiahanp@scbg.ac.cn (H.X.); linyb@scib.ac.cn (Y.L.); tianqian@scbg.ac.cn (Q.T.)

3 Key Laboratory of Geospatial Technology for the Middle and Lower Yellow River Regions (Henan University), Ministry of Education, College of Environment and Planning, Henan University, Kaifeng 475004, China

4 Department of Environmental Sciences, College of Natural Sciences, University of Puerto Rico, P.O. Box 70377, San Juan, PR 00936-8377, USA; xzou2015@163.com

* Correspondence: zhoulx@scbg.ac.cn; Tel.: +86-020-3725-2977

Received: 28 December 2018; Accepted: 19 February 2019; Published: 21 February 2019

Abstract: In order to gain more detailed knowledge of the CO_2 concentration gradient in forest soil profiles and to better understand the factors that control CO_2 concentration along forest soil profiles, we examined the soil surface CO_2 flux, soil properties and soil profile CO_2 concentration in upright (CK), inverted and mixed soil columns with a depth of 60 cm in two subtropical forests in China from May 2008 to December 2009. The results showed that: (1) The SOC (soil organic carbon), TN (total N) and microbial biomass were higher in the deeper layers in the inverted soil column, which was consistent with an increase in CO_2 concentration in the deeper soil layer. Furthermore, the biogeochemical properties were homogenous among soil layers in the mixed soil column. (2) CO_2 concentration in the soil profile increased with depth in CK while soil column inversion significantly intensified this vertical stratification as the most active layer (surface soil) was now at the bottom. The stratification of CO_2 concentration along the soil profile in the mixed soil column was similar to that in CK but it was not intensified after soil was mixed. (3) The soil surface CO_2 flux did not significantly change after the soil column was inverted. The surface CO_2 flux rate of the mixed soil column was higher compared to that of the inverted soil column but was not significantly different from CK. Our results indicated that the profile soil CO_2 production was jointly controlled by soil properties related to CO_2 production (e.g., SOC content and soil microbial biomass) and those related to gas diffusion (e.g., soil bulk density and gas molecular weight), but the soil surface CO_2 flux was mainly determined by soil surface temperature and may be affected by the intensity of soil disturbance.

Keywords: CO_2 production and diffusion; soil properties; CO_2 emission; surface soil layer

1. Introduction

An increase in atmospheric CO_2 concentration is considered to be one of the main causes for global warming [1,2]. As the largest terrestrial source and potential sink for CO_2, soil is particularly important in the global carbon cycle [3–7]. All CO_2 produced in the soil would be emitted through soil

surface efflux on a long-term basis [8]. The soil profile CO_2 concentration was reported to drive and accelerate this surface emission process [9] and therefore, this would influence the carbon balance of the forest. Some models estimated the soil CO_2 effluxes from the soil CO_2 concentration profiles [10–12]. Thus, we need to gain more detailed knowledge of the soil profile CO_2 concentration in order to better assess its contribution to soil surface CO_2 emission and global warming.

The majority of the forest soil CO_2 is produced in the surface layer since the majority of SOM (soil organic matter) and roots are distributed in the surface soil. However, the soil profile CO_2 concentration is high in the deep soil layer and low in the surface soil, which is the opposite to the production source layer [13]. Microbial biomass acts as both a source and sink for nutrients and participates in C, N and P transformation. Although it contributes less than 5% to SOM, it plays an active role in the soil C cycle [14]. The soil profile CO_2 concentration depends on both the processes of CO_2 production and diffusion. Studies have shown that soil CO_2 production and diffusion often has a strong and remarkable dependence on temperature and moisture [15–17]. It was also affected by soil properties, such as soil organic matter, total N (TN) and bulk density, root dynamics and microbial biomass [18,19]. However, there were limited studies focused on the relationship between the variation of soil properties and soil CO_2 concentration.

Agricultural practice, such as tillage, plays an important role in the storage and release of C within the terrestrial C cycle. The conventional intensive tillage was found to increase the emission of CO_2 by 16.0% in a subtropical rice farm [20]. Significantly greater CO_2 fluxes were also observed in subtropical paddy ecosystems after tillage operations [21]. Tillage disturbance does not occur as frequently as croplands in forests but during the process of restoring damaged ecosystems, tree planting and occasionally tillage are usual practices. Consequently, soil mixing is inevitable during ploughing.

In the present study, we manipulated a soil column experiment with upright, inverted and mixed soil columns in order to investigate the soil surface CO_2 flux, the distribution of CO_2 concentration in soil profiles and their influencing factors. The field site was a forest restoration ecosystem. We mixed the soil in "mixed" columns to identify the influence of "tillage" disturbance on soil CO_2. The purpose of our study was to examine the dependence of soil profile CO_2 concentration on soil properties in order to better understand the mechanism of the vertical stratification of soil profile CO_2 concentration and the relationship of soil profile CO_2 with soil surface CO_2 flux.

2. Materials and Methods

2.1. Study Area

The study was conducted over a 20-month period (from May 2008 to December 2009) in two subtropical plantation forests at the Heshan Hilly Land Interdisciplinary Experimental Station (112°50′ E, 22°34′ N), Guangdong Province, China. These selected forests included a coniferous forest (CF) mixed by Pinus massoniana lamb, Cunninghamia lanceolata (lamb) Hook and a broad-leaved forest (BF) dominated by Schima wallichii Choisy. The soil of the field site was an Orthic Acrisol [22] and the surface soil pH was about 4.0. The soil SOC (soil organic carbon) was 13.08 and 19.26 g kg^{-1} while the TN was 0.99 and 1.11 g kg^{-1} in CF and BF, respectively. The trees were about 25 years old when the current experiment started in 2008.

2.2. Experimental Design and Sample Analysis

A randomized block design with six replicates for each treatment was used in the soil column manipulation experiment. The soil column treatments were: (1) Upright soil column (CK); (2) inverted soil column (Inverted); and (3) mixed soil column (Mixed). The soil pillar was carefully dug and sheathed in the PVC (polyvinyl chloride) pipe to make a soil column cylinder. Each soil column had a diameter of 40 cm and a depth of 60 cm. In the upright and inverted soil columns, the soil pillar was undisturbed but in the mixed soil column, the topsoil and subsoil were thoroughly mixed. All soil columns were sealed at the bottom and placed back into the original location where the soil column

was manipulated. Each soil column was equipped with gas tubes and three-way stopcocks at depths of 20, 40 and 60 cm to sample soil CO_2 while a water tube was added at the bottom to sample the dissolved soil organic carbon and to avoid waterlog (Figure A1). Several holes with a diameter of 2 cm were made onto the wall of the PVC pipe to allow for the free exchange of soil air. All vegetation and litter fall were removed carefully from the soil surface of each soil column and were not present during the experiment period, which was achieved without disturbing the soil. All these manipulations were completed in May 2008.

We measured the soil surface CO_2 flux for each column once per month with the static chamber-gas chromatograph (GC) technique [23] from May 2008 to December 2009. PVC chamber with a diameter of 20 cm and a height of 20 cm was gently inserted 2 cm below the soil. Gas samples were collected four times at 10 min intervals from each soil column with 60 mL polypropylene syringes. Measurements were always made between 09:00 and 11:00 as suggested by Xu and Qi to represent the diurnal averages [19,24,25]. Soil CO_2 concentrations at depths of 20, 40 and 60 cm were sampled after the surface measurements and were determined using GC within 24 h. The soil temperature at depths of 5, 20, 40 and 60 cm was recorded every 0.5 h with an iButton DS1923 digital thermometer equipped in the soil column.

Gas flux was calculated based on the soil surface gas concentration change within the chamber over the measurement period, which was estimated as the slope of linear regression between concentration and time. It was expressed in the following equation [26]:

$$F = \frac{\Delta m}{\Delta t} \cdot D \frac{V}{A} = hD \frac{\Delta m}{\Delta t} \quad (1)$$

where F is the gas flux (mg m^{-2} h^{-1}); h is the height of the chamber (m); D is the gas density in the chamber ($D = n/v = P/RT$, in mg m^{-3} where P is the air pressure; T is the temperature inside of the chamber and R is the air constant; $\triangle m/\triangle t$ denotes the linear slope of concentration changing with time over the measurement period.

The soil along the profiles was sampled in May and November both in 2008 and 2009. All soil samples were sieved with a 2 mm sieve before analysis. Soil water content (SWC) was measured by oven-drying for 48 h at 105 °C; SOC was determined by the dichromate oxidation method; soil TN was estimated by Kjeldahl digestion with UV spectrophotometric analysis [27]; and soil bulk density was determined by the intact soil core method. The soil microbial biomass and community structure was analyzed using the phospholipid fatty acids (PLFAs) method as described by Bossio and Scow [28]. Different PLFAs were considered to represent different groups of soil microorganisms. The abundance of individual fatty acids was calculated based on the 19:0 internal standard concentrations. Bacteria were identified by 10 PLFAs (i15:0, a15:0, 15:0, i16:0, 16: 1ω7, i17:0, a17:0, 17:0, cy17:0 and cy19:0) while 18:2ω6c and 18:1ω9c were used as the indicators of fungal biomass [29]. The ratio of fungal PLFAs to bacterial PLFAs was used to estimate the ratio of fungal to bacterial biomass (F/B) in soil [30]. The results of soil properties were the average of four measurements.

2.3. Statistical Analysis

A repeated measures analysis of variance (RM ANOVA) was performed to examine the monthly changes in CO_2 concentration and the soil surface CO_2 flux. Two-way ANOVA and LSD (least significant difference) tests were performed to compare the physicochemical and microbial traits among forest types and soil treatments. All statistics were performed using IBM SPSS Statistics 21 (IBM Corporation, New York, NY, USA) and SigmaPlot 12.5 (Systat Software Inc., San Jose, CA, USA).

3. Results

3.1. Precipitation and Air Temperature

The annual precipitation of the site was 1319.6 mm and 1525.6 mm while the average temperature was 21.60 °C and 22.49 °C in 2008 and 2009, respectively. The precipitation from May to September (high temperature period, monthly mean temperature >25 °C) in 2008 was 922.60 mm, which was significantly less than that in the same period in 2009 (1148.20 mm). The mean air temperature was 26.95 °C in this period in 2008, which was lower by 0.62 °C compared to 2009 (Figure A2). The mean soil temperature at a depth of 5 cm was 24.73 °C in CF in the study period, which was higher by 1.29 °C compared to BF.

3.2. Variation of Soil Profile CO_2 Concentration

Large variations of CO_2 concentration in soil profiles were observed both throughout time and with different depths in all treatments (Figure 1a–f). In general, the CO_2 concentration increased with depth, with the highest concentrations observed at a depth of 60 cm. CO_2 concentrations in soil profiles were quite different between the two years, with the peak accumulation having occurred in the high temperature period of the second year. The CO_2 concentration in the BF soil was higher than that in the CF soil.

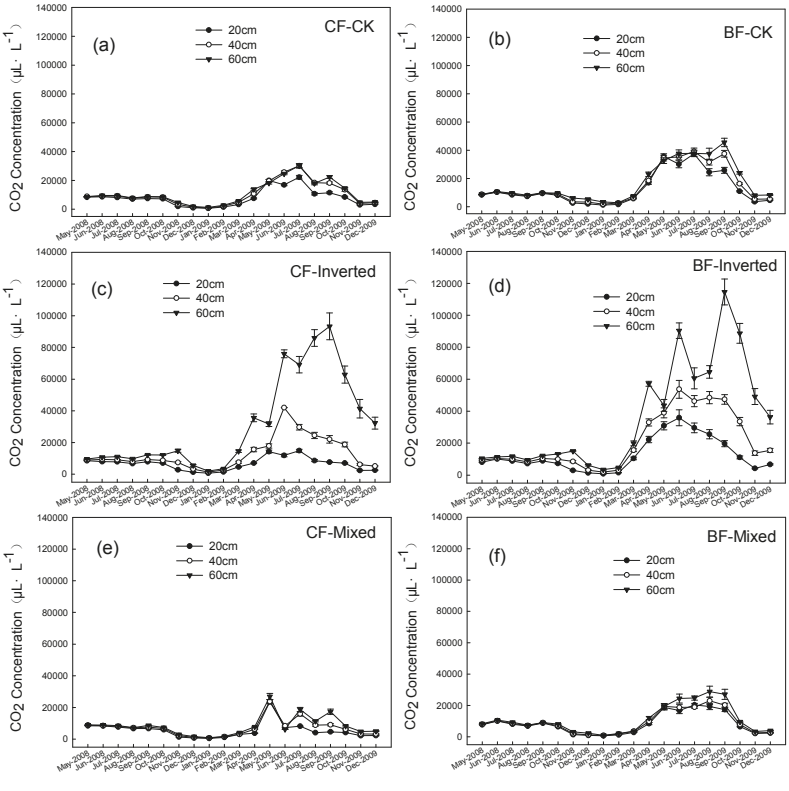

Figure 1. Seasonal variations of CO_2 concentration along soil profiles in a coniferous forest (CF) and a broad-leaved forest (BF). Different soil column treatments were: (**a**) CF-CK (upright soil column); (**b**) BF-CK; (**c**) CF-Inverted; (**d**) BF-Inverted; (**e**) CF-Mixed; and (**f**) BF-Mixed. Data are shown as means ± SE, $n = 6$.

The average CO_2 concentration in CF at a depth of 60 cm was 1.1×10^4 $\mu L \cdot L^{-1}$, which was 39% higher than that in 20 cm. The CO_2 concentration in the inverted soil column at a depth of 60 cm reached 3.2×10^4 $\mu L \cdot L^{-1}$, which was about 4.8 times that of the 20 cm. In other words, the vertical stratification of CO_2 concentration in the soil profile was intensified in the inverted soil column compared to CK. In the mixed soil columns, the CO_2 concentration in each layer was lower than CK. Similar patterns were observed in BF, which showed that the inverted soil column intensified the stratification of CO_2 concentrations in soil profiles, while CO_2 concentrations in the "Mixed" soil column were lower than CK despite still maintaining its stratification.

3.3. Seasonal Variation of Soil Surface CO_2 Flux

Soil surface CO_2 flux rates varied significantly during the study period, with higher CO_2 flux rates observed during the summer both in BF and CF (Figure 2a,b). The repeated measures analyses of variance indicated a significant interaction between months and treatments ($p < 0.001$). The average soil surface CO_2 flux rates in CF were 185.69, 155.70 and 201.81 mg m^{-2} h^{-1} for the CK, inverted and mixed soil columns, respectively. In BF, the rates were 183.42, 159.95 and 197.70 mg m^{-2} h^{-1}, respectively. The soil surface CO_2 flux rates of the inverted soil column were 13%–16% lower than CK while that of the "mixed" soil column were somewhat higher although these differences were not significant. However, soil surface CO_2 flux rates of the "mixed" soil column was significantly higher than that in the inverted soil column in BF ($p < 0.05$). Soil surface CO_2 flux rates from CF did not significantly differ from the rates measured in BF.

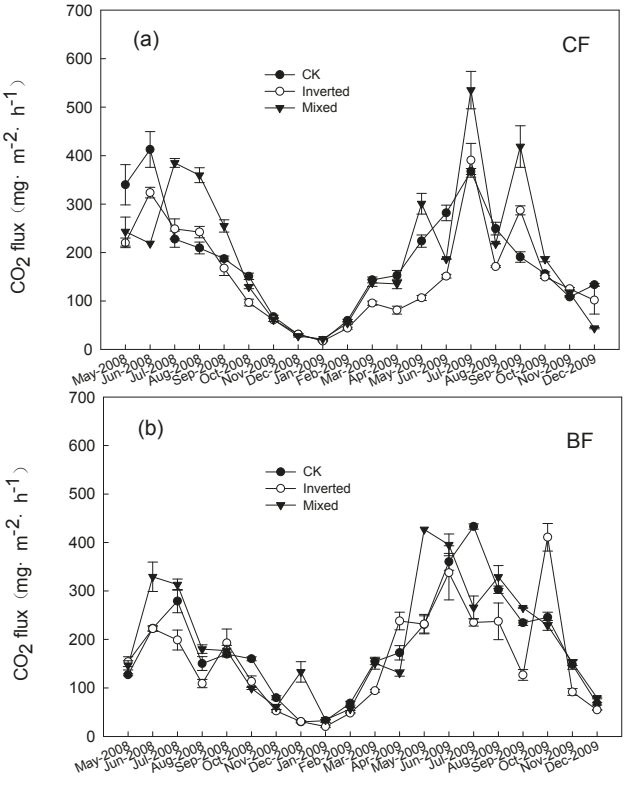

Figure 2. Fluxes of CO_2 in a coniferous forest (CF) (**a**) and a broad-leaved forest (BF) (**b**) in different soil column treatments: CK, inverted and mixed. Error bars represent standard errors of the mean ($n = 6$).

3.4. Soil Biogeochemical Properties in Different Columns

The SOC (at a depth of 0–20 cm) was significantly higher in the BF soil than in the CF soil ($p < 0.05$, Table 1). SWC, TN and bulk density did not differ between the two forests. In the upright soil column, the SOC and TN in the topsoil were significantly higher than in the subsoil ($p < 0.05$) while the soil bulk density was higher in the subsoil. Naturally, the opposite pattern was observed in the inverted soil column, which showed that SOC and TN were higher in "new subsoil" but soil bulk density was higher in the "new topsoil". In the mixed soil column, all measured soil properties did not differ significantly among the three soil layers.

Table 1. Soil physical and chemical properties by depth and soil columns manipulation, including soil water content (SWC), total organic carbon (TOC), total nitrogen (TN) and bulk density. Error bars represent the standard errors of the mean ($n = 4$). Different letters represent significant differences (LSD test, $p < 0.05$).

Forest Type	Treatments	Profile	SWC (%)	SOC ($g \cdot kg^{-1}$)	TN ($mg \cdot L^{-1}$)	Bulk Density ($g \cdot cm^{-3}$)
CF	CK	0–20 cm	19.66 ± 4.00a	13.09 ± 2.74a	1.17 ± 0.14a	1.40 ± 0.05a
		20–40 cm	18.95 ± 2.54a	7.62 ± 2.21b	0.83 ± 0.18b	1.48 ± 0.06a
		40–60 cm	19.93 ± 2.97a	5.75 ± 1.45b	0.70 ± 0.10b	1.48 ± 0.08a
	Inverted	0–20 cm	19.08 ± 3.21a	5.98 ± 1.00b	0.66 ± 0.15b	1.49 ± 0.02a
		20–40 cm	20.04 ± 1.86a	6.17 ± 1.76b	0.71 ± 0.20b	1.46 ± 0.11ab
		40–60 cm	21.36 ± 2.58a	10.12 ± 2.98a	0.99 ± 0.20a	1.35 ± 0.09b
	Mixed	0–20 cm	20.19 ± 2.63a	10.89 ± 1.82a	0.97 ± 0.18a	1.31 ± 0.03a
		20–40 cm	21.04 ± 2.67a	9.25 ± 1.35a	0.94 ± 0.16a	1.30 ± 0.05a
		40–60 cm	21.80 ± 1.53a	9.42 ± 0.69a	0.90 ± 0.16a	1.28 ± 0.09a
BF	CK	0–20 cm	23.15 ± 1.82a	17.25 ± 1.53a	1.42 ± 0.41a	1.39 ± 0.02b
		20–40 cm	21.07 ± 2.15a	6.97 ± 1.94b	0.81 ± 0.29b	1.55 ± 0.05a
		40–60 cm	21.44 ± 1.60a	4.76 ± 1.54b	0.68 ± 0.33b	1.48 ± 0.08a
	Inverted	0–20 cm	20.15 ± 1.82a	5.51 ± 1.44b	0.75 ± 0.41a	1.39 ± 0.09a
		20–40 cm	20.62 ± 2.51a	5.31 ± 1.49b	0.76 ± 0.31a	1.48 ± 0.10a
		40–60 cm	23.29 ± 1.83a	12.79 ± 5.54a	1.15 ± 0.29a	1.39 ± 0.02a
	Mixed	0–20 cm	21.80 ± 2.31a	9.43 ± 2.16a	0.97 ± 0.33a	1.32 ± 0.08a
		20–40 cm	22.22 ± 1.57a	9.18 ± 3.01a	0.92 ± 0.21a	1.35 ± 0.03a
		40–60 cm	22.50 ± 3.93a	8.33 ± 2.22a	0.96 ± 0.40a	1.32 ± 0.04a

In the upright soil columns, the mean total soil microbial biomass (PLFA), fungal biomass, bacterial biomass and F/B ratio all decreased with depth both in CF and BF soil (Table 2). In the inverted soil column, bacterial biomass was higher in the "new subsoil" while fungal biomass was higher in the "new topsoil". In the mixed soil column, the biogeochemical properties were homogenous among different soil layers.

Table 2. Soil microbial community characters in each soil layer over all manipulated soil columns. PLFA, total PLFA; Fun, fungi; Bac, Bacteria; F/B, the ratio of fungal to bacterial biomass. Error bars represent the standard errors of the mean ($n = 4$). Different letters represent significant differences (LSD test, $p < 0.05$).

Forest Type	Treatments	Profile	PLFA ($nmol \cdot g^{-1}$)	Fun (mol%)	Bac (mol%)	F/B%
CF	CK	0–20 cm	6.34 ± 3.52a	4.14 ± 1.34a	28.64 ± 5.76a	14.69 ± 4.23a
		20–40 cm	4.07 ± 2.24a	1.99 ± 0.98ab	21.33 ± 8.61b	10.75 ± 6.12a
		40–60 cm	4.15 ± 2.30a	1.53 ± 1.12b	17.86 ± 4.93b	8.89 ± 5.83a
	Inverted	0–20 cm	5.45 ± 2.66a	3.52 ± 3.39a	17.39 ± 3.31b	19.64 ± 18.31a
		20–40 cm	4.72 ± 2.25a	1.18 ± 0.72a	17.06 ± 3.36b	7.34 ± 4.67b
		40–60 cm	5.10 ± 1.90a	2.94 ± 0.51a	27.51 ± 6.05a	11.18 ± 4.54a
	Mixed	0–20 cm	7.31 ± 4.60a	5.01 ± 2.60a	27.25 ± 3.00a	17.43 ± 8.86a
		20–40 cm	5.57 ± 2.73a	3.21 ± 0.89a	25.28 ± 3.84a	12.09 ± 3.37a
		40–60 cm	5.45 ± 1.77a	2.76 ± 0.56a	25.83 ± 2.10a	10.19 ± 2.06a

Table 2. *Cont.*

Forest Type	Treatments	Profile	PLFA (nmol·g^{-1})	Fun (mol%)	Bac (mol%)	F/B%
BF	CK	0–20 cm	10.55 ± 1.92a	3.35 ± 1.90a	24.24 ± 6.24a	13.04 ± 5.24a
		20–40 cm	7.75 ± 1.94a	2.05 ± 0.74a	20.83 ± 3.85a	9.79 ± 4.14a
		40–60 cm	6.23 ± 1.05b	0.98 ± 0.60a	14.37 ± 3.15b	7.32 ± 4.10a
	Inverted	0–20 cm	6.54 ± 1.55a	3.71 ± 4.90a	16.79 ± 3.93a	8.46 ± 4.25a
		20–40 cm	6.83 ± 2.49a	1.39 ± 0.41a	18.38 ± 3.64a	8.81 ± 3.39a
		40–60 cm	7.11 ± 0.96a	1.74 ± 0.48a	21.24 ± 1.06a	8.93 ± 1.67a
	Mixed	0–20 cm	7.05 ± 2.27a	2.21 ± 2.04a	20.96 ± 4.47a	9.88 ± 8.07a
		20–40 cm	8.49 ± 2.37a	1.44 ± 1.30a	16.15 ± 6.37a	8.19 ± 5.49a
		40–60 cm	9.10 ± 3.08a	1.32 ± 1.11a	16.32 ± 4.66a	7.93 ± 4.95a

3.5. Correlations of Soil CO_2 Concentration and Temperature

The dependence of soil CO_2 concentration on temperature was strong and consistent in two forests in the CK and mixed soil columns (Figure 3a–f). The relationship was well fit by an exponential growth regression model ($p < 0.001$). The temperature explained 26%–76% of the variation in soil CO_2 concentration in the upright and mixed soil columns. In the inverted soil columns, this dependence was significantly weaker.

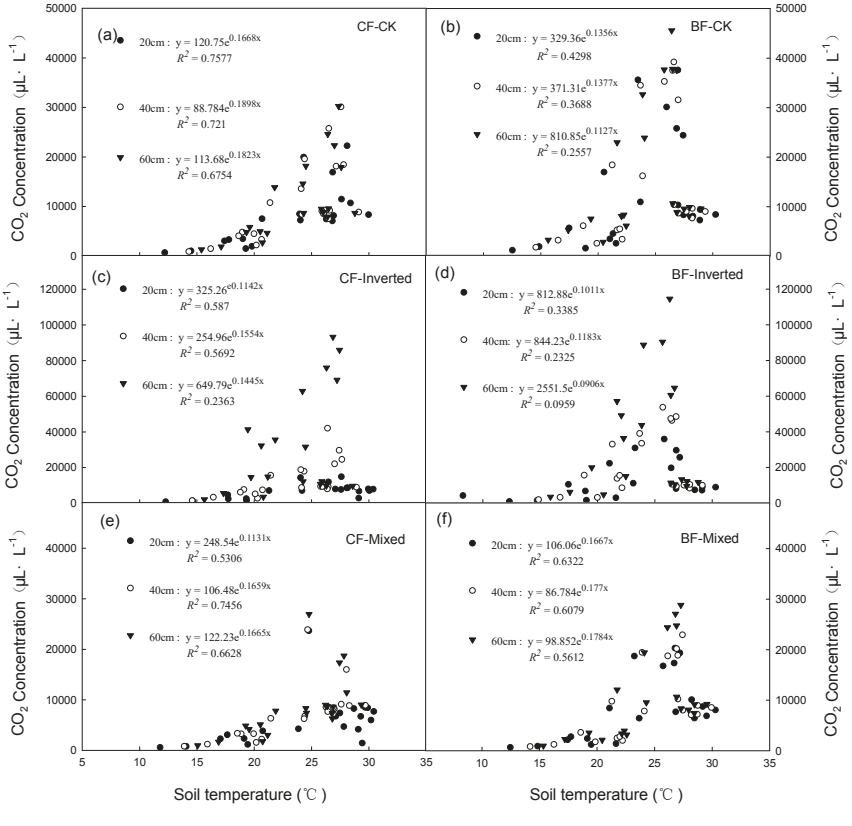

Figure 3. Relationship between soil profile CO_2 concentration and soil temperature. Different soil column treatments were: (**a**) CF-CK; (**b**) BF-CK; (**c**) CF-Inverted; (**d**) BF-Inverted; (**e**) CF-Mixed; and (**f**) BF-Mixed.

4. Discussion

4.1. Effects of Environment Variables on CO_2 Concentration in Soil Profiles and Soil Surface CO_2 Flux

In general, the soil CO_2 concentration was greater in the deeper soil layer regardless of the way that the soil columns were manipulated in the present study. We considered that this was mainly due to the difficulty of CO_2 diffusion within the soil profile to the atmosphere [15]. Studies have demonstrated that the molecular diffusion trait is the most important factor affecting CO_2 transportation within the soil profile. Furthermore, this was strongly dependent on soil porosity, which was closely related to soil moisture [9]. Rainfall could lead to an increase in soil moisture and a decrease in CO_2 diffusivity, which would subsequently result in CO_2 accumulation in soil and increase the CO_2 concentration in deep soil [16]. Our data also showed that CO_2 concentration in soil profiles increased with the seasonal temperature rise, which was probably due to an increase in soil microbial respiration with increasing temperature. This suggests that temperature is also a major factor that influences CO_2 concentration along the soil profile. The summer of 2009 was relatively hotter and wetter than the summer of 2008 during the study period, which resulted in a significantly higher CO_2 concentration in the summer of 2009 thus, verifying that temperature and moisture are major factors determining soil CO_2 concentration.

4.2. Soil Properties and Soil CO_2 Concentration Stratification

The inverted soil column was found to intensify the stratification of CO_2 concentration due to the replacement of the subsoil with the original topsoil. In this case, the SOC, TN and microbial biomass were higher in the deeper layer in the inverted soil column, which was consistent with an increase in CO_2 concentration in the deeper soil layer. SOC and TN provide energy and nutrients for microbial growth and thus, the CO_2 in the soil profiles mainly resulted from microbial activity. In addition, the higher soil bulk density in the "new topsoil" in the inverted soil column would have a negative effect on CO_2 emission from the soil since CO_2 diffusion within the soil profile depends on soil porosity, which is tied closely with soil bulk density.

As we observed, soil organic carbon, total nitrogen and microbial biomass were often higher in original topsoil and they coincided with higher CO_2 production. However, the soil CO_2 concentration was generally higher in the deeper soil layer. Furthermore, soil properties in the mixed soil columns did not differ significantly among soil layers but the CO_2 concentration along the soil profile showed a clear stratification. These results indicated that although CO_2 concentration was highly influenced by soil properties, it was the gravity that determined the vertical distribution of soil CO_2 concentration since the molecular weight of CO_2 is greater than air.

4.3. CO_2 Profile Concentration and its Relationship to Soil Surface CO_2 Flux

The surface CO_2 flux rates of the mixed soil column were 8%–9% higher than those in CK although these were not statistically significantly. This was much less than those in the croplands under conventional tillage [20,21]. Soil profile CO_2 is transported into the atmosphere primarily by diffusion and air turbulence at the forest soil surface, which could significantly impact the carbon balance of the forest ecosystem [31,32]. These important processes often occurred near the soil surface but had little effect on the subsoil CO_2 storage. Wiaux et al. [10] observed that approximately 90%–95% of the surface CO_2 fluxes originated from the top 10 cm of the soil profile. On one hand, the upward movement of CO_2 is a slow process limited by soil surface texture and turbulence. On the other hand, CO_2 has the tendency to sink down along the soil profile as the molecular weight of CO_2 is heavier than the average molecular weight of air [13].

In the present study, it is important to note that soil column inversion significantly intensified the vertical stratification of soil profile CO_2 concentration. However, this did not intensify soil surface CO_2 flux rate, which was even lower compared to CK. In contrast, soil column mixing increased the soil surface CO_2 flux to some extent (although this was not statistically significant). C content in BF

in the topsoil was 32% more than that in CF, while the soil surface CO_2 flux rates from BF were not significantly different from those in CF. These results suggested that CO_2 production was stimulated by the increased CO_2 production sources (SOC, TN and microbial communities) while surface soil CO_2 exchange could be altered by changing the soil texture (i.e., soil bulk density) and soil surface temperature (mean soil temperature at a depth of 5 cm was 1.29 °C higher in CF than in BF).

5. Conclusions

The soil profile CO_2 concentration appeared to be strongly affected by environmental factors (temperature and precipitation) and soil properties (SOC, TN, soil bulk density and microbial communities) in the current study. The surface CO_2 fluxes rates remained relatively stable when the CO_2 concentration in soil profile was increased to a significant extent. These results increased our understanding of the factors influencing CO_2 concentration in forest soil profile and the relationship of soil profile CO_2 with soil surface CO_2 flux. We concluded that the interaction of soil properties and environmental factors controlled the CO_2 production in the soil profile, but the soil surface CO_2 emission could be affected by the intensity of the disturbance or soil temperature variation. Although all CO_2 produced in the soil would be eventually emitted to the atmosphere through soil surface efflux on a long-term basis, CO_2 stored in the subsoil may be relatively stable in the deeper soil layers.

Author Contributions: Data curation, X.W. and Q.T.; formal analysis, X.W.; funding acquisition, J.L. and H.X.; investigation, X.W., Y.L. and Q.T.; project administration, S.F. and L.Z.; supervision, S.F.; writing—original draft, X.W.; writing—review and editing, X.Z. and W.Z.

Funding: This research was funded by the National Natural Science Foundation of China, grant numbers 41501268 and 30771704; and GDAS' Project of Science and Technology Development, grant number 2019GDASYL-0103060 and 2018GDASCX-0107.

Acknowledgments: We thank Dima Chen for advice on the content and Xingquan Rao and Heshan Station for providing meteorological data. We thank Yanmei Xiong for improving the English of this manuscript. We are grateful to the editors and the three anonymous reviewers for helpful comments on the manuscript.

Conflicts of Interest: The authors declare no conflicts of interest.

Appendix A

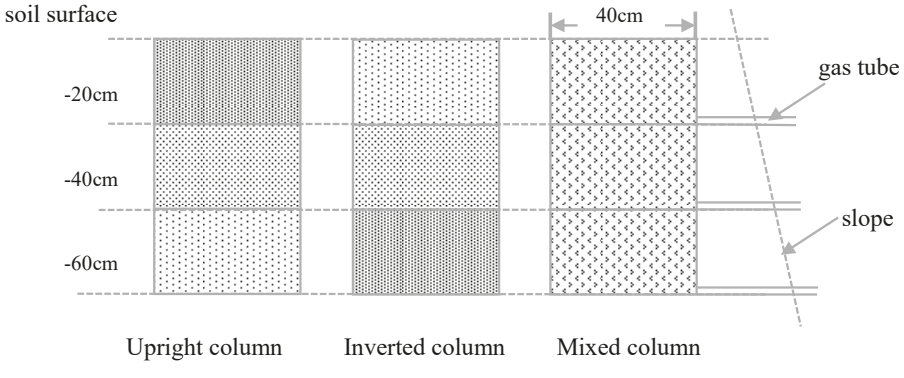

Figure A1. Diagram depicting soil column manipulation for field measurements of CO_2.

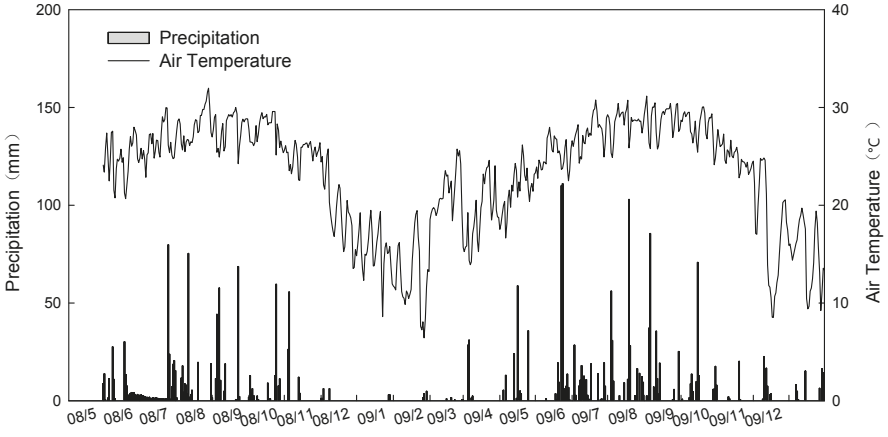

Figure A2. Precipitation and air temperature in Heshan station during the study period.

References

1. Houghton, J.T.; Meira-Filho, L.G.; Callander, B.A.; Harris, N. *Climate Change 1995: The Science of Climate Change*; Kathenberg, N., Maskell, K., Eds.; Cambridge University Press: New York, NY, USA, 1996.
2. Stocker, T.F.; Qin, D.; Plattner, G.K.; Tignor, M.; Allen, S.K.; Boschung, J.; Nauels, A.; Xia, Y. *Climate Change: The Physical Science Basis*; Bex, V., Midgley, P.M., Eds.; Cambridge University Press: New York, NY, USA, 2013.
3. Grüning, M.M.; Germeshausen, F.; Thies, C.; L.-M.-Arnold, A. Increased forest soil CO_2 and N_2O emissions during insect infestation. *Forests* **2018**, *9*, 612. [CrossRef]
4. Lee, S.; Yim, J.; Son, Y.; Son, Y.; Kim, R. Estimation of forest carbon stocks for national greenhouse gas inventory reporting in south Korea. *Forests* **2018**, *9*, 625. [CrossRef]
5. Schlesinger, W.H.; Andrews, J.A. Soil respiration and the global carbon cycle. *Biogeochemistry* **2000**, *48*, 7–20. [CrossRef]
6. Valentini, R.; Matteucci, G.; Dolman, A.J.; Schulze, E.D.; Rebmann, C.; Moors, E.J.; Granier, A.; Gross, P.; Jensen, N.O.; Pilegaard, K.; et al. Respiration as the main determinant of carbon balance in European forests. *Nature* **2000**, *404*, 861–865. [CrossRef] [PubMed]
7. Raich, J.W.; Schlesinger, W.H. The global carbon-dioxide flux in soil respiration and its relationship to vegetation and climate. *Tellus B* **1992**, *44*, 81–99. [CrossRef]
8. Maier, M.; Schack-Kirchner, H.; Hildebrand, E.E.; Schindler, D. Soil CO_2 efflux vs. soil respiration: Implications for flux models. *Agric. For. Meteorol.* **2011**, *151*, 1723–1730. [CrossRef]
9. Pihlatie, M.; Pumpanen, J.; Rinne, J.; Ilvesniemi, H.; Simojoki, A.; Hari, P.; Vesala, T. Gas concentration driven fluxes of nitrous oxide and carbon dioxide in boreal forest soil. *Tellus B* **2007**, *59*, 458–469. [CrossRef]
10. Wiaux, F.; Vanclooster, M.; Van-Oost, K. Vertical partitioning and controlling factors of gradient-based soil carbon dioxide fluxes in two contrasted soil profiles along a loamy hillslope. *Biogeosciences* **2015**, *12*, 4637–4649. [CrossRef]
11. Tang, J.W.; Baldocchi, D.D.; Qi, Y.; Xu, L.K. Assessing soil CO_2 efflux using continuous measurements of CO_2 profiles in soils with small solid-state sensors. *Agric. For. Meteorol.* **2003**, *118*, 207–220. [CrossRef]
12. Maier, M.; Schack-Kirchner, H. Reply to comment on "Using the gradient method to determine soil gas flux: A review". *Agric. For. Meteorol.* **2014**, *197*, 256–257. [CrossRef]
13. Luo, Y.Q.; Zhou, X.H. Processes of CO_2 transport from soil to the atmosphere. In *Soil Respiration and the Environment*; Elsevier Inc.: Amsterdam, The Netherlands, 2006; pp. 61–76.
14. Hopkins, D.W.; Sparrow, A.D.; Shillam, L.L.; English, L.C.; Dennis, P.G.; Novis, P. Enzymatic activities and microbial communities in an antarctic dry valley soil: Responses to c and n supplementation. *Soil Biol. Biochem.* **2008**, *40*, 2130–2136. [CrossRef]
15. Risk, D.; Kellman, L.; Beltrami, H. Carbon dioxide in soil profiles: Production and temperature dependence. *Geophys. Res. Lett.* **2002**, *29*, 111–114. [CrossRef]

16. Jassal, R.; Black, A.; Novak, M.; Morgenstern, K.; Nesic, Z.; Gaumont-Guay, D. Relationship between soil CO_2 concentrations and forest-floor CO_2 effluxes. *Agric. For. Meteorol.* **2005**, *130*, 176–192. [CrossRef]
17. Albanito, F.; Saunders, M.; Jones, M.B. Automated diffusion chambers to monitor diurnal and seasonal dynamics of the soil CO_2 concentration profile. *Eur. J. Soil Sci.* **2009**, *60*, 507–514. [CrossRef]
18. Billings, S.A.; Richter, D.D.; Yarie, J. Soil carbon dioxide fluxes and profile concentrations in two boreal forests. *Can. J. For. Res.* **1998**, *28*, 1773–1783. [CrossRef]
19. Xu, M.; Qi, Y. Soil-surface CO_2 efflux and its spatial and temporal variations in a young ponderosa pine plantation in northern California. *Glob. Chang. Biol.* **2001**, *7*, 667–677. [CrossRef]
20. Zhang, Z.S.; Cao, C.G.; Guo, L.J.; Li, C.F. Emissions of CH_4 and CO_2 from paddy fields as affected by tillage practices and crop residues in central china. *Paddy Water Environ.* **2016**, *14*, 85–92. [CrossRef]
21. Li, C.F.; Kou, Z.K.; Yang, J.H.; Cai, M.L.; Wang, J.P.; Cao, C.G. Soil CO_2 fluxes from direct seeding rice fields under two tillage practices in central China. *Atmos. Environ.* **2010**, *44*, 2696–2704. [CrossRef]
22. FAO. *World Reference Base for Soil Resources 2006*; World Soil Resources Report; FAO: Rome, Italy, 2006; p. 103.
23. Wang, Y.S.; Wang, Y.H. Quick measurement of CH_4, CO_2 and N_2O emissions from a short-plant ecosystem. *Adv. Atmos. Sci.* **2003**, *20*, 842–844.
24. Larionova, A.A.; Rozonova, L.N.; Samoylov, T.I. Dynamics of gas exchange in the profile of a gray forest soil. *Sov. Soil Sci.* **1989**, *24*, 1359–1372.
25. Jian, J.S.; Steele, M.K.; Day, S.D.; Quinn, T.R.; Hodges, S.C. Measurement strategies to account for soil respiration temporal heterogeneity across diverse regions. *Soil Biol. Biochem.* **2018**, *125*, 167–177. [CrossRef]
26. Zhou, C.Y.; Zhou, G.Y.; Zhang, D.Q.; Wang, Y.H.; Liu, S.Z. CO_2 efflux from different forest soils and impact factors in Dinghu Mountain, China. *Sci. China Ser. D* **2005**, *48*, 198–206.
27. Liu, G. *Analysis of Soil Physical and Chemical Properties and Description of Soil Profiles*; China Standard: Beijing, China, 1996.
28. Bossio, D.A.; Scow, K.M. Impacts of carbon and flooding on soil microbial communities: Phospholipid fatty acid profiles and substrate utilization patterns. *Microb. Ecol.* **1998**, *35*, 265–278. [CrossRef] [PubMed]
29. Frostegard, A.; Baath, E. The use of phospholipid fatty acid analysis to estimate bacterial and fungal biomass in soil. *Biol. Fert. Soils* **1996**, *22*, 59–65. [CrossRef]
30. Baath, E.; Anderson, T.H. Comparison of soil fungal/bacterial ratios in a pH gradient using physiological and PLFA-based techniques. *Soil Biol. Biochem.* **2003**, *35*, 955–963. [CrossRef]
31. Massman, W.J.; Sommerfeld, R.A.; Mosier, A.R.; Zeller, K.F.; Hehn, T.J.; Rochelle, S.G. A model investigation of turbulence-driven pressure-pumping effects on the rate of diffusion of CO_2, N_2O and CH_4 through layered snow packs. *J. Geophys. Res.-Atmos.* **1997**, *102*, 18851–18863. [CrossRef]
32. Bowling, D.R.; Massman, W.J. Persistent wind-induced enhancement of diffusive CO_2 transport in a mountain forest snowpack. *J. Geophys. Res.-Biogeo.* **2011**, *116*, 352–370. [CrossRef]

forests

MDPI

Article

Methane Emission from Mangrove Wetland Soils Is Marginal but Can Be Stimulated Significantly by Anthropogenic Activities

Xiawan Zheng [1,2,3], Jiemin Guo [3,4], Weimin Song [1,5], Jianxiang Feng [3,6] and Guanghui Lin [1,2,3,*]

1 Ministry of Education Key Laboratory for Earth System Modeling, Department of Earth System Science, Tsinghua University, Beijing 100084, China; zhengxw16@mails.tsinghua.edu.cn (X.Z.); wmsong2005@163.com (W.S.)
2 Joint Center for Global Change Studies, Beijing 100875, China
3 Graduate School at Shenzhen, Tsinghua University, Shenzhen 518055, China; jguo3@uwyo.edu (J.G.); weifejix@163.com (J.F.)
4 Department of Botany, University of Wyoming, Laramie, WY 82071, USA
5 Yantai Institute of Coastal Zone Research, Chinese Academy of Science, Yantai 264006, China
6 School of Life Sciences, Sun Yat-sen University, Guangzhou 510275, China
* Correspondence: lingh@mail.tsinghua.edu.cn; Tel.: +86-010-62797230

Received: 21 October 2018; Accepted: 22 November 2018; Published: 27 November 2018

Abstract: Mangrove wetland soils have been considered as important sources for atmospheric CH_4, but the magnitude of CH_4 efflux in mangrove wetlands and its relative contribution to climate warming compared to CO_2 efflux remains controversial. In this study, we measured both CH_4 and CO_2 effluxes from mangrove soils during low or no tide periods at three tidal zones of two mangrove ecosystems in Southeastern China and collected CH_4 efflux data from literature for 24 sites of mangrove wetlands worldwide. The CH_4 efflux was highly variable among our field sites due to the heterogeneity of mangrove soil environments. On average, undisturbed mangrove sites have very low CH_4 efflux rates (ranging from 0.65 to 14.18 μmol m^{-2} h^{-1}; median 2.57 μmol m^{-2} h^{-1}), often less than 10% of the global warming potentials (GWP) caused by the soil CO_2 efflux from the same sites (ranging from 0.94 to 9.50 mmol m^{-2} h^{-1}; median 3.67 mmol m^{-2} h^{-1}), even after considering that CH_4 has 28 times more GWP over CO_2. Plant species, study site, tidal position, sampling time, and soil characteristics all had no significant effect on mangrove soil CH_4 efflux. Combining our field measurement results and literature data, we demonstrated that the CH_4 efflux from undisturbed mangrove soils was marginal in comparison with the CO_2 efflux in most cases, but nutrient inputs from anthropogenic activities including nutrient run-off and aquaculture activities significantly increased CH_4 efflux from mangrove soils. Therefore, CH_4 efflux from mangrove wetlands is strongly influenced by anthropogenic activities, and future inventories of CH_4 efflux from mangrove wetlands on a regional or global scale should consider this phenomenon.

Keywords: greenhouse gas emission; soil respiration; coastal wetlands; anthropogenic effect

1. Introduction

Global wetlands are considered as important carbon sinks for sequestering high amounts of carbon dioxide (CO_2) from the atmosphere and contain more than 30% of the world's organic carbon in the soils, despite accounting for only 5%–8% of the global terrestrial surface [1–3]. Mangrove wetlands could be key ecosystems in addressing climate regulation through their high productivity and effective carbon (C) sequestration rates [4–7]. The global carbon sequestration rate in mangrove wetlands is on average 174 g C m^{-2} $year^{-1}$, corresponding to about 10%–15% of global coastal ocean carbon storage [8]. Organic-rich soils dominate in mangrove carbon storage, accounting for 49%–98% of

carbon stocks in mangrove wetlands [9,10]. However, the buried carbon may releases back into the atmosphere as gaseous products such as CO_2 and methane (CH_4) [1]. Meanwhile, wetlands are also identified as major CH_4 sources for the atmosphere, emitting 177 to 284 Tg CH_4 $year^{-1}$, corresponding to approximately 40% of the total global CH_4 emission [11]. CH_4 has a global warming potential 28 times greater than that of CO_2 on a 100-year timescale and directly contributes to about 20% of recent climate warming, despite the fact its concentration is two orders of magnitude lower than that of CO_2 [12]. Thus, proper quantification of CH_4 efflux from mangrove wetlands is critical to evaluating its effect on climate warming mitigation. Additional knowledge of mangrove wetlands' CH_4 emission will further provide guidance on mangrove wetlands restoration efforts to mitigate atmospheric CO_2 increase.

CH_4 efflux from mangrove soils is generally identified to be low but highly variable [13–16]. The practice of mangrove carbon budget has shown that carbon burial, soil respiration, and soil CH_4 emission are 24 Tg C $year^{-1}$, 36 Tg C $year^{-1}$, and 2 Tg C $year^{-1}$, respectively [8], assuming a mangrove extent area of 138,000 km^2 [17]. Low CH_4 production and emission is mainly due to the presence of high sulfate in mangrove soil, which allows sulfate-reducing bacteria to outcompete CH_4-producing bacteria [18–20]. Additionally, mangrove ecosystems are inundated by periodic tides and receive nutrient input from anthropogenic activities, which provides an anaerobic environment and high availability of substrate for methanogenesis [21]. Recent studies reported a significant amount of CH_4 efflux from mangrove wetland soils [21–23] and claimed that the contribution of CH_4 efflux to climate warming was non-negligible in the estuarine mangrove wetlands, which could account for 9.3%–32.7% plant CO_2 sequestration [24]. Thus, considerable uncertainty still exists regarding the magnitude of mangrove soil CH_4 efflux and its contribution to climate warming, which requires further study.

The carbon stocks in mangrove wetlands of China play an essential role in global oceanic carbon cycling and differ among mangrove species in subtropical and tropical regions [25]. Large spatio-temporal variations in CH_4 efflux have been observed in mangrove soils [18,23,26]. Previous studies indicated that CH_4 efflux varied among different tidal positions, probably due to differences in soil temperature, salinity, and pH [27]. Temporal variation in CH_4 efflux could be explained by soil temperature, the position of the water table, and the availability of suitable substrate [23,28,29]. Meanwhile, mangrove wetlands in China are facing greater pollution pressure due to chemical discharge from aquaculture activity and sea-wall construction [30]. However, there are few studies that investigate human perturbations such as nutrient loading from aquaculture ponds on mangrove soil CH_4 efflux even though these activities can significantly change these factors [7,26].

In this study, we measured both soil CH_4 and CO_2 effluxes from mangrove wetland soils during low or no tide periods at three tidal zones of two mangrove ecosystems in Southeastern China and collected available CH_4 efflux data from literature for global mangrove wetlands. The aims of this study were to identify the magnitude of CH_4 efflux in mangroves wetlands with and without the influence of anthropogenic activities and to evaluate the relative contribution of CH_4 efflux over CO_2 efflux from mangrove wetland soils to climate warming.

2. Materials and Methods

2.1. Study Site Description

The study was conducted in two mangrove wetlands in Southeastern China, including Zhangjiang Estuary Mangrove National Natural Reserve (23°55′49″ N, 117°24′54″ E, abbreviated as the ZJ (Zhangjiang Estuary) site) and Qinglan Harbour Mangrove Provincial Natural Reserve (19°37′48″ N, 110°46′12″ E, abbreviated as the QL (Qinglan Harbour) site) (Figure 1).

ZJ site is located in an estuary of the Zhangjiang River, Yunxiao County, Fujian Province, China, with a subtropical marine monsoon climate. The monthly mean air temperature ranged from 13.5 °C in January to 28.9 °C in August, and the annual mean air temperature was 21.2 °C. Annual mean rainfall was 1714.5 mm, most of which occurred during the wet season from April to September.

Tides were semidiurnal, with an annual mean tidal-level variation of 2.32 m. The salinity of the seawater ranged from 12 to 26 ppt. The vegetation was dominated by *Kandelia obovata* Sheue, Liu & Yong (red mangrove), *Aegiceras corniculatum* (L.) Blanco (black mangrove), and *Avicennia marina* (Forssk.) Vierh. (grey mangrove), mixed with some other less common mangrove species such as *Bruguiera gymnorrhiza* (L.) Savigny (black mangrove) and *Acanthus ilicifolius* L. (holy mangrove) [31].

QL site, situated in Wenchang County, Hainan Province, China, experienced a tropical monsoon climate. Annual mean air temperature was 23.9 °C, and the lowest monthly mean temperature was 18.3 °C in January. The annual precipitation was 1974 mm, of which more than 82% occurred during the wet season from May to October. Tides were semi-diurnal, and the tidal-level ranged from 0.01 m to 2.38 m, with the largest tidal-level variation of 2.07 m in one tidal cycle. The dominant mangrove species at QL site, which had the largest number of mangrove species in China, were *Bruguiera sexangula* (Lour.) Poir. (upriver orange mangrove), *Sonneratia caseolaris* (L.) Engl. (mangrove apple), *Lumnitzera racemosa* Willd. (tonga mangrove), *Ceriops tagal* (Pers.) C.B.Rob. (spurred mangrove), and *Rhizophora apiculata* Blume (red mangrove) communities [32,33].

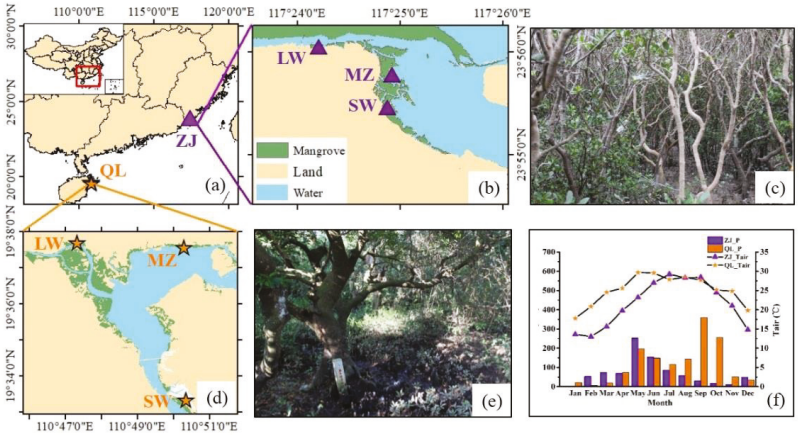

Figure 1. Map of sampling location and climatic conditions. (**a**) Geographical location of Zhangjiang Estuary (ZJ) and Qinglan Harbour (QL) mangrove wetlands. (**b**,**c**) Sampling sites and a typical scene from ZJ mangrove forest. (**d**,**e**) Sampling sites and a typical scene from QL mangrove forest. (**f**) Monthly precipitation (P, mm) and monthly air temperature (T, °C) from ZJ and QL mangrove wetlands. LW: landward zone, MZ: middle zone, and SW: seaward zone.

2.2. Measurements of Soil CH_4 and CO_2 Effluxes

Sampling campaigns were undertaken in July 2013 (represented wet season) and February 2014 (represented dry season) at ZJ site, and in August 2016 (represented wet season) and November 2017 (represented dry season) at QL site. For each sampling time, measurements were conducted in three tidal positions: landward zone (LW), middle zone (MZ), and seaward zone (SW), with the exception of SW at ZJ site during the dry season due to heavy rainfall making the site inaccessible. At each sampling position, four chambers were set up, and four replicated samples were collected on the same day at each site for a total of twelve samples. During low or no tide periods in the day time, we measured environmental variables and collected samples for laboratory analyses. The soil inundation and exposure duration were similar among three tidal positions and four replicates samples.

Gas effluxes from the soil were quantified through the standard static (closed) chamber technique [23]. Measurements were taken using PVC chambers (diameter 20 cm, length 15 cm, volume 4.50 L, and enclosing 0.025 m^2). The open end of chamber was slightly inserted into the soil to a depth of 2–3 cm to ensure minimal lateral gas leakage. A controllable valve above the chamber was left open for 30 min prior to sampling, which is adequate to remove impacts of root disturbance caused by the

chamber insertion, and then the valve was closed during the whole measurements time. Deployment time was set at 2 h, with sampling at 0, 30, 60, 90, and 120 min intervals. Headspace gas was mixed carefully through the vent tube, and 8 ml gas samples were collected using a 50 mL gas-tight syringe equipped with a luer-lock valve (SGE Trajan Scientific and Medical Pty Ltd., Melbourne, Australia). Gas samples were then transferred into pre-evacuated gas sampling bags or vials for storage (Dalian Delin Gas Packing Inc., Dalian, Liaoning, China). The air temperature inside the chamber was measured simultaneously with the gas sampling.

All samples were transported to laboratory and analyzed within 24 h using an Agilent 7890A gas chromatograph (Agilent Technologies Inc., Wilmington, DE, USA) equipped with a flame ionization detector (FID) and a Poropak-Q column. The column and detector temperatures were set at 60 °C and 130 °C, respectively, with nitrogen as the carrier gas at a flow rate of 1200 mL s^{-1}. Standard curves were gained by injecting a series volume of pure CH_4 (99.992%) and CO_2 (99.999%) in high purity N_2 (99.999%, HKO Co Ltd., Hong Kong, China). The CH_4 and CO_2 concentrations were quantified by calculating the peak areas of samples against standards of similar concentration ranges. During the gas measurement, standard gas (40 mL L^{-1} CH_4 and 2000 mL L^{-1} CO_2) was analyzed every 10 samples to ensure data quality. Gas effluxes were calculated based on a linear least squares fit of the time series of gas concentrations. Data were accepted if the slope of the linear fit had a $R^2 > 0.80$.

2.3. Measurements of Environmental Factors

For each chamber measurement, soil cores (0–10 cm surface soil) were collected using a hand-held PVC tube after gas sampling. The soil samples were divided into two subsamples: fresh soil and air-dried soil. Soil moisture content was determined by oven-drying of 7 g fresh soil at 105 °C to a constant weight. Soil inorganic N (NH_4^+-N and NO_3^--N) contents were extracted with 2 M KCl from fresh soil samples and then analyzed using a UV-2501PC UV–VIS spectrophotometer (Shimadzu Inc., Japan) [23]. While both NH_4^+-N and NO_3^--N extraction methods require fresh soil samples, the samples from ZJ-SW during the wet season and ZJ-LW and ZJ-MZ during the dry season were dried before we could take any measurements. Air-dried soil was sieved through a 2 mm sieve. The pH and salinity were measured at a *w* (soil): *v* (water) of 1:5 and 1:2.5 soil slurry using an electrochemistry benchtop meter, Orion™ Versa Star Pro™ (Thermo Fisher Scientific Inc., Beverly, MA, USA). Soil total carbon content (TC), total nitrogen content (TN), and C:N ratio of air-dried soil were measured using the an elementar analyzer (Vario EL III, Elementar Analysensysteme GmbH Inc., Hanau, Germany). Analysis of soil characteristics all followed the standard methods described by Page et al. (1982), and data were expressed in term of 105 °C oven-dried weight.

2.4. Conversion to CO_2—Equivalent Efflux

The global warming potential for CH_4 was converted to CO_2 equivalents using a multiplier of 28 for 100-year timescale [34] to compare their global warming effects.

2.5. Collecting CH_4 Efflux Data from Literature

A total of 24 studies of CH_4 efflux from mangrove soil were reviewed (Table S2). These studies were selected because the same static chamber method was used as our study, which made the results comparable. We divided the mangrove wetlands into undisturbed and anthropogenic sites according to the eutrophic status of the chosen study sites (Table S3). Undisturbed sites are defined as not affected by nutrient input from anthropogenic activities involving agricultural, domestic, aquaculture, or other run-off from treatment plants as indicated by the reference's study site descriptions. Anthropogenic sites are those known to be influenced by activities described above.

2.6. Statistical Analysis

Two-way analysis of variance (ANOVA) was used to determine significance of differences between means of soil characteristics and effluxes of CH_4 and CO_2 among tidal positions and sampling time.

If the difference was significant at $p < 0.05$, a Post-hoc Turkey test was used to determine where the difference lay. All data were expressed as means ± standard error (SE) with four replicates. Paired *t*-test was used to compare the differences in soil characteristics and effluxes of CH_4 and CO_2 among tropical and subtropical mangrove wetlands. Pearson correlation coefficient values (*r*) were calculated to determine the relationship between soil characteristics and CH_4 and CO_2 effluxes. All analysis processes were performed using SPSS 21.0 for Windows (SPSS Inc., Chicago, IL, USA).

3. Results

3.1. Soil CH_4 and CO_2 Effluxes

CH_4 efflux was highly variable among the sampling sites, for most sampling sites; CH_4 efflux was small and almost negligible, ranging from 0.65 ± 0.91 to 14.18 ± 6.35 μmol m^{-2} h^{-1}, while at the landward zone in Zhangjiang Estuary site (abbreviated as ZJLW) during the wet season, CH_4 efflux was about 10 times higher than the highest value found at other sites (123.59 ± 41.79 μmol m^{-2} h^{-1}) (Figure 2a,b and Table S1). CO_2 efflux ranged from 0.94 ± 0.41 to 9.50 ± 2.70 mmol m^{-2} h^{-1}, and the highest and lowest values were recorded at landward and seaward zones in Qinglan Harbour mangrove wetland during wet season (Figure 2c, Figure 2d and Table S1). No significant difference was found in soil CH_4 and CO_2 effluxes between ZJ and QL sites ($p = 0.173$ and $p = 0.111$).

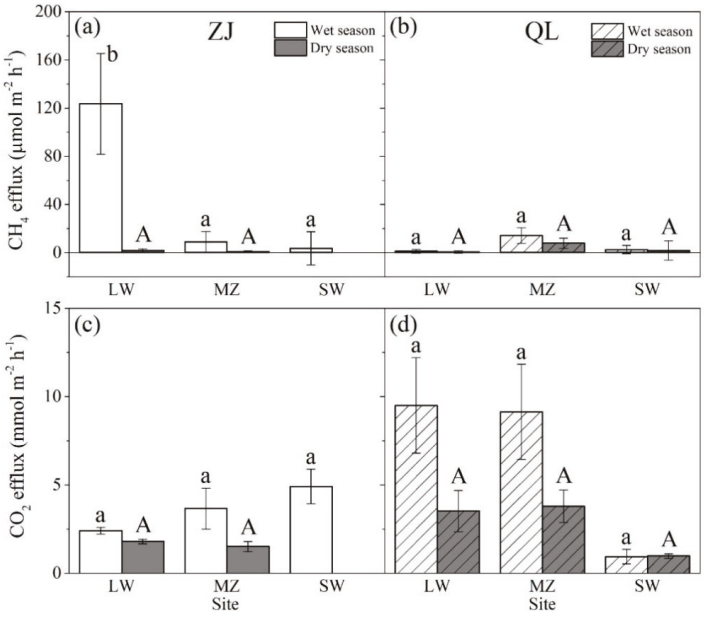

Figure 2. CH_4 and CO_2 effluxes from ZJ and QL mangrove soils. (**a**,**b**) Comparison of the mean soil CH_4 efflux among three tidal positions during wet and dry seasons at ZJ and QL site. (**c**,**d**) Comparison of the mean soil CO_2 efflux among three tidal positions during wet and dry seasons at ZJ and QL site. Error bars represent the standard error (SE) of the means ($n = 4$). Different letters indicate significant differences among tidal positions for each period (wet and dry seasons) according to analysis of variance (ANOVA) test (Turkey HSD test, $p < 0.05$). Site abbreviations were the same as Figure 1.

At ZJ site, CH_4 efflux ranged from 0.73 ± 0.73 to 123.59 ± 41.79 μmol m^{-2} h^{-1} (Figure 2a), and significant differences in CH_4 efflux among tidal positions and sampling time were found ($p = 0.006$ and $p = 0.002$, respectively). The highest and lowest CH_4 values were recorded at landward zone during wet season and middle zone during dry season, respectively. Soil CH_4 efflux was higher

in wet season than that in the dry season at all sites. The CO_2 efflux ranged from 1.52 ± 0.29 to 4.91 ± 0.98 mmol m^{-2} h^{-1} and did not differ significantly with tidal positions and seasons ($p = 0.160$ and $p = 0.108$) (Figure 2c).

At QL site, the value of soil CH_4 efflux ranged from 0.65 ± 0.91 to 14.18 ± 6.35 μmol m^{-2} h^{-1} and showed no significant differences among different tidal positions and sampling time ($p > 0.05$) (Figure 2b). CH_4 efflux at the middle zone was the highest, followed by the CH_4 efflux at seaward zone. The CO_2 efflux ranged from 0.94 ± 0.41 to 9.50 ± 2.70 mmol m^{-2} h^{-1} (Figure 2d) and changed with tidal position and sampling time significantly ($p = 0.045$ and $p = 0.042$, respectively). The lowest value of CO_2 efflux was measured at seaward zone, and highest CO_2 efflux was observed during wet season rather than dry season.

3.2. Soil Characteristics

Soil characteristics measured during wet and dry season at ZJ and QL sites are shown in Table 1. There were significant differences in soil temperature, pH, TC content, TN content, and C:N ratio among subtropical (ZJ site) and tropical (QL site) mangrove wetlands ($p < 0.05$). The mangrove soils had higher pH values (ranging from 6.62 ± 0.16 to 7.43 ± 0.14) at QL site than that at ZJ site (ranging from 5.46 ± 0.31 to 7.11 ± 0.03). Higher soil temperature, TC content, TN content, and C:N ratio were detected at QL site than at ZJ site ($p < 0.05$). Salinity and soil moisture content were not significantly different between QL site and ZJ site and were not significantly influenced by tidal positions and sampling time ($p > 0.05$).

At ZJ site, significantly higher soil temperatures were observed in the wet season rather than dry season ($p = 0.015$). Tidal position had significant effect on pH, TN content, and C:N ratio ($p < 0.05$). Lowest pH but highest TC content, TN content, and C:N ratio were observed in the middle zone ($p < 0.05$).

At QL site, both soil temperature and C:N ratio were significantly different between wet and dry season. Higher soil temperature and a lower C:N ratio were observed in wet season ($p < 0.05$). The pH value, NH_4^+-N content, NO_3^--N content, TN content, TC content, and C:N ratio were significantly affected by tidal position ($p < 0.05$). With an increase in tidal positions, salinity, pH value, and C:N ratio gradually increased, while the NH_4^+-N content, NO_3^--N content, TN content, and TC content gradually decreased.

Table 1. Key characteristics for mangrove soils at various study sites measured during wet and dry seasons.

Mangrove Wetland	Season	Study Site	Species	T_{soil}	Salinity (ppt)	pH	Soil Moisture Content	NH_4^+-N (ug g^{-1})	NO_3^--N (ug g^{-1})	TN (%)	TC (%)	C:N Ratio
ZJ	Wet season	LW	KO	27.19 ± 0.19c	2.07 ± 0.25a	5.46 ± 0.31a	0.85 ± 0.15a	9.50 ± 0.92	0.14 ± 0.04	0.15 ± 0.03a	1.82 ± 0.18a	12.50 ± 1.07b
		MZ	KO	27.74 ± 0.05c	5.70 ± 0.66ab	7.11 ± 0.03c	0.89 ± 0.23a	9.09 ± 0.88	0.15 ± 0.05	0.15 ± 0.01a	1.36 ± 0.01a	9.25 ± 0.35a
		SW	KO	27.42 ± 0.09c	7.70 ± 1.45ab	6.82 ± 0.03ab	1.04 ± 0.45a			0.17 ± 0.01a	1.96 ± 0.18a	11.44 ± 0.65ab
	Dry season	LW	KO	17.35 ± 0.19a	9.00 ± 1.27b	6.23 ± 0.10b	0.75 ± 0.07a			0.16 ± 0.02a	1.98 ± 0.16a	12.29 ± 0.47b
		MZ	KO	18.47 ± 0.09b	15.55 ± 2.56c	7.01 ± 0.14c	0.81 ± 0.50a			0.14 ± 0.01a	1.49 ± 0.09a	10.90 ± 0.31ab
		SW	KO									
QL	Wet season	LW	BS, HL	29.00D	12.09 ± 1.37A	6.81 ± 0.05AB	1.85 ± 0.25B	8.02 ± 0.90B	4.31 ± 0.45B	0.73 ± 0.10B	11.48 ± 2.00AB	15.44 ± 0.93A
		MZ	BS, RA	28.90D	17.84 ± 5.91AB	6.62 ± 0.16A	0.56 ± 0.12A	3.11 ± 0.55A	1.28 ± 0.13A	0.24 ± 0.05A	4.01 ± 0.66AB	17.03 ± 0.61A
		SW	Mixed	30.50E	25.91 ± 4.22B	6.85 ± 0.02AB	0.51 ± 0.01A	3.17 ± 0.13A	1.63 ± 0.05A	0.08 ± 0.01A	4.48 ± 0.12AB	57.81 ± 7.33B
	Dry season	LW	KO	25.18 ± 0.07B	11.12 ± 1.21A	7.30 ± 0.11BC	2.08 ± 0.39B	8.14 ± 1.10B	3.55 ± 0.35B	0.79 ± 0.11B	12.41 ± 2.58B	15.10 ± 0.89A
		MZ	KO	23.34 ± 0.03A	15.60 ± 0.67AB	6.76 ± 0.16A	0.60 ± 0.14A	2.26 ± 0.75A	1.42 ± 0.30A	0.19 ± 0.05A	3.52 ± 0.88A	19.47 ± 0.74B
		SW	KO	25.45 ± 0.01C	19.90 ± 0.30AB	7.43 ± 0.14C	0.44 ± 0.06A	2.26 ± 0.33A	1.31 ± 0.01A	0.07 ± 0.01A	4.75 ± 0.16AB	74.26 ± 7.84C

ZJ: Zhangjiang Estuary Mangrove National Natural Reserve; QL: Qinglan Harbour Mangrove Provincial Natural Reserve; LW: Landward zone; MZ: Middle zone; SW: Seaward zone; KO: *Kandelia obovata* Sheue, Liu & Yong (red mangrove) community; BS: *Bruguiera sexangula* (Lour.) Poir. (upriver orange mangrove) community; HL: *Heritiera littoralis* Aiton (looking-glass mangrove) community; RA: *Rhizophora apiculata* Blume (red mangrove) community; Mixed: Mixed species community. Mean and standard error (SE) of four replicates are shown ($n = 4$). Different letters indicated significant differences among different sampling sites according to analysis of variance (ANOVA) test ($p < 0.05$).

3.3. The Relationship between Gas Effluxes and Soil Characteristics

Among soil characteristics measured in current study, soil temperature and pH were correlated with CO_2 efflux. The soil temperature had positive effect on CO_2 efflux ($p = 0.011$, $r = 0.342$), while pH had negative effect on it ($p < 0.001$, $r = -0.506$). No significant relationship among CH_4 efflux and any soil characteristics was recorded in this study.

4. Discussions

4.1. Magnitude of CH_4 Efflux from Mangrove Wetland Soils

Combining our data and literature data, we found CH_4 efflux from undisturbed mangrove wetlands was negligible but can be stimulated significantly by anthropogenic activities (Figure 3). The results from our direct field measurements indicated that low CH_4 efflux was recorded in undisturbed mangrove soils of Southeastern China, ranging from 0.65 ± 0.91 to 14.18 ± 6.35 μmol m^{-2} h^{-1}, which was consistent with the results found by others in nearby undisturbed mangrove areas [35–37]. The highest CH_4 efflux (123.59 ± 41.79 μmol m^{-2} h^{-1}) was observed at landward zone in ZJ mangrove wetland, probably due to large and frequent discharge of freshwater as indicated by very low salinity at this site (as low as 2 ppt) (Table 1). This result was similar to the CH_4 efflux in the Jiulong River mangrove, which was also heavily influenced by human activities and positively correlated with NH_4^+-N, organic carbon, and total Kjeldahl nitrogen [24]. Mangrove ecosystems are rich in carbon but nutrient-poor; in particular, they are limited by nitrogen and phosphorus [38]. Anthropogenic nutrient input improves microbial metabolic process, enhancing more emission of CH_4 efflux from soils into the atmosphere [39].

In addition, the CH_4 efflux data from literature for 24 sites of mangrove wetlands worldwide showed that mangroves affected by anthropogenic activities (ranging from 0.19 to 5168.62 μmol m^{-2} h^{-1} with the median values of 52.80 μmol m^{-2} h^{-1}) had emission rates 14 times higher than those from undisturbed mangroves (ranging from −6.05 to 79.00 μmol m^{-2} h^{-1} with the median of 3.57 μmol m^{-2} h^{-1}). These CH_4 efflux data revealed that the mangroves affected by anthropogenic activities made a greater contribution to climate warming rather than those undisturbed or not heavily disturbed mangrove forests. Anthropogenic activities cause significant increases in CH_4 emission, and if anthropogenic activities continue at the current pace without protective measures, these ecosystems could become potential major sources of CH_4 emission and decrease their ability to store carbon in the future [40]. The current study divided the mangrove wetlands into undisturbed and affected by anthropogenic activities based on whether the chosen study sites have involved agricultural, domestic, aquaculture, or other run-off from treatment plants in the references. Further research is needed to quantify the stimulation effect of nutrient input from anthropogenic activities on CH_4 emissions, combined with controlled experiments and microbial community analysis to model the extent of change.

4.2. Contribution of CH_4 Efflux from Mangrove Wetlands to Climate Warming

We calculated CH_4:CO_2 efflux ratio and CH_4:CO_2 warming effect ratio to evaluate the relative role of CH_4 efflux for warming potentials (Figure 4) among different tidal zones in two mangrove wetlands. The CH_4:CO_2 efflux ratio ranged from $-0.06\% \pm 0.32\%$ to $0.45\% \pm 0.57\%$ in most sampling sites except for the disturbed ZJLW site ($4.95\% \pm 1.46\%$). Considering CH_4 global warming potential in 100-year term, CH_4 accounted for $-0.63\% \pm 3.21\%$ to $4.54\% \pm 5.79\%$ of the warming effect, a relatively minor contributor to CO_2 equivalents, except at the ZJLW site, which was $50.37\% \pm 14.85\%$, making it a highly significant contributor. A higher CH_4:CO_2 warming effect ratio had been reported in the Jiulong River mangrove (10.30% to 48.35%) [24] and Futian mangrove (18.36% to 255.96%) [21] in South China, which received significant amounts of anthropogenic nutrient inputs. This reveals that the magnitude and contribution of CH_4 efflux from undisturbed mangrove soils to climate warming

was marginal in comparison with CO_2 efflux, but could be a potential major contributor to warming effect under the influence of anthropogenic activities.

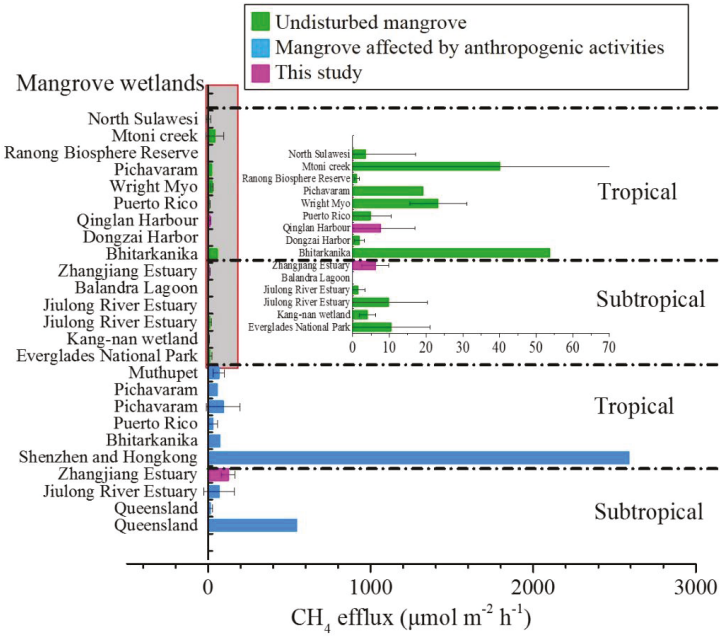

Figure 3. Comparison of CH_4 efflux from undisturbed mangrove wetlands and mangroves wetlands affected by anthropogenic activities. Detailed information on the literature sources of CH_4 efflux data is provided in Table S2. Nutrient concentrations and assignment of eutrophic status from mangrove wetlands are shown in Table S3.

In addition, the global median CH_4 efflux in mangrove wetlands (3.57 and 52.80 μmol m^{-2} h^{-1} for undisturbed mangroves and mangroves affected by anthropogenic activities, respectively) was negligible in contrast to other wetlands, such as freshwater wetlands (69.44 to 6944.44 μmol m^{-2} h^{-1}) (Chmura et al., 2003), peatlands (31.39 to 59.93 μmol m^{-2} h^{-1}) [41], and rice paddies (709.38 μmol m^{-2} h^{-1}) [42]. This indicates that mangrove wetlands were not significant contributors to global wetland CH_4 budget compared with other wetlands. Recent studies have also found that mangrove soils acted as a net carbon sink after subtracting the effects of CH_4 emission from carbon sequestration [43]. Overall, mangrove wetlands should be restored and protected to mitigate climate warming without great concern for warming effect caused by CH_4 emission.

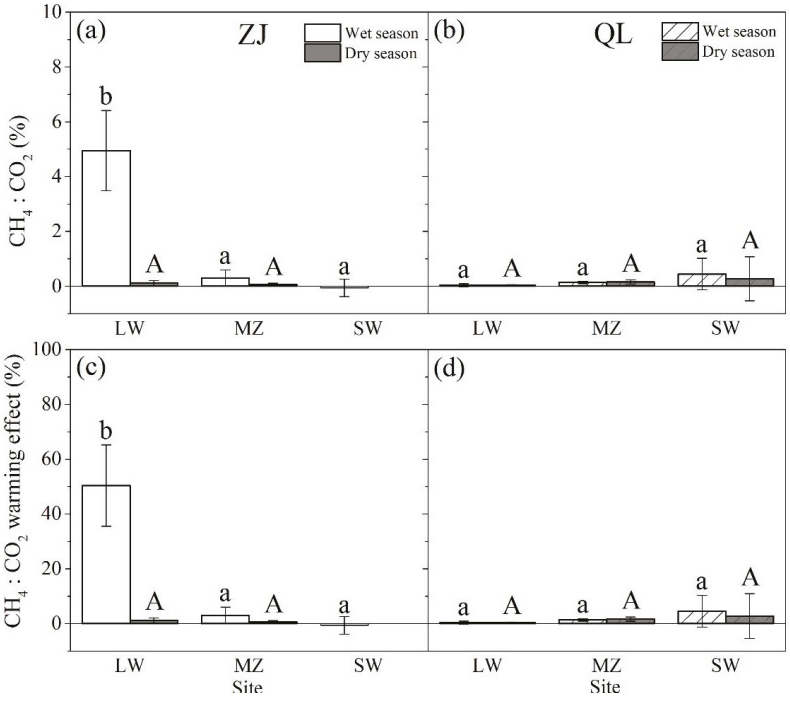

Figure 4. CH_4:CO_2 effluxes ratio and CH_4:CO_2 warming effect ratio from ZJ and QL mangrove wetlands. (**a**–**b**) Comparison of CH_4:CO_2 effluxes ratio among three tidal positions during wet and dry seasons at ZJ and QL sites. (**c**–**d**) Comparison of CH_4:CO_2 warming effect ratio among three tidal positions during wet and dry seasons at ZJ and QL site. Site abbreviations were the same as Figure 1.

5. Conclusions

The current study suggests that undisturbed mangrove soils were minor contributors to climate warming, but the CH_4 efflux from mangrove wetlands was significantly increased by nutrient inputs from anthropogenic activities including nutrient run-off and aquaculture activities. This phenomenon should be considered in order to better quantify the emission of CH_4 from regional or global mangrove wetlands and to evaluate the potential roles of constructed or restored mangrove wetlands for mitigating climate warming.

Supplementary Materials: The following are available online at http://www.mdpi.com/1999-4907/9/12/738/s1, Table S1: CH_4 and CO_2 effluxes from ZJ and QL mangrove wetlands; Table S2: summary of CH_4 efflux data as reported by authors or calculated from literature in other mangrove wetlands; and Table S3: nutrient concentrations and assignment of eutrophic status.

Author Contributions: G.L. conceived and designed the experiment. X.Z., J.G., W.S. and J.F conducted the experiment and collected data. X.Z. and G.L. analyzed the data and wrote the initial draft of the manuscript. All authors contributed to the editing and revising of the final version of the manuscript. The authors approved the final version for publication and agree to be held accountable for the content therein.

Funding: This research described in this paper was supported financially by National Basic Research Program of China (973 Program); Ministry of Science and Technology, China (2013CB956601); Shenzhen Basic Research Discipline Layout Project, Shenzhen Science and Technology Innovation Committee, China (JCYJ20150529164918736); and the Ocean Open Public Fund Project, State Oceanic Administration, China (201305021).

Acknowledgments: We thank Jianzhang Chen for assistance in the elemental and Gas Chromatograph analyses, and Guangqiang Zheng, Jie Liang, Ziyao Yang and Jiacheng Lv for their assistances in field sampling and measurements. We thank Chris Feng for improving the English of this manuscript.

Conflicts of Interest: The authors declare no conflict of interest.

References

1. Mitsch, W.J.; Bernal, B.; Nahlik, A.M.; Mander, Ü.; Zhang, L.; Anderson, C.J.; Jørgensen, S.E.; Brix, H. Wetlands, carbon, and climate change. *Landsc. Ecol.* **2012**, *28*, 583–597. [CrossRef]
2. Sun, L.; Song, C.; Lafleur, P.M.; Miao, Y.; Wang, X.; Gong, C.; Qiao, T.; Yu, X.; Tan, W. Wetland-atmosphere methane exchange in Northeast China: A comparison of permafrost peatland and freshwater wetlands. *Agric. For. Meteorol.* **2017**, *249*, 239–249. [CrossRef]
3. Mitra, S.; Wassmann, R.; Vlek, P.L.G. An appraisal of global wetland area and its organic carbon stock. *Curr. Sci.* **2005**, *88*, 25–35.
4. McLeod, E.; Chmura, G.L.; Bouillon, S.; Salm, R.; Björk, M.; Duarte, C.M.; Lovelock, C.E.; Schlesinger, W.H.; Silliman, B.R. A blueprint for blue carbon: Toward an improved understanding of the role of vegetated coastal habitats in sequestering CO_2. *Front. Ecol. Environ.* **2011**, *9*, 552–560. [CrossRef]
5. Sitoe, A.; Mandlate, L.; Guedes, B. Biomass and Carbon Stocks of Sofala Bay Mangrove Forests. *Forests* **2014**, *5*, 1967–1981. [CrossRef]
6. Cui, X.; Liang, J.; Lu, W.; Chen, H.; Liu, F.; Lin, G.; Xu, F.; Luo, Y.; Lin, G. Stronger ecosystem carbon sequestration potential of mangrove wetlands with respect to terrestrial forests in subtropical China. *Agric. For. Meteorol.* **2018**, *249*, 71–80. [CrossRef]
7. Lu, W.; Xiao, J.; Liu, F.; Zhang, Y.; Liu, C.; Lin, G. Contrasting ecosystem CO_2 fluxes of inland and coastal wetlands: A meta-analysis of eddy covariance data. *Glob. Chang. Biol.* **2017**, *23*, 1180–1198. [CrossRef] [PubMed]
8. Alongi, D.M. Carbon cycling and storage in mangrove forests. *Ann. Rev. Mar. Sci.* **2014**, *6*, 195–219. [CrossRef] [PubMed]
9. Benson, L.; Glass, L.; Jones, T.; Ravaoarinorotsihoarana, L.; Rakotomahazo, C. Mangrove Carbon Stocks and Ecosystem Cover Dynamics in Southwest Madagascar and the Implications for Local Management. *Forests* **2017**, *8*, 190. [CrossRef]
10. Donato, D.C.; Kauffman, J.B.; Murdiyarso, D.; Kurnianto, S.; Stidham, M.; Kanninen, M. Mangroves among the most carbon-rich forests in the tropics. *Nat. Geosci.* **2011**, *4*, 293–297. [CrossRef]
11. Ciais, P.; Sabine, C.; Manyothers, I.; Patra, P.; Ciais, P.; Sabine, C.; Manyothers, I.; Patra, P. *Chapter 6: Carbon and Other Biogeochemical Cycles*; Cambridge University Press: Cambridge, UK, 2014.
12. Stocker, T.F.; Qin, D.; Plattner, G.-K.; Tignor, M.; Allen, S.K.; Boschung, J.; Nauels, A.; Xia, Y.; Bex, V.; Midgley, P.M. *Climate Change 2013: The Physical Science Basis. Contribution of Working Group I to the Fifth Assessment Report of the Intergovernmental Panel on Climate Change*; Cambridge University Press: Cambridge, UK; New York, NY, USA, 2013; pp. 465–570.
13. Harriss, R.C.; Sebacher, D.I.; Bartlett, K.B.; Bartlett, D.S.; Crill, P.M. Sources of atmospheric methane in the south Florida environment. *Glob. Biogeochem. Cycle* **1988**, *2*, 231–243. [CrossRef]
14. Sotomayor, D.; Corredor, J.E.; Morell, J.M. Methane flux from mangrove sediments along the southwestern coast of Puerto Rico. *Estuaries* **1994**, *17*, 140–147. [CrossRef]
15. Kristensen, E. *Carbon Balance in Mangrove Sediments: The Driving Processes and Their Controls*; Gendai Tosho: Kanagawa, Japan, 2007; pp. 61–78.
16. Chen, G.C.; Ulumuddin, Y.I.; Pramudji, S.; Chen, S.Y.; Chen, B.; Ye, Y.; Ou, D.Y.; Ma, Z.Y.; Huang, H.; Wang, J.K. Rich soil carbon and nitrogen but low atmospheric greenhouse gas fluxes from North Sulawesi mangrove swamps in Indonesia. *Sci. Total Environ.* **2014**, *487*, 91–96. [CrossRef] [PubMed]
17. Giri, C.; Ochieng, E.; Tieszen, L.L.; Zhu, Z.; Singh, A.; Loveland, T.; Masek, J.; Duke, N. Status and distribution of mangrove forests of the world using earth observation satellite data. *Glob. Ecol. Biogeogr.* **2011**, *20*, 154–159. [CrossRef]
18. Biswas, H.; Mukhopadhyay, S.K.; Sen, S.; Jana, T.K. Spatial and temporal patterns of methane dynamics in the tropical mangrove dominated estuary, NE coast of Bay of Bengal, India. *J. Mar. Syst.* **2007**, *68*, 55–64. [CrossRef]
19. Segarra, K.E.A.; Comerford, C.; Slaughter, J.; Joye, S.B. Impact of electron acceptor availability on the anaerobic oxidation of methane in coastal freshwater and brackish wetland sediments. *Geochim. Cosmochim. Acta* **2013**, *115*, 15–30. [CrossRef]

20. Nobrega, G.N.; Ferreira, T.O.; Neto, M.S.; Queiroz, H.M.; Artur, A.G.; Mendonca, E.D.; Silva, E.D.; Otero, X.L. Edaphic factors controlling summer (rainy season) greenhouse gas emissions (CO_2 and CH_4) from semiarid mangrove soils (NE-Brazil). *Sci. Total Environ.* **2016**, *542*, 685–693. [CrossRef] [PubMed]
21. Chen, G.C.; Tam, N.F.Y.; Ye, Y. Summer fluxes of atmospheric greenhouse gases N_2O, CH_4 and CO_2 from mangrove soil in South China. *Sci. Total Environ.* **2010**, *408*, 2761–2767. [CrossRef] [PubMed]
22. Mukhopadhyay, S.; Biswas, H.; De, T.; Sen, B.; Sen, S.; Jana, T. Impact of Sundarban mangrove biosphere on the carbon dioxide and methane mixing ratios at the NE Coast of Bay of Bengal, India. *Atmos. Environ.* **2002**, *36*, 629–638. [CrossRef]
23. Allen, D.E.; Dalal, R.C.; Rennenberg, H.; Meyer, R.L.; Reeves, S.; Schmidt, S. Spatial and temporal variation of nitrous oxide and methane flux between subtropical mangrove sediments and the atmosphere. *Soil Biol. Biochem.* **2007**, *39*, 622–631. [CrossRef]
24. Chen, G.; Chen, B.; Yu, D.; Tam, N.F.Y.; Ye, Y.; Chen, S. Soil greenhouse gas emissions reduce the contribution of mangrove plants to the atmospheric cooling effect. *Environ. Res. Lett.* **2016**, *11*, 124019. [CrossRef]
25. Liu, H.; Ren, H.; Hui, D.; Wang, W.; Liao, B.; Cao, Q. Carbon stocks and potential carbon storage in the mangrove forests of China. *J. Environ. Manag.* **2014**, *133*, 86–93. [CrossRef] [PubMed]
26. Wang, H.T.; Liao, G.S.; D'Souza, M.; Yu, X.Q.; Yang, J.; Yang, X.R.; Zheng, T.L. Temporal and spatial variations of greenhouse gas fluxes from a tidal mangrove wetland in Southeast China. *Environ. Sci. Pollut. Res.* **2016**, *23*, 1873–1885. [CrossRef] [PubMed]
27. Chauhan, R.; Datta, A.; Ramanathan, A.L.; Adhya, T.K. Factors influencing spatio-temporal variation of methane and nitrous oxide emission from a tropical mangrove of eastern coast of India. *Atmos. Environ.* **2015**, *107*, 95–106. [CrossRef]
28. Walter, B.P.; Heimann, M. A process-based, climate-sensitive model to derive methane emissions from natural wetlands: Application to five wetland sites, sensitivity to model parameters, and climate. *Glob. Biogeochem. Cycle* **2000**, *14*, 745–765. [CrossRef]
29. Inubushi, K.; Furukawa, Y.; Hadi, A.; Purnomo, E.; Tsuruta, H. Seasonal changes of CO_2, CH_4 and N_2O fluxes in relation to land-use change in tropical peatlands located in coastal area of South Kalimantan. *Chemosphere* **2003**, *52*, 603–608. [CrossRef]
30. Zai-Wang, Z.; Xiang-Rong, X.; Yu-Xin, S.; Shen, Y.; Yong-Shan, C.; Jia-Xi, P. Heavy metal and organic contaminants in mangrove ecosystems of China: A review. *Environ. Sci. Pollut. Res. Int.* **2014**, *21*, 11938–11950.
31. Lin, P. *The Comprehensive Report of Science Investigation on the Natural Reserve of Mangrove Wetland of Zhangjiang Estuary in Fujian*; Xiamen University Press: Xiamen, China, 2001.
32. Ding, H.; Yao, S.; Chen, J. Authigenic pyrite formation and re-oxidation as an indicator of an unsteady-state redox sedimentary environment: Evidence from the intertidal mangrove sediments of Hainan Island, China. *Cont. Shelf Res.* **2014**, *78*, 85–99. [CrossRef]
33. Guo, Z.Z.; Guo, Y.; Wen, W.; Cao, M.; Guo, J.; Li, Z. Soil carbon sequestration and its relationship with soil pH in Qinglangang mangrvoe wetlands in Hainan island (in Chinese). *Sci. Silvae Sin.* **2014**, *50*, 8–15.
34. Myhre, G.; Shindell, D.; Bréon, F.-M.; Collins, W.; Fuglestvedt, J.; Huang, J.; Koch, D.; Lamarque, J.-F.; Lee, D.; Mendoza, B. Anthropogenic and natural radiative forcing. *Clim. Chang.* **2013**, *423*, 658–740.
35. Lu, C.Y.; Wong, Y.S.; Tam, N.F.; Ye, Y.; Lin, P. Methane flux and production from sediments of a mangrove wetland on Hainan Island, China. *Mangroves Salt Marshes* **1999**, *3*, 41–49. [CrossRef]
36. Alongi, D.M.; Pfitzner, J.; Trott, L.A.; Tirendi, F.; Dixon, P.; Klumpp, D.W. Rapid sediment accumulation and microbial mineralization in forests of the mangrove Kandelia candel in the Jiulongjiang Estuary, China. *Estuar. Coast. Shelf Sci.* **2005**, *63*, 605–618. [CrossRef]
37. Chen, Y.P.; Chen, G.C.; Ye, Y. Coastal vegetation invasion increases greenhouse gas emission from wetland soils but also increases soil carbon accumulation. *Sci. Total Environ.* **2015**, *526*, 19–28. [CrossRef] [PubMed]
38. Alongi, D. Impact of Global Change on Nutrient Dynamics in Mangrove Forests. *Forests* **2018**, *9*, 596. [CrossRef]
39. Kreuzwieser, J.; Buchholz, J.; Rennenberg, H. Emission of Methane and Nitrous Oxide by Australian Mangrove Ecosystems. *Plant Biol.* **2003**, *5*, 423–431. [CrossRef]
40. Purvaja, R.; Ramesh, R. Natural and Anthropogenic Methane Emission from Coastal Wetlands of South India. *Environ. Manag.* **2001**, *27*, 547–557. [CrossRef]

41. Abdalla, M.; Hastings, A.; Truu, J.; Espenberg, M.; Mander, Ü.; Smith, P. Emissions of methane from northern peatlands: A review of management impacts and implications for future management options. *Ecol. Evolut.* **2016**, *6*, 7080–7102. [CrossRef] [PubMed]
42. Chen, H.; Zhu, Q.A.; Peng, C.H.; Wu, N.; Wang, Y.F.; Fang, X.Q.; Jiang, H.; Xiang, W.H.; Chang, J.; Deng, X.W.; et al. Methane emissions from rice paddies natural wetlands, lakes in China: Synthesis new estimate. *Glob. Chang. Biol.* **2013**, *19*, 19–32. [CrossRef] [PubMed]
43. Cabezas, A.; Mitsch, W.J.; MacDonnell, C.; Zhang, L.; Bydałek, F.; Lasso, A. Methane emissions from mangrove soils in hydrologically disturbed and reference mangrove tidal creeks in southwest Florida. *Ecol. Eng.* **2018**, *114*, 57–65. [CrossRef]

forests

MDPI

Article

Effect of Woodchips Biochar on Sensitivity to Temperature of Soil Greenhouse Gases Emissions

Irene Criscuoli [1,*], Maurizio Ventura [1], Andrea Sperotto [1], Pietro Panzacchi [1,2] and Giustino Tonon [1]

[1] Faculty of Science and Technology, Free University of Bolzano/Bozen, Piazza Università, 5, 39100 Bolzano, Italy

[2] Centro di Ricerca per le Aree Interne e gli Appennini (ArIA), Università degli Studi del Molise, via Francesco De Sanctis 1, 86100 Campobasso, Italy

* Correspondence: irene.criscuoli@unibz.it; Tel.: +39-0471-017765

Received: 17 June 2019; Accepted: 14 July 2019; Published: 17 July 2019

Abstract: Research Highlights: Biochar is the carbonaceous product of pyrolysis or the gasification of biomass that is used as soil amendment to improve soil fertility and increase soil carbon stock. Biochar has been shown to increase, decrease, or have no effect on the emissions of greenhouse gases (GHG) from soil, depending on the specific soil and biochar characteristics. However, the temperature sensitivity of these gas emissions in biochar-amended soils is still poorly investigated. Background and Objectives: A pot experiment was set up to investigate the impact of woodchips biochar on the temperature sensitivity of the main GHG (CO_2, CH_4, and N_2O) emissions from soil. Materials and Methods: Nine pots (14 L volume) were filled with soil mixed with biochar at two application rates (0.021 kg of biochar/kg of soil and 0.042 kg of biochar/kg of soil) or with soil alone as the control (three pots per treatment). Pots were incubated in a growth chamber and the emissions of CO_2, CH_4, and N_2O were monitored for two weeks with a cavity ring-down gas analyzer connected to three closed dynamic chambers. The temperature in the chamber increased from 10 °C to 30 °C during the first week and decreased back to 10 °C during the second week, with a daily change of 5 °C. Soil water content was kept at 20% (w/w). Results: Biochar application did not significantly affect the temperature sensitivity of CO_2 and N_2O emissions. However, the sensitivity of CH_4 uptake from soil significantly decreased by the application of biochar, reducing the CH_4 soil consumption compared to the un-amended soil, especially at high soil temperatures. Basal CO_2 respiration at 10 °C was significantly higher in the highest biochar application rate compared to the control soil. Conclusions: These results confirmed that the magnitude and direction of the influence of biochar on temperature sensitivity of GHG emissions depend on the specific GHG considered. The biochar tested in this study did not affect soil N_2O emission and only marginally affected CO_2 emission in a wide range of soil temperatures. However, it showed a negative impact on soil CH_4 uptake, particularly at a high temperature, having important implications in a future warmer climate scenario and at higher application rates.

Keywords: CO_2; CH_4; N_2O; soil; biochar; sensitivity; temperature

1. Introduction

Forest management can contribute to climate change mitigation by allocating woody biomass to bioenergy production, thus displacing fossil fuel use [1]. Among the energy conversion processes that can utilize woody biomass as feedstock, pyrolysis and gasification are acknowledged to be promising technologies in terms of carbon (C) budget [2]. During pyrolysis and gasification, biomass is thermally degraded through heating (300–1200 °C) under the complete or partial exclusion of oxygen. The volatile components of biomass are therefore released in the form of syngas, that can be used to produce

thermal energy, electricity, or an oily fuel, and the leftover by-product of this process is charcoal [3]. In the last two decades, this C-rich, solid material has been proposed as a soil amendment with the name of biochar [4].

Due to its chemical structure, biochar is supposed to be particularly recalcitrant to soil degradation [5], even if estimations of its mean residence time vary from decades to millennia, depending on the starting feedstock, the production conditions, and the characteristics of the amended soil [6–8]. Biochar has been shown to improve soil characteristics and plant productivity in agricultural and forest ecosystems [9–13] as well as reduce nutrient losses from soil [14–16]. For these reasons, biochar has been proposed in forest restoration as a replacement to other forms of organic amendments and liming agents, particularly in degraded sites [9]. Applying biochar to forest soils may therefore contribute to mitigate climate change through the increase of soil C stock, improve soil characteristics, and allow at the same time the valorization of the woody biomass gasification chain, by turning what is now considered a waste into a resource.

However, little research has been conducted on biochar in forest ecosystems compared to agricultural crops [1,13,17] and most of the information on charcoal in forest ecosystems in the literature derives from studies on wildfires [18].

To evaluate the real climate change mitigation potential of biochar, its impact on greenhouse gases (GHG) emissions from soil has to be accounted. In fact, it is estimated that soil emissions of carbon dioxide (CO_2), methane (CH_4), and nitrous oxide (N_2O) represent 35%, 47%, and 53% of the total annual global emissions of these greenhouse gases (GHG), respectively [19,20]. Biochar has been shown to affect soil GHG emissions in different ways, depending on biochar and soil characteristics. For example, biochar application decreased [21], increased [22,23], or had no effect [24–26] on soil CO_2 emissions. Different results have also been obtained for CH_4. Biochar can in fact contribute to mitigate CH_4 emissions from flooded soils under anoxic conditions, while in non-flooded soils, especially if neutral or alkaline, biochar may decrease soil CH_4 uptake [27]. Finally, biochar has been shown to strongly reduce soil N_2O emissions in different situations, even if increases in emissions have been observed as well [28].

While different studies have examined the effect of biochar application on GHG soil emissions, only a few have evaluated the impact that specific environmental parameters exert on these emissions in biochar-amended soils. Soil temperature is known to be the most important driver of GHG fluxes from soil [20,29,30], as well as of biochar oxidation and decomposition [31]. However, the effect of temperature on GHG fluxes in biochar-amended soil has been poorly investigated. Understanding the role of temperature is fundamental to assessing the effect of biochar on GHG emissions in different climatic conditions and in the context of climate change.

The overall aim of this study was to assess the effect of biochar on temperature sensitivity and basal emission of soil GHG fluxes. In particular, soil CO_2, CH_4, and N_2O fluxes were measured in soils amended with woodchip biochar at two application rates and in un-amended (control) soils. During the experiment, the soil moisture was kept constant at 20% (w/w) in all treatments and the temperature ranged between 10 °C and 30 °C.

We hypothesized that the application of biochar could affect the sensitivity to temperature and the basal value of CO_2, N_2O, and CH_4 flux.

Our experimental results partially confirmed our hypothesis. In fact, biochar application did not affect the temperature sensitivity of CO_2 and N_2O fluxes, while it significantly reduced that of CH_4 flux. On the contrary, basal respiration significantly increased for CO_2 by biochar application.

2. Materials and Methods

2.1. Experimental Set Up and Soil and Biochar Characteristics

The soil used in the experiment was sampled near Merano (Bolzano Province, Northern Italy, 46°40′0.181″ N, 11°11′39.282″ E; about 600 m a.s.l.). The soil was sandy-loam soil (USDA classification),

with 64% sand, 29% silt, and 7% clay. The soil organic carbon (SOC) content was 2.4 ± 0.8% and soil pH was 6.4 ± 0.2. The soil water content at field capacity, calculated using the SPAW model (USDA-ARS) was 20% (v/v). The soil was sieved to a 8 mm mesh size to remove stones and coarse organic matter fragments.

The biochar used in the experiment consisted of small particles (<5 mm) and was obtained from conifer woodchips, at approximately 500 °C, through fast pyrolysis (Record Immobiliare S.r.l., Lunano, Pesaro-Urbino, Italy). Biochar was characterized by a bulk density of 0.165 g cm^{-3} and C:N ratio of 151. A detailed physicochemical characterization of the biochar used in this experiment is provided in Table 1.

Table 1. Physicochemical characterization of the biochar used in the present work.

Parameter	Unit	Value	Uncertainty
pH	-	12.4	± 0.5
Sieve fraction <5 mm	%	100	± 10
Sieve fraction <2 mm	%	97	± 10
Sieve fraction <0.5 mm	%	70	± 7
Max. water retention	% w/w	86	± 7
Ash (550 °C)	%	31	± 3
Total C	%	58.9	-
C from $CaCO_3$	%	1.1	-
Organic C	%	57	± 5
H:C molar ratio	-	0.10	± 0.01
Total N	%	0.39	± 0.04
Total P	%	0.64	
Total K	%	3.5	± 0.5
PAHs [1]	mg/kg	<1	

[1] Polycyclic aromatic hydrocarbons.

B1 and B2 treatments were prepared by mixing biochar and the sieved soil at two rates: 0.021 kg of biochar kg^{-1} of soil (dry weight) (B1), and 0.042 kg of biochar kg^{-1} of soil (dry weight) (B2), respectively. The two mixing rates corresponded to field biochar application doses of 25 ton ha^{-1} and 50 ton ha^{-1}, respectively, considering a field biochar incorporation depth of 20 cm and are in line with the biochar dosages used in the majority of previous studies in forest ecosystems [9]. Biochar and soil mixtures where then homogenized with a concrete mixer.

The experiment was set up in July 2018 in a growth chamber at the Laimburg research center for Agriculture and Forestry located in Auer/Ora (BZ), Northern Italy. A total of 9 pots (45 cm × 25 cm × 21 cm, 14 L volume) were filled with soil mixed with biochar or with un-amended soil as the control. A total of 3 replicates (pots) were prepared for each treatment. The pots were stored in the growth chamber for two weeks at 10 °C temperature. The temperature in the chamber was then increased from 10 °C to 30 °C during one week (first week of experiment), and from 30 °C back to 10 °C during the following week (second week of experiment), with an overnight change of 5 °C per day. The lowest temperature (10 °C) was chosen because it is a standard temperature used internationally to compare the soil respiration of different experimental sites or treatments, the so called basal soil respiration at 10 °C (R_{10}) [32]. The highest temperature (30 °C) was chosen because the maximum monthly temperature measured in Merano between 2011 and 2017 was on average 29.1 °C [33]. In order to isolate the effect of soil temperature, excluding any effect of soil humidity on soil GHG fluxes, soil moisture was kept constant at 20% (w/w) in all treatments. Soil water content at the beginning of the experiment was measured in each pot by collecting a soil subsample (~10 g of soil) and drying it for 24 h at 105 °C. The amount of water to be added daily to the soil was calculated as the difference between the actual weight of the pot and the theoretical weight if the soil moisture was equal to 20% (w/w).

2.2. Measurement of Soil GHG Fluxes

The emissions of GHG from the soil were measured by a gas analyzer CRDS (Picarro Inc., Santa Clara, CA, USA), connected to 3 closed dynamic chambers (eosAC Autochamber, Eosense Inc., Dartmouth, NS, Canada) operated by a multiplexer (eosMX, Eosense Inc., Dartmouth, NS, Canada). The chambers were installed on PVC (polymerizing vinyl chloride) collars (15.2 cm diameter, 7 cm height) inserted into the soil, 1 per pot, for 4 cm. Fluxes of CO_2 (μmol m^{-2} s^{-1}), N_2O, and CH_4 (nmol m^{-2} s^{-1}) were measured daily from the 3 experimental treatments by manually moving one chamber (leaving the collars on the soil) on the 3 pots of each treatment. The measurements on each pot lasted for 10 min. A valve delay of 66 s was set at the beginning and at the end of each measurement to account for the time needed to draw the air from the chamber, analyze the gas concentrations, and then recirculate the air sample back to the chamber through a tubing length of 30 m. During measurements, the soil temperature (°C) was measured at a 5 cm soil depth by a RT-1 Rugged Soil Temperature Sensor (Decagon Devices, Inc., Pullman, WA, USA).

2.3. Data Analysis

After the elimination of data associated with system malfunctioning, soil CO_2 flux (soil respiration) measured in the different treatments were related to soil temperature using the following exponential model:

$$Fs = R_{10}\, e^{b(T-10)} \quad (1)$$

where *Fs* is the soil CO_2 flux, *T* is the soil temperature (°C) at 5 cm depth, and R_{10} is the basal soil respiration, i.e., the value of Fs at the reference temperature of 10 °C. The model parameters R_{10} and *b* were estimated by nonlinear regression analysis. The apparent sensitivity of CO_2 flux to soil temperature was determined by the Q_{10} temperature coefficient as follows:

$$Q_{10} = e^{10b} \quad (2)$$

Fluxes of CH_4 and N_2O were related to soil temperature using a linear model:

$$Fs = R_{10} + b(T-10) \quad (3)$$

where *Fs* is the soil CH_4 or N_2O flux, *T* is the soil temperature (°C) at 5 cm depth, and R_{10} is the basal emission at 10 °C. Parameters R_{10} and *b* (slope of the regression line) are estimated by linear regression analysis.

For each gas, the linear regression models obtained in the different experimental treatments were then compared by Analysis of Covariance (ANCOVA) to analyze the effect of biochar on the sensitivity of GHG fluxes to temperature. Equation (1) was linearized with a log-transformation of CO_2 efflux data before analysis. At first the slopes of the linear regression model were compared and then only when the slopes were not significantly different, and the intercepts of the regression lines were also compared. In case ANCOVA highlighted significant differences, post-hoc individual comparisons were performed with the Tukey's HSD test. The homogeneity of variances was checked before analysis by plotting the residual vs. fitted values. When this condition was not fulfilled, a square root transformation was applied to the data before analysis. Statistical analysis was performed using the software R (version 3.4.2) [34].

3. Results

The highest CO_2 emission rates were observed in the biochar-treated soils (Figure 1). Biochar application did not significantly affect the Q_{10} value of CO_2 fluxes, while it significantly increased R_{10} of CO_2 when applied at the highest rate in comparison to the control (Figure 1 and Table 2).

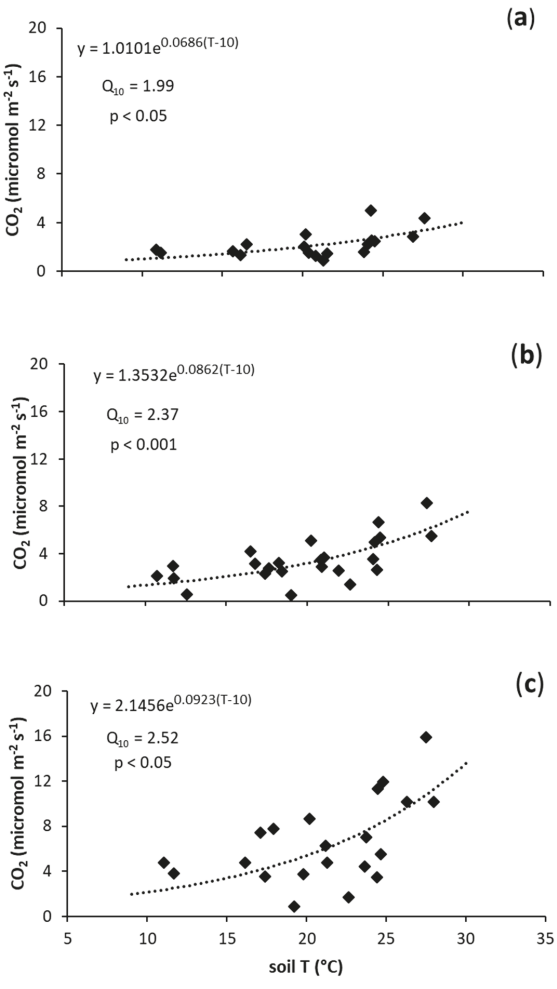

Figure 1. Relationship between CO_2 fluxes (μmol m^{-2} s^{-1}) and soil temperature (°C) in: (**a**) N (control treatment); (**b**) B1 (0.021 kg of biochar/kg of soil); and (**c**) B2 (0.042 kg of biochar/kg of soil).

A negative CH_4 flux, i.e., a net CH_4 consumption in the soil, was observed in all treatments (Figure 2). The temperature sensitivity of soil CH_4 uptake significantly decreased following biochar application, showing a reduction in CH_4 uptake in biochar-amended soil in comparison to the control (Table 2). This effect was dependent on the biochar application rate and was particularly evident in the B2 treatment (Figure 2, Table 2). At this application rate, CH_4 flux was not significantly affected by soil temperature (slope: −0.0087) and its flux was always close to zero (Figure 2, Table 2).

Table 2. Results of Analysis of Covariance (ANCOVA) and the post-hoc Tukey test for a pairwise comparison of the slopes and intercepts of the linear models relating the fluxes of CO_2, CH_4, and N_2O to soil temperature (T, °C) in the treatments N (control), B1 (0.021 kg of biochar/kg of soil), and B2 (0.042 kg of biochar/kg of soil). Different letters indicate significant differences between model parameters determined for each soil treatment ($p < 0.05$) in the table.

	Model Parameters			
	b		**R_{10}**	
CO_2				
N	0.0686	a	1.0101	a
B1	0.0862	a	1.3532	ab
B2	0.0923	a	2.1456	b
CH_4				
N	−0.0378	a	−1.2309	a
B1	−0.0389	b	0.0229	a
B2	−0.0087	c	0.1022	a
N_2O				
N	0.0078	a	−0.0066	a
B1	0.0131	a	−0.0141	a
B2	0.0068	a	0.0262	a

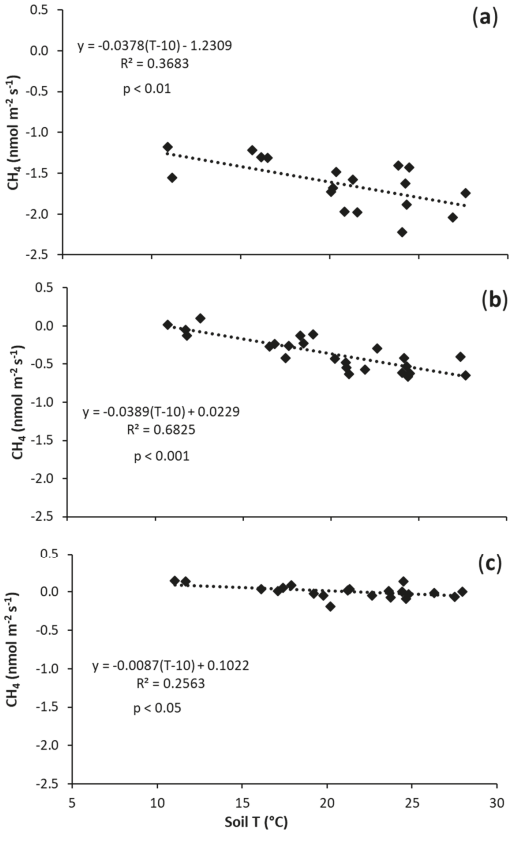

Figure 2. Relationship between CH_4 fluxes (nmol m^{-2} s^{-1}) and soil temperature (°C) in: (**a**) N (control treatment); (**b**) B1 (0.021 kg of biochar/kg of soil); and (**c**) B2 (0.042 kg of biochar/kg of soil).

The highest N_2O emissions from the soil were observed in the B1 treatment in comparison with control and B2, but the sensitivity of N_2O emissions from the soil, as well as the N_2O basal emission, were not significantly affected by the application of biochar (Figure 3, Table 2).

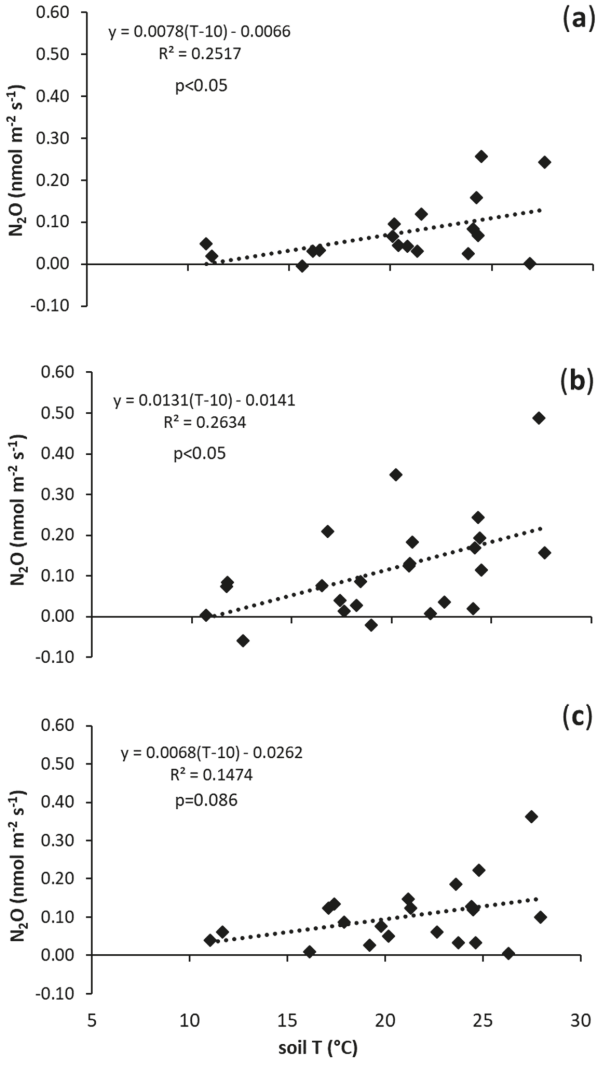

Figure 3. Relationship between N_2O fluxes (nmol m^{-2} s^{-1}) and soil temperature (°C) in: (**a**) N (control treatment); (**b**) B1 (0.021 kg of biochar/kg of soil); and (**c**) B2 (0.042 kg of biochar/kg of soil).

4. Discussion

Soil temperature is known to be the most important driver of GHG fluxes from soil [20,29,30], as well as of biochar oxidation and decomposition [31]. The temperature sensitivity of GHG fluxes is therefore a key parameter to predict the impact that global warming will have on the flux of GHG [35,36].

In our experiment, we observed a positive exponential relationship between CO_2 fluxes and the temperature in biochar-amended soils. This relation was typically observed in forest and plantation

ecosystems [25,26,30,37,38]. The absence of a significant modification of the Q_{10} after the application of biochar (Figure 1, Table 2) was coherent with what was observed in previous studies with different biochars and application rates [26,37,39]. However, this result is inconsistent with other studies that reported a decrease [40–42] or an increase [25,43] to the temperature sensitivity of CO_2 emissions. These contrasting results derives from the complexity of the factors involved. In fact, the Q_{10} of biochar was expected to be higher than the less recalcitrant native soil organic matter (SOM) [44], but the sensitivity of CO_2 fluxes in biochar-amended soils also depends on the impact that biochar has on the Q_{10} of the native soil's organic matter [45]. Moreover, results can also change according to the incubation temperature range and soil type. More specifically, a smaller sensitivity was expected in soils with high clay, Fe, and Al oxides content as well as with an acidic pH [46].

In the present study, basal soil respiration increased significantly in the soil that was amended with biochar at a higher application rate. A R_{10} increase was found for heterotrophic respiration in different environments such as apple orchards [26] and the desert [47] after the application of biochar produced from wood and cotton straw, respectively. A significant increase in R_{10} for total soil respiration was also observed in soils amended with poultry litter biochar [48].

These results have been attributed to an increase of microbial biomass and/or activity [26,48]. The stimulation of soil microbes can derive from the decomposition of the labile fraction of biochar, consisting of bio-oils and condensation products [49–53]. However, the degradation of the more recalcitrant C compounds cannot be excluded [54]. This mechanism can be the main driver of the increased CO_2 efflux observed after biochar application in both agricultural and forest ecosystems [17,26]. Moreover, we cannot exclude that the increased CO_2 fluxes derive from an increased decomposition of the native soil's organic matter, the so-called priming effect (PE). In fact, a positive PE has been observed in several short term studies [55,56], especially in sandy soils [52], while in the long term, a protection of native organic matter from decomposition (negative PE) is generally observed in biochar-amended soils [23,57]. A boost in soil microbiota activity can also be due to a shift in soil properties such as soil aeration [58]. Biochar is characterized by a high porosity, which may have increased soil gas permeability and oxygen availability for soil microbes. Moreover, even if the soil water content was kept constant during the incubation experiment, the presence of biochar may have affected the availability of soil water by soil microorganisms. Biochar can in fact alter soil water potential [59,60], which is known to impact soil microbial population and activity [61].

Non-flooded soils in an oxic condition usually show a CH_4-sink capacity [62], as CH_4 is oxidized by soil methanotrophic bacteria, and the rate of CH_4 oxidation depends on soil temperature [63]. This trend was also observed in the present study, as CH_4 consumption increased linearly with soil temperature (Figure 2). The decreased sensitivity to soil temperature of CH_4 flux in biochar-treated soil means that biochar decreased CH_4 consumption at a higher soil temperature, while at a lower soil temperature this effect was less pronounced. In their meta-analysis, Jeffery et al. [27] showed that the application of biochar from woody feedstock, produced at temperatures between 400 °C and 600 °C, decreases soil CH_4 uptake in non-flooded soils, especially in neutral or alkaline soil pH. Results of the present study are in line with these findings as our biochar was produced from wood chips at approximately 500 °C, and the soil water content was kept at 20%. Non-flooded upland soils contribute to approximately 15% of global CH_4 oxidation [64], therefore biochar application may decrease net CH_4 oxidation, reducing the climate change mitigation potential of these soils. However, few studies examined the sensitivity of CH_4 soil flux to temperature. Our study showed that the reduction of soil CH_4 uptake induced by biochar increased with soil temperature. This effect could therefore more pronounced under warmer climatic conditions and may worsen within the context of global warming. Moreover, the reduction of sensitivity to temperature for CH_4 was much more evident in the B2 treatment, which suggests not using high biochar application rates in order to preserve the soil CH_4 uptake capacity. However, a significant increase in soil CH_4 uptake [37,65] and sensitivity to temperature [37] was observed in some experiments in non-flooded soils, contradicting the results of

the present work and showing that the relation between biochar, soil, and CH_4 emissions is complex and hard to predict.

The mechanism behind the reduction of CH_4 oxidation might be a modification of the methanogenic/methanotrophic bacteria ratio in biochar-amended soils [66], and the release of chemicals with a toxic effect on the methanotrophic bacteria population, such as ethylene [67]. In addition, even if the soil water content was kept constant, biochar may have altered soil water potential and water availability for soil bacteria.

Soil N_2O emissions in the present work increased linearly with the temperature in all soil treatments and the application of biochar did not affect temperature sensitivity or basal soil N_2O emissions (Figure 3, Table 2). These results confirm a previous study by [68] but are in contrast with other studies, reporting a significant reduction of N_2O flux sensitivity to temperature, both in subtropical [37] and continental climate [69]. In a meta-analysis by Cayuela et al. [28], an average reduction of 54% in N_2O emissions has been reported in biochar-treated soils. In this case, the variability observed in the experimental results has been shown to depend on different characteristics of biochar (feedstock used, pyrolysis conditions, and C/N ratio) and soil. In particular, when biochar is applied to drained soils with a coarse texture, reduction in N_2O emissions has not been observed [28,70]. In our experiment, soil moisture was kept at a relatively low value, not exceeding the field capacity of the sandy-loam textured soil. In these conditions, it was likely that N_2O emission was not promoted and the effect of biochar was consequently not relevant.

In previous studies, an observed reduction of N_2O emissions from soils was explained by a toxic effect on soil microbes involved in N_2O production of Polycyclic aromatic hydrocarbons (PAHs) [71,72]. The PAHs content in the biochar used in this study was very low (Table 1) and therefore a toxic effect on soil biota was unlikely.

A decrease of soil N_2O emissions has also been associated with a shift in the soil's physical properties, such as a reduction in soil compaction [73]. This mechanism cannot have occurred in our experiment, as it was set up in controlled conditions and the soil was not subjected to compaction.

The reduction of N_2O emissions observed in previous studies has also been attributed to the sorption of reactive N on biochar surfaces and the reduction of its availability for N_2O emitting reactions. However, this mechanism is observed in case of biochar production at temperatures higher than 600 °C [74,75]. The absence of the biochar effect on the sensitivity to temperature of N_2O emission would suggest that biochar will not affect the emission of this powerful greenhouse gas in warmer climatic conditions.

It has to be considered that the short experimental duration of this study might limit the validity of the results to the first period after the application of biochar [76,77]. Therefore, these results may not be representative of the effect of biochar on long-term GHG emissions from soil in field application.

5. Conclusions

Before concluding if biochar application to soil is a forest management practice that is able to mitigate climate change, an evaluation of its effect on soil GHG emission is fundamental. The results of the present work show that biochar addition to soil did not significantly affect the sensitivity of CO_2 and N_2O fluxes, while it slightly increased the CO_2 basal soil respiration in case of a high application rate, indicating that biochar application would not affect the emission of these gases in warmer climatic conditions. However, the significant decrease of the temperature sensitivity of soil CH_4 uptake indicated that biochar can induce an important reduction of the soil CH_4 sink potential, in particular in a warmer environment, and this effect can become more relevant in a global warming scenario. Moreover, the reduction of sensitivity to temperature for CH_4 was much more evident in the case of the higher application rate, suggesting that high biochar dosages should be avoided in order to preserve the soil CH_4 uptake capacity.

The observed effects seem to depend on specific biochar characteristics (temperature of production, low content of PAHs) and soil characteristics (sandy-loam, drained soil). However, long-term field

studies are advisable in order to guarantee a thorough understanding of the impact of biochar on GHG emissions from soil.

Author Contributions: Conceptualization, G.T.; Methodology, G.T., M.V., and I.C.; validation, M.V., G.T., I.C., and P.P.; Formal analysis, I.C. and M.V.; Investigation, I.C., A.S.; Resources, I.C., P.P., A.S., and M.V.; Data Curation, I.C., A.S.; Writing—original draft preparation, I.C. and M.V.; Writing—review and editing, I.C., M.V., P.P., and G.T.; Visualization, I.C. and M.V.; Supervision, G.T.; Project administration, G.T.; Funding acquisition, G.T.

Funding: This research was funded by the Wood-Up project (Optimization of WOOD gasification chain in South Tyrol to produce bioenergy and other high-value green products to enhance soil fertility and mitigate climate change, EFRE-FESR 2014–2020, project number 1028), funded by the European Regional Development Fund of the European Union and the Autonomous Province of Bolzano/Bozen.

Acknowledgments: The authors would like to thank the Laimburg Research Center for the availability of the climatic chamber, and Christian Ceccon and Christian Grümer from the Free University of Bolzano for their support in soil sample preparation and analysis.

Conflicts of Interest: The authors declare no conflict of interest. The funders had no role in the design of the study, in the collection, analyses, or interpretation of data, in the writing of the manuscript, or in the decision to publish the results.

References

1. Cowie, A.; Barton, C.; Singh, B.; Ximenes, F.; Stone, C. Climate Change Impacts and Research Priorities for the Forestry Sector. In *DPI Priority Actions for Climate Change Workshop*; NSW Department of Primary Industries: Orange, NSW, Australia, 2007.
2. Lehmann, J. A Handful of Carbon. *Nature* **2007**, *447*, 143–144. [CrossRef] [PubMed]
3. Bridgwater, A.V. The Production of Biofuels and Renewable Chemicals by Fast Pyrolysis of Biomass. *Int. J. Glob. Energy Issues* **2007**, *27*, 160–203. [CrossRef]
4. Lehmann, J. Bio-Energy in the Black. *Front. Ecol. Environ.* **2007**, *5*, 381–387. [CrossRef]
5. Downie, A.; Munroe, P. Characteristics of Biochar—Physical and Structural Properties. In *Biochar for Environmental Management: Science, Technology and Implementation*; Lehmann, J., Joseph, S., Eds.; Earthscan: London, UK, 2009; pp. 13–29.
6. Lehmann, J.; Abiven, S.; Kleber, M.; Pan, G.; Singh, B.P.; Sohi, S.P.; Zimmerman, A.R. Persistence of Biochar in Soil. In *Biochar for Environmental Management: Science, Technology and Implementation*; Lehmann, J., Joseph, S., Eds.; Routledge: New York, NY, USA, 2015; pp. 235–282.
7. Criscuoli, I.; Alberti, G.; Baronti, S.; Favilli, F.; Martinez, C.; Calzolari, C.; Pusceddu, E.; Rumpel, C.; Viola, R.; Miglietta, F. Carbon Sequestration and Fertility after Centennial Time Scale Incorporation of Charcoal into Soil. *PLoS ONE* **2014**, *9*, e91114. [CrossRef] [PubMed]
8. Gurwick, N.P.; Moore, L.A.; Kelly, C.; Elias, P. A Systematic Review of Biochar Research, with a Focus on Its Stability in Situ and Its Promise as a Climate Mitigation Strategy. *PLoS ONE* **2013**, *8*, e75932. [CrossRef] [PubMed]
9. Thomas, S.C.; Gale, N. Biochar and Forest Restoration: A Review and Meta-Analysis of Tree Growth Responses. *New For.* **2015**, *46*, 931–946. [CrossRef]
10. Biederman, L.; Harpole, W.S. Biochar and Its Effects on Plant Productivity and Nutrient Cycling: A Meta-Analysis. *GCB Bioenergy* **2012**, *5*, 202–214. [CrossRef]
11. Liu, X.; Zhang, A.; Ji, C.; Joseph, S.; Bian, R.; Li, L.; Pan, G.; Paz-Ferreiro, J. Biochar's Effect on Crop Productivity and the Dependence on Experimental Conditions—A Meta-Analysis of Literature Data. *Plant Soil* **2013**, *373*, 583–594. [CrossRef]
12. Criscuoli, I.; Baronti, S.; Alberti, G.; Rumpel, C.; Giordan, M.; Camin, F.; Ziller, L.; Martinez, C.; Pusceddu, E.; Miglietta, F. Anthropogenic Charcoal-Rich Soils of the XIX Century Reveal That Biochar Leads to Enhanced Fertility and Fodder Quality of Alpine Grasslands. *Plant Soil* **2017**, *411*, 499–516. [CrossRef]
13. Li, Y.; Hu, S.; Chen, J.; Mueller, K.; Li, Y.; Fu, W.; Lin, Z.; Wang, H. Effects of Biochar Application in Forest Ecosystems on Soil Properties and Greenhouse Gas Emissions: A Review. *J. Soils Sediments* **2018**, *18*, 546–563. [CrossRef]
14. Ventura, M.; Sorrenti, G.; Panzacchi, P.; George, E.; Tonon, G. Biochar Reduces Short-Term Nitrate Leaching from a Horizon in an Apple Orchard. *J. Environ. Qual.* **2013**, *42*, 76–82. [CrossRef] [PubMed]

15. Major, J.; Steiner, C.; Downie, A.; Lehmann, J. Biochar Effects on Nutrient Leaching. In *Biochar for Environmental Management: Science, Technology and Implementation*; Lehmann, J., Joseph, S., Eds.; Routledge, Earthscam: New York, NY, USA, 2015; pp. 271–287.
16. Sorrenti, G.; Ventura, M.; Toselli, M. Effect of Biochar on Nutrient Retention and Nectarine Tree Performance: A Three-Year Field Trial. *J. Plant Nutr. Soil Sci.* **2016**, *179*, 1–11. [CrossRef]
17. Johnson, M.S.; Webster, C.; Jassal, R.S.; Hawthorne, I.; Black, T.A. Biochar Influences on Soil CO_2 and CH_4 Fluxes in Response to Wetting and Drying Cycles for a Forest Soil. *Sci. Rep.* **2017**, *7*, 6480. [CrossRef] [PubMed]
18. Stavi, I. Biochar Use in Forestry and Tree-Based Agro-Ecosystems for Increasing Climate Change Mitigation and Adaptation. *Int. J. Sustain. Dev. World Ecol.* **2013**, *20*, 166–181. [CrossRef]
19. Solomon, S.; Qin, D.; Manning, M.; Chen, Z.; Marquis, M.; Averyt, K.B.; Tignor, M.M.B.; Miller, H.L. *Climate Change 2007: The Physical Science Basis. Contribution of Working Group I to the Fourth Assessment Report of the Intergovernmental Panel on Climate Change*; Cambridge University Press: Cambridge, UK; New York, NY, USA, 2007.
20. Oertel, C.; Matschullat, J.; Zurba, K.; Zimmermann, F.; Erasmi, S. Greenhouse Gas Emissions from Soils—A Review. *Chemie der Erde—Geochemistry* **2016**, *76*, 327–352. [CrossRef]
21. Case, S.D.; McNamara, N.P.; Reay, D.S.; Whitaker, J. Can Biochar Reduce Soil Greenhouse Gas Emissions from a Miscanthus Bioenergy Crop? *GCB Bioenergy* **2014**, *6*, 76–89. [CrossRef]
22. Novak, J.M.; Busscher, W.J.; Watts, D.W.; Laird, D.A.; Ahmedna, M.A.; Niandou, M.A.S. Short-Term CO_2 Mineralization after Additions of Biochar and Switchgrass to a Typic Kandiudult. *Geoderma* **2010**, *154*, 281–288. [CrossRef]
23. Ventura, M.; Alberti, G.; Panzacchi, P.; Delle Vedove, G.; Miglietta, F.; Tonon, G. Biochar Mineralization and Priming Effect on SOM Decomposition. Results from a Field Trial in a Short Rotation Coppice in Italy. In *EGU General Assembly Conference Abstracts*; EGU General Assembly: Vienna, Austria, 2016; Volume 18, p. 9109.
24. Scheer, C.; Grace, P.R.; Rowlings, D.W.; Kimber, S.; van Zwieten, L. Effect of Biochar Amendment on the Soil-Atmosphere Exchange of Greenhouse Gases from an Intensive Subtropical Pasture in Northern New South Wales, Australia. *Plant Soil* **2011**, *345*, 47–58. [CrossRef]
25. Wang, Z.; Li, Y.; Chang, S.X.; Zhang, J.; Jiang, P.; Zhou, G.; Shen, Z. Contrasting Effects of Bamboo Leaf and Its Biochar on Soil CO_2 Efflux and Labile Organic Carbon in an Intensively Managed Chinese Chestnut Plantation. *Biol. Fertil. Soils* **2014**, *50*, 1109–1119. [CrossRef]
26. Ventura, M.; Zhang, C.; Baldi, E.; Fornasier, F.; Sorrenti, G.; Panzacchi, P.; Tonon, G. Effect of Biochar Addition on Soil Respiration Partitioning and Root Dynamics in an Apple Orchard. *Eur. J. Soil Sci.* **2014**, *65*, 186–195. [CrossRef]
27. Jeffery, S.; Verheijen, F.G.A.; Kammann, C.; Abalos, D. Biochar Effects on Methane Emissions from Soils: A Meta-Analysis. *Soil Biol. Biochem.* **2016**, *101*, 251–258. [CrossRef]
28. Cayuela, M.L.; van Zwieten, L.; Singh, B.P.; Jeffery, S.; Roig, A.; Sánchez-Monedero, M.A. Biochar's Role in Mitigating Soil Nitrous Oxide Emissions: A Review and Meta-Analysis. *Agric. Ecosyst. Environ.* **2014**, *191*, 5–16. [CrossRef]
29. Reichstein, M.; Beer, C. Soil Respiration across Scales: The Importance of a Model-Data Integration Framework for Data Interpretation. *J. Plant Nutr. Soil Sci.* **2008**, *171*, 344–354. [CrossRef]
30. Shen, Y.; Zhu, L.; Cheng, H.; Yue, S.; Li, S. Effects of Biochar Application on CO_2 Emissions from a Cultivated Soil under Semiarid Climate Conditions in Northwest China. *Sustainability* **2017**, *9*, 1482. [CrossRef]
31. Nguyen, B.T.; Lehmann, J.; Hockaday, W.C.; Joseph, S.; Masiello, C.A. Temperature Sensitivity of Black Carbon Decomposition and Oxidation. *Environ. Sci. Technol.* **2010**, *44*, 3324–3331. [CrossRef] [PubMed]
32. Lloyd, J.; Taylor, A. On the Temperature Dependence of Soil Respiration. *Funct. Ecol.* **1994**, *8*, 315–323. [CrossRef]
33. Provincia Autonoma di Bolzano. Valori Medi Delle Temperature Massime e Minime—Merano/Quarazze cod. 23200MS. Available online: http://www.provincia.bz.it/meteo/download/23200MS-TS-MeranoQuarazze-MeranGratsch.pdf (accessed on 8 July 2019).
34. Ihaka, R.; Gentleman, R. R: A Language for Data Analysis and Graphics. *J. Comput. Graph. Stat.* **1996**, *5*, 299–314.

35. Luo, Y.; Wan, S.; Hui, D.; Wallace, L.L. Acclimatization of Soil Respiration to Warming in a Tall Grass Prairie. *Nature* **2001**, *413*, 622–625. [CrossRef]
36. Zhou, T.; Shi, P.; Hui, D.; Luo, Y. Global Pattern of Temperature Sensitivity of Soil Heterotrophic Respiration (Q10) and Its Implications for Carbon-Climate Feedback. *J. Geophys. Res.* **2009**, *114*, 1–9. [CrossRef]
37. Lu, X.; Li, Y.; Wang, H.; Singh, B.P.; Hu, S.; Luo, Y.; Li, J.; Xiao, Y.; Cai, X.; Li, Y. Responses of Soil Greenhouse Gas Emissions to Different Application Rates of Biochar in a Subtropical Chinese Chestnut Plantation. *Agric. For. Meteorol.* **2019**, *271*, 168–179. [CrossRef]
38. Li, Y.; Li, Y.; Chang, S.X.; Yang, Y.; Fu, S.; Jiang, P.; Luo, Y.; Yang, M.; Chen, Z.; Hu, S.; et al. Biochar Reduces Soil Heterotrophic Respiration in a Subtropical Plantation through Increasing Soil Organic Carbon Recalcitrancy and Decreasing Carbon-Degrading Microbial Activity. *Soil Biol. Biochem.* **2018**, *122*, 173–185. [CrossRef]
39. Bamminger, C.; Poll, C.; Marhan, S. Offsetting Global Warming-Induced Elevated Greenhouse Gas Emissions from an Arable Soil by Biochar Application. *Glob. Chang. Biol.* **2018**, *24*, 318–334. [CrossRef] [PubMed]
40. Pei, J.; Zhuang, S.; Cui, J.; Li, J.; Li, B.; Wu, J.; Fang, C. Biochar Decreased the Temperature Sensitivity of Soil Carbon Decomposition in a Paddy Field. *Agric. Ecosyst. Environ.* **2017**, *249*, 156–164. [CrossRef]
41. Chen, J.; Sun, X.; Zheng, J.; Zhang, X.; Liu, X.; Bian, R.; Li, L.; Chneg, K.; Zheng, J.; Pan, G. Biochar Amendment Changes Temperature Sensitivity of Soil Respiration and Composition of Microbial Communities 3 Years after Incorporation in an Organic Carbon-Poor Dry Cropland Soil. *Biol. Fertil. Soils* **2018**, *54*, 175–188. [CrossRef]
42. He, X.; Du, Z.; Wang, Y.; Lu, N.; Zhang, Q. Sensitivity of Soil Respiration to Soil Temperature Decreased under Deep Biochar Amended Soils in Temperate Croplands. *Appl. Soil Ecol.* **2016**, *108*, 204–210. [CrossRef]
43. Zhou, G.; Zhou, X.; Zhang, T.; Du, Z.; He, Y.; Wang, X.; Shao, J.; Cao, Y.; Xue, S.; Wang, H.; et al. Biochar Increased Soil Respiration in Temperate Forests but Had No Effects in Subtropical Forests. *For. Ecol. Manage.* **2017**, *405*, 339–349. [CrossRef]
44. Conant, R.; Steinweg, J.; Haddix, M.; Paul, E.; Plante, A.; Six, J. Experimental Warming Shows That Decomposition Temperature Sensitivity Increases with Soil Organic Matter Recalcitrance. *Ecology* **2008**, *89*, 2384–2391. [CrossRef]
45. Fang, Y.; Singh, B.P.; Matta, P.; Cowie, A.L.; Van Zwieten, L. Temperature Sensitivity and Priming of Organic Matter with Different Stabilities in a Vertisol with Aged Biochar. *Soil Biol. Biochem.* **2017**, *115*, 346–356. [CrossRef]
46. Fang, Y.; Singh, B.P.; Singh, B. Temperature Sensitivity of Biochar and Native Carbon Mineralisation in Biochar-Amended Soils. *Agric. Ecosyst. Environ.* **2014**, *191*, 158–167. [CrossRef]
47. Liao, N.; Li, Q.; Zhang, W.; Zhou, G.; Ma, L.; Min, W.; Ye, J.; Hou, Z. Effects of Biochar on Soil Microbial Community Composition and Activity in Drip-Irrigated Desert Soil. *Eur. J. Soil Biol.* **2016**, *72*, 27–34. [CrossRef]
48. Mierzwa-Hersztek, M.; Klimkowicz-Pawlas, A.; Gondek, K. Influence of Poultry Litter and Poultry Litter Biochar on Soil Microbial Respiration and Nitrifying Bacteria Activity. *Waste Biomass Valorization* **2018**, *9*, 379–389. [CrossRef]
49. Kolb, S.E.; Fermanich, K.J.; Dornbush, M.E. Effect of Charcoal Quantity on Microbial Biomass and Activity in Temperate Soils. *Soil Sci. Soc. Am. J.* **2009**, *73*, 1173–1181. [CrossRef]
50. Zimmerman, A.R. Abiotic and Microbial Oxidation of Laboratory-Produced Black Carbon (Biochar). *Environ. Sci. Technol.* **2010**, *44*, 1295–1301. [CrossRef] [PubMed]
51. Kuzyakov, Y.; Bogomolova, I.; Glaser, B. Biochar Stability in Soil: Decomposition during Eight Years and Transformation as Assessed by Compound-Specific 14C Analysis. *Soil Biol. Biochem.* **2014**, *70*, 229–236. [CrossRef]
52. Wang, J.; Xiong, Z.; Kuzyakov, Y. Biochar Stability in Soil: Meta-Analysis of Decomposition and Priming Effects. *GCB Bioenergy* **2016**, *8*, 512–523. [CrossRef]
53. Ventura, M.; Alberti, G.; Panzacchi, P.; Delle Vedove, G.; Miglietta, F.; Tonon, G. Biochar Mineralization and Priming Effect in a Poplar Short Rotation Coppice from a 3-Year Field Experiment. *Biol. Fertil. Soils* **2019**, *55*, 67–78. [CrossRef]
54. Anderson, C.R.; Condron, L.M.; Clough, T.J.; Fiers, M.; Stewart, A.; Hill, R.A.; Sherlock, R.R. Biochar Induced Soil Microbial Community Change: Implications for Biogeochemical Cycling of Carbon, Nitrogen and Phosphorus. *Pedobiologia* **2011**, *54*, 309–320. [CrossRef]

55. Zimmerman, A.R.; Gao, B.; Ahn, M.Y. Positive and Negative Carbon Mineralization Priming Effects among a Variety of Biochar-Amended Soils. *Soil Biol. Biochem.* **2011**, *43*, 1169–1179. [CrossRef]
56. Maestrini, B.; Nannipieri, P.; Abiven, S. A Meta-Analysis on Pyrogenic Organic Matter Induced Priming Effect. *GCB Bioenergy* **2015**, *7*, 577–590. [CrossRef]
57. Fidel, R.B.; Laird, D.A.; Parkin, T.B. Impact of Six Lignocellulosic Biochars on C and N Dynamics of Two Contrasting Soils. *GCB Bioenergy* **2017**, *9*, 1279–1291. [CrossRef]
58. Zhou, Z.; Guo, C.; Meng, H. Temperature Sensitivity and Basal Rate of Soil Respiration and Their Determinants in Temperate Forests of North China. *PLoS ONE* **2013**, *8*, e81793. [CrossRef] [PubMed]
59. Laird, D.A.; Fleming, P.; Davis, D.D.; Horton, R.; Wang, B.; Karlen, D.L. Impact of Biochar Amendments on the Quality of a Typical Midwestern Agricultural Soil. *Geoderma* **2010**, *158*, 443–449. [CrossRef]
60. Novak, J.M.; Busscher, W.J.; Watts, D.W.; Amonette, J.E.; Ippolito, J.A.; Lima, I.M.; Gaskin, J.; Das, K.C.; Steiner, C.; Ahmedna, M.; et al. Biochars Impact on Soil-Moisture Storage in an Ultisol and Two Aridisols. *Soil Sci.* **2012**, *177*, 310–320. [CrossRef]
61. Sinegani, A.A.S.; Maghsoudi, J. The Effects of Water Potential on Some Microbial Populations and Decrease Kinetic of Organic Carbon in Soil Treated with Cow Manure under Laboratory Conditions. *J. Appl. Sci. Environ. Manag.* **2011**, *15*, 179–188. [CrossRef]
62. Suwanwaree, P.; Robertson, G.P. Methane Oxidation in Forest, Successional, and No-till Agricultural Ecosystems: Effects of Nitrogen and Soil Disturbance. *Soil Sci. Soc. Am. J.* **2005**, *69*, 1722–1729. [CrossRef]
63. Luo, G.J.; Kiese, R.; Wolf, B.; Butterbach-Bahl, K. Effects of Soil Temperature and Moisture on Methane Uptake and Nitrous Oxide Emissions across Three Different Ecosystem Types. *Biogeosciences* **2013**, *10*, 3205–3219. [CrossRef]
64. Powlson, D.S.; Goulding, K.W.T.; Willison, T.W.; Webster, C.P.; Hütsch, B.W. The Effect of Agriculture on Methane Oxidation in Soil. *Nutr. Cycl. Agroeco.* **1997**, *49*, 59–70. [CrossRef]
65. Karhu, K.; Mattila, T.; Bergström, I.; Regina, K. Biochar Addition to Agricultural Soil Increased CH_4 Uptake and Water Holding Capacity—Results from a Short-Term Pilot Field Study. *Agric. Ecosyst. Environ.* **2011**, *140*, 309–313. [CrossRef]
66. Feng, Y.; Xu, Y.; Yu, Y.; Xie, Z.; Lin, X. Mechanisms of Biochar Decreasing Methane Emission from Chinese Paddy Soils. *Soil Biol. Biochem.* **2012**, *46*, 80–88. [CrossRef]
67. Spokas, K.A.; Baker, J.M.; Reicosky, D.C. Ethylene: Potential Key for Biochar Amendment Impacts. *Plant Soil* **2010**, *333*, 443–452. [CrossRef]
68. Deem, L.M.; Yu, J.; Crow, S.E.; Deenik, J.; Penton, C.R. Biochar Increases Temperature Sensitivity of Soil Respiration and N2O Flux. 2016. Available online: https://biochar-us.org/presentation/biochar-increases-temperature-sensitivity-soil-respiration-and-n2o-flux (accessed on 8 July 2019).
69. Chang, J.; Clay, D.E.; Clay, S.A.; Chintala, R.; Miller, J.M.; Schumacher, T. Biochar Reduced Nitrous Oxide and Carbon Dioxide Emissions from Soil with Different Water and Temperature Cycles. *Agron. Soils Environ. Qual.* **2016**, *108*, 2214–2221. [CrossRef]
70. Curtin, D.; Campbell, C.A.; Jalil, A. Effects of Acidity on Mineralization: PH-Dependence of Organic Matter Mineralization in Weakly Acidic Soils. *Soil Biol. Biochem.* **1998**, *30*, 57–64. [CrossRef]
71. Maliszewska-Kordybach, B.; Klimkowicz-Pawlas, A.; Smreczak, B.; Janusauskaite, D. Ecotoxic Effect of Phenanthrene on Nitrifying Bacteria in Soils of Different Properties. *J. Environ. Qual.* **2007**, *36*, 1635–1645. [CrossRef] [PubMed]
72. Guo, G.X.; Deng, H.; Qiao, M.; Yao, H.Y.; Zhu, Y.G. Effect of Long-Term Wastewater Irrigation on Potential Denitrification and Denitrifying Communities in Soils at the Watershed Scale. *Environ. Sci. Technol.* **2013**, *47*, 3105–3113. [CrossRef]
73. Rogovska, N.; Laird, D.; Cruse, R.; Fleming, P.; Parkin, T.; Meek, D. Impact of Biochar on Manure Carbon Stabilization and Greenhouse Gas Emissions. *Soil Sci. Soc. Am. J.* **2011**, *75*, 871–879. [CrossRef]
74. Clough, T.J.; Condron, L.M.; Kammann, C.; Müller, C. A Review of Biochar and Soil Nitrogen Dynamics. *Agronomy* **2013**, *3*, 275–293. [CrossRef]
75. Singh, B.P.; Hatton, B.; Balwant, S.; Cowie, A.L.; Kathuria, A. Influence of Biochars on Nitrous Oxide Emission and Nitrogen Leaching from Two Contrasting Soils. *J. Environ. Qual.* **2010**, *39*, 1224–1235. [CrossRef]
76. Fidel, R.; Laird, D.; Parkin, T. Effect of Biochar on Soil Greenhouse Gas Emissions at the Laboratory and Field Scales. *Soil Syst.* **2019**, *3*, 8. [CrossRef]

77. Spokas, K.A. Impact of Biochar Field Aging on Laboratory Greenhouse Gas Production Potentials. *GCB Bioenergy* **2013**, *5*, 165–176. [CrossRef]

forests

MDPI

Article

Biochar Is Comparable to Dicyandiamide in the Mitigation of Nitrous Oxide Emissions from *Camellia oleifera* Abel. Fields

Bangliang Deng [1,2], Haifu Fang [1], Ningfei Jiang [3], Weixun Feng [1], Laicong Luo [1], Jiawei Wang [1], Hua Wang [4], Dongnan Hu [1], Xiaomin Guo [1] and Ling Zhang [1,*]

1 Key Laboratory of Silviculture, College of Forestry, Jiangxi Agricultural University, Nanchang 330045, China; bangliangdeng@gmail.com (B.D.); fanghaifu11@163.com (H.F.); fwx1754090341@126.com (W.F.); Luolaicong@126.com (L.L.); wjw_bjfu@163.com (J.W.); dnhu98@163.com (D.H.); gxmjxau@163.com (X.G.)
2 Department of Plant Pathology, North Carolina State University, Raleigh, NC 27695, USA
3 Seed Management Station, Jiande Agricultural and Rural Burea, Jiande 311600, China; jiangningfei2009@163.com
4 College of Land Resources and Environment, Jiangxi Agricultural University, Nanchang 330045, China; mengyiwanghua@sina.com
* Correspondence: lingzhang09@126.com; Tel.: +86-0791-8381-3243

Received: 25 October 2019; Accepted: 25 November 2019; Published: 27 November 2019

Abstract: *Research Highlights*: Intensive nitrogen (N) application for agricultural purposes has substantially increased soil nitrous oxide (N_2O) emissions. Agricultural soil has great potential in the reduction of N_2O emissions, and applications of biochar and nitrification inhibitors may be useful for mitigating agricultural soil N_2O emissions. *Background and Objectives: Camellia oleifera* Abel. is an important woody oil plant in China. However, intensive N input in *C. oleifera* silviculture has increased the risk of soil N_2O emissions. As an important greenhouse gas, N_2O is characterized by a global warming potential at a 100-year scale that is 265 times that of carbon dioxide. Thus, mitigation of soil N_2O emissions, especially fertilized soils, will be crucial for reducing climate change. *Materials and Methods*: Here, we conducted an in situ study over 12 months to examine the effects of *C. oleifera* fruit shell-derived biochar and dicyandiamide (DCD) on soil N_2O emissions from a *C. oleifera* field with intensive N application. *Results*: A three-fold increase of cumulative soil N_2O emissions was observed following N application. Cumulative N_2O emissions from the field with N fertilization were reduced by 36% and 44% with biochar and DCD, respectively. While N_2O emissions were slightly deceased by biochar, the decrease was comparable to that by DCD. *Conclusions*: Results indicated that biochar may mitigate soil N_2O emissions substantially and similarly to DCD under specific conditions. This result should be examined by prolonged and multi-site studies before it can be generalized to broader scales.

Keywords: biochar; *Camellia oleifera*; DCD; nitrification inhibitor; nitrous oxide

1. Introduction

Increased atmospheric greenhouse gases (GHGs) as a result of human activities contribute substantially to global warming. Nitrous oxide (N_2O) is an important component of GHGs [1] and is a dominant ozone-depleting substance [2]. Concentrations of atmospheric N_2O increased from 270 ppb in the 18th century to a new high at 329.9 ppb in 2017 [3]. Specifically, the global warming potential at a 100-year scale of N_2O is 265 times that of carbon dioxide [1]. Considering its important role in global warming, reduction of N_2O emissions is crucial for the mitigation of global climate change.

Soil is the largest source of N_2O emissions at 13 Tg N_2O-N year^{-1}. Human activities have contributed 7 Tg N_2O-N year^{-1} thus far in the 21st century [4]. Intensive nitrogen (N) applications for

agricultural purposes have induced input of 79 Tg synthetic N and 7.4 Tg N of livestock manure per year [5,6]. Therefore, agricultural soil has large potential in the reduction of N_2O emissions and hence for the mitigation of global climate change.

Biochar and nitrification inhibitor applications are useful strategies for N_2O emission mitigation [7–10]. Biochar is produced by slow pyrolysis of organic matter under high temperatures and an anaerobic environment [11]. Biochar application reduced N_2O emissions caused by N fertilization by 33% [7]; this was ascribed to increased soil pH [12] or N immobilization [7]. In addition, 70% of N_2O emissions are emitted from microbial-driven nitrification and denitrification processes [4], which could be effectively inhibited by nitrification inhibitors. Nitrification inhibitors are a class of organic compounds that inhibit the activity of nitrifying nitrifiers, including synthetic nitrification inhibitors such as dicyandiamide (DCD), nitrapyrin, and 3, 4-dimethylpyrazole phosphate, and biological nitrification inhibitors such as methyl 3-(4-hydroxyphenyl) propionate [13] and brachialactone [14]. Nitrification inhibitors reduced N_2O emissions by 44% via inhibition of nitrifying nitrifiers [15]. As a commonly used nitrification inhibitor, DCD deactivates the activity of ammonium monooxygenase enzyme (a copper co-factor enzyme), and hence N_2O emissions [16].

Camellia oleifera Abel. is one of the world's four main woody edible oil crops, with a long cultivation history and wide cultivation area in subtropical China [17] due to the beneficial effects of its oil on human health [18]. *C. oleifera* is mainly cultivated in Typic Hapludult Ultisols (red soil) with lower soil fertility [17,19]. Therefore, intensive N input has been used to increase the yield of *C. oleifera* oil. However, large amounts of N input increase the risk of nitrate N (NO_3^--N) leaching and gaseous N losses, such as N_2O emissions and ammonia volatilization [20,21]. While large amounts of *C. oleifera* fruit shells have been dumped without use, it might be an ideal feedstock for producing biochar for the mitigation of N_2O emissions [22].

Here, we conducted study using biochar derived from *C. oleifera* fruit shells and DCD to examine their effects in the mitigation of N_2O emissions from a *C. oleifera* field with intensive ammonium nitrate (NH_4NO_3) fertilization. We predicted that *C. oleifera* fruit shell-derived biochar or DCD may effectively mitigate soil N_2O emissions.

2. Materials and Methods

2.1. Study Site and Soil Collection

This study was conducted at a *C. oleifera* plantation covering 200 ha in Yongxiu county, Jiangxi province, China (29.16° N, 115.77° E) from 25 February 2017 to 16 March 2018. The *C. oleifera* plantation has been intensively managed more than 10 years, with each individual tree distributed 2 m or 3 m apart. Compound fertilizer with 14% N was applied at the rate of 300 mg plant^{-1}. In this region, there is a subtropical monsoon climate with a mean annual precipitation of 1561 mm and a mean annual air temperature of 17.5 °C (the monthly mean temperature ranges from 2.4 °C in January to 33.4 °C in July) (http://www.worldclim.org). Soil was classified as Typic Hapludult (red soil). Soil characteristics were obtained by collecting soil samples from 12 randomly selected sites and pooled together for measurement. The basic characteristics were as follows: bulk density, 1.42 g cm^{-3}; pH, 4.45; total organic carbon (TOC), 11.06 g kg^{-1}; total N (TN), 1.18 g kg^{-1}; dissolved organic carbon (DOC), 0.28 g kg^{-1}; dissolved organic N (DON), 39.78 mg kg^{-1}; ammonium N (NH_4^+-N), 4.52 mg kg^{-1}; NO_3^--N, 1.37 mg kg^{-1}.

2.2. Experimental Design and Field Procedures

This study was conducted using a randomized design with four treatments (including Control, N only, N with Biochar, N with DCD) and four replications (N = 16, four soil amelioration treatment × four replicates). Biochar was produced by pyrolyzing *C. oleifera* fruit shell at 450 °C without oxygen for 1 h and was applied at the rate of 500 g plant^{-1}(equivalent to 10 t ha^{-1}). Biochar characteristics were: pH, 9.49; TOC, 743.89 g kg^{-1}; TN, 5.14 g kg^{-1}; DOC, 1.57 g kg^{-1}; DON, 14.28 mg kg^{-1}; NH_4^+-N,

2.24 mg kg^{-1}; NO_3^--N, 2.65 mg kg^{-1}. DCD was applied by 2% (DCD/N) [22]. Two years before the study, the studied area was intensively managed but no fertilization was applied. In the study, N was applied by 20 g NH_4NO_3-N $plant^{-1}$ (equivalent to 400 kg NH_4NO_3-N ha^{-1}). Sixteen *C. oleifera* trees with similar size (mean ground diameter: 6.52 cm) were randomly selected and 0.5 m^2 plots were established under the crown of each plant for measurement of N_2O fluxes. Nitrogen, biochar, or DCD were thoroughly mixed and applied in all plots.

Static opaque chamber method was used for measurement of N_2O fluxes. Plastic collars with a groove (inner diameter = 16.7 cm, height = 10 cm, groove = 9 cm) were installed inside each plot. The collar groove was filled with water to seal the open-bottomed chamber (inner diameter = 19.5 cm, height = 80 cm) covered with foam and aluminum for minimizing temperature variation [23]. Gas samples were collected at minutes 0, 5, 10, and 15 min from chamber closing using a syringe, and were stored in aluminum foil gas sample bags before analysis.

Fluxes of N_2O were measured 21 times from 25 February, 2017 to 16 March, 2018 at days 4, 8, 12, 19, 26, 32, 46, 62, 77, 93, 111, 130, 140, 161, 175, 190, 210, 248, 287, 339, and 384. Air temperature, soil temperature, and moisture (10 cm depth) were monitored simultaneously when N_2O fluxes were measured. Meanwhile, soil NH_4^+-N and NO_3^--N (0–20 cm layer) were measured nine times over the study on days 62, 93, 130, 161, 210, 248, 287, 339, and 384.

2.3. Analysis of Soil and Biochar Characteristics

Concentrations of soil and biochar NH_4^+-N and NO_3^--N were extracted by 2 mol L^{-1} KCl solution and measured by a discrete analyzer (Smartchem 200, Rome, Italy). Dissolved organic carbon and DON were extracted by 0.5 mol L^{-1} K_2SO_4 and measured by element analyzer (Multi N/C 3100, Jena Germany). pH was measured by soil (1:2.5, *w/w*) or biochar (1:5, *w/w*) suspensions using pH meter and air-dried samples passed through 0.2-mm sieve (Mettler Toledo, Shanghai, China). Total organic carbon and TN were also analyzed by an element analyzer (Variomax CNS Analyzer, Elementar GmbH, Hanau, Germany) using samples passed through a 0.15-mm sieve.

2.4. Measurement of Soil N_2O Emission Rates and Cumulative Soil N_2O Emissions

Nitrous oxide concentration in each sample was determined using gas chromatograph (Agilent 7890B, Santa Clara, CA, USA). In situ measurements were conducted on sunny days with minimal partial pressure of water vapor. Nitrous oxide fluxes (F, μg m^{-2} h^{-1}) were calculated by [23,24]:

$$F = P \times V \times \frac{\Delta c}{\Delta t} \times \frac{1}{RT} \times M \times \frac{1}{S} \quad (1)$$

where P stands for standard atmospheric pressure (Pa) (which should be adjusted if partial pressure of water vapor of chamber air taken into consideration [25]), V refers to the volume of chamber headspace (m^3), $\Delta c/\Delta t$ means the rate of N_2O (ppb) concentration change with time based on linear regressions [26,27], R stands for universal gas constant (m^3 mol^{-1} K^{-1}), T is the absolute air temperature (K), M means the molecular mass of N_2O (g mol^{-1}), and S indicates the collar area (m^2).

Cumulative soil N_2O emissions (E, μg m^{-2}) were calculated by [28]:

$$E = \sum_{i=1}^{n} \frac{(F_i + F_{i+1})}{2} \times (t_{i+1} - t_i) \times 24 \quad (2)$$

where F indicates soil N_2O emission rates (μg m^{-2} h^{-1}), i means the ith measurement, $(t_{i+1} - t_i)$ refers to the time span (days) between two measurements, and n means the total number of the measurements.

2.5. Statistical Analysis

One-way analysis of variance (ANOVA) was performed to examine dependence of cumulative N_2O emissions on N, biochar and DCD treatments. Repeated-measures ANOVA was used to examine

dependence of soil temperature, moisture, NH_4^+-N, NO_3^--N and N_2O emission rates on biochar and DCD treatments. Tukey's honestly significant difference (HSD) tests were used for identifying the significant differences among treatments in ANOVA. Follow-up contrasts were conducted for significant repeated-measures ANOVA results. Pairwise correlation analysis was applied to examine relationship between environment factor, inorganic N and soil N_2O emission rate. All statistical analyses were carried out using JMP 9.0. Software (Gary, NC, USA) at $\alpha = 0.05$.

3. Results

Application of N, biochar, or DCD significantly influenced soil N_2O emission rates ($F = 8.34$, $p = 0.0029$) and cumulative N_2O emissions ($F = 6.68$, $p = 0.0067$) compared to control from the *C. oleifera* field. No significant results were observed in soil temperature, moisture, NH_4^+-N, and NO_3^--N (Figures 1 and 2). Compared with N treatment, N + DCD ($F = 7.94$, $p = 0.0155$) or N + biochar ($F = 5.69$, $p = 0.0344$) treatments showed lower soil N_2O emission rates, but no significant differences were observed between N + DCD and N + biochar treatments ($F = 0.19$, $p = 0.67$; Figure 3). Overall, N, biochar, or DCD treatments significantly impacted soil N_2O emission rates over the 12-month study ($F = 10.11$, $p = 0.0013$; Figure 3).

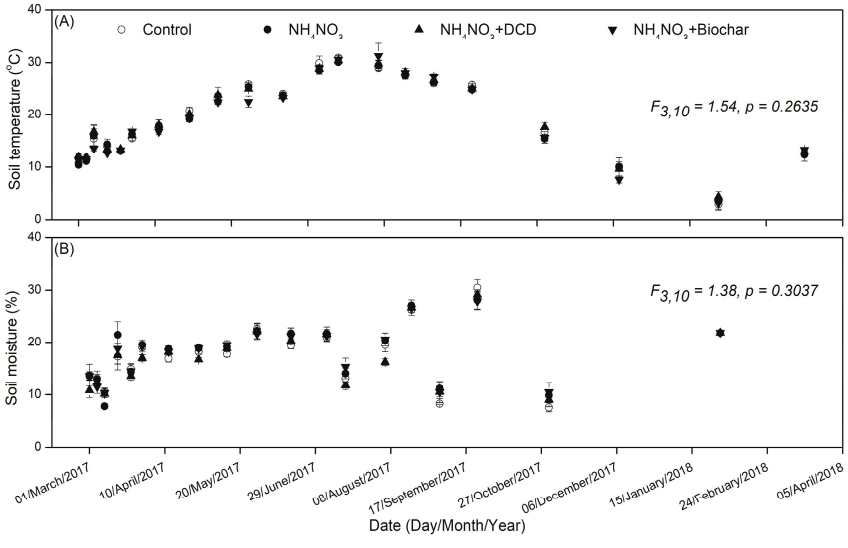

Figure 1. Soil (**A**) temperature and (**B**) moisture (mean ± standard error) over the 12-month study in *Camellia oleifera* Abel. field with the N and mitigation treatments. Repeated-measure one-way analysis of variance results are shown. N: nitrogen; DCD: dicyandiamide; NH_4NO_3: ammonium nitrate.

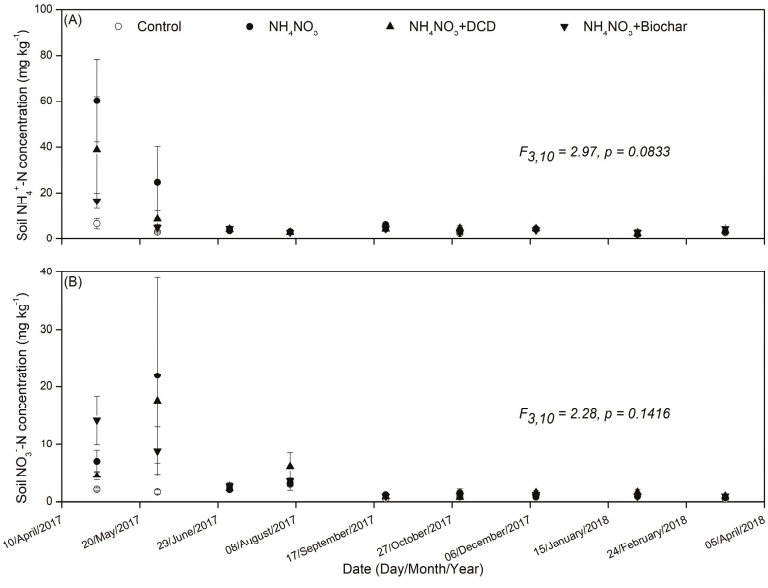

Figure 2. Soil inorganic N dynamics, including (**A**) NH_4^+-N and (**B**) NO_3^--N (mean ± standard error), over the 12-month study in *Camellia oleifera* Abel. field with the N and mitigation treatments. Repeated-measure one-way analysis of variance results are shown. N: nitrogen; NH_4^+-N: ammonium nitrogen; NO_3^--N: nitrate nitrogen; DCD: dicyandiamide; NH_4NO_3: ammonium nitrate.

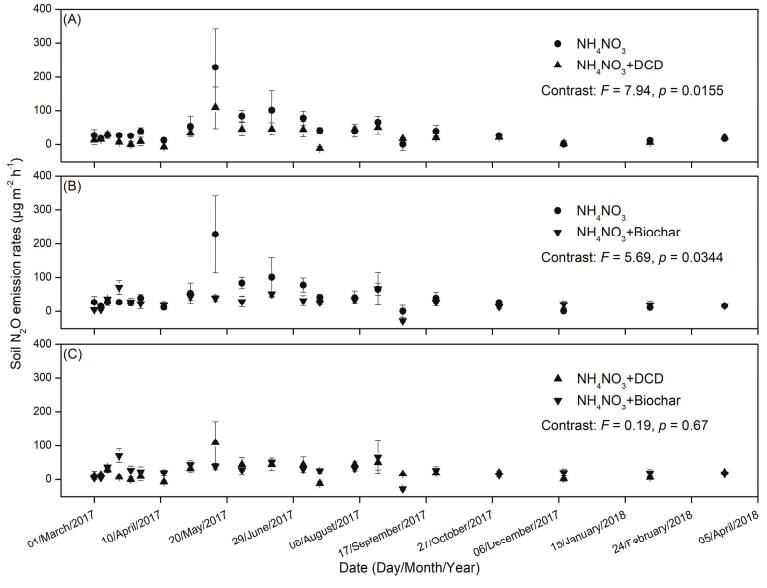

Figure 3. Soil N_2O emissions (mean ± standard error) from soil with N, or N with DCD or biochar in a *Camellia oleifera* Abel. field. (**A**) NH_4NO_3 vs. NH_4NO_3 + DCD; (**B**) NH_4NO_3 vs. NH_4NO_3 + Biochar; (**C**) NH_4NO_3 + DCD vs. NH_4NO_3 + Biochar. Repeated-measure one-way analysis of variance and follow-up contrast results are shown. N: nitrogen; DCD: dicyandiamide; NH_4NO_3: ammonium nitrate; N_2O: nitrous oxide.

Nitrogen treatment increased cumulative soil N_2O emissions (control vs. N, 92.14 ± 47.01 vs. 375.10 ± 60.30 mg m^{-2}, respectively). DCD reduced the increase of cumulative soil N_2O emissions caused by N addition, but no significant differences were observed between N + DCD and N + biochar treatments (Figure 4, N + DCD vs. N + biochar, 211.89 ± 35.88 vs. 238.34 ± 30.65 mg m^{-2}). The soil N_2O emission rate positively correlated with soil temperature, moisture, NH_4^+-N, and NO_3^--N (Table 1).

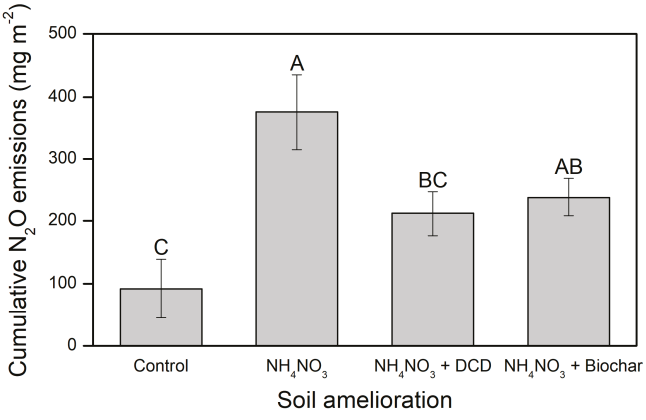

Figure 4. Cumulative soil N_2O emissions (mean ± SE) from the *Camellia oleifera* Abel. field as affected by N fertilization, DCD, or biochar treatments. Bars connected by the same letter are not significantly different in post-hoc tests at $\alpha = 0.05$. N: nitrogen; DCD: dicyandiamide; NH_4NO_3: ammonium nitrate; N_2O: nitrous oxide.

Table 1. Pairwise correlations among soil environmental factors, inorganic nitrogen and soil N_2O emission rate.

Parameters	Soil Temperature	Soil Moisture	NH_4^+-N	NO_3^--N
Soil moisture	0.275 ***			
NH_4^+-N	0.051	−0.050		
NO_3^--N	0.188 *	−0.003	0.414 ***	
N_2O	0.216 ***	0.201 ***	0.285 ***	0.221 **

*, $p < 0.05$; **, $p < 0.01$; ***, $p < 0.001$. NH_4^+-N: ammonium nitrogen; NO_3^--N: nitrate nitrogen; N_2O: nitrous oxide.

4. Discussion

Nitrous oxide emitted from *C. oleifera* plantation was monitored over one year in situ study to investigate effects of biochar or DCD on soil N_2O emissions following application of N fertilization. Soil N_2O emission rates were decreased by biochar or DCD in fertilized soil and the decrease was comparable between two treatments (Figure 3). However, the cumulative soil N_2O emissions caused by NH_4NO_3 fertilization were reduced by DCD application to levels comparable to the control treatment (Figure 4).

4.1. Nitrogen Fertilization Stimulated Soil N_2O Emissions

Nitrogen fertilization stimulated cumulative soil N_2O emissions from *C. oleifera* plantation (Figure 4). N fertilization generally alters activities of N-transforming microorganisms via input of available N substrate [29], stimulating the processes of microbial-driven nitrification and denitrification and subsequent soil N_2O emissions [30,31]. In general, soil N_2O emissions were increased by N input with nonlinear responses [32]. Indeed, the soil N_2O emission rate was positively correlated with NH_4^+-N and NO_3^--N (Table 1). Furthermore, intensive N fertilization, especially NH_4^+-N fertilization, often results in soil acidification [33,34]. Changes in soil pH may regulate soil N_2O emissions via

altering the abundance and composition of N-transforming microorganisms [35–37]. For example, abundances of ammonia-oxidizing bacteria (AOB) were more sensitive to N addition than that of ammonia-oxidizing archaea (AOA) (+ 326% vs. + 27%) [35]. Soil acidification induced by intensive N fertilization results in a high ratio of $N_2O/(N_2O+N_2)$ in the previous study [38]. Therefore, N addition might alter the abundance and composition of AOB and AOA via acidifying soil, hence stimulating N_2O emissions.

In our study, positive correlations between N_2O emission rate and soil temperature or soil moisture were observed (Table 1). A previous study demonstrated that soil temperature and moisture can explain up to 86% variations of N_2O emissions [39]. Soil N_2O emissions varied with soil temperature in specific ranges [28,40], which may relate to different optimum temperatures of N-transforming microorganisms with or without N fertilization and different soil types [37,41]. Compared with soil temperature, soil moisture is the main factor impacting soil N_2O emissions. Consistently, soil N_2O emitted from a wheat–maize plantation showed a positive correlation with a soil water-filled pore space (WFPS) [42]. However, higher soil moisture with lower oxygen content was beneficial to denitrification [30,43] and potentially decrease soil N_2O emissions [44,45]. For example, WFPS at 67–76% was the optimum moisture environment for emitting N_2O [46]. Similarly, N_2O emitted from a rice-rapeseed rotation soil was higher in 60% WFPS than flooding in an incubation experiment [36]. Therefore, moisture effects of soil N_2O emissions may depend on soil type and present non-linear correlations.

4.2. Biochar Reduced Soil N_2O Emission Rates as Affected by N Fertilization

In fertilized soil, N_2O emission rates were significantly decreased and cumulative N_2O emissions were decreased by 36% by biochar (Figures 3B and 4), indicating biochar could be an ideal strategy for N_2O mitigations in *C. oleifera* plantations with N fertilization. Indeed, soil N_2O emissions with N fertilization were decreased 33% by biochar in a meta-analysis study [7]. Biochar-suppressed soil N_2O emissions may be relative, limiting the availability of NO_3^--N to denitrifiers [47,48] or altering the N transformation process rather than limiting the availability of NH_4^+-N or NO_3^--N to N-transforming microorganisms [49]. In addition, biochar could also impose toxic effects on urease activity and subsequent generation of NH_4^+-N by introducing polycyclic aromatic hydrocarbons, heavy metals, and free radicals into soil [50], which may suppress soil N_2O emissions via reducing the N substrate with respect to N-transforming microorganisms.

Biochar addition may suppress soil N_2O emissions by increasing soil pH [12]. The activity of N_2O-reductase was generally higher with higher soil pH [31]. Indeed, the pH of *C. oleifera* fruit shell-derived biochar was higher than that of the acid soil in *C. oleifera* plantations. While an acid soil improvement study showed that liming by dolomite addition could substantially mitigate N_2O emissions via increasing *nosZ* gene abundance [36,51], biochar application could also increase soil pH of the acid *C. oleifera* field soil, which might have also been accompanied by enhanced activities of N_2O-reducing enzymes and hence suppressed N_2O emissions. Moreover, the negative effects of biochar on N_2O emissions could also be induced by its buffer capacity rather than pH, in which biochar acted as "electron shuttle" and replaced NO_3^- as electron sink during denitrification [52]. However, the application of *C. oleifera* fruit shell-derived biochar stimulated N_2O emissions in a previous incubation study [22], which might have been caused by the short-term time scale of incubation study and further indicated the importance of in situ studies. Future studies are still needed for thoroughly understanding of *C. oleifera* fruit shell-derived biochar effects on N_2O emissions and its prolonged effects in mitigation of soil N_2O emissions.

4.3. DCD Reduced Soil N_2O Emissions as Affected by N Fertilization

Cumulative soil N_2O emissions were reduced 44% by DCD application in soil with N fertilization treatment (Figures 3A and 4), which indicated that the application of DCD is an effective strategy for mitigating soil N_2O emissions in *C. oleifera* plantations with intensive N fertilization. DCD has been proved to be effective in reducing average N_2O emission rates following NH_4NO_3 addition in a

previous study [22]. In agreement, DCD reduced soil N_2O emissions following $(NH_4)_2SO_4$ addition by suppressing *amoA* genes and stimulating *nosZ* genes [53]. Nitrification and denitrification are two main pathways producing N_2O [30,31,54]. Application of nitrification inhibitors can suppress soil N_2O emissions [15,16] by inhibiting the activity of ammonium monooxygenase enzyme involved in nitrification process [16]. Thereby, application of DCD generally decreases abundance of *amoA* genes and hence soil N_2O emissions.

4.4. Biochar and DCD Effects on Soil N_2O Emissions

While N fertilization significantly increased soil N_2O emissions compared with control treatment, DCD application decreased soil N_2O emissions to similar levels as control treatment (Figures 3A and 4). Even though biochar addition treatment did not significantly decrease N_2O emissions from soil with N, the slight decrease in cumulative N_2O emissions may potentially mitigate N_2O emissions in prolonged study, which should be examined in future studies. However, DCD application significantly decreased cumulative N_2O emissions and no significant difference was observed between control and DCD treatment (Figure 4), indicating DCD was effective in mitigation of N_2O emissions from *C. oleifera* field relative to biochar. No significant differences were observed between DCD and biochar treatments in their effects on N_2O emission rates (Figures 3C and 4), indicating biochar application could be considered as a potential mitigation strategy of soil N_2O. Similarly, both DCD and biochar reduced the yield-scaled N_2O following N fertilization, while biochar showed stronger effects than DCD in N_2O mitigation in a sweet corn field [55].

5. Conclusions

This study is the first in examining the effects of DCD and biochar derived from *C. oleifera* fruit shells on mitigation of soil N_2O emissions. Application of biochar and DCD showed comparable effects in mitigation of the N_2O emission rate in a *C. oleifera* field with intensive N fertilization practice, with biochar slightly decreasing and DCD significantly decreasing cumulative N_2O emissions. This might have implications for the disposal of dumped byproducts in management of *C. oleifera* and represent an ideal way to enhance both the economic and ecological benefits of the *C. oleifera* industry. If this pattern presents in other plantations, the combined effects of biochar and nitrification inhibitors on soil N_2O emissions should be focused upon in the future. However, the potential effects of biochar derived from *C. oleifera* fruit shell on cumulative N_2O emissions in prolonged studies and other kinds of ecosystems should be examined in future in order to provide guidance for intensive management of *C. oleifera* plantations and disposal of byproducts.

Author Contributions: Conceptualization, L.Z. and B.D.; methodology, L.Z. and B.D.; software, L.Z. and B.D.; validation, H.F., N.J., H.W., and D.H.; investigation, B.D., H.F., and N.J.; resources, L.Z. and X.G.; data curation, B.D., H.F., N.J., and J.W.; writing—original draft preparation, B.D.; writing—review and editing, L.Z., N.J., H.W., J.W., W.F., L.L., and X.G.; project administration, B.D., H.F., and L.Z.; funding acquisition, L.Z.

Funding: This research was funded by the National Natural Science Foundation of China, Grant Numbers 41967017 and 41501317, and the Jiangxi Education Department, Project Number GJJ160348. Bangliang Deng was supported by China Scholarship Council for study in the United States.

Acknowledgments: Thanks are given to Liya Zheng, Xiang Zheng, Qian Li, Xi Yuan, Shuli Wang, Xintong Xu, and Jianwei Wang for their help in laboratory and field work.

Conflicts of Interest: The authors have declared that no competing interests exist.

References

1. IPCC. *Synthesis Report, Climate Change 2014*; IPCC: Geneva, Switzerland, 2014; pp. 1–164.
2. Ravishankara, A.R.; Daniel, J.S.; Portmann, R.W. Nitrous oxide (N_2O): The dominant ozone-depleting substance emitted in the 21st century. *Science* **2009**, *326*, 123–125. [CrossRef] [PubMed]
3. WMO. *WMO Greenhouse Gas Bulletin: The State of Greenhouse Gases in the Atmosphere Based on Global Observations Through 2017*; Atmospheric Environment Research Division: Geneva, Switzerland, 2018; pp. 1–8.

4. Fowler, D.; Coyle, M.; Skiba, U.; Sutton, M.A.; Cape, J.N.; Reis, S.; Sheppard, L.J.; Jenkins, A.; Grizzetti, B.; Galloway, J.N.; et al. The global nitrogen cycle in the twenty-first century. *Philos. Trans. R. Soc. B Biol. Sci.* **2013**, *368*, 1–13. [CrossRef]
5. Gerber, J.S.; Carlson, K.M.; Makowski, D.; Mueller, N.D.; Garcia De Cortazar-Atauri, I.; Havlík, P.; Herrero, M.; Launay, M.; O'Connell, C.S.; Smith, P.; et al. Spatially explicit estimates of N_2O emissions from croplands suggest climate mitigation opportunities from improved fertilizer management. *Glob. Chang. Biol.* **2016**, *22*, 3383–3394. [CrossRef] [PubMed]
6. Carlson, K.M.; Gerber, J.S.; Mueller, N.D.; Herrero, M.; MacDonald, G.K.; Brauman, K.A.; Havlik, P.; Connell, C.S.; Johnson, J.A.; Saatchi, S.; et al. Greenhouse gas emissions intensity of global croplands. *Nat. Clim. Chang.* **2017**, *7*, 63–68. [CrossRef]
7. He, Y.; Zhou, X.; Jiang, L.; Li, M.; Du, Z.; Zhou, G.; Shao, J.; Wang, X.; Xu, Z.; Hosseini Bai, S.; et al. Effects of biochar application on soil greenhouse gas fluxes: A meta-analysis. *GCB Bioenergy* **2017**, *9*, 743–755. [CrossRef]
8. Gu, J.; Nie, H.; Guo, H.; Xu, H.; Gunnathorn, T. Nitrous oxide emissions from fruit orchards: A review. *Atmos. Environ.* **2019**, *201*, 166–172. [CrossRef]
9. Liu, Q.; Liu, B.; Zhang, Y.; Hu, T.; Lin, Z.; Liu, G.; Wang, X.; Ma, J.; Wang, H.; Jin, H.; et al. Biochar application as a tool to decrease soil nitrogen losses (NH_3 volatilization, N_2O emissions, and N leaching) from croplands: Options and mitigation strength in a global perspective. *Glob. Chang. Biol.* **2019**, *25*, 2077–2093. [CrossRef]
10. Shrestha, B.; Chang, S.; Bork, E.; Carlyle, C. Enrichment planting and soil amendments enhance carbon sequestration and reduce greenhouse gas emissions in agroforestry systems: A review. *Forests* **2018**, *9*, 369. [CrossRef]
11. Johannes, L.; Stephen, J. *Biochar for Environmental Management*; Routledge: New York, NY, USA, 2015; pp. 1–944.
12. Obia, A.; Cornelissen, G.; Mulder, J.; Dörsch, P. Effect of soil pH increase by biochar on NO, N_2O and N_2 production during denitrification in acid soils. *PLoS ONE* **2015**, *10*, 1–19. [CrossRef]
13. Zakir, H.A.; Subbarao, G.V.; Pearse, S.J.; Gopalakrishnan, S.; Ito, O.; Ishikawa, T.; Kawano, N.; Nakahara, K.; Yoshihashi, T.; Ono, H.; et al. Detection, isolation and characterization of a root-exuded compound, methyl 3-(4-hydroxyphenyl) propionate, responsible for biological nitrification inhibition by sorghum (*Sorghum bicolor*). *New Phytol.* **2008**, *180*, 442–451. [CrossRef]
14. Subbarao, G.V.; Nakahara, K.; Hurtado, M.P.; Ono, H.; Moreta, D.E.; Salcedo, A.F.; Yoshihashi, A.T.; Ishikawa, T.; Ishitani, M.; Ohnishi-Kameyama, M.; et al. Evidence for biological nitrification inhibition in *Brachiaria* pastures. *Proc. Natl. Acad. Sci. USA* **2009**, *106*, 17302–17307. [CrossRef] [PubMed]
15. Qiao, C.; Liu, L.; Hu, S.; Compton, J.E.; Greaver, T.L.; Li, Q. How inhibiting nitrification affects nitrogen cycle and reduces environmental impacts of anthropogenic nitrogen input. *Glob. Chang. Biol.* **2015**, *21*, 1249–1257. [CrossRef] [PubMed]
16. Ruser, R.; Schulz, R. The effect of nitrification inhibitors on the nitrous oxide (N_2O) release from agricultural soils-a review. *J. Plant Nutr. Soil Sci.* **2015**, *178*, 171–188. [CrossRef]
17. Liu, J.; Wu, L.; Chen, D.; Li, M.; Wei, C. Soil quality assessment of different *Camellia oleifera* stands in mid-subtropical China. *Appl. Soil Ecol.* **2017**, *113*, 29–35. [CrossRef]
18. Yuan, J.; Wang, C.; Chen, H.; Zhou, H.; Ye, J. Prediction of fatty acid composition in *Camellia oleifera* oil by near infrared transmittance spectroscopy (NITS). *Food Chem.* **2013**, *138*, 1657–1662. [CrossRef]
19. Liu, C.; Chen, L.; Tang, W.; Peng, S.; Li, M.; Deng, N.; Chen, Y. Predicting potential distribution and evaluating suitable soil condition of oil tea *Camellia* in China. *Forests* **2018**, *9*, 487. [CrossRef]
20. Martins, M.R.; Sant Anna, S.A.C.; Zaman, M.; Santos, R.C.; Monteiro, R.C.; Alves, B.J.R.; Jantalia, C.P.; Boddey, R.M.; Urquiaga, S. Strategies for the use of urease and nitrification inhibitors with urea: Impact on N_2O and NH_3 emissions, fertilizer-^{15}N recovery and maize yield in a tropical soil. *Agric. Ecosyst. Environ.* **2017**, *247*, 54–62. [CrossRef]
21. Liu, S.; Lin, F.; Wu, S.; Ji, C.; Sun, Y.; Jin, Y.; Li, S.; Li, Z.; Zou, J. A meta-analysis of fertilizer-induced soil NO and combined NO+N_2O emissions. *Glob. Chang. Biol.* **2017**, *23*, 2520–2532. [CrossRef]
22. Deng, B.; Wang, S.; Xu, X.; Wang, H.; Hu, D.; Guo, X.; Shi, Q.; Siemann, E.; Zhang, L. Effects of biochar and dicyandiamide combination on nitrous oxide emissions from *Camellia oleifera* field soil. *Environ. Sci. Pollut. Res.* **2019**, *26*, 4070–4077. [CrossRef]

23. Zhang, L.; Wang, S.; Liu, S.; Liu, X.; Zou, J.; Siemann, E. Perennial forb invasions alter greenhouse gas balance between ecosystem and atmosphere in an annual grassland in China. *Sci. Total Environ.* **2018**, *642*, 781–788. [CrossRef]
24. Zhang, L.; Ma, X.; Wang, H.; Liu, S.; Siemann, E.; Zou, J. Soil respiration and litter decomposition increased following perennial forb invasion into an annual grassland. *Pedosphere* **2016**, *26*, 567–576. [CrossRef]
25. Carter, M.R.; Gregorich, E.G. *Soil Sampling and Methods of Analysis*; CRC Press: Boca Raton, IL, USA, 2007; pp. 1–1224.
26. Pärn, J.; Verhoeven, J.T.A.; Butterbach-Bahl, K.; Dise, N.B.; Ullah, S.; Aasa, A.; Egorov, S.; Espenberg, M.; Järveoja, J.; Jauhiainen, J.; et al. Nitrogen-rich organic soils under warm well-drained conditions are global nitrous oxide emission hotspots. *Nat. Commun.* **2018**, *9*, 1–8. [CrossRef]
27. Domeignoz-Horta, L.A.; Philippot, L.; Peyrard, C.; Bru, D.; Breuil, M.; Bizouard, F.; Justes, E.; Mary, B.; Léonard, J.; Spor, A. Peaks of in situ N_2O emissions are influenced by N_2O-producing and reducing microbial communities across arable soils. *Glob. Chang. Biol.* **2018**, *24*, 360–370. [CrossRef] [PubMed]
28. He, T.; Yuan, J.; Luo, J.; Wang, W.; Fan, J.; Liu, D.; Ding, W. Organic fertilizers have divergent effects on soil N_2O emissions. *Biol. Fertil. Soils* **2019**, *55*, 685–699. [CrossRef]
29. Lourenço, K.S.; Dimitrov, M.R.; Pijl, A.; Soares, J.R.; Do Carmo, J.B.; van Veen, J.A.; Cantarella, H.; Kuramae, E.E. Dominance of bacterial ammonium oxidizers and fungal denitrifiers in the complex nitrogen cycle pathways related to nitrous oxide emission. *GCB Bioenergy* **2018**, *10*, 645–660. [CrossRef]
30. Pauleta, S.R.; Dell Acqua, S.; Moura, I. Nitrous oxide reductase. *Coord. Chem. Rev.* **2013**, *257*, 332–349. [CrossRef]
31. Hu, H.; Chen, D.; He, J. Microbial regulation of terrestrial nitrous oxide formation: Understanding the biological pathways for prediction of emission rates. *FEMS Microbiol. Rev.* **2015**, *39*, 729–749. [CrossRef]
32. Shcherbak, I.; Millar, N.; Robertson, G.P. Global metaanalysis of the nonlinear response of soil nitrous oxide (N_2O) emissions to fertilizer nitrogen. *Proc. Natl. Acad. Sci. USA* **2014**, *111*, 9199–9204. [CrossRef]
33. Tian, D.; Niu, S. A global analysis of soil acidification caused by nitrogen addition. *Environ. Res. Lett.* **2015**, *10*, 24019. [CrossRef]
34. Matson, P.A.; McDowell, W.H.; Townsend, A.R.; Vitousek, P.M. The globalization of N deposition: Ecosystem consequences in tropical environments. *Biogeochemistry* **1999**, *46*, 67–83. [CrossRef]
35. Carey, C.J.; Dove, N.C.; Beman, J.M.; Hart, S.C.; Aronson, E.L. Meta-analysis reveals ammonia-oxidizing bacteria respond more strongly to nitrogen addition than ammonia-oxidizing archaea. *Soil Biol. Biochem.* **2016**, *99*, 158–166. [CrossRef]
36. Shaaban, M.; Wu, Y.; Khalid, M.S.; Peng, Q.; Xu, X.; Wu, L.; Younas, A.; Bashir, S.; Mo, Y.; Lin, S.; et al. Reduction in soil N_2O emissions by pH manipulation and enhanced *nosZ* gene transcription under different water regimes. *Environ. Pollut.* **2018**, *235*, 625–631. [CrossRef] [PubMed]
37. Blum, J.; Su, Q.; Ma, Y.; Valverde-Pérez, B.; Domingo-Félez, C.; Jensen, M.M.; Smets, B.F. The pH dependency of N-converting enzymatic processes, pathways and microbes: Effect on net N_2O production. *Environ. Microbiol.* **2018**, *20*, 1623–1640. [CrossRef] [PubMed]
38. Qu, Z.; Wang, J.; Almøy, T.; Bakken, L.R. Excessive use of nitrogen in Chinese agriculture results in high $N_2O/(N_2O+N_2)$ product ratio of denitrification, primarily due to acidification of the soils. *Glob. Chang. Biol.* **2014**, *20*, 1685–1698. [CrossRef]
39. Schindlbacher, A. Effects of soil moisture and temperature on NO, NO_2, and N_2O emissions from European forest soils. *J. Geophys. Res.* **2004**, *109*, 1–12. [CrossRef]
40. Pinheiro, P.L.; Recous, S.; Dietrich, G.; Weiler, D.A.; Schu, A.L.; Bazzo, H.L.S.; Giacomini, S.J. N_2O emission increases with mulch mass in a fertilized sugarcane cropping system. *Biol. Fertil. Soils* **2019**, *55*, 511–523. [CrossRef]
41. Yin, C.; Fan, F.; Song, A.; Fan, X.; Ding, H.; Ran, W.; Qiu, H.; Liang, Y. The response patterns of community traits of N_2O emission-related functional guilds to temperature across different arable soils under inorganic fertilization. *Soil Biol. Biochem.* **2017**, *108*, 65–77. [CrossRef]
42. Chen, T.; Oenema, O.; Li, J.; Misselbrook, T.; Dong, W.; Qin, S.; Yuan, H.; Li, X.; Hu, C. Seasonal variations in N_2 and N_2O emissions from a wheat–maize cropping system. *Biol. Fertil. Soils* **2019**, *55*, 539–551. [CrossRef]
43. Quick, A.M.; Reeder, W.J.; Farrell, T.B.; Tonina, D.; Feris, K.P.; Benner, S.G. Nitrous oxide from streams and rivers: A review of primary biogeochemical pathways and environmental variables. *Earth-Sci. Rev.* **2019**, *191*, 224–262. [CrossRef]

44. Chen, H.; Mothapo, N.V.; Shi, W. Soil moisture and pH control relative contributions of fungi and bacteria to N_2O production. *Microb. Ecol.* **2015**, *69*, 180–191. [CrossRef]
45. Burgin, A.J.; Groffman, P.M. Soil O_2 controls denitrification rates and N_2O yield in a riparian wetland. *J. Geophys. Res. Biogeosci.* **2012**, *117*, 1–10. [CrossRef]
46. Chen, Z.; Ding, W.; Xu, Y.; Müller, C.; Yu, H.; Fan, J. Increased N_2O emissions during soil drying after waterlogging and spring thaw in a record wet year. *Soil Biol. Biochem.* **2016**, *101*, 152–164. [CrossRef]
47. Van Zwieten, L.; Singh, B.P.; Kimber, S.W.L.; Murphy, D.V.; Macdonald, L.M.; Rust, J.; Morris, S. An incubation study investigating the mechanisms that impact N_2O flux from soil following biochar application. *Agric. Ecosyst. Environ.* **2014**, *191*, 53–62. [CrossRef]
48. Case, S.D.C.; McNamara, N.P.; Reay, D.S.; Whitaker, J. The effect of biochar addition on N_2O and CO_2 emissions from a sandy loam soil - The role of soil aeration. *Soil Biol. Biochem.* **2012**, *51*, 125–134. [CrossRef]
49. Case, S.D.C.; McNamara, N.P.; Reay, D.S.; Stott, A.W.; Grant, H.K.; Whitaker, J. Biochar suppresses N_2O emissions while maintaining N availability in a sandy loam soil. *Soil Biol. Biochem.* **2015**, *81*, 178–185. [CrossRef]
50. Liu, Y.; Dai, Q.; Jin, X.; Dong, X.; Peng, J.; Wu, M.; Liang, N.; Pan, B.; Xing, B. Negative impacts of biochars on urease activity: High pH, heavy metals, polycyclic aromatic hydrocarbons, or free radicals? *Environ. Sci. Technol.* **2018**, *52*, 12740–12747. [CrossRef]
51. Shaaban, M.; Hu, R.; Wu, Y.; Younas, A.; Xu, X.; Sun, Z.; Jiang, Y.; Lin, S. Mitigation of N_2O emissions from urine treated acidic soils by liming. *Environ. Pollut.* **2019**, *225*, 113237. [CrossRef]
52. Cayuela, M.L.; Sánchez-Monedero, M.A.; Roig, A.; Hanley, K.; Enders, A.; Lehmann, J. Biochar and denitrification in soils: When, how much and why does biochar reduce N_2O emissions? *Sci. Rep.* **2013**, *3*, 1–7. [CrossRef]
53. Wang, Q.; Hu, H.W.; Shen, J.P.; Du, S.; Zhang, L.M.; He, J.Z.; Han, L.L. Effects of the nitrification inhibitor dicyandiamide (DCD) on N_2O emissions and the abundance of nitrifiers and denitrifiers in two contrasting agricultural soils. *J. Soils Sediments* **2017**, *17*, 1635–1643. [CrossRef]
54. Kuypers, M.M.M.; Marchant, H.K.; Kartal, B. The microbial nitrogen-cycling network. *Nat. Rev. Microbiol.* **2018**, *16*, 263–276. [CrossRef]
55. Yi, Q.; Tang, S.; Fan, X.; Zhang, M.; Pang, Y.; Huang, X.; Huang, Q. Effects of nitrogen application rate, nitrogen synergist and biochar on nitrous oxide emissions from vegetable field in south China. *PLoS ONE* **2017**, *12*, 1–15. [CrossRef]

forests

MDPI

Article

Estimation of Forest Carbon Stocks for National Greenhouse Gas Inventory Reporting in South Korea

Sun Jeoung Lee [1,3], Jong Su Yim [1], Yeong Mo Son [2], Yowhan Son [3] and Raehyun Kim [4,*]

1 Division of Forest Industry, National Institute of Forest Science, 57 Hoegi-ro, Seoul 02455, Korea; sunjlee1020@korea.kr (S.J.L.); yimjs@korea.kr (J.S.Y.)
2 Division of Forest Welfare, National Institute of Forest Science, 57 Hoegi-ro, Seoul 02455, Korea; treelove@korea.kr
3 Department of Environmental Science and Ecological Engineering, Graduate School, Korea University, 145 Anam-ro, Seoul 02841, Korea; yson@korea.ac.kr
4 Division of Global Forestry, National Institute of Forest Science, 57 Hoegi-ro, Seoul 02455, Korea
* Correspondence: rhkim@korea.kr; Tel.: +82-2-961-2871

Received: 14 September 2018; Accepted: 5 October 2018; Published: 10 October 2018

Abstract: The development of country-specific emission factors in relation to the Agriculture, Forestry, and Other Land Use (AFOLU) sector has the potential to improve national greenhouse gas inventory systems. Forests are carbon sinks in the AFOLU that can play an important role in mitigating global climate change. According to the United Nations Framework Convention on Climate Change (UNFCCC), signatory countries must report forest carbon stocks, and the changes within them, using emission factors from the Intergovernmental Panel on Climate Change (IPCC) or from country-specific values. This study was conducted to estimate forests carbon stocks and to complement and improve the accuracy of national greenhouse gas inventory reporting in South Korea. We developed country-specific emissions factors and estimated carbon stocks and their changes using the different approaches and methods described by the IPCC ($IPCC_{EF}$: IPCC default emission factors, CS_{FT}: country-specific emission factors by forest type, and CS_{SP}: country-specific emission factors by species). CS_{FT} returned a result for carbon stocks that was 1.2 times higher than the value using $IPCC_{EF}$. Using CS_{SP}, CO_2 removal was estimated to be 60,648 Gg CO_2 per year with an uncertainty of 22%. Despite a reduction in total forest area, forests continued to store carbon and absorb CO_2, owing to differences in the carbon storage capacities of different forest types and tree species. The results of this study will aid estimations of carbon stock changes and CO_2 removal by forest type or species, and help to improve the completeness and accuracy of the national greenhouse gas inventory. Furthermore, our results provide important information for developing countries implementing Tier 2, the level national greenhouse gas inventory systems recommended by the IPCC.

Keywords: carbon stock changes; forest; greenhouse gas inventory; IPCC; South Korea

1. Introduction

According to the United Nations Framework Convention on Climate Change (UNFCCC), all parties are obligated to submit annual national greenhouse gas inventory reports for all emissions and removals, including those associated with the Agriculture, Forestry, and Other Land Use sector (AFOLU). Specifically, the Paris Agreement states that "parties shall account for their Nationally Determined Contributions (NDC)" [1]. The mitigation contributions of parties (included in the NDCs) should be accounted for in the context of the Paris Agreement and are expected to be based on greenhouse gas inventory reporting methodology.

All countries have made efforts to improve inventory reporting systems and tier levels given respective national circumstances, in accordance with the principles of Transparency,

Accuracy, Consistency, Comparability, and Completeness (TACCC) under the UNFCCC [1,2]. The Intergovernmental Panel on Climate Change (IPCC) guidelines provide three different tier levels for calculating the national greenhouse gas inventory, which relate to the activity data and emission factors in the AFOLU [2,3]. In general, using complementary data and moving to a methodology at higher tiers can improve the accuracy of the inventory and reduce uncertainty [2,3]. Most developing countries, including South Korea, have not been able to report on the carbon stocks from all carbon pools [4,5]. Estimating all carbon pools would represent a major improvement in completeness, which is linked to comparability and accuracy for national greenhouse gas inventory systems, and would also affect the greenhouse gas mitigation targets in NDC.

Dependent upon tree growth rate, forest ecosystems are able to remove CO_2 from the atmosphere; as such, they are the largest terrestrial carbon sink [6]. For this reason, Annex I countries under the UNFCCC should report the national emissions and removal of greenhouse gases associated with the forest sector in AFOLU [2,7]. To calculate greenhouse gas emissions and their removal, national forest inventories (NFIs) represent a key source of information [8]. Although relatively few countries carry out NFIs more frequently than every 5 or even 10 years, the national reports normally rely on projected quantities of carbon emissions and removal from forests and land use change for the reporting period [9,10].

Forests cover 64% of the total land area in South Korea, and they play an important role in the mitigation of greenhouse gases through carbon sequestration [11,12]. South Korean forests were a carbon source releasing carbon at a rate of 0.5 Tg C year^{-1} during 1954–1973; however, they have been acting as carbon sinks with a carbon sequestration rate of 12.6 Tg C year^{-1} since 1974 [12]. The annual carbon balance of South Korean forests from 1954 to 2012 was 8.3 Tg C year^{-1} [12]. Studies into forest carbon stocks have been also conducted to establish the greenhouse gas inventory system of the forestry sector in South Korea. The South Korean national greenhouse gas inventory system is based on country-specific emission factors and activity data from NFIs and on official statistics by forest type [5]. To complement the national greenhouse gas inventory system and improve its accuracy, a number of studies have focused on the emission factors in all carbon pools in South Korea [13–17]; a few case studies have also estimated total carbon stocks at the national scale using modeling [12].

Owing partly to a limited range of activity data, previous studies have focused on the above and belowground biomass in South Korean forests [5]. The purpose of this study was to develop country-specific emission factors and to examine the methodology in order to enhance the completeness and accuracy of national greenhouse gas inventory reporting using those factors.

2. Materials and Methods

2.1. Estimating Country-Specific Emission Factors

In order to develop country-specific emission factor for biomass, soil, and litter, we distributed the number of samples in proportion of growing stock by tree species (Figures S1 and S2). The major tree species of Korea were selected and sampled. Red pine (*Pinus densiflora* Siebold & Zucc.), Oak (*Quercus* spp.), and Larch (*Larix kaempferi* (Lamb.) Carrière) were sampled from all over the country; Hinoki-cypress (*Chamaecyparis obtuse* (Siebold & Zucc.) Endl.), Japanese cedar (*Cryptomeria japonica* (Thunb. ex L. f.) D. Don), Black pine (*Pinus thunbergii* Parl.), and other species that are distributed locally, were collected from relevant regions. The carbon emission factors of the carbon pools (biomass, soil, and litter) in Korean forests were estimated from 226 sampling plots during the 2007–2015 period; each sampling plot had an area of 20 × 20 m. In total, 16 tree species were sampled, representing about 77% of the total growing stock in South Korean forests. We measured the height and diameter at breast height of selected sample trees from each plot. These trees were then divided into branches, leaves, twigs, and roots, after which their respective fresh weights were measured. From the 226 sampling plots, we additionally selected 119 plots to estimate soil and litter carbon stocks for eight tree species across South Korea. Litter samples included humus, fallen leaves, and twigs (smaller than 10 cm in

diameter) [18]. Soil pits were dug at each sampling plot, and soil was sampled at depths of 0–10, 10–20, 20–30, and 30–50 cm [18]. Biomass, litter, and soil samples were brought to the laboratory for further analysis.

The dry mass of biomass and litter samples was measured after oven-drying at 85 °C at a constant weight. Soil samples from depths of 0–10 cm, 10–20 cm, 20–30 cm, and 30–50 cm were passed through a 2-mm sieve to remove coarse fragments and roots. Soil bulk density was estimated as the proportion of the dry mass of all mineral soils to the volume of the corer, while the coarse fregments content was estimated as the ratio between the dry mass of coarse fregments to mineral soils, both of which were based on the mass remaining after oven-drying at 105 °C. The carbon concentrations of the litter and mineral soil were determined using an elemental analyzer (vario Macro, Elementar Analysensysteme GmbH, Langenselbold, Germany). Biomass emission factors such as basic wood density (WD), biomass expansion factors (BEF), and the root to shoot ratio (R) were calculated using the dry mass, fresh mass, and volume. The WD was calculated as the ratio of dry-weight to fresh volume using the water displacement method [18]. The BEF was calculated as the ratio of aboveground biomass (stem, branches, leaves, and twigs) to the stem biomass. The R was calculated as the ratio of root biomass to aboveground biomass [18]. Litter carbon stocks (C ton/ha) were calculated using the dry mass multiplied by carbon concentration, and mineral soil carbon stocks (C ton/ha) were calculated as the sum of each soil depth multiplied by bulk density, coarse fregments content, and carbon concentration [18]. However, the country-specific emission factors for deadwood carbon stocks were calculated as the volume of the residences and tree mortality from the NFI data, multiplied by carbon conversion factors from previous studies in South Korea [19,20]. Uncertainty analysis was calculated using the error propagation equation from the IPCC guidelines [3];

$$\text{Uncertainty} = \frac{0.5 \times (95\% CI\ width)}{\mu} \times 100 \quad (1)$$

where $CI\ width$ is the width of the 95% confidence interval and μ is the mean value following the IPCC methodology [3]. Emission factors of other coniferous forest and other deciduous forest except for deadwood carbon stocks were calculated by weighted average using the growing stock proportions in South Korean forest.

2.2. Estimating Carbon Stocks in Biomass, Soil, and Dead Organic Matter

We adopted three different approaches for estimating carbon stocks. The first approach ($IPCC_{EF}$) was applied according to IPCC default emission factors, where it is assumed that soil and dead organic matter do not change with forest management, forest type, or disturbance regime. The second approach (CS_{FT}) was applied according to country-specific emission factors in regard to forest type, while the third approach (CS_{SP}) was applied according to country-specific emission factors for tree species (Table 1).

Table 1. Three approaches for carbon stock estimation.

Resolution	Forest Type		Species
Approach	**$IPCC_{EF}$**	**CS_{FT}**	**CS_{SP}**
Biomass	E	E	E
Litter	NE	E	E
Soil	NE	E	E
Deadwood	NE	E	E

$IPCC_{EF}$: Intergovernmental Panel on Climate Change (IPCC) default emission factors, CS_{FT}: country-specific emission factors by forest type, CS_{SP}: country-specific emission factors by species, E: estimated, NE: not estimated.

In the case of $IPCC_{EF}$ and CS_{FT}, forest areas and growing stocks were taken from national greenhouse gas inventory reports [5], after which the carbon stocks in above and belowground biomass,

soil, litter, and deadwood were calculated using IPCC default emission factors for coniferous species (WD: 0.49, BEF: 1.30, and R: 0.32), deciduous species (WD: 0.58, BEF: 1.40, and R: 0.26), and carbon fraction (0.50) [3], along with country-specific emission factors developed by this study. If there was no country-specific emission factor by tree species, we applied emission factors of other coniferous or deciduous forests by tree species.

On the other hand, NFI data was used for CS_{SP} because official statistics for the growing stocks of tree species do not currently exist. The NFI provides data on merchantable growing stocks and the number of points for each tree species, while data on whole-tree biomass is needed to estimate biomass carbon pools. Specifically, we used data from the 5th and 6th NFI, which were conducted between 2006–2010 and 2011–2015, respectively, and included a nationally consistent sampling frame and plot design (Figure 1). In reference to the 6th NFI, 149 plots were not resampled at the original plots from the 5th NFI; however, 430 new plots were established for sampling. In order to estimate the area of forest types and tree species, we used the proportions of the sub-points in the specific stand for each species, multiplied by the known land area:

$$A_h = A \times p_h, (where,\ p_h = \frac{n_h}{n}) \quad (2)$$

where A_h is the total area by tree species; A is the forest area on the basis of the official statistics of the Korea Forest Service (KFS) and Greenhouse Gas Inventory and Research Center of Korea (GIR) [5,21,22]; p_h is the proportion of points that are of h; n is the number of total points for forest types; n_h is the number of points for h; and h is the tree species. The area of mixed forest was divided into 'other coniferous' and 'other deciduous' forests. The total growing stocks of each species was calculated using the growing stocks per ha and the species area, while the total growing stock was stratified by random sampling of each species.

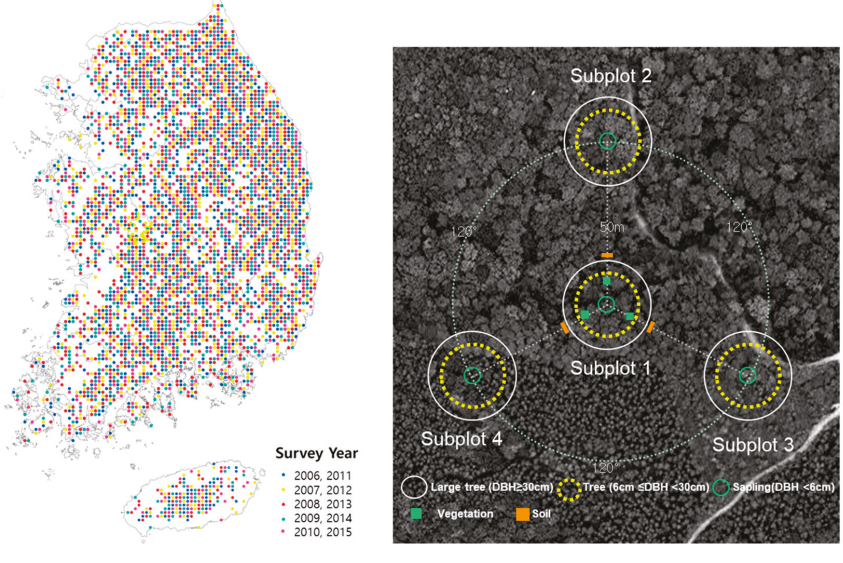

Figure 1. Permanent sample plots in the South Korean National Forest Inventory (NFI).

Total carbon stocks in biomass were calculated using area, growing stocks, biomass expansion factors, basic wood density, and the root to shoot ratio; total carbon stocks in soil and dead organic matter were calculated as the area multiplied by their carbon stocks (C ton/ha) developed by this study [3]. Annual changes in biomass, soil, and dead organic matter were estimated using the IPCC

stock changes method [3]. Specifically, the IPCC stipulates that the activity data for soil and dead organic matter have a transition period of 20 years [3]; in other words, the forest area for estimated carbon stocks should remain constant over a 20-year period. As the forest area in our study has decreased since 1970, we assumed that the forest area in the base year was equal to that of 20 years ago. Uncertainty was calculated using the error propagation equation in accordance with IPCC guidelines [3]. The uncertainty in tree growing stocks from official statistics assumes 0.05% from the previous study, while the uncertainty in IPCC default values is assumed to be 50% [3,11]. All statistical analyses were conducted using the proc GLM procedures of the SAS 9.4 software. And Tukey's HSD test was used to identify the significantly different means ($p < 0.05$).

3. Results

3.1. Estimation of Country-Specific Emission Factors

Emission factors for each carbon pool are shown in Tables 2 and 3. The biomass, calculated as basic wood density (WD, expressed in t dry matter/m^3), ranged from 0.35 to 0.50 for coniferous species and from 0.46 to 0.83 for deciduous species. Deciduous species generally had higher basic wood density than coniferous species (Table 2). Basic wood density was highest for *Q. acuta*, a deciduous species, and lowest for *C. japonica*, a coniferous species (Table 2). Biomass expansion factors (BEF) ranged from 1.31 to 1.74 for coniferous species, and from 1.24 to 1.70 for deciduous species. The root to shoot ratio (R) ranged from 0.20 to 0.36 for coniferous species and from 0.19 to 0.48 for deciduous species (Table 2).

Coniferous species generally had higher litter carbon stocks than deciduous species ($P < 0.05$), while mineral soil carbon stocks were lower in coniferous forest than in deciduous forest ($P > 0.05$; Table 3). However, there was no difference in deadwood carbon stocks between coniferous forest and deciduous forest (Table 3).

Uncertainty in emission factors for biomass ranged from 2% to 12% for WD, 4% to 16% for BEF, and 6% to 33% for R, respectively. Uncertainty for carbon stocks in soil, litter, and deadwood ranged from 27% to 41%, 16% to 27%, and 8% to 1211%, respectively. Soil and dead organic matter had higher uncertainties than biomass; in particular, the uncertainty in deadwood had a large variation owing to lack of NFI sampling points for some tree species.

Table 2. Country-specific emission factors for biomass by tree species.

Forest Type	Species	WD (t dry matter/m^3)	BEF	R
Coniferous forest	*Chamaecyparis obtusa*	0.43 (4%) ^{fg}	1.35 (9%) ^{cd}	0.20 (33%) ^{e}
	Cryptomeria japonica	0.35 (4%) ^{h}	1.31 (6%) ^{cd}	0.23 (12%) ^{de}
	Larix kaempferi	0.45 (6%) ^{efg}	1.34 (8%) ^{cd}	0.29 (15%) ^{bcde}
	Pinus densiflora (Gangwon)	0.42 (12%) ^{fg}	1.48 (12%) ^{abcd}	0.26 (14%) ^{cde}
	P. densiflora (Jungbu)	0.47 (4%) ^{efg}	1.41 (6%) ^{bcd}	0.25 (6%) ^{cde}
	P. koraiensis	0.41 (6%) ^{hg}	1.74 (13%) ^{a}	0.28 (14%) ^{cde}
	P. rigida	0.50 (4%) ^{de}	1.33 (12%) ^{cd}	0.36 (29%) ^{bcd}
	P. thunbergii	0.48 (6%) ^{ef}	1.52 (13%) ^{abcd}	0.29 (19%) ^{bcde}
	Other coniferous forest	0.46 (6%)	1.43 (8%)	0.27 (13%)
Deciduous forest	*Betula platyphylla*	0.55 (4%) ^{d}	1.30 (6%) ^{cd}	0.29 (16%) ^{bcde}
	Liriodendron tulipifera	0.46 (10%) ^{efg}	1.24 (6%) ^{d}	0.23 (27%) ^{de}
	Quercus acuta	0.83 (5%) ^{a}	1.70 (16%) ^{ab}	0.19 (20%) ^{e}
	Q. acutissima	0.72 (6%) ^{b}	1.45 (6%) ^{abcd}	0.31 (26%) ^{bcde}
	Q. mongolica	0.66 (3%) ^{bc}	1.60 (8%) ^{abc}	0.39 (23%) ^{abc}
	Q. serrata	0.66 (5%) ^{bc}	1.55 (8%) ^{abcd}	0.43 (21%) ^{ab}
	Q. variabilis	0.72 (2%) ^{b}	1.34 (4%) ^{cd}	0.32 (15%) ^{bcde}
	Robinia pseudoacacia	0.64 (11%) ^{c}	1.47 (8%) ^{abcd}	0.48 (17%) ^{a}
	Other deciduous forest	0.68 (3%)	1.51 (7%)	0.36 (20%)

WD: basic woody density, BEF: Biomass expansion factor, R: root to shoot ratio. Values with different letters indicate significant differences among tree species at $p < 0.05$ and with those in parenthesis representing uncertainty (%).

Table 3. Carbon stocks in soil and dead organic matter

Forest Type	Species	Litter (C ton/ha)	Soil (C ton/ha)	Deadwood (C ton/ha)	
				5th NFI	6th NFI
Coniferous forest	*Chamaecyparis obtusa*	-	-	1.59 (108%)	3.26 (156%)
	Cryptomeria japonica	-	-	4.37 (90%)	3.50 (179%)
	Larix kaempferi	7.01 (27%) [ab]	46.71 (36%)	2.98 (25%)	2.63 (32%)
	Pinus densiflora (Gangwon)	9.03 (16%) [ab]	53.16 (41%)	1.97 (20%)	2.46 (28%)
	P. densiflora (Jungbu)	11.85 (27%) [a]	37.83 (28%)	1.82 (14%)	1.98 (12%)
	P. koraiensis	7.36 (26%) [ab]	37.77 (29%)	2.78 (31%)	1.51 (57%)
	P. rigida	7.95 (25%) [ab]	36.35 (40%)	1.99 (24%)	3.73 (37%)
	P. thunbergii			2.18 (28%)	1.94 (38%)
	Other coniferous forest	11.25 (25%)	38.75 (32%)	2.11 (38%)	1.90 (55%)
Deciduous forest	*Betula platyphylla*	-	-	1.11 (290%)	0.71
	Liriodendron tulipifera	-	-		0.13
	Quercus acuta	-	-	6.49 (1211%)	0.19
	Q. acutissima	5.07 (19%) [b]	64.30 (27%)	1.55 (33%)	1.27 (38%)
	Q. mongolica	7.30 (20%) [ab]	64.02 (34%)	1.55 (15%)	2.48 (21%)
	Q. serrata	-	-	0.76 (41%)	1.83 (37%)
	Q. variabilis	6.49 (20%) [ab]	57.09 (35%)	1.43 (21%)	1.56 (19%)
	Robinia pseudoacacia	-	-	2.14 (50%)	2.42 (37%)
	Other deciduous forest	6.63 (20%)	55.68 (33%)	1.60 (11%)	2.20 (8%)

Values with different letters indicate significant differences among tree species at $p < 0.05$ with those in parenthesis representing uncertainty (%).

3.2. Estimation of Forest Area and Growing Stock by Tree Species

The estimated forest areas and growing stocks from the 5th NFI and 6th NFI are shown in Table 3. The estimated forest areas (1000 ha) in 2010 were 2581 for coniferous forest, 1865 mixed forest, and 1719 for deciduous forest; the estimated forest areas (1000 ha) for 2015 were 2339 for coniferous forest, 1706 for mixed forest, and 2029 for deciduous forest. Coniferous and mixed forests were converted to deciduous forest, with conversion rates of 9.36% and 8.53%, respectively. The conversion rate of forest area comprised of coniferous species was highest for *P. rigida,* followed by *P. densiflora* (Gangwon), and *L. kaempferi* (Table 3). The growing stock showed increases for all forest types, despite the reduction in forest area over the last five years. The estimated growing stock increased from 832 to 970 M m^3 during the research period (2010–2015), while according to official statistics, South Korean forests increased from 800 to 925 M m^3 during the same period (Table 4). The change in growing stock ranged from −6 M m^3 (*P. rigida*) to 15 M m^3 (*P. densiflora* [Jungbu]) for coniferous species, and from 0.07 M m^3 (*Q. acuta*) to 62 M m^3 (other deciduous forest) for deciduous species (Table 4).

Table 4. Estimated areas and growing stocks by tree species.

Forest Type	Species	Area (1000 ha)		Growing Stock (1000 m^3)	
		2010	2015	2010	2015
Coniferous forest	*Chamaecyparis obtusa*	19 (0.2%)	25 (0.3%)	2377 ± 320	3898 ± 433
	Cryptomeria japonica	14 (0.2%)	14 (0.2%)	3680 ± 346	4850 ± 367
	Larix kaempferi	200 (2.5%)	173 (2.1%)	38,062 ± 1036	41,528 ± 1075
	Pinus densiflora (Gangwon)	363 (4.5%)	312 (3.9%)	62,836 ± 1244	62,316 ± 1271
	P. densiflora (Jungbu)	1315 (4.5%)	1176 (14.5%)	199,213 ± 2261	213,985 ± 2363
	P. koraiensis	126 (16.3%)	116 (1.4%)	16,844 ± 727	20,835 ± 841
	P. rigida	267 (1.6%)	200 (2.5%)	41,126 ± 1009	34,642 ± 946
	P. thunbergii	173 (3.3%)	177 (2.2%)	20,083 ± 870	25,959 ± 1072
	Other coniferous forest	104 (2.2%)	146 (1.8%)	12,649 ± 679	19,425 ± 958

Table 4. *Cont.*

Forest Type	Species	Area (1000 ha)		Growing Stock (1000 m^3)	
		2010	2015	2010	2015
Mixed forest		1865 (28.9%)	1706 (29.1%)	246,042 ± 2033	274,331 ± 2064
Deciduous forest	*Betula platyphylla*	6 (0.1%)	6 (0.1%)	160 ± 18	348 ± 34
	Liriodendron tulipifera	-	1 (0.0%)	-	82 ± 32
	Quercus acuta	1 (0.0%)	1 (0.0%)	177 ± 27	244 ± 18
	Q. acutissima	66 (1.5%)	78 (1.6%)	6301 ± 281	9544 ± 346
	Q. mongolica	472 (10.7%)	415 (8.6%)	62,721 ± 698	64,431 ± 714
	Q. serrata	31 (0.7%)	38 (0.8%)	3248 ± 207	4783 ± 259
	Q. variabilis	221 (5.0%)	235 (4.9%)	32,085 ± 602	40,607 ± 685
	Robinia pseudoacacia	58 (1.3%)	59 (1.2%)	5306 ± 233	7254 ± 299
	Other deciduous forest	865 (19.6%)	1196 (24.8%)	78,913 ± 960	141,146 ± 1363
Total		6165 (100%)	6074 (100%)	831,821 ± 3463	970,210 ± 3473

Values indicate the mean and standard error of stratified random sampling.

3.3. Estimation of Carbon Stocks and Their Changes in Biomass, Litter, Deadwood, and Soil

The estimated carbon stocks and their changes from 2010 to 2015 are shown in Figure 2. Applying IPCC default emission factors ($IPCC_{EF}$) demonstrated that carbon stocks increased by 57,363 Gg C (15.99%) from 2010 to 2015, with an increase of 15.55% in deciduous forests and 15.11% in coniferous forests (Figure 2). Our estimation of CO_2 removal was 42,067 Gg CO_2 per year, with an uncertainty of 35%. Furthermore, in applying IPCC default emission factors, we assumed that the soil and dead organic matter did not change [3]. Applying country-specific emission factors by forest type (CS_{FT}), total carbon stocks increased by 66,569 Gg C (8.47%) from 2010 to 2015, with increases of 15.48%, 0.13%, and 9.32% for biomass, soil, and deadwood, respectively, and a decrease of 3.65% for litter. Additionally, the estimation of CO_2 removal was 48,817 Gg CO_2 per year with an uncertainty of 17% (Figure 3); this CO_2 removal value was about 1.16 times that of $IPCC_{EF}$, which only estimates biomass using the IPCC default emission factors.

In terms of country-specific emission factors by tree species (CS_{SP}), total carbon stocks were increased by 82,702 Gg C (10.41%) from 2010 to 2015 (Figure 2). The carbon pools in biomass and dead wood increased by 19.20% and 14.67%, respectively, while those in litter and soil decreased by 3.17% and 0.21%, respectively. These results indicated a higher total carbon stock than CS_{FT}, despite the reduction of carbon stocks in litter and soil with CS_{SP}. The total carbon stocks of the tree species increased, with the exception of *P. densiflora* (Gangwon), *P. densiflora* (Jungbu), *P. rigida*, and *L. kaempferi* in coniferous forests, and *Q. mongolica* in deciduous forests. The CO_2 removal for CS_{SP} was 60,648 Gg CO_2, with an uncertainty of 22% (Figure 3). Estimated by species (CS_{SP}), CO_2 removal value was about 1.24 times greater than that estimated by forest type (CS_{FT}).

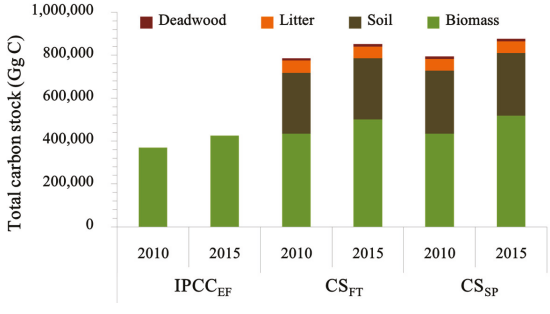

Figure 2. Total carbon stock in each approach. $IPCC_{EF}$: Intergovernmental Panel on Climate Change (IPCC) default emission factors, CS_{FT}: country-specific emission factors by forest type, CS_{SP}: country-specific emission factors by species.

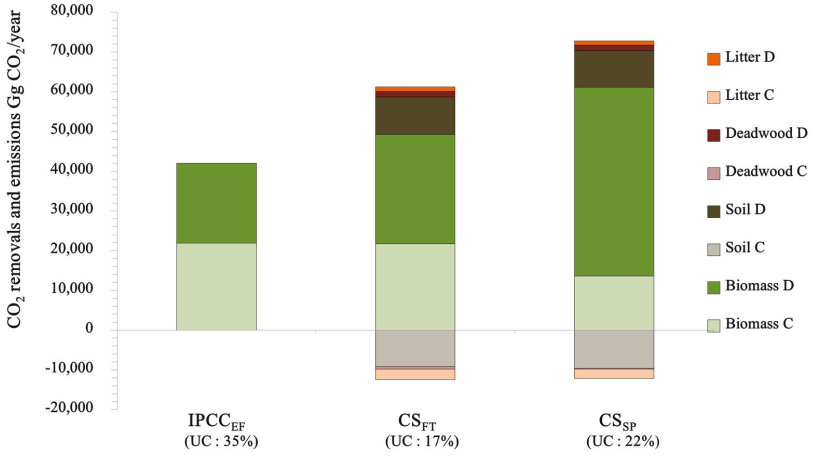

Figure 3. CO_2 removals (+) and emissions (−), and their uncertainty (UC) in each approach. C: coniferous forest, D: deciduous forest, $IPCC_{EF}$: Intergovernmental Panel on Climate Change (IPCC) default emission factors, CS_{FT}: country-specific emission factors by forest type, CS_{SP}: country-specific emission factors by species.

4. Discussion

4.1. Development and Implications of Country-Specific Emission Factors

Using country-specific emission factors can complement other methods of national greenhouse gas inventory reporting and thereby offer improved accuracy. The IPCC [3] report a basic wood density (D) that ranges from 0.31 to 0.49 for coniferous species and 0.35 to 0.58 for deciduous species; however, our results yielded a basic wood density for deciduous forest that ranged from 0.46 to 0.83. Similarly, Kim et al. [23] found that the basic wood density of deciduous species ranged from 0.58 to 0.88 in Korean forests. Past studies have consistently found that basic wood density is higher in deciduous forests than in coniferous forests [3,23,24]. In the IPCC guidelines, the BEF ranges from 1.15 to 4.2 for coniferous species and from 1.15 to 3.2 for deciduous species in temperate regions. Although the IPCC and some other studies have found that BEF can depend on stand age and structure [3,24–26], we did not consider stand age in this study because other researchers have reported that BEF is not dependent upon stand age, but instead reflects stand density, which affects crown density [27,28]. Our results for R were also similar to those from previous studies at global and regional scales [3,23,28]. Additionally, the IPCC [3] report R ranges of 0.23–0.46 for coniferous species and 0.24–0.45 for deciduous species.

The IPCC guidelines do not stipulate default values in regard to the carbon stock of soil and dead organic matter, which do not change in the Tier 1 method; therefore, comparison with our results was not possible. The litter carbon stock was similar to the ranges indicated by previous studies focused on Korean forests; for example, Kim et al. [29] reported that the litter carbon stock (Mg C/ha) in Korean forests ranges from 6.7 to 8.5 for pine forests, 4.6 to 5.0 for oak forests, and 6.5 to 7.0 for larch forests [29]. Other studies have reported litter carbon stocks of 7.2 for coniferous forests and 4.8 for deciduous forests at the national scale [11], as litter carbon stocks are generally given to be higher for coniferous species than for deciduous species [11,29]. Furthermore, the literature shows that litter carbon stock is influenced by the varying composition and decomposition rates of different species [30,31]. Our study showed that litter carbon stock was highest for *P. densiflora* (Jungbu) in coniferous species. Moreover, we found that there was a large degree of variation between forests in terms of soil and deadwood carbon stocks. Another study focusing on *L. kaempferi* reported that carbon stocks (t C/ha) ranged from 45.43 to 165.48 in soil and from 0.1 to 3.4 in deadwood [32]; another study reported that soil carbon stocks were 83.2 t C/ha in deciduous forests and 59.1 t C/ha in coniferous

forests at the national scale [11]. Although there was a large degree of variation in the carbon stock values for soil and dead organic matter, our results are nevertheless within the range of results from previous studies. Furthermore, our results have been verified by GIR for the period 2013 to 2017, except for carbon stocks in deadwood, and this implies that the results are appropriate for use as country-specific emission factors in South Korea.

Most of the uncertainty levels for the emission factors of each carbon pool, except for deadwood, were estimated to be in the range of 10 to 40%, which is consistent with findings from previous studies [3,33]. The uncertainty levels for the deadwood were high in *Q. acuta* due to small sampling plots from NFI as *Q. acuta* occupied a small area in South Korea. In the EU, most countries use emission factors constructed from country-specific studies, although other countries continue to apply international studies or IPCC default emission factors. This trend is promising, as country-specific studies lead to more accurate estimations of carbon stocks in comparison with the use of IPCC default emission factors [34]. Additionally, it is difficult to estimate uncertainty when using IPCC default emission factors, due to the lack of statistical information. However, if country-specific emission factors are used, the uncertainty surrounding emission factors can be estimated. Therefore, it is considered good practice that countries use country-specific emission factors for national greenhouse gas inventory reporting [3].

4.2. Carbon Stocks and Their Changes for Use in National Greenhouse Gas Inventory Reporting

In this study, we estimated the carbon stocks in biomass, soil, litter, and deadwood for use in national greenhouse gas inventory reporting. The removal amount (expressed in Gg CO_2) varied from 42,067 to 60,648 per year, depending upon which of the three approaches was used. These results—specifically the increase of total carbon stocks in biomass and deadwood, which accounted for more than 50% of forest carbon storage—have shown that South Korean forests have stored carbon and absorbed CO_2. According to the NFI survey period, the age class was found to have increased [35], which would have affected the carbon stocks of biomass and deadwood, consistent with findings from studies based on forests in China and the US [36,37]. Large stocks of woody debris commonly occur in mature forests that have a large amount of living biomass [38]. However, forest age is also expected to affect the amount of woody debris at the local scale, and often a greater amount of woody debris is found in young growth stands than in other stands [39].

The CO_2 removal based on the CS_{FT} was about 1.16 times higher than that based on the $IPCC_{EF}$. The application of country-specific emission factors would reflect national circumstances [2] and improve accuracy over IPCC default emission factors, despite differences in previously reported CO_2 removal rates (48,507 Gg CO_2 per year) for forests [5]. These differences are due to the estimate of all carbon pools when estimating carbon stocks in Korean forests. We estimated soil and dead organic matter using the country-specific emission factors and NFI data as a way to improve the completeness of the national greenhouse gas inventory system for the forest sector. In terms of methodology, this difference might be due to using three year moving average data [2,3,5] in contrast to this study, which used single year data.

The application of country-specific emission factors for each species (CS_{SP}) yielded different results from the application of country-specific emission factors for forest type (CS_{FT}). These differences were reflected in changes of area for each species and differences in their carbon stocks from NFI data. In particular, the total growing stock for *P. rigida* has decreased during last five years, consistent with reporting that area of *P. rigida* has decreased owing to age [40]. The species also has high biomass emission factors, which would have an effect on the overall amount of CO_2 removal (Table 2).

According to the IPCC, the CS_{FT} and CS_{SP} approaches represent higher-level inventory reporting systems than the $IPCC_{EF}$, which lacks the accuracy and completeness of CS_{FT} and CS_{SP}. The CS_{FT} estimate reflects a simple difference between two forest types, whereas the CS_{SP} is based on several consecutive change estimates from permanent plots by species. The use of CS_{SP} would improve accuracy in regard to growing stock, as in the case of Finland [9]. Most EU countries could use their

NFIs, which provide information on aboveground biomass [34]. Aboveground biomass is derived from growing stock, which is collected by NFIs. Additionally, other carbon pools may also be based on the data collected in NFIs.

The CS approach has lower uncertainty that does the IPCC approach. While the CS_{SP} approach has higher uncertainty that does the CS_{FT} approach, the uncertainty is in regard to precision rather than accuracy [3,41]. The total uncertainty of net CO_2 removal was high owing to the high uncertainty of soil and dead organic matter despite the low uncertainty in biomass. The CS_{SP}, which appears to be a more complementary and accurate estimation method, includes the estimation of carbon stock changes by tree species. With increasing coverage of the inventory, there is increasing accuracy in terms of the estimated total greenhouse gas emissions, even though the precision of estimated of net emissions might decrease [41].

In order to achieve accuracy and completeness, Annex I countries should also report CO_2 removals and emissions for all carbon pools using country-specific emission factors and models [9,42]. The results of this study are applicable to the improvement of greenhouse gas inventory systems in regard to domestic forests; furthermore, they provide information in regard to greenhouse gas inventory methodology to countries that do not yet have country-specific emission factors. However, it is also necessary to review the Tier 3–level reporting detailed in the UNFCCC report. In addition, an annual land-use change matrix should be established to improve the accounting of changes in carbon stocks for national greenhouse gas inventory systems.

5. Conclusions

The purpose of this study was to examine the methodology for enhancing the completeness and accuracy of national greenhouse gas inventory reporting using Korean forest survey data. The application of country-specific emission factors gave an estimated CO_2 removal value that was 1.2 times greater than for the IPCC default emission factors. In order to improve completeness and accuracy, we estimated CO_2 absorption by all carbon pools and each tree species, which gave a result of 60,648 Gg CO_2 per year with 22% uncertainty. Despite the reduction in total forest area, forests still store carbon and absorb CO_2 owing to differences in the carbon storage capacities of several species. Our results will aid in the development of South Korea's greenhouse gas inventory systems—or those of countries without country-specific emission factors—by improving the calculation of carbon stocks and CO_2 removal by species. However, it would be necessary to construct a land use change matrix, after which our study would be useful for the implementation of Tier 2–level national greenhouse gas inventory systems, as recommended by the IPCC.

Supplementary Materials: The following are available online at http://www.mdpi.com/1999-4907/9/10/625/s1, Figure S1: Location of studied sites for emission factor in biomass, soil, and litter by coniferous species; Figure S2: Location of studied sites for emission factor in biomass, soil, and litter by deciduous species.

Author Contributions: S.J.L., Y.M.S., Y.S., and R.K. conceived and designed the study; S.J.L. J.S.Y., and R.K. analyzed the data; S.J.L. and R.K. wrote the paper.

Funding: This research was funded by Korea Forest Service (Korea Forestry Promotion Institute), grant number (2017044C10-1819-BB01).

Acknowledgments: This study was carried out with support from the R&D Program for Forest Science Technology (Project No. 2017044C10-1819-BB01) provided by the Korea Forest Service (Korea Forestry Promotion Institute).

Conflicts of Interest: The authors declare no conflict of interest.

References

1. UNFCCC. The Paris Agreement. 2015. Available online: https://unfccc.int/process-and-meetings/the-paris-agreement/the-paris-agreement (accessed on 28 September 2018).
2. IPCC. *IPCC Guidelines for National Greenhouse Gas Inventory*; IPCC/IGES: Hayama, Japan, 2006.
3. IPCC. *Good Practice Guidance for Land Use, Land-Use Change and Forestry*; IPCC/IGES: Hayama, Japan, 2003.

4. FAO (Food and Agriculture organization). *Estimating Greenhouse Gas Emissions in Agriculture*; FAO: Rome, Italy, 2015.
5. GIR (Greenhouse Gas Inventory and Research Center of Korea). *National Greenhouse Gas Inventory Report 2017*; GIR: Seoul, Korea, 2017.
6. Pan, Y.; Birdsey, R.A.; Fang, J.; Houghton, R.; Kauppi, P.E.; Kurz, W.A.; Phillips, O.L.; Shvidenko, A.; Lewis, S.L.; Canadell, J.G.; et al. A large and persistent carbon sink in the world's forests. *Science* **2011**, *333*, 988–993. [CrossRef] [PubMed]
7. UNFCCC. COP 15 2009. Available online: https://unfccc.int/meetings/copenhagen_dec_2009/session/6262/php/view/decisions.php (accessed on 28 September 2018).
8. Baritz, R.; Strich, S. Forests and the national greenhouse gas inventory of Germany. *Biotechnol. Agron. Soc. Environ.* **2000**, *4*, 265–271.
9. Statistics Finland. *Greenhouse Gas Emissions in Finland 1990∼2013*; Statistics Finland: Helsinki, Finland, 2015.
10. Federal Environment Agency. *Submission under the United Nations Framework Convention on Climate Change and the Kyoto Protocol 2015*; Federal Environment Agency: Dessau, Germany, 2015.
11. KFS (Korea Forest Service); Kofpi (Korea Forestry Promotion Institute). *Assessment of the Korea's Forest Resource*; Kopfi: Seoul, Korea, 2013.
12. Lee, J.; Yoon, T.K.; Han, S.; Kim, S.; Yi, M.J.; Park, G.S.; Kim, C.; Son, Y.M.; Kim, R.; Son, Y. Estimating the carbon dynamics of South Korean forests from 1954 to 2012. *Biogeoscience* **2014**, *11*, 4637–4650. [CrossRef]
13. Son, Y.M.; Kim, R.H.; Kang, J.T.; Lee, K.S.; Kim, S.W. A practical application and development of carbon emission factors. *J. Korean For. Soc.* **2014**, *103*, 593–598. [CrossRef]
14. Son, Y.M.; Kim, R.H.; Lee, K.H.; Pyo, J.K.; Kim, S.W.; Hwang, J.S.; Lee, S.J.; Park, H. *Carbon Emission Factors and Biomass Allometric Equations by Species in Korea*; KFRI: Seoul, Korea, 2014.
15. Lee, S.J.; Yim, J.S.; Kang, J.T.; Kim, R.; Son, Y.; Park, G.W.; Son, Y.M. Application and development of carbon emissions factors for deciduous species in Republic of Korea—*Robinia pseudoacacia, Betula platyphylla*, and *Liriodendron tulipifera*. *J. Clim. Chang. Res.* **2017**, *8*, 393–399. [CrossRef]
16. Pyo, J.K.; Son, Y.M.; Lee, K.H.; Kim, R.H.; Kim, Y.H.; Lee, Y.J. Estimating the uncertainty and validation of basic wood density for *Pinus densiflora* in Korea. *J. Korean For. Soc.* **2010**, *99*, 929–933.
17. Pyo, J.K.; Son, Y.M.; Jang, G.M.; Lee, Y.J. Uncertainty assessment of emission fators for *Pinus densiflora* unsung Monte Carlo simulation technique. *J. Korean For. Soc.* **2013**, *102*, 477–483. [CrossRef]
18. KFRI (Korea Forest Research Institute). *Survey Manual for Biomass and Soil Carbon*; KFRI: Seoul, Korea, 2010.
19. Yoon, T.K.; Chung, H.; Kim, R.H.; Noh, N.J.; Seo, K.W.; Lee, S.K.; Jo, W.; Son, Y. Coarse woody debris mass dynamics in temperate natural forests of Mt. Jumbong, Korea. *J. Ecol. Field Biol.* **2011**, *34*, 115–125. [CrossRef]
20. KFS (Korea Forest Service). *Improvement of Forest Carbon Accounting System for Post 2020 Climate Change Regime*; KFS: Daejeon, Korea, 2016.
21. KFS (Korea Forest Service). *Statistical Yearbook of Forest*; KFS: Daejeon, Korea, 2016.
22. KFS (Korea Forest Service). *Statistical Yearbook of Forest*; KFS: Daejeon, Korea, 2011.
23. Kim, H.; Kim, H.J.; Lee, K.H.; Son, Y.M.; Lee, K.S.; Lee, S.H. Biomass conversion factors for tree species and verification of applicability for national factors in Korea. *J. Korean Soc. Appl. Biol. Chem.* **2011**, *54*, 758–762. [CrossRef]
24. Lehtonen, A.; Mäkipää, R.; Heikkinen, J.; Sievänen, R.; Liski, J. Biomass expansion factor (BEFs) for Scote pine, Norway spruce and birch according to stand age for boreal forests. *For. Ecol. Manag.* **2004**, *188*, 211–224. [CrossRef]
25. Van Camp, N.; Walle, I.V.; Mertens, J.; De Neve, S.; Samson, R.; Lust, N.; Lemeur, R.; Boeckx, P.; Lootens, P.; Beheydt, D.; et al. Inventory-based carbon stock of Flemish forests: A comparison of European biomass expansion factors. *Ann. For. Sci.* **2004**, *61*, 677–682. [CrossRef]
26. Seo, Y.O.; Lee, Y.J.; Pyo, J.K.; Kim, R.; Son, Y.M.; Lee, K.H. Uncertainty analysis of stem density and biomass expansion factor for *Pinus rigida* in Korea. *J. Korean For. Soc.* **2011**, *100*, 149–153.
27. Kim, C.; Lee, K.S.; Son, Y.M.; Cho, H.S. Allometric equations and biomass expansion factors in and age-sequence of black pine (*Pinus thunbergii*) stands. *J. Korean For. Soc.* **2013**, *102*, 543–549. [CrossRef]
28. Noh, N.J.; Son, Y.; Kim, J.S.; Kim, R.; Seo, K.Y.; Seo, K.W.; Koo, J.W.; Kyung, J.H.; Park, I.H.; Lee, Y.J.; et al. A study on estimation of biomass, stem density and biomass expansion factor for stand age class of Japanese larch (*Larix leptolepis*) stands in Gapyeong area. *J. Korean For. Environ.* **2006**, *25*, 1–8.

29. Kim, S.; Kim, C.; Han, S.H.; Lee, S.T.; Son, Y. A multi-site approach toward assessing the effect of thinning on soil carbon contents across temperature pine, oak, and larch forests. *For. Ecol. Manag.* **2018**, *424*, 62–70. [CrossRef]
30. Berg, B. Litter decomposition and organic matter turn-over in northern forest soils. *For. Ecol. Manag.* **2000**, *133*, 13–22. [CrossRef]
31. Schulp, C.J.E.; Nabuurs, G.; Verburg, P.H.; Waal, R.W. Effect of tree species on carbon stocks in forest floor and mineral soil and implication for soil carbon inventories. *For. Ecol. Manag.* **2008**, *256*, 482–490. [CrossRef]
32. Ko, S. *Influence of Thinning on Carbon Storage in Soil, Forest Floor and Coarse Woody Debris of Larix kaempferi Stands in Korea*; Korea University: Seoul, Korea, 2013.
33. FAO (Food and Agriculture organization). *Global Forest Resource Assessment 2005*; FAO: Rome, Italy, 2006.
34. Cienciala, E.; Tomppo, E.; Snorrason, A.; Broadmeadow, M.; Colin, A.; Dunger, K.; Exnerova, Z.; Lasserre, B.; Petersson, H.; Privitzer, T.; et al. Preparing emission reporting from forests: Use of national forest inventories in European countries. *Silva Fennica* **2007**, *42*, 73–88. [CrossRef]
35. KFS (Korea Forest Service); Kofpi (Korea Forestry Promotion Institute). *Assessment of the Korea's Forest Resources*; Kofpi: Seoul, Korea, 2017.
36. Woodall, C.W.; Balters, B.F.; Oswalt, S.N.; Domke, G.M.; Toney, C.; Gray, A.N. Biomass and carbon attributes of downed woody materials in forests of the United States. *Forest. Ecol. Manag.* **2013**, *305*, 48–59. [CrossRef]
37. Zhu, J.; Hu, H.; Tao, S.; Chi, X.; Li, P.; Jiang, L.; Ji, C.; Zhu, J.; Tang, Z.; Pan, Y.; et al. Carbon stocks and changes of dead organic matter in China's forests. *Nat. Commun.* **2017**, *8*, 151. [CrossRef] [PubMed]
38. Smith, J.E.; Heath, L.S.; Skog, K.E.; Birdsey, R.A. *Methods of Calculating Forest Ecosystem and Harvested Carbon with Standard Estimates for Forests Types of the United State*; USDA: Newtown Square, PA, USA, 2006.
39. Coomes, D.A.; Allen, R.B. Effect of size, competition and altitude on tree growth. *J. Ecol.* **2007**, *95*, 1084–1097. [CrossRef]
40. Seo, Y.O.; Jung, S.C.; Lee, Y.J. Estimation of carbon storage for *Pinus rigida* stands in Muju. *Korean J. Environ. Ecol.* **2016**, *30*, 399–405. [CrossRef]
41. Monni, S.; Peltoniemi, M.; Palosuo, T.; Lehtonen, A.; Mäkipää, R.; Savolainen, I. Uncertainty of forest carbon stock changes—Implications to total uncertainty of GHG inventory of Finland. *Clim. Chang.* **2007**, *81*, 391–413. [CrossRef]
42. Swedish Environmental Protection Agency. *National Inventory Report 2015 Sweden*; Swedish Environmental Protection Agency: Stockholm, Sweden, 2015.

MDPI
St. Alban-Anlage 66
4052 Basel
Switzerland
Tel. +41 61 683 77 34
Fax +41 61 302 89 18
www.mdpi.com

Forests Editorial Office
E-mail: forests@mdpi.com
www.mdpi.com/journal/forests

MDPI
St. Alban-Anlage 66
4052 Basel
Switzerland

Tel: +41 61 683 77 34
Fax: +41 61 302 89 18

www.mdpi.com

ISBN 978-3-03928-667-6